Design, Synthesis and Photophysical Characterisation of N-Containing Organic Emitters and Their Metal Complexes

Ana Maria Garrote Cañas

Submitted in accordance with the requirements for the degree of

Doctor of Philosophy

The University of Leeds

School of Chemistry

December 2017

The candidate confirms that the work submitted is their own, except where work which has formed part of jointly authored publications has been included. The contribution of the candidate and the other authors to this work has been explicitly indicated below. The candidate confirms that appropriate credit has been given within the thesis where reference has been made to the work of others.

In Chapter 3 A. Garrote Cañas carried out the synthesis and evaluation of the photophysical properties with the exception to computational analysis, which was conducted by Dr N. Martsinovich.

.

Acknowledgements

It is an honour for me to express my gratitude and deep regards to all the people who provided their unselfish support and help. Your encouragement enabled me to complete this thesis.

Firstly, thanks to my supervisor Dr Natalia Sergeeva for giving me the opportunity to do the PhD.

I would like to show my great thanks to my colleagues, especially Ellana, Saskia and Yunhan. Without you the long hours in the Lab would have been really boring. A big thank you to Lewis, James, Ryan, Seb, Lauren, Lydia, Pablo, Alberto, Kate, Victor, Ben, Dan, Lynda Forbes, David Fogarty, Chris Pask…the friendship between us is my most precious experience in England.

I cannot express enough thanks to Justin, who has been my rock and without him I could never have submitted this thesis.

I would like to thank my family, my parents and "yaya" for their unconditional support and helping me to become the person that I am today. They have taught me an incredible amount and I have blossomed into who I am through their amazing moral and values. And especially to my "mug" for his guidance, encouragement and support.

Thank you all for supporting me through this difficult time and believing in me.

Last but not least, I should thank Ed Sheeran for keeping me company during the long nights of writing.

Abstract

This study aimed to design novel N-containing heterocyclic compounds, utilising different synthetic strategies to tune the photophysical properties of these compounds. This research was focussed on three families of compounds: indoles, hydrazones and phenanthrolines.

Hydrazones were proved to be useful precursors for the preparation of the bis(indoyl) derivatives *via* a double Fischer indole synthesis. Structural modifications and their effect on the photophysical properties were studied. Also, the pH response and metal sensing ability of these compounds were investigated.

Despite the popularity of research involving indoles, a vast majority focusses on the development of new materials *via* functionalisation of the C-2 position. This thesis described two different strategies to modulate the photophysical properties of materials through a) structural modification of the organic framework aimed at altering its electron distribution and b) a use of metals aimed at the formation of organometallic complexes.

Finally, the synthesis of five novel phenanthroline ligands was explored using two different strategies. Photophysical properties of the novel phenanthroline derivatives were investigated. Also, the synthesis of Ir(III) phenanthroline complexes was carried out and their photophysical properties were evaluated.

Contents

List of Figures

List of Schemes

List of Tables

List of Abbreviations

δ	Chemical shift
λ_{max}	Maximum wavelength of light
°C	Degrees Celsius
2D-COSY	Two dimensional correlation spectroscopy
Abs	Absorbance
Aq	Aqueous
Ar	Aromatic
BdH	Biacetylhydrazone
BINAP	(1,1′-Binaphthalene-2,2′-diyl)bis(diphenylphosphine)
BIP	Bis(indolyl)pyridine
Bpy	2,2'-Bipyridyl
Cat	Catalyst
dcbp	4,40 -dicarboxy-2,20 -bipyridine
DCM	Dichloromethane
DEB	Diethyl butyryl
DFT	Density functional theory
DMPU	N,N'-dimethylpropyleneurea
DMSO	Dimethyl Sulfoxide
DMU	Dimethyl urea
DNBF	4,6-dinitrobenzofuroxan
E^+	Electrophile
E_g	Band gap
Em.	Emission
En	Ethylenediamine
Eq.	Equivalents
G_0	Ground state
G*	Excited state
$H_2BIA(OCH_3)$	2,5-Bis[(5-methoxy)-1H-indol-2-yl]thiazole
$H_2BIP(H)$	2,6-Bis(1H-indol-2-yl)pyridine

$H_2BIP(OCF_3)$	2,6-Bis[(5-trifluoromethoxy)-1H-indol-2-yl]pyridine
$H_2BIP(OCH_3)$	2,6-Bis[(5-methoxy)-1H-indol-2-yl]pyridine
$H_2BIT(OCH_3)$	2,5-Bis[(5-methoxy)-1H-indol-2-yl]thiophene
HMBC	Heteronuclear multiple bond correlation spectroscopy
HMPA	Hexamethylphosphoric triamide
HOMO	Highest Occupied Molecular Orbital
HSQC	Heteronuclear single quantum coherence spectroscopy
Hz	Hertz
ILCT	Intraligand-charge-transfer
Imidazo-Phen	1H-Imidazo[4,5-f][1,10]phenanthroline
IR	Infra-Red
ISC	Intersystem crossing
LC	Ligand centred
LDA	Lithiumdi(isopropyl)amide
LiHMDS	Lithium bis(trimethylsilyl)amide
LiTMP	Lithium 2,2,6,6-tetramethylpiperidine
LUMO	Lowest Unoccupied Molecular Orbital
m/z	Mass-to-charge ratio
MC	Metal centred
MLCT	Metal-to-ligand charge-transfer transitions
mp	Melting point
MS	Mass Spectrometry
MW	Microwave
NBS	N-Bromosuccinimide
NMR	Nuclear Magnetic Resonance
Nu^-	Nucleophile
Phen	Phenanthroline
PMTDA	Pentamethyldiethylenetriamine
ppm	Parts per million
PL	Photoluminiscence
Ppy	2-2’-Bipyridyl

p-TSA	*p*-toluenesulfonic acid
Py	Pyridine
r.t	Room temperature
sat	Saturated
SOC	Spin–orbit coupling
TA	Tartaric acid
TBA	Tetrabutyl ammonium
TBAF	Tetra-n-butylammonium fluoride
TCT	2,4,6-trichloro-1,2,5-triazine
TFA	Trifluoroacteic acid
TMDA	Tetrarnethylethylenediamine
TMS	Trimethylsilane
TMSCl	Trimethylsilyl chloride
TPPMS	Sodium triphenylphosphine-*m*-sulfonate
Tpy	2,2′:6′,2″-Terpyridine
TsCl	*p*-Toluenesulfonyl chloride
UV	Ultraviolet
UV-vis	Ultraviolet-visible

“If a cluttered desk is a sign of a cluttered mind, of what, then, is an empty desk a sign?”

Albert Einstein

Chapter 1 Introduction

Light has been one of the biggest human fascinations since antiquity[1]. It is no wonder the sun was considered a god by ancient civilizations. The Egyptians named their sun god Ra **(Figure 1-1)**. These were the same people who used the seed of a plant found in the Nile River to treat skin diseases (Leukodermia). After ingestion and exposure to sunlight, the skin regained its original pigment.[2] This is one of many instances where processes, promoted by the sun, lead the development and evolution of life as we know it, although sometimes we may not be aware of it.[3]

At least one organic photoreaction is older than mankind; photosynthesis[4]. While attempting to explain plant growth, people discovered the process of photosynthesis. This is the most obvious example of photochemistry which causes chemical change driven by the light. Although, photochemistry also uses the physical processes, they are not involved in any chemical alterations in chemical identity. Scientists have extensively investigated the interactions of light with matter, enriching the field of photochemistry.

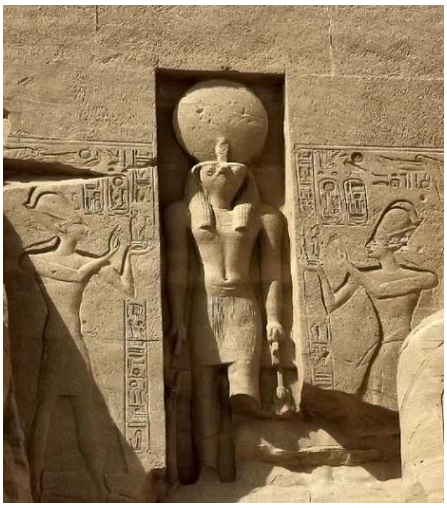

Figure 1-1 The Egyptian god Ra (© Bill Stanley)[5]

1.1 The energy of light: Ground and excited states

Upon light excitation of suitable wavelength, the molecule transfers into an electronic excited state (G*). Each excited state has its own electronic configuration different from that of the ground state owing to different physical and chemical properties. Electronic spectroscopy can

be used to monitor these transitions. The transitions from the ground state (G_0) of a molecule gives rise to the bands observed in absorption spectra and are responsible for the colour. A loss of energy by the molecule in the excited states (G*) can follow either a radiative or a non-radiative pathway.[6]

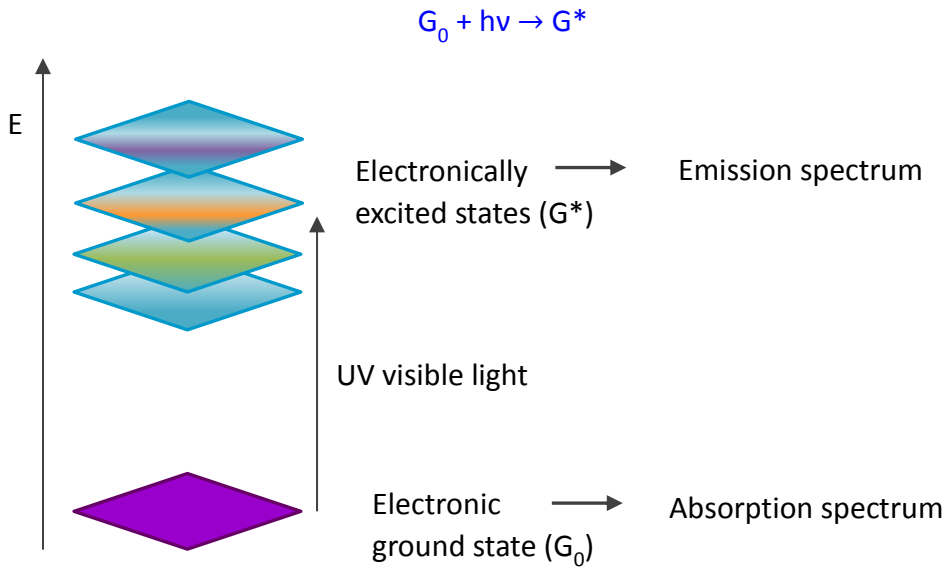

Figure 1-2 Electronic transitions involved in excitation with a photon of suitable energy

1.2 Principles of excited state deactivation[7, 8]

A molecule in an excited state will return to the ground state within a short period of time. The most common deactivation process is non-radiative decay. Here, an excess of energy can either be transferred into the vibration, rotation and translation of surrounding molecules or the molecule can undergo thermal degradation. The radiative decay process from an excited state involves the emission of a photon.[9]

The photophysical pathways for relaxation are reflected in the Jablonski diagram **(Figure 1-3)**. S represents singlet state and T triplet state of the molecule. In **Figure 1-3**, the electronic energy levels are defined by S_0, S_1 and S_2 (arranged by energy). Each electronic level consists of vibrational levels (0-3) and rotational levels (omitted for simplicity of viewing). The process of absorption is reflected as a vertical transition from S_0 to S_1 or S_2 (depending on the energy of the incoming photon). According to the Franck-Condon principle[10], in many cases the excited molecules will be in a higher vibrational level (of the electronic excited state). These excited vibrational states are often referred to as “hot states". According to Kasha's rule, a return to the ground state is most likely to take place from the lowest vibrational level of the

first excited state ($S_{1,0}$).[11] The radiative decay (emission of a photon) from an excited state is called luminescence . Depending on the nature of the excited state, luminescence can be divided into two categories, fluorescence and phosphorescence.

1. Fluorescence is the emission of light from a singlet excited state. This process is favourable as it does not involve a change in the electron spin multiplicity. It occurs in the order of 10^{-9} to 10^{-6} seconds.

2. Phosphorescence is the emission of light from a triplet excited state, in which the excited electron has the same spin as the electron in the ground state. These transitions are forbidden. Consequently, phosphorescence is a much slower process in comparison to fluorescence. It continues even after the excitation source is turned off (10^{-4} to 10^{2} seconds or over). Phosphorescence involves intersystem crossing (change in the electron spin multiplicity).

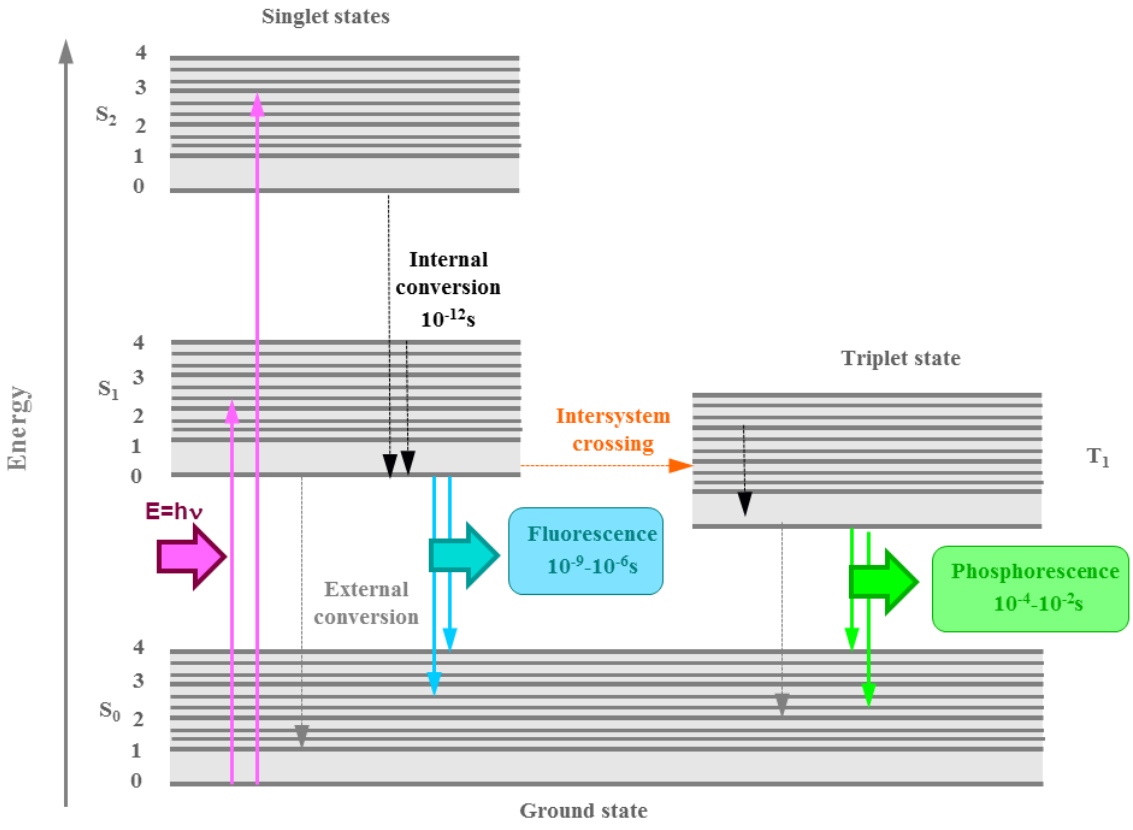

Figure 1-3 Jablonski diagram for absorption, fluorescence and phosphorescence

There is a variety of non-radiative processes to dissipate the excess of energy:

1. Vibrational relaxation refers to collisions of molecules with excited species and solvent. This process is very rapid ($<10^{-12}$ s). Therefore, fluorescence almost always involves the transition from the lowest vibrational level of the excited state.

2. Internal conversion involves the spontaneous change from the initial electronic state to a lower energy electronic state of the same multiplicity (10^{-14} to 10^{-12} seconds). The excess of energy is usually converted into vibrational energy.

3. External conversion involves deactivation of the excited electronic state involving the interaction between the excited state and the solvent. Solvents with high viscosity and low temperatures slow down this deactivation process diminishing the collision number.

4. Intersystem crossing is a crossover process which is enhanced if the vibrational levels of two states overlap. It is more common in molecules that contain heavy atoms, such as iridium, leading to a reduction in fluorescence.

Consequently, this thesis aims to develop and study a variety of strategies to tune photophysical properties of novel N-containing emitters. These are one of the most important and commonly used ligands in coordination chemistry[12-14]. Therefore, three families of two or more donor atom nitrogen-containing heterocycles were investigated: hydrazones, indoles and phenanthrolines.

Chapter 2 Synthesis and Characterisation of Bis(2,6-diacetylphenylhydrazones)

2.1 Introduction

Since the middle of the 20th century[15], the chemistry of hydrazones has dynamically evolved. In particular, aryl hydrazones are a versatile class[16] of compounds due to their ease of preparation, stability, conformational flexibility and tendency toward crystallinity. Their structural features display versatile behaviour in metal coordination, acting as multidentate ligands by forming coloured chelates. Potentially, heterocyclic hydrazones can coordinate to the metal through the nitrogen atoms either alone or together with the central heteroatom. The colourful chelates can then be used in a selective determination of cationic or anionic species, which has made them active components of chemosensors.[17]

In addition, they have been used as precursors for the synthesis of a variety of heterocycles, including thousands[18] of indoles *via* the Fischer indole synthesis. They are widely used in organic synthesis due to their capability to react with electrophiles and nucleophiles. The hydrazone group contains two connected nitrogen atoms which are both nucleophilic, although the amino type nitrogen is more reactive than the imine nitrogen atom[19, 20].

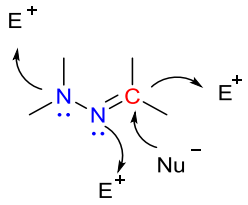

Figure 2-1 Reactivity and active centres of hydrazone group

Owing to their properties, hydrazones and their metal complexes have been employed in various fields including metal and covalent organic frameworks[21-25], sensors[26], analytical[27], biological[28, 29] and medicinal chemistry[30-34].

Hydrazones are usually synthesised by three different pathways: (i) condensation of hydrazine with aldehydes or ketones[35], (ii) reaction involving a diazonium salt and β-ketoester under basic conditions (Japp-Klingemann)[36] and (iii) Pd-catalysed[18] reaction of aryl halides with hydrazine derivatives (Buchwald-Hartwig).

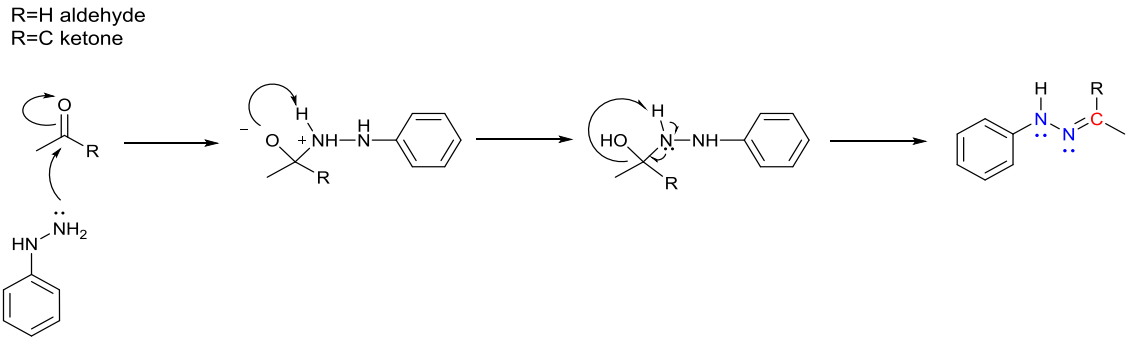

Scheme 2.1 Mechanism of the condensation reaction of hydrazine with a carbonyl compound

The Japp-Klingemann reaction involves two steps. The first process is the coupling between a diazonium salt and a malonic acid derivative. Here, an unstable azo compound gives a hydrazone following decarboxylation.[37]

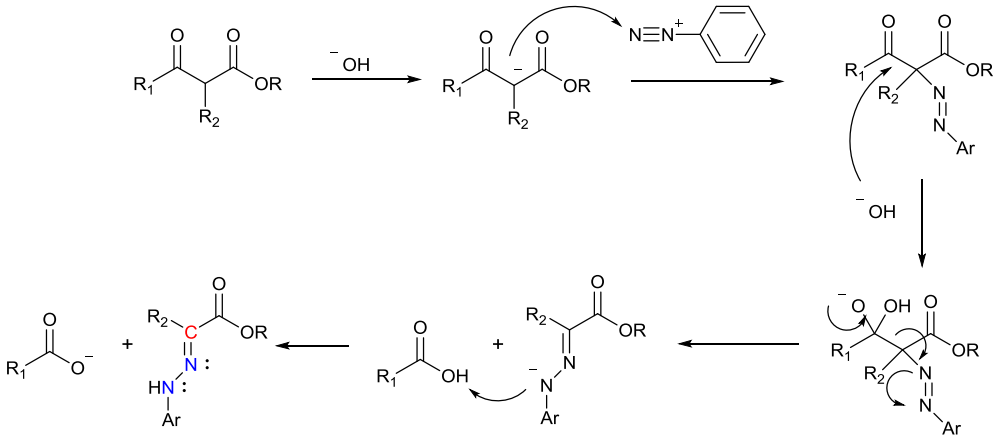

Scheme 2.2 Mechanism of the Japp-Klingemann coupling reactions

Buchwald-Hartwig coupling is a palladium catalysed reaction for the formation of C-N bonds. In 1995 Buchwald[38] and Hartwig[39] reported independently the reaction of arylhalides with nitrogen nucleophiles, such as hydrazine, using base (stoichiometric amounts).

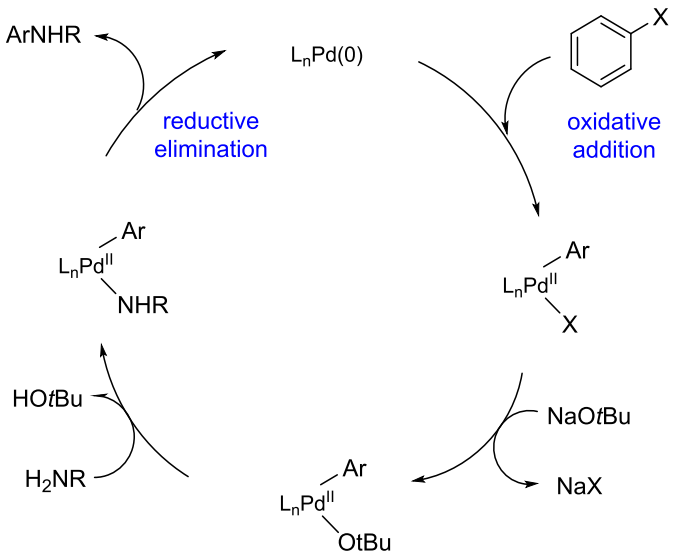

Scheme 2.3 General mechanism of the Buchwald-Hartwig coupling

2.1.1 Bis(phenylhydrazone)derivatives as ancillary ligands

N-Containing heterocycles, containing electron-withdrawing imine nitrogen(s) (C=N), have attracted interest for their ability to form metal complexes[40]. 2,2'-Bipyridyl (bpy) **(S.1)** and 2,2′:6′,2″-terpyridine (tpy) **(S.4)** systems are the most commonly used. In the middle of the 20th century, biacetylhydrazone (bdH) **(S.2)** and its derivatives emerged as alternatives to the well-known complexing agent, 2,2'-bypyridine **(S.1)**[41]. BdH **(S.2)** is a bidentate ligand with two imine N-atom donors capable of bonding with metals. 2-Pyridinal methylamine **(S.3)** contains both, the cyclic amine and the imine functional group. In addition, ligands containing the trimethine structural unit **(S.5)**, comprising a cyclic amine and imine group, emerge as alternatives to the previous mentioned frameworks.

Curry, *Robinson* and *Busch* show that 2,6-diacetylpyridinebis(phenylhydrazone) ligands **(S.6)** function as planar tridentate ligands. A replacement of hydrogen(s) at the amino group can significantly decrease the donor strength of the ligand due to an increase in the steric hindrance and disruption of the planarity. [42]

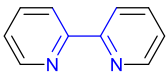

Bpy (S.1)

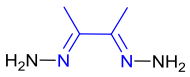

BdH (S.2)

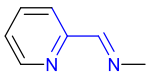

2-pyridinal methylamine (S.3)

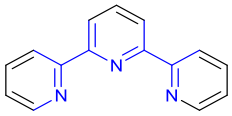

Tpy (S.4)

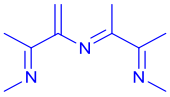

Trimethine (S.5)

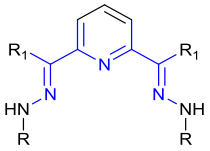

2,6-diacetylpyridine bis(phenylhydrazone) (S.6)

Figure 2-2 Examples of N-bidental ligands and N-tridental ligands

2.2 Design and synthesis of bis(phenylhydrazone)derivatives

Hydrazones are a versatile class of compounds due to their ease of preparation. Their applicability in a wide range of applications has resulted in extensive use in organic synthesis, especially as intermediates for the preparation of heterocyclic compounds[43, 44].

Six substrates were screened as potential precursors for the synthesis of bis(indolyl) derivatives. To understand the influence of substituents on the cyclisation, R=OCH_3 and R=OCF_3 were selected as electron-donating and withdrawing groups respectively and for comparison with a non-substituted substrate (R=H). Our "selection/exclusion" criteria for the substrates was based on five factors:

1. relatively low cost
2. relatively low toxicity
3. mild reaction conditions
4. yields above 60%
5. ease of purification e.g. washing, precipitation or recrystallisation (N-arylhydrazones are easily enolisable, and are unstable to purification by flash chromatography)[45]

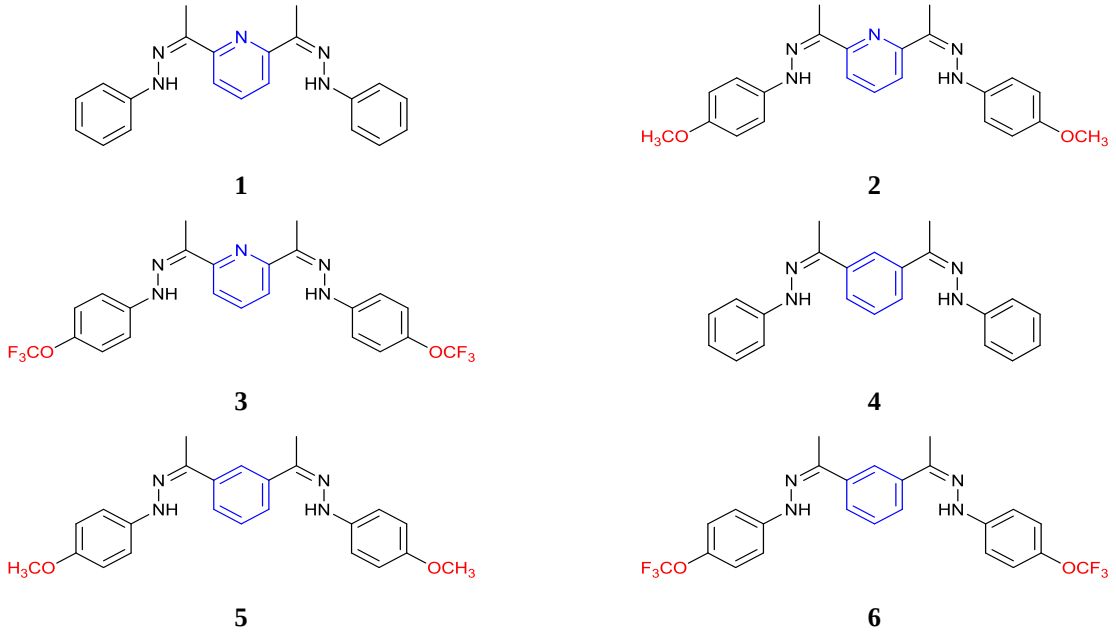

Figure 2-3 Target structures of bis(phenylhydrazones)

The synthesis of bis(phenylhydrazone)pyridines **(1-3)** and bis(phenylhydrazone)benzenes **(4-6)** was accomplished by using a (standard) condensation protocol[42, 46], reacting the appropriate hydrazine with 2,6-diacetylpyridine or 1,3-diacetylbenzene respectively **(Scheme 2.4)**.

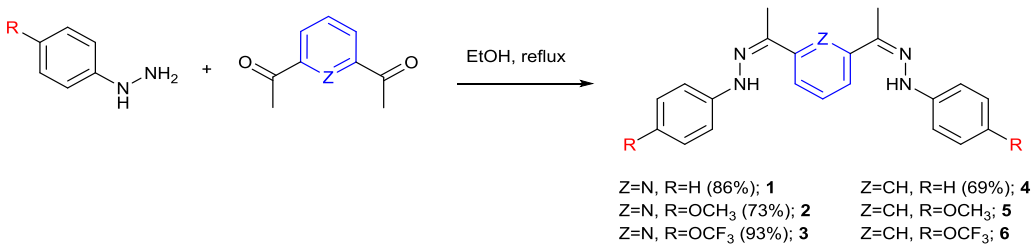

Scheme 2.4 Synthesis of bis(phenylhydrazones)

The synthesis of compounds **1-3** provided products as solids that can be easily precipitated resulting in the yields of 73%-93%. Compound **4** was obtained in the yield of 80% using solvent diffusion (EtOH-Ether, inner-outer). However, compounds **4-6** were more difficult to isolate. For compounds **5** and **6**, repeated attempts at recrystallisation or precipitation (varying solvents) failed. The attempts to form exclusively bishydrazones **5** and **6** without the presence of mono-adducts proved to be unsuccessful. Compounds **5** and **6** failed the "selection/exclusion" criteria and were thus removed from further studies.

2.3 Synthesis of pyridinyl bis(phenylhydrazone) metal complexes

Metal ions play an important role in biological processes, increasing their interest as biomarkers or drugs for early diagnosis and treatment of diseases. Cancer is one of the most common diseases causing human suffering and death [47, 48]. Due to the toxicity of cis-platin[49], a well-known chemotherapeutic drug, platinum[50] and ruthenium [51, 52] have been commonly explored. However, there is an emerging interest in the use of cheaper first-row coordination compounds[53 54, 55].

In addition, imine nitrogen (C=N) linkage possess remarkable antibacterial, antifungal, anticancer and antimalarial activities.

For the synthesis of bis(phenylhydrazone)pyridine derivative complexes, a variety of metal salts were used to examine the coordination number preferred. Two different approaches were used:

1. Conventional synthesis of the metal complexes followed by crystal growth using solvent layering, slow evaporation, vapour diffusion and crystallisation.
2. Vapour diffusion technique[56, 57], which is a popular method for simultaneous complex and crystal formation.

The conventional synthesis was used to screen the conditions. The reaction was carried out in open air, rapidly adding a solution of the ligand (flask A) to a solution of the metal salt (flask B). **Table 2-1** summarises the different conditions for the attempted synthesis of metal complexes using hydrazones **1-3** as ligands.

Table 2-1 Examples of metal complexes *via* conventional synthesis

R	Solvent	Metal source	Ratio (L:M) Result
OCH_3	EtOH (dry)	$KAuCl_4$	1:1
OCH_3	DCM (dry)	PtCl2	1:1
OCH_3	Acetone	$Cu(ClO_4).6H_2O$	2:1
H	Acetone	$Cu(ClO_4).6H_2O$	2:1
OCH_3	Acetone	$Zn(ClO_4).6H_2O$	2:1
OCH_3	EtOH	$Zn(ClO_4).6H_2O$	2:1
H	Acetone	$Zn(ClO_4).6H_2O$	2:1
OCF_3	Acetone	$Zn(ClO_4).6H_2O$	2:1
OCF_3	EtOH	$Zn(ClO_4).6H_2O$	2:1
OCF_3	EtOH	$Cu(ClO_4).6H_2O$	2:1
OCF_3	EtOH	$Co(ClO_4).6H_2O$	2:1
OCF_3	EtOH	AlCl3	2:1

Vapour diffusion allows a metal complex and crystal growth in the same vial. Generally, a saturated solution, prepared by dissolving a few milligrams of the ligand in a suitable solvent, was added to the metal salt in a vial. The mixture in the vial was then placed in a larger vial that contained a small volume of solvent, in which the resulting metal complex is insoluble. The outer vial was then sealed. The vapour of the volatile solvent from the larger vial slowly diffuses through the holes in the inner vial. This lead to formation of crystals of the metal complex suitable for X-ray examination. **Table 2-2** summarises the different conditions for the attempted synthesis of metal complexes using hydrazones **1-3** as ligands.

Table 2-2 Examples of metal complexes *via* vapour diffusion

Entry	R	Solvent inner vial	Solvent outer vial	Metal salt	Ratio (L:M) Result	
1	H	Acetone	Hexane	$Zn(ClO_4).6H_2O$	1:1	2:1
2	H	Acetone	Hexane	$ZnCl_2$	1:1	2:1
3	H	Acetone	Hexane	$Cu(ClO_4).6H_2O$	1:1	2:1
4	H	Acetone	Hexane	$AlCl_3$	2.1	
5	H	Acetone	Hexane	μ-Ir-dimer	1:1	2.1
6	H	Acetone	Hexane	$EuCl_3$	1:1	2.1
7	OCH_3	EtOH/DCM	Diethyl ether	$Zn(ClO_4).6H_2O$	1:1	2.1
8	OCH_3	EtOH/DCM	Diethyl ether	$Cu(ClO_4).6H_2O$	1:1	2:1
9	OCH_3	EtOH/DCM	Diethyl ether	$AlCl_3$	2:1	
10	OCH_3	EtOH/DCM	Diethyl ether	$Pt(PhCN)_2Cl_2$	2:1	
11	OCH_3	EtOH/DCM	Diethyl ether	μ-Ir-dimer	1:1	
12	OCH_3	EtOH/DCM	Diethyl ether	$EuCl_3$	2:1	
13	OCF_3	EtOH/DCM	Diethyl ether	$Zn(ClO_4).6H_2O$	1:1	2:1
14	OCF_3	EtOH/DCM	Diethyl ether	$Cu(ClO_4).6H_2O$	1:1	2:1
15	OCF_3	EtOH/DCM	Diethyl ether	$AlCl_3$	2:1	
16	OCF_3	EtOH/DCM	Diethyl ether	$Pt(PhCN)_2Cl_2$	2:1	
17	OCF_3	EtOH/DCM	Diethyl ether	μ-Ir-dimer	1:1	2.1
18	OCF_3	EtOH/DCM	Diethyl ether	$EuCl_3$	1:1	2.1

2.3.1 X-Ray crystal structures

The ligands with a trimethine motif were investigated. Ligands **1-3** can coordinate to the metals through the three nitrogen atoms. X-Ray analysis of Zn^{2+} and Cu^{2+} complexes of bishydrazones, with a stoichiometric ratio of ligand to metal 2:1, revealed an octahedral arrangement; the colour of the complexes were orange and brown-green, respectively.

The crystal structures of bis-[2,6-diacetylpyridine(phenylhydrazone)] Zn(II) diperchlorate **(Zn.1)** and bis-[2,6-diacetylpyridine(phenylhydrazone)] Cu(II) diperchlorate **(Cu.1)** complexes are shown in **Figure 2-4**. Both complexes crystallised in a monoclinic cell and were solved in the $P2_1$ space group with three cations, six $[ClO_4]^-$ counter ions and one molecule of water in the asymmetric unit. The only difference was that the zinc complex **(Zn.1)** crystallised as orange blocks while the copper complex **(Cu.1)** crystallised as brown blocks.

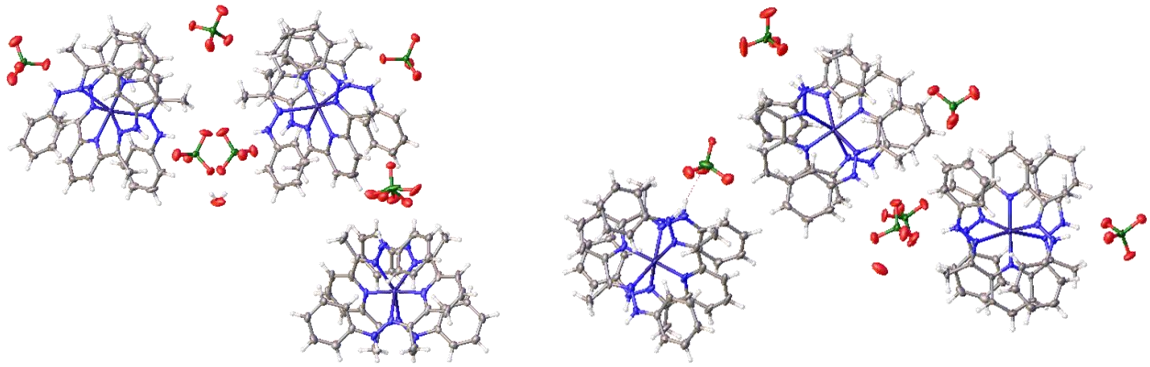

Zn.1 **Cu.1**

Figure 2-4 Crystal structures of 2,6-diacetylpyridine(phenylhydrazone) Zn (Zn.1) and Cu(Cu.1) diperchlorate complexes

The crystal structure of bis-[2,6-diacetylpyridine(phenylhydrazone)] Zn(II) tetrachloridozincate complex **(Zn.1.1)** is shown in **Figure 2-5**. The orange compound crystallised in a monoclinic cell and was solved in the *P*2/*n* space group with four cations, four $[ZnCl_4]^{2-}$ counter ions and acetone, water and hexane in the asymmetric unit. The $[ZnCl_4]^{2-}$ anions were formed in the presence of an excess of Cl anions from the $ZnCl_2$ salt[58-60].

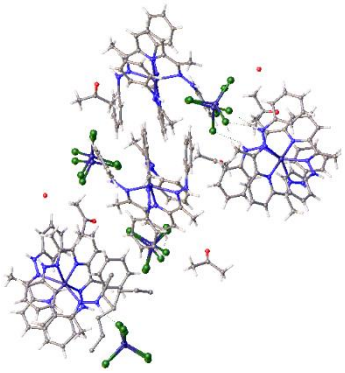

Zn.1.1

Figure 2-5 Crystal structures of bis-[2,6-diacetylpyridine(phenylhydrazone)] Zn(II) tetrachloridozincate (Zn.1.1)

The crystal structures of bis-[2,6-diacetylpyridine(4-trifluoromethoxyphenylhydrazone)] Zn(II) diperchlorate **(Zn.3)** and bis-[2,6-diacetylpyridine(4-trifluoromethoxy phenylhydrazone)] Cu(II) diperchlorate **(Cu.3)** complexes are shown in **Figure 2-6**. Both complexes crystallised in a monoclinic cell. However, **Zn.3** was solved in the *Cc* space group with one cation and two anions in the asymmetric unit while **Cu.3** was solved in the *C*2/*c* space

group with half a cation and two half perchlorate anions in the asymmetric unit. In addition, **Zn.3** crystallised as orange prisms while **Cu.3** crystallised as brown fragments.

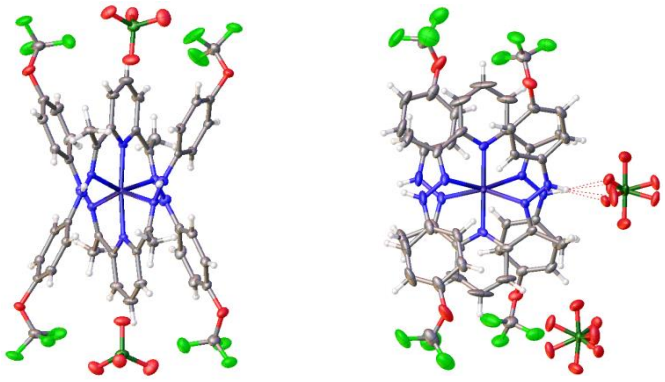

Zn.3 **Cu.3**

Figure 2-6 Crystal structures of 2,6-diacetylpyridine(4-trifluoromethoxyphenyl hydrazone) Zn (Zn.3) and Cu(Cu.3) diperchlorate complexes

The crystal structure of bis-[2,6-diacetylpyridine(4-methoxyphenylhydrazone)] Zn(II) diperchlorate complex **(Zn.2)** is shown in **Figure 2-7.** The compound crystallised (as brown plates) in an orthorhombic cell and was solved in the *Fddd* space group with a quarter of a cation and half a perchlorate counter ion in the asymmetric unit.

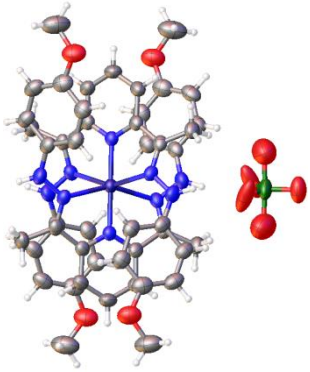

Zn.2

Figure 2-7 Crystal structure of 2,6-diacetylpyridine(4-methoxyphenylhydrazone) Cu(II) diperchlorate complex (Zn.2)

2.4 Analysis of bis(phenylhydrazone)derivatives

2.4.1 Photophysical properties of bis(phenylhydrazone)derivatives

The photophysical properties of the resulting bis(phenylhydrazone)derivatives **(1-4)** were investigated in three different solvents. Compound **4** was found to be an exception due to low solubility in acetonitrile[1]. The different conformation adopted by the molecule influenced the interactions of lone pairs present in the nitrogen atoms. Therefore, the spectral shift, intensity or shape change can be attributed to specific solute-solute interaction and solute-solvent interaction[61].

Absorption spectroscopy was used to study the photophysical behaviour of compounds **1-4** in different solvents. The bishydrazones showed the absorption maxima in the range of 344-360 nm **(Figure 2-8)**. While the extinction coefficient values were dependent on the solvent choice, the position of the main band is almost independent.

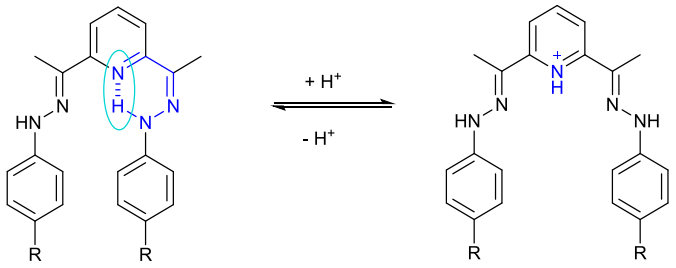

Scheme 2.5 Intramolecular interaction in compounds 1-4 *via* H-bonding

The record of the spectra in solvents of different polarity The absorption profiles of compounds **1** and **4** are not altered by the solvent polarity **(Figure** 2-8**.1** and **Figure 2-8.4)**. However, compound **2** and **3** present two additional bands in acetonitrile and dichloromethane **(Figure 2-8.2** and **Figure 2-8.3)**. From these results, it can be concluded that only the compounds with substituents (**2** and **3**) are affected by a decrease in the solvent polarity. The introduction of substituents alters the magnitude and direction of the permanent dipole moments and electron distribution, and can allow the formation of a more stable exciplex. As a result, the spectral

[1] Spectroscopic measurements were performed using the same concentration range (10^{-5} M)

shifts can be attributed to solute-solute or solute solvent interactions *via* the formation of H-bonding.

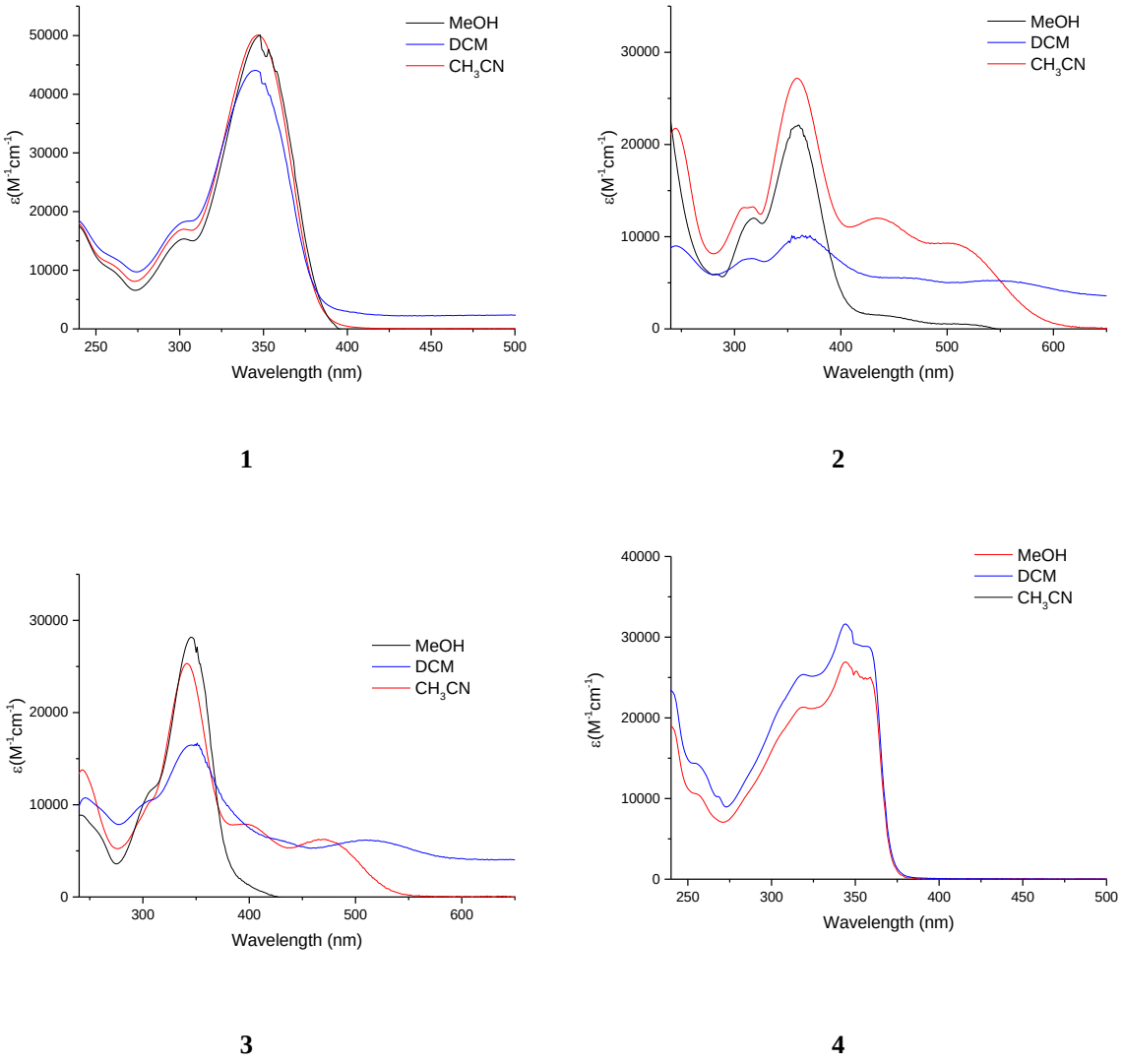

Figure 2-8 Absorbance spectra of 1-4 in methanol, acetonitrile and dichloromethane

The emission properties of pyridine-based hydrazones **1-3** and benzene-based hydrazone **4** were investigated. Compound **4** was the only emissive material, showing that the use of a different bridge unit such as benzene can affect the luminescent properties. Interestingly, compounds **1** and **4** have similar framework structures, where the pyridine bridging unit in **1** is replaced by benzene in **4**. However, the results show that compound **4** exhibits a quantum yield of Φ =38%, while emission of compound **1** is non-existent.

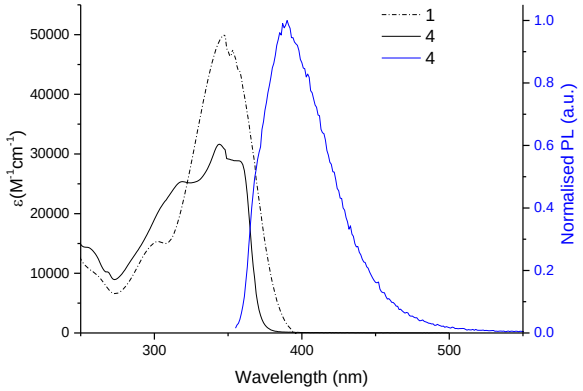

Figure 2-9 Absorption and normalised emission (energy of excitation 338nm) profile of compounds 1 and 4 in dichloromethane

2.4.2 Acidochromism: reversible pH-induced molecular change

The sensing ability of the aryl-hydrazones 1-4 was investigated. The pH response was studied upon addition of trifluoroacteic acid (TFA) (1.3×10^{-2} M) to the solutions of hydrazones **1-4** in ethanol ($2.2\text{-}2.8\times10^{-5}$ M). The reversibility of the protonation process was explored by the addition of tetra-*n*-butylammonium fluoride (TBAF) solution (1.0×10^{-2} M) to the protonated species. The presence of an isosbestic point in the absorption spectra of compounds **1-3** suggests the coexistence of two different species which were associated with the protonation of the pyridine-nitrogen. Hydrazones **1-3** displayed a noticeable colour change from colourless (pH>7) to yellow, burgundy and orange, respectively, at acidic pH.

Compound **1** shows two absorption bands in the UV region at λ_{max}=303 nm and at λ_{max}=348 nm **(Figure 2-10)**. Upon addition of Tetra-n-butylammonium fluoride

Trifluoroacteic acidTFA (1.3×10^{-2} M), two new bands are observed in the visible region at λ_{max}=428 nm and at λ_{max}=496 nm. These bands are responsible for the yellow colour of the molecule and can be attributed to the protonation of the pyridine unit **(Figure 2-10)**. Protonation of the pyridine unit is also confirmed with X-ray analysis **(Figure 2-11)**.

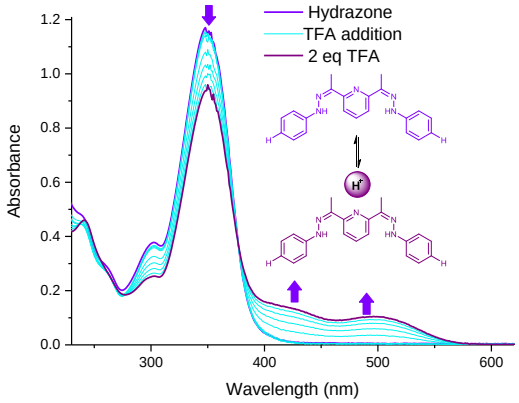

Figure 2-10 Spectrophotometric titration of compound 1 (2.2×10^{-5} M) with TFA (1.3×10^{-2} M) in EtOH

Figure 2-11 shows the normalised absorbance intensity variation upon addition of 2 eq of TFA.

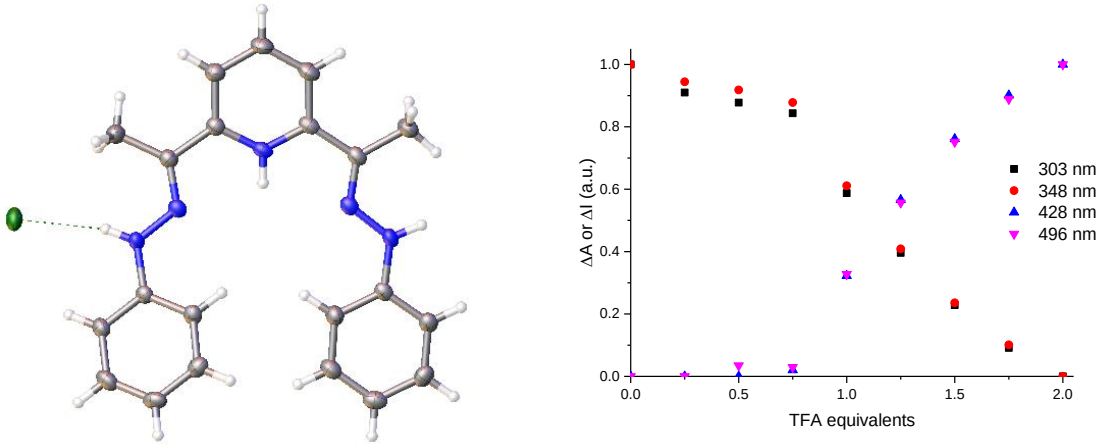

Figure 2-11 Crystal structure of protonated 2,6-diactetylpyridinebis(phenylhydrazone) (left). Normalised absorption variation upon addition of TFA at 303 nm, 348 nm, 428 nm and 496nm (right)

Compound **2** displays a remarkable colour change from colourless at pH>7 to burgundy at pH<7. It shows four absorption bands in the UV-vis spectral region at λ_{max}=318 nm, λ_{max}=362 nm, λ_{max}=451 nm and at λ_{max}=530 nm **(Figure 2-12)**. Upon addition of TFA (1.3×10^{-2} M), there is an increase in the intensities of the bands at 451 nm and 530 nm along with a decrease in the intensities of the bands at λ_{max}=318 nm and λ_{max}=362 nm. These peaks are responsible for enhancing the red colour already observed in the solution as a result of the protonation of the pyridine unit. Also, the X-ray analysis shows that **2** exists in the protonated form under neutral conditions **(Figure 2-13)**. Reversibility of the protonation is tested by the

addition of *n*-tetrabutylammonium fluoride solution (1.0×10^{-2} M, in THF/EtOH) to an acidified solution of **2**. The disappearance of the bands at λ_{max}=451 nm and at λ_{max}=530 associated with the protonated form of **2** is observed. At a basic pH, hydrazone **2** shows a shoulder at λ_{max}=318 nm and an intense band at λ_{max}=362 nm in the UV region.

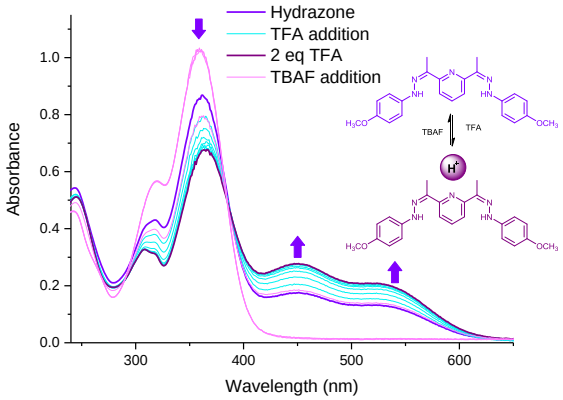

Figure 2-12 Spectrophotometric titration of compound 2 (2.6×10^{-5} M) with TFA (1.3×10^{-2} M, up to 2 equivalents) in EtOH, followed by deprotonation of 2 by addition of TBAF (1.0×10^{-2} M, in THF/EtOH)

Figure 2-13 shows the normalised absorbance intensity variation upon addition of 2 eq of TFA.

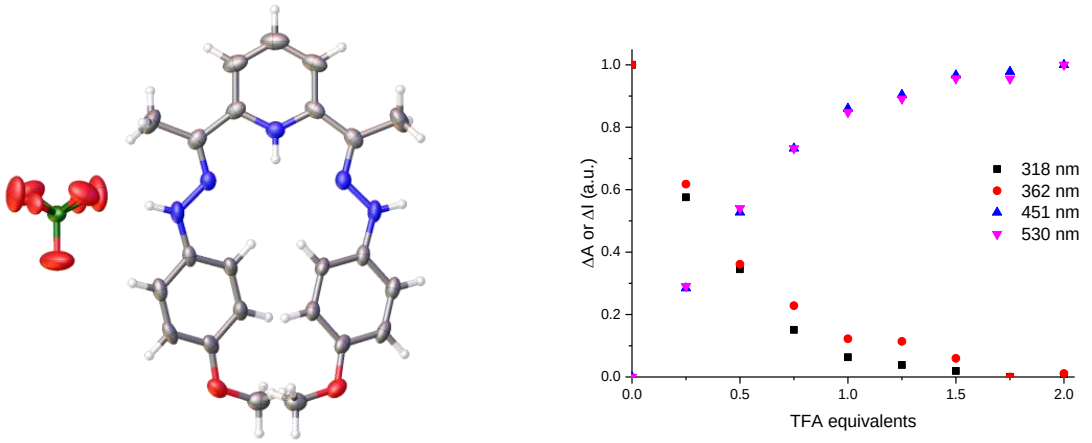

Figure 2-13 Crystal structure of protonated 2,6-diactetylpyridinebis(4-methoxyphenylhydrazone) (left). Normalised absorption variation upon addition of TFA at 318 nm, 362 nm, 451 nm and 530 nm (right).

Compound **3** displays a colour change from colourless at pH>7 to orange pH<7. Four absorption bands can be observed in the UV-vis spectral region at λ_{max}=308 nm, λ_{max}=347 nm λ_{max}=407 nm and at λ_{max}=483 nm **(Figure 2-14)**. Upon the addition of TFA (1.3×10^{-2} M) there

is an increase in the intensity of the bands at 407 nm and 483 nm along with a decrease of λ_{max}=308 nm and λ_{max}=347 nm bands. These bands are responsible for enhancing the orange colour already observed in the solution as a result of the protonation of the pyridine unit. Also, the X-ray analysis shows that compound **3** already exists in the protonated form under neutral conditions **(Figure 2-15)**. Reversibility of the protonation is studied by the addition of TBAF solution (1.0×10^{-2} M, in THF/EtOH). A disappearance of the bands at λ_{max}=407 nm and at λ_{max}=483 associated with the protonated form of **3** has been observed. In solution of pH>7, hydrazone **3** shows a shoulder at λ_{max}=308 nm and an intense band at λ_{max}=347 nm in the UV region.

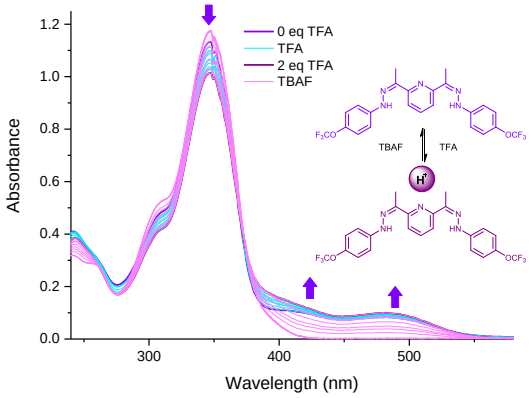

Figure 2-14 Spectrophotometric titration of compound 3 (2.4×10^{-5} M) in EtOH with TFA (1.3×10^{-2} M, up to 2 equivalents) in EtOH, followed by deprotonation by addition of (1.0×10^{-2} M, in THF/EtOH)

Figure 2-15 shows the normalised absorbance intensity variation upon addition of 2 eq of TFA.

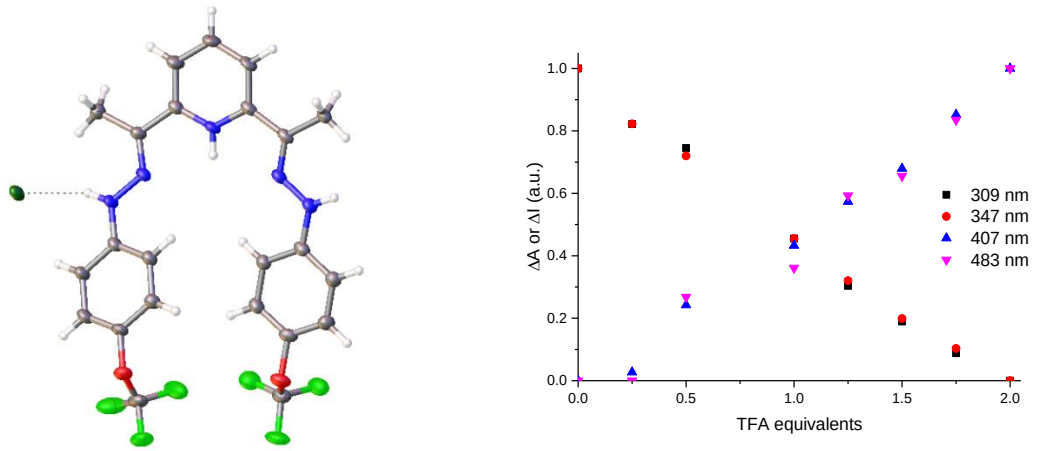

Figure 2-15 Crystal structure of protonated 2,6-diactetylpyridinebis(4-trifluoromethoxyphenylhydrazone) (left). Normalised absorption variation upon addition of TFA at 309 nm, 347 nm, 407nm and 483 nm) (right).

Compound **4** shows two absorption bands in the UV region at λ_{max}=319 nm and at λ_{max}=362 nm and a blue emission at λ_{em}=387 nm **(Figure 2-16)**. However, no significant change is observed in either absorption or emission spectra upon the addition of TFA (1.3×10^{-2} M), due to the absence of protonation event.

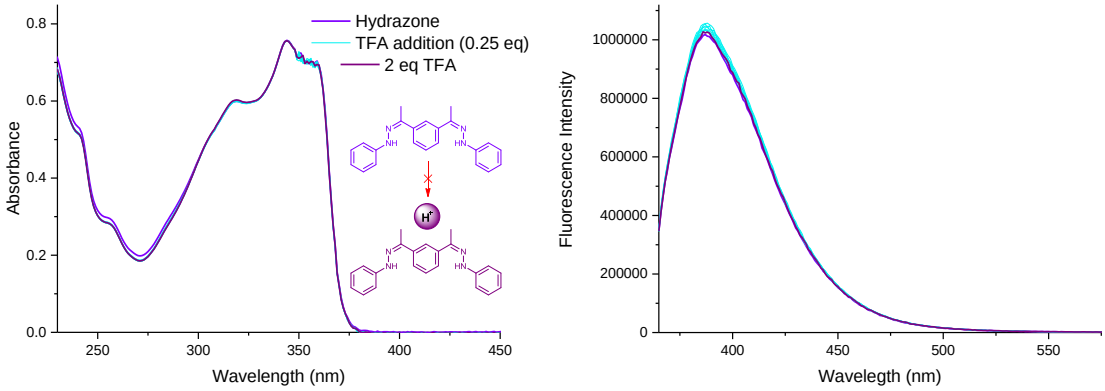

Figure 2-16 Spectrophotometric titration of compound 4 (2.8×10^{-5} M) with TFA (1.3×10^{-2} M) in EtOH (left). Emission (energy of excitation 350 nm) of compound 4 (2.8×10-5 M) in EtOH solution upon addition of TFA (1.3×10^{-2} M) (right)

2.4.3 Hydrazones Cu^{2+} and Zn^{2+} detection *via* metal complex formation

Zinc (Zn^{2+}) and copper (Cu^{2+}) are the second and third most abundant metal ions, after Fe^{2+}, in the human body[62, 63]. Both play a crucial role in the biological processes[64, 65] involved in neurological disorders such as Alzheimer's and Parkinson's[66-68]. Therefore, the potential of

hydrazones **(1-4)** for selective detection of Cu^{2+} and Zn^{2+} ions was investigated *via* UV-vis spectrophotometric titrations. An isosbestic point was observed during the titrations of **1-4** with Cu^{2+} ions strongly indicating the formation of copper-hydrazone complexes of **1-4**. However, the isosbestic points were only observed for hydrazones **1-3** upon titration with Zn^{2+} ions. The titration of **4** with Zn^{2+} ions did not lead to substantial changes in UV-vis spectrum, indicating that **4** has no sensitivity for Zn^{2+}ions.

2.4.3.1 Sensing Cu^{2+} ions *via* metal-hydrazone complex formation

A dramatic change in the absorption spectrum of hydrazone **1** in ethanol (2.3×10^{-5} M) is observed upon the titration with a solution of copper perchlorate hexahydrate (3.2×10^{-3} M) in EtOH. As shown in **Figure 2-17**, upon addition of Cu^{2+}, the peaks at λ_{max}=303 nm and λ_{max}=349 nm gradually decrease with a new peak developing at λ_{max}=447 nm. The presence of the isosbestic points indicate the formation of a metal-hydrazone complex through the coordination with the –NH and the pyridine nitrogen. This led to a drastic colour change which was clearly detectable to the naked eye.

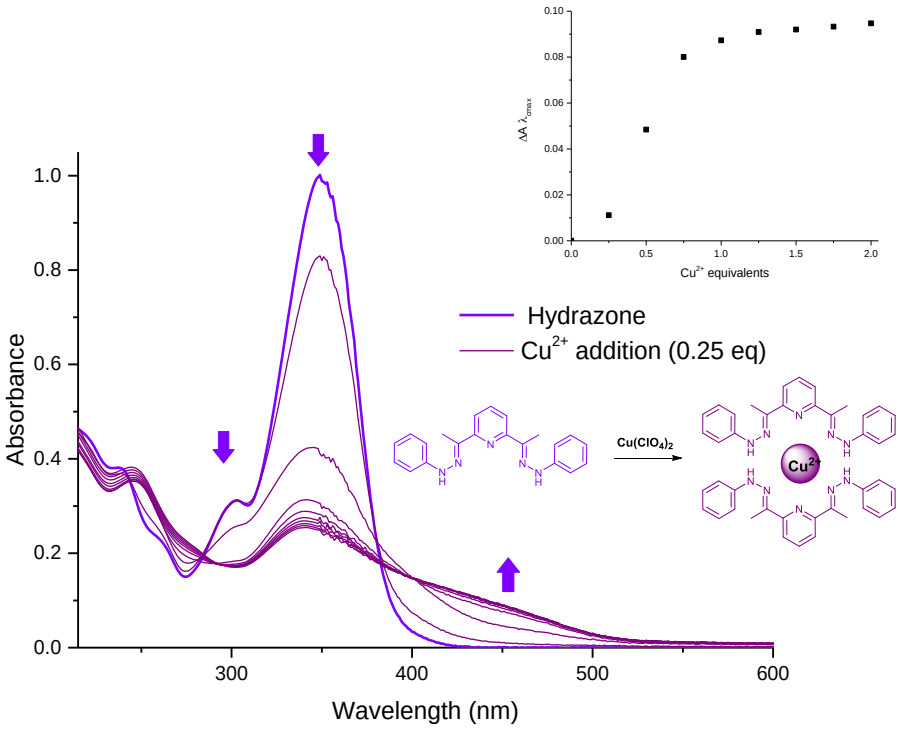

Figure 2-17 Spectrophotometric titration of compound 1 (2.3×10^{-5} M) with a solution of copper perchlorate hexahydrate (3.2×10^{-3} M, up to 2.0 equivalents) in EtOH

A dramatic change in the absorption profile of hydrazone **2** in ethanol (2.6×10^{-5} M) is observed upon the titration of the solution with a solution of copper perchlorate hexahydrate (3.2×10^{-3}

M) in EtOH. As shown in **Figure 2-18**, upon addition of Cu^{2+}, the peaks at λ_{max}=318 nm and λ_{max}=362 nm gradually decrease. Due to the presence of the shoulders at λ_{max}=451 nm and λ_{max}=530 nm prior to the addition of Cu^{2+}, the resultant spectrum became very complex. However, upon the addition of Cu^{2+} the metal complex formation is clearly evident through an abrupt intensity decrease of the absorbance of the ligand main band.

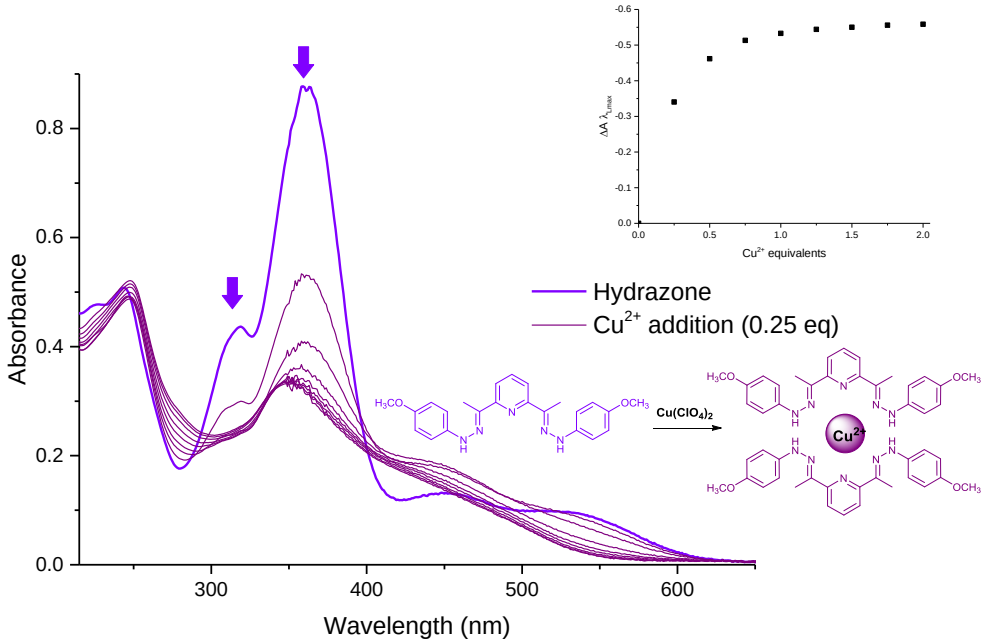

Figure 2-18 Spectrophotometric titration of compound 2 (2.6×10^{-5} M) with a solution of copper perchlorate hexahydrate (3.2×10^{-3} M, up to 2.0 equivalents) in EtOH

A significant change in the absorption spectrum of hydrazone **3** in ethanol (2.3×10^{-5} M) is detectable upon the titration with a solution of copper perchlorate hexahydrate (3.2×10^{-3} M) in EtOH. As shown in **Figure 2-19**, upon addition of Cu^{2+}, the peaks at λ_{max}=308 nm and λ_{max}=347 nm gradually decrease with a new peak emerging at λ_{max}=414 nm. The presence of the isosbestic points indicates the formation of a metal-hydrazone complex through the coordination with the –NH and the pyridine nitrogen. This was clearly detectable to the naked eye through a colour change of the solution.

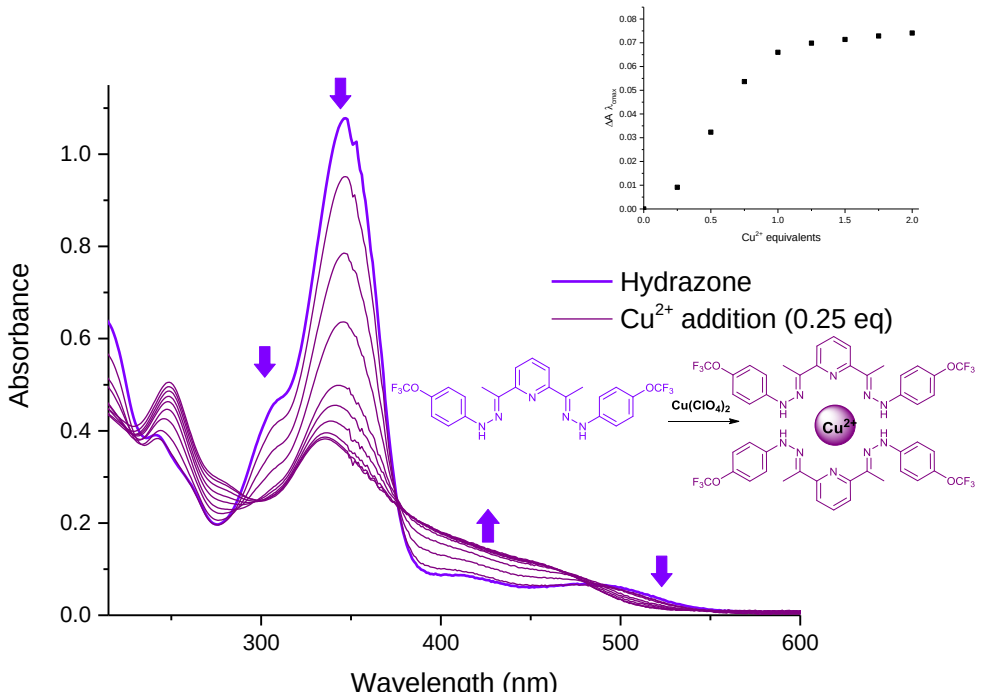

Figure 2-19 Spectrophotometric titration of compound 3 (2.3×10^{-5} M) with a solution of copper perchlorate hexahydrate (3.2×10^{-3} M, up to 2.0 equivalents) in EtOH

A dramatic change in the absorption spectrum of hydrazone **4** in ethanol (2.8×10^{-5} M) is observed upon the titration with a solution of copper perchlorate hexahydrate (3.2×10^{-3} M) in EtOH. As shown in **Figure 2-20**, upon addition of Cu^{2+}, the peaks at λ_{max}=319 nm and λ_{max}=344 nm gradually decrease with a new peak developing at λ_{max} =398 nm. The presence of the isosbestic points indicates the formation of a metal-hydrazone complex most likely through the coordination of the Cu(II) with the –NH nitrogen atoms.

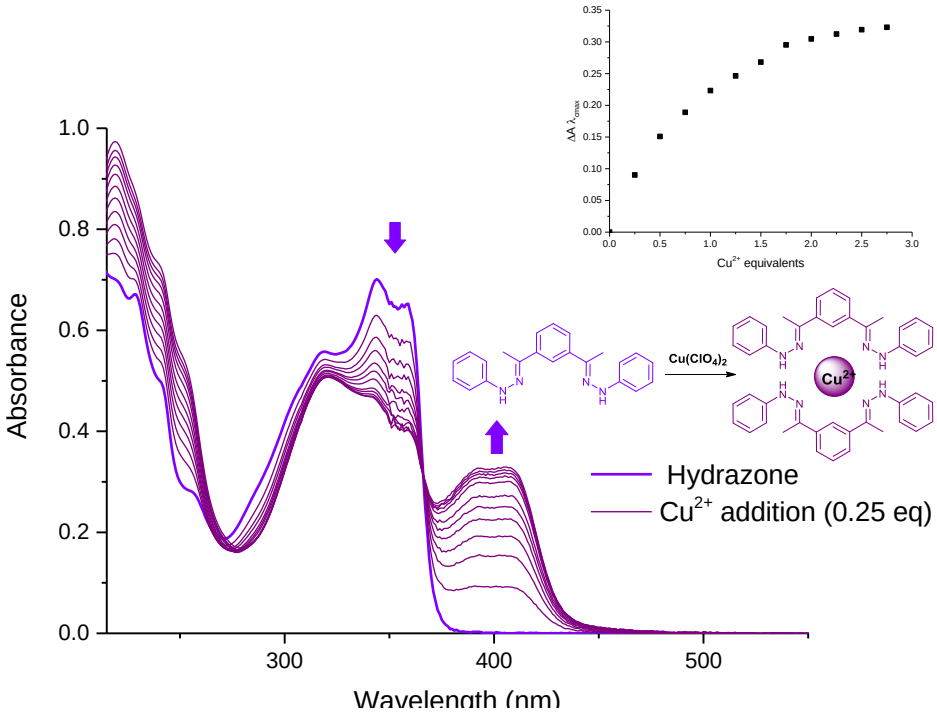

Figure 2-20 Spectrophotometric titration of compound 4 (2.8×10^{-5} M) with a solution of copper perchlorate hexahydrate (3.2×10^{-3} M, up to 3.0 equivalents) in EtOH

2.4.3.2 Sensing Zn^{2+} ions *via* metal-hydrazone complex formation

A change in the absorption spectrum of hydrazone **1** in ethanol (2.1×10^{-5} M) is observed upon the titration with a solution of zinc perchlorate hexahydrate (3.0×10^{-3} M) in EtOH. As shown in **Figure 2-20**, upon addition of Zn^{2+}, the peaks at λ_{max}=302 nm and λ_{max}=350 nm gradually decrease with a new peak emerging at λ_{max}=405 nm. The presence of the isosbestic points indicates the formation of a metal-hydrazone complex through the coordination with the –NH and the pyridine nitrogen. This was detected by the naked eye through a colour change of the solution.

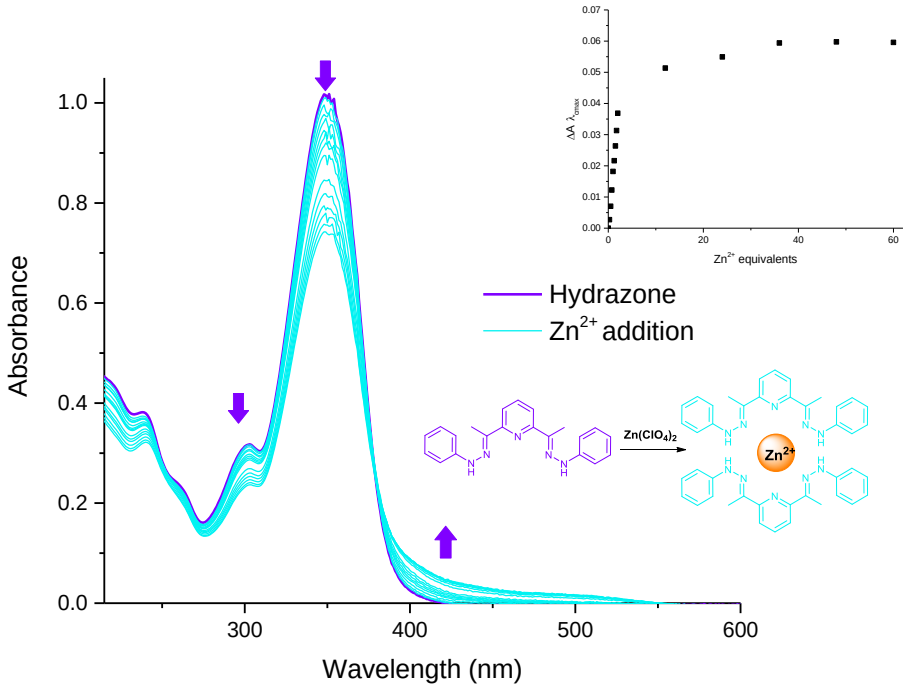

Figure 2-21 Spectrophotometric titration of compound 1 (2.1×10^{-5} M) with a solution of copper perchlorate hexahydrate (3.0×10^{-3} M, up to 60.0 equivalents) in EtOH

A change in the absorption spectrum of hydrazone **2** (1.8×10^{-5} M) is recorded upon the titration of the solution with a solution of zinc perchlorate hexahydrate (3.0×10^{-3} M) in EtOH. As shown in **Figure 2-22**, upon addition of Zn^{2+}, the peaks at λ_{max}=318 nm and λ_{max}=362 nm gradually decrease with a new peak developing at λ_{max}=422 nm. The presence of the isosbestic points confirmes the formation of a metal-hydrazone complex through the coordination with the –NH and the pyridine nitrogen. The accompanying colour change was visible to the naked eye.

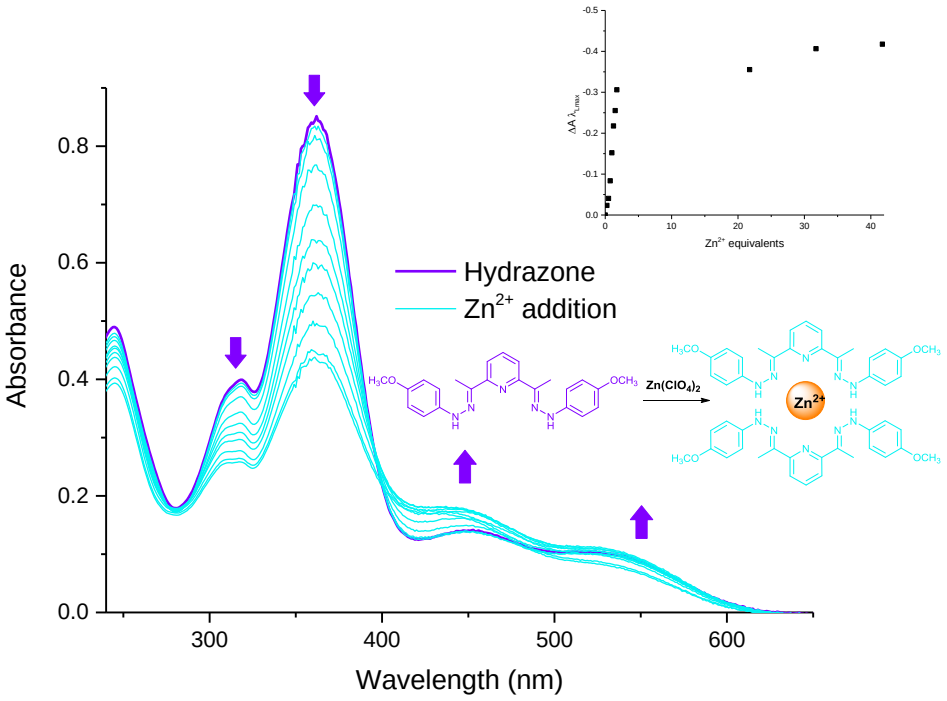

Figure 2-22 Spectrophotometric titration of compound 2 (1.8×10^{-5} M) with a solution of copper perchlorate hexahydrate (3.0×10^{-3} M, up to 41.8 equivalents) in EtOH

A change in the absorption spectrum of hydrazone **3** in ethanol (2.3×10^{-5} M) is observed upon titration with a solution of zinc perchlorate hexahydrate (3.0×10^{-3} M) in EtOH. As shown in **Figure 2-23,** upon addition of Zn^{2+}, the peaks at λ_{max}=308 nm and λ_{max}=347 nm gradually decrease with a new peak developing at λ_{max}=394 nm. The presence of the isosbestic point indicates the formation of a well-defined complex through the coordination with the –NH and the pyridine nitrogen. This led to a colour change which was detected by the naked eye.

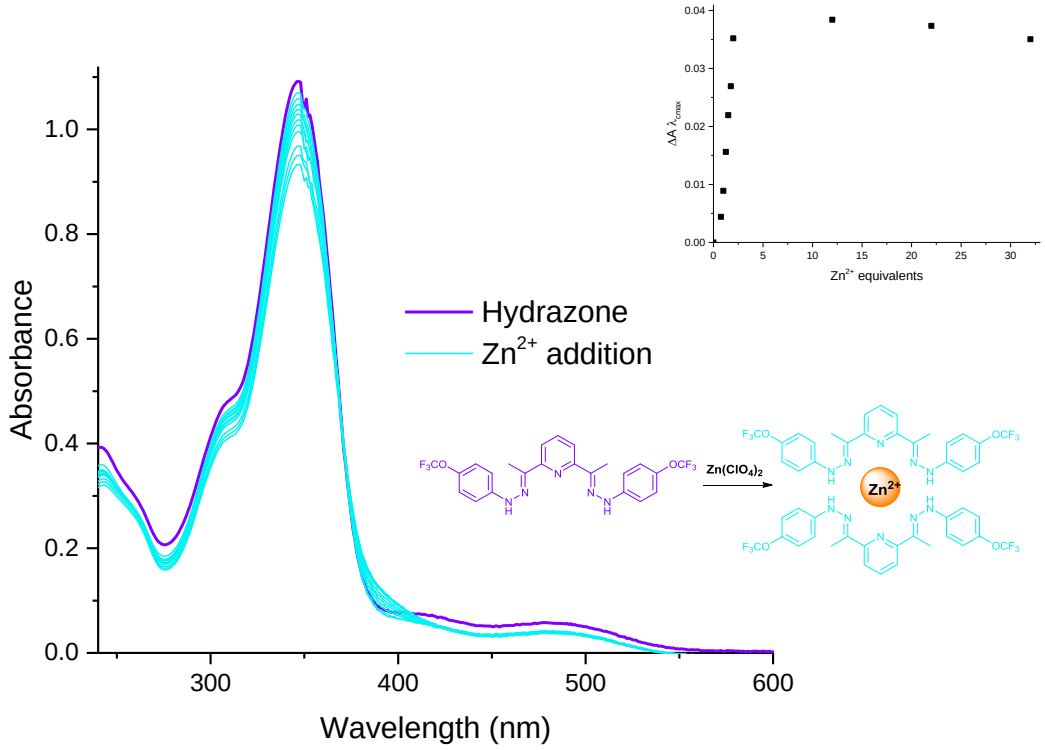

Figure 2-23 Spectrophotometric titration of compound 3 (2.3×10^{-5} M) with a solution of copper perchlorate hexahydrate (3.0×10^{-3} M, up to 41.8 equivalents) in EtOH

No significant change in the absorption spectrum of compound **4** in ethanol (2.3×10^{-5} M) is observed upon titration of the solution with a solution of zinc perchlorate hexahydrate (3.0×10^{-3} M) in EtOH, as shown in **Figure 2-24**. The minor change in the intensity of the absorption is a consequence of the dilutions.

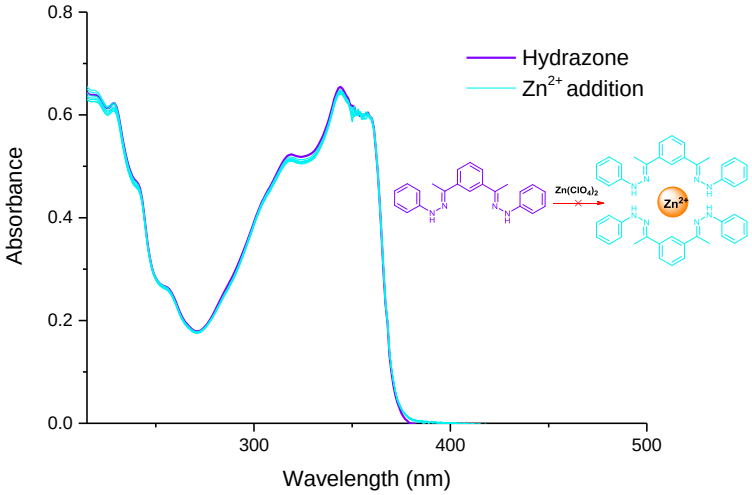

Figure 2-24 Spectrophotometric titration of compound 4 (2.3×10^{-5} M) with a solution of copper perchlorate hexahydrate (3.0×10^{-3} M, up to 2.0 equivalents) in EtOH

Figure 2-25 summarises the Cu^{2+} and Zn^{2} sensing ability of pyridine-based hydrazones **1-3** and benzene-based hydrazone **4**. All hydrazones **(1-4)** showed higher sensitivity towards Cu^{2+} ions than for the detection of Zn^{2+} ions. This is a consequence of the d^{10} electronic configuration of Zn^{2+} inhibiting MLCT electronic transitions. Comparing the sensitivity of hydrazones **1-3** for the detection of Cu^{2+} ions, hydrazone **1** showed the highest sensing ability. An increase in the steric hindrance of the phenyl group of the hydrazones resulted in a decrease in the donor strength of the ligands. In addition, the compounds **1-3** showed higher detection in comparison to compound **4**, most likely due to the coordination with the metal atom through the nitrogen atom of the pyridine bridging unit.

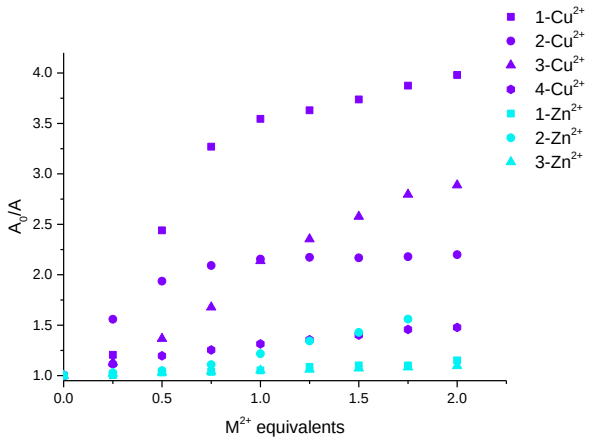

Figure 2-25 Comparison of the spectral changes during the titration of hydrazones 1-4 with a solution of Cu^{2+} and Zn^{2+} (0-2 equivalents)

2.5 Conclusion

In conclusion, four 2,6-diacetylbis(phenylhydrazone) derivatives were successfully synthesised. Factors which make them interesting examples include: relatively easy synthesis (yields up to 93%), good solubility in organic solvents, easy purification process, stability, tendency toward crystallinity and the use of relatively cheap precursors. In addition, simple structural modifications allowed the tuning of the photophysical properties.

The impact of structural modification to hydrazones **1-4** on their photophysical properties was studied. Analysis of hydrazones **1-4** in different solvents revealed a solvatochromic effect for the phenyl-substituted hydrazones. Here, hydrazones **2** and **3** showed a larger solvatochromic shift with solvents of a lower polarity. The photoluminescence properties were also analysed, but only hydrazone **4** was an efficient emitter (Φ =38%).

UV-Vis spectrophotometric titrations of hydrazones **1-4** were conducted to explore their sensing behaviour towards cationic species. Pyridine-based hydrazones **1-3** showed substantial changes upon addition of TFA. A replacement of pyridine by a benzene central unit in hydrazone **4** resulted in no response to changes in pH solution. This highlighted that the signal recognition motif, in response to pH, was localised on the pyridine unit. Protonation of the pyridine unit was also confirmed by X-ray analysis. In addition, the reversibility of the protonation process for hydrazones **1-3** was successfully demonstrated using TBAF.

The Cu^{2+} and Zn^{2+} sensing behaviour of the hydrazones **1-4** was also investigated *via* UV-vis spectroscopy. The results demonstrate that despite an apparent similarity in ion size and the

chemical properties of Cu^{2+} and Zn^{2} ions, their mode of interaction with the hydrazones **1-4** was substantially different . The hydrazones **1-4** were more sensitive for the detection of Cu^{2+} than for the detection of Zn^{2+} .

In addition, the colour changes can be clearly observed by the naked eye providing a convenient and reliable sensing strategy for pH, Cu^{2+} and Zn^{2} ion detection as biomarkers for early detection of incipient diseases. The cations sensing can potentially be used to unmask homeostatic failure in absence of pathological conditions[69].

2.6 Experimental

2.6.1 General techniques

All chemicals were obtained from Sigma Aldrich, Alfa Aesar, VWR and Across and used without further purification. Anhydrous solvents were obtained from a PureSolv MD6 solvent purification system. ^{1}H NMR and ^{13}C NMR spectra were recorded on a Bruker Advanced 500 spectrometer. Chemical shifts (δ) are reported in parts per million (ppm) relative to the residual solvent peak and peaks are described as singlet (s), doublet (d), triplet (t), quartet (q), sextet (sex), multiplet (m), broad singlet (br) and coupling constants (J) are quoted in Hertz (Hz). Spectra were recorded in chloroform-d, dichloromethane-d_2 or deuterated DMSO-d_6 and were measured at room temperature unless otherwise stated. Where needed, two dimensional correlation spectroscopy (2D-COSY), heteronuclear single quantum coherence spectroscopy (HSQC) and heteronuclear multiple bond correlation spectroscopy (HMBC) were used in order to aid assignment. The progress of reactions was monitored by TLC and purified by column chromatography using silica gel 60 (40-63μm). High resolution mass spectrometry (HRMS) was performed on Bruker MaXis Impact (EI+) by positive and negative electrospray ionisation. The accepted experimental error was <4 ppm. High performance liquid chromatography (HPLC) was performed on an Agilent 1100 Infinity Series equipped with a UV detector and Ascentis Express C_{18} reverse phase column, using MeCN/water (50-95%) containing 0.1% TFA, at a flow rate of 0.5 mL min^{-1} over a period of 12 minutes. Infrared spectra (IR) were recorded in solid phase on a Bruker Alpha Platinum ATR FTIR spectrometer with vibrational frequencies given in cm^{-1}. Melting points were measured on a Stuart SMP30. The electronic absorption spectra were recorded on a Cary 100 UV-vis scanning spectrometer. The fluorescence spectra were recorded on a FluoroMax-3 spectrofluorimeter. Quantum yields of fluorescence were measured by the relative method using optically dilute solutions.

2.6.2 Experiments

2.6.2.1 2,6-Diactetylpyridine-bis(phenylhydrazone) (1)[42]

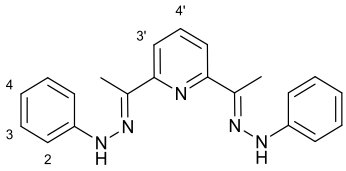

A solution of 2,6-diacetylpyridine (915 mg, 5.6 mmol) and phenylhydrazine (1.10 mL, 11.2 mmol) in dry EtOH (10 mL) was refluxed for 45 min. The reaction mixture was cooled to room temperature. The resulting white powder was collected by suction filtration, washed with cold ethanol and dried under vacuum to yield compound **1** as a pale yellow-white solid (1.66 g, 86%). **^{1}H NMR** (500 MHz, C_2D_6O) δ ppm 9.49 (s, 2H, NH), 8.01 (d, *J* = 7.9 Hz, 2H, 3'-H), 7.76 (t, *J* = 7.9 Hz, 1H, 4'-H), 7.33 (dd, *J* = 7.9, 1.2 Hz, 4H, 2-H), 7.26 (t, *J* = 7.9 Hz, 4H, 3-H), 6.81 (tt, *J* = 7.9, 1.2 Hz, 2H, 4-H), 2.45 (s, 6H, CH_3). **^{13}C NMR** (125 MHz, C_2D_6O) δ ppm 154.9, 145.6, 141.5, 136.2, 128.9, 119.3, 117.4, 113.0, 11.0; **m/z (ES+):** Found: 366.1692 [M+Na], requires: 366.1689; **IR ν_{max}/cm^{-1} (solid):** 3341, 3012, 2927, 1600, 1561, 1245, 1162, 1139, 746, 693; **M.pt:** 218-220.5 °C.

2.6.2.2 2,6-Diactetylpyridine-bis(4-methoxyphenylhydrazone) (2)

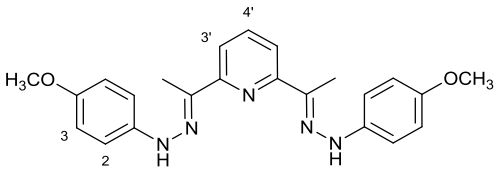

The same procedure as described for compound **1** was followed using 4-methoxyphenylhydrazine hydrochloride (664 mg, 3.8 mmol) and 2,6-diacetylpyridine (310 mg, 1.9 mmol). Compound **2** was isolated as a dark purple solid (785 mg, 73%). **^{1}H NMR** (400 MHz, $CDCl_3$ + EtOH) δ ppm 11.14 (s, 2H, NH), 7.80 (t, *J* = 8.1 Hz, 1H, 4'-H), 7.39 (d, *J* = 9.0 Hz, 4H, 3-H), 7.02 (d, *J* = 8.1 Hz, 2H, 3'-H), 6.43 (d, *J* = 9.0 Hz, 4H, 2-H), 3.66 (s, 6H, OCH_3), 2.38 (s, 6H, CH_3); **^{13}C NMR** (125 MHz, C_2D_6O) δ ppm 154.2, 138.0, 118.9, 115.4, 114.5, 55.2, 11.6; **m/z (ES+):** Found: 426.1905 [M+Na], requires: 426.1900; **IR ν_{max}/cm^{-1} (solid):** 3393, 3187, 2994, 2831, 1502, 1412, 1270, 1231, 816; **M.pt:** 178-181 °C.

2.6.2.3 2,6-Diactetylpyridine-bis(4-trifluoromethoxyphenylhydrazone) (3)

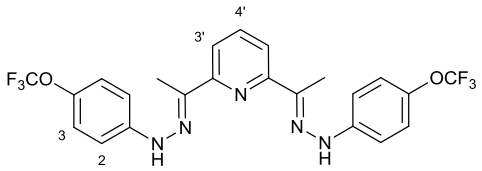

The same procedure as described for compound **1** was followed using 4-trifluoromethoxyphenylhydrazine hydrochloride (2.29 g, 10.0 mmol) and 2,6-diacetylpyridine (816 mg, 5.0 mmol). Compound **3** was isolated by gravity filtration as a bright orange solid (2.40 g, 93%). **^{1}H NMR** (500 MHz, MeOD) δ ppm 8.49 (t, *J* = 8.1 Hz, 1H, 4'-H), 8.01 (d, *J* = 8.1 Hz, 2H, 3'-H), 7.60 – 7.27 (m, 4H, 3-H), 7.06 (d, *J* = 9.0 Hz, 4H, 2-H), 2.44 (s, 6H, CH_3); **^{13}C NMR** (125 MHz, MeOD) δ ppm 149.1, 148.4, 145.2, 144.1, 132.6, 123.5, 122.0 (q, J_{F-C} = 254.9 Hz),121.8, 116.6, 11.5; **m/z (ES+):** Found: 534.1333 [M+Na], requires: 534.1335; **IR ν_{max}/cm^{-1} (solid):** 3150, 3073, 2955, 2906, 1540, 1504, 1439, 1248, 1193, 1159, 1142, 844; **M.pt:** 271.3-272.8 °C.

2.6.2.4 1,3-Diactetylbenzene-bis(phenylhydrazone) (4)

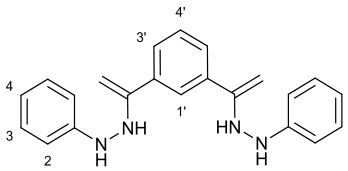

The same procedure as described for compound **1** was followed using phenylhydrazine hydrochloride (0.84 mL, 8.5 mmol) and 1,3-diacetylbenzene (460 mg, 2.8 mmol). Compound **4** was isolated as a gold solid (666 mg, 69%). **^{1}H NMR** (300 MHz, C_2D_6O + EtOH) δ ppm 9.92 (s, 2H, Ph), 7.76 (dd, *J* = 8.9, 6.7 Hz, 1H, 4'-H), 7.70 – 7.62 (m, 2H, 3'-H), 7.52 (s, 2H, Ph), 7.44 (d, *J* = 8.8 Hz, 2H, Ph), 7.26 (s, 2H, Ph), 7.13 (dd, *J* = 8.8, 1.4 Hz, 2H, Ph), 7.05 (d, *J* = 1.4 Hz, 2H, Ph), 4.82 (s, 4H, CH_2); **^{13}C NMR** (100 MHz, EtOH + C_2D_6O) δ ppm 149.5, 143.6, 143.5, 138.4, 137.6, 135.0, 129.3, 122.0, 120.0, 118.9, 117.5, 113.7, 112.1, 101.5, 31.1; **m/z (ES+):** Found: 343.4060 [M+H], requires: 343.4460; **IR ν_{max}/cm^{-1} (solid): M.pt:** 229-231 °C.

Chapter 3 Synthesis and Characterisation of Bis(indolyl)derivatives

The following chapter covers the synthesis of four novel bis(indolyl)derivatives and a comprehensive and detailed study of their photophysical properties. The synthetic routes have been designed to understand the substrate reactivity and to evaluate their synthetic applicability. In order to improve the applicability of the bis(indolyl)derivatives, it is very important to understand the driving factors that allow tuning of photophysical properties and therefore, the effectiveness and applicability of those materials. Three interesting examples for tuning of the photophysical properties of these compounds, two of which successful, are:

1. The effect of increasing the electronic delocalisation along the backbone of the molecules.

2. The effect of different substituents.

3. The unsuccessful strategy of using the bis(indolyl)derivatives as chelating agents.

3.1 Indole

Indole is ubiquitous and one of the most abundant heterocyclic structures in nature**.** It was isolated for the first time by Baeyer from the treatment of indigo **(S.7)** with oleum[70]. Since the 1950s its importance has grown impressively because it and its derivatives are part of biologically significant compounds. For example, tryptophan **(S.8)** which is an essential amino acid and a constituent of most proteins. Serotonin **(S.9)**[71], a vasoconstrictor that plays a part in conducting impulses to the brain and cardiovascular function. Complex alkaloids are clinically used anticancer agents[72] (cause the inhibition of mitosis or cell division), vinblastine **(S.10)**[73] isolated from *Catharanthus roseus*, is particularly interesting as it contains both an indole and an indoline motif and *Cypridina luciferin* **(S.11)**[74] which is an indole-based substrate responsible for the biluminiscence produced by ostracod crustaceans. It participates in the luminescent enzyme system “luciferin-luciferase”.

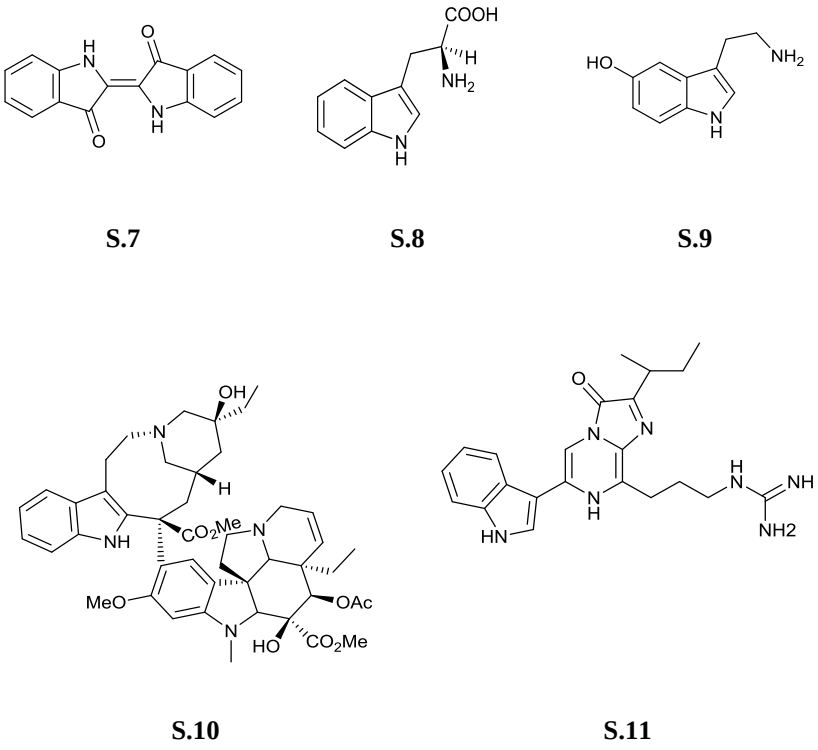

Figure 3-1 Naturally occurring indole-containing products

3.2 Indole synthesis

Due to a wide range of biological and medicinal applications, such as chemosensors[75, 76], regulators of neurological and physiological functions[77], anticancer agents[72, 78] and antidiabetic drugs[79] (applications developed most recently), the synthesis of indoles and its derivatives have been well-established[80, 81]. Many of these synthetic approaches involve the annulation of a five member ring to an existing (functionalised) benzene ring. With a few exceptions such as those proceeding through the pyrrole[82] functionalization or methods in which both rings are formed simultaneously[83]. There are four bonds in the five-membered indole ring. Synthesis of indoles are often named and classified[84] dependent on the last bond formed, this is shown in the **Figure 3-2.**

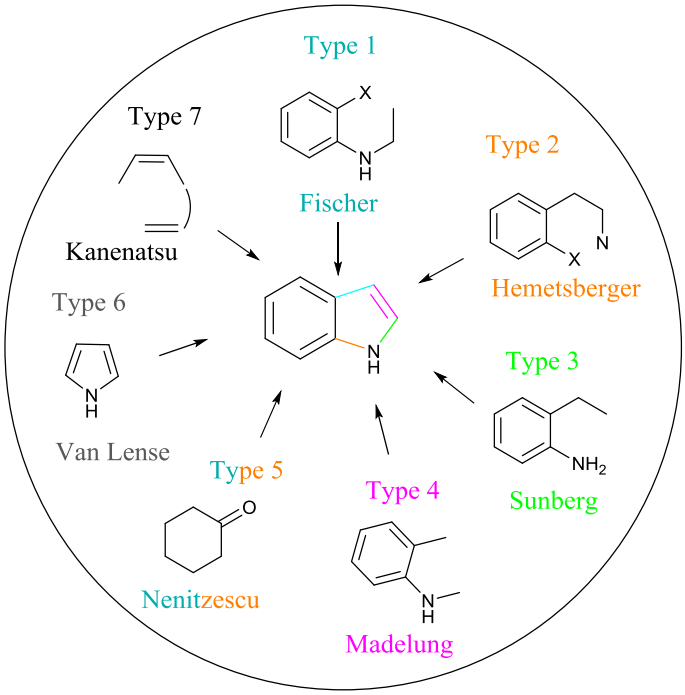

Figure 3-2 Types of indole synthesis, classified by the last bond formed (showing an example)

Type 1 and 2 involve bond formation to an aromatic carbon (occupied only by H) or functionalised. Type 3 has a C-N bond formation, type 4 involves a C-C bond formation and type 5 involves generation of the benzene ring from an existing cyclohexane. As previously mentioned, not all of the indoles are formed from a functionalised benzene ring. Type 6 takes place through pyrrole[85] and type 7 through the construction of both rings.

3.2.1 Fischer indole synthesis

First reported in 1883[43], the Fischer indole reaction is still the most versatile, efficient and highly used method for the synthesis of indole intermediates. In many cases the reaction of a substituted phenylhydrazine with an aldehyde or ketone leads to the phenylhydrazone, which undergoes cyclic [3,3]-sigmatropic rearrangement under acid catalysis which allows the NH_3 elimination leading to the desired indole **(Scheme 3.1)**[86].

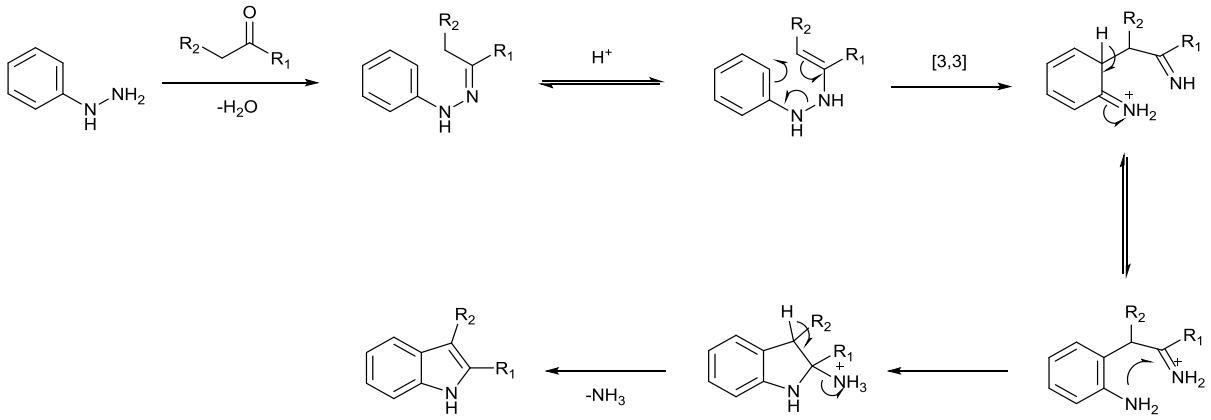

Scheme 3.1 Accepted mechanism for the Fischer indole synthesis

This reaction meets all the requirements of a modern indole synthesis in its convenience and simplicity. Allowing the attachment of different substituents at the C-2 and C-3 positions and on the aromatic ring, by using different ketones or aldehydes and substituted hydrazine derivatives. This also includes a relative tolerance to a wide range of compatible functional groups at the aromatic ring allowing direct formation of substituted indoles without the need for further modifications.

The main drawback is a limited number of commercially available aryl hydrazines and their toxicity[87, 88]. Mono- and unsubstituted hydrazines are readily available; however, the ring closure leading to the final indole can occur at two different positions resulting in the formation of regioisomers. This does not apply when symmetrical or *ortho*-substituted hydrazines are used.

3.2.1.1 Precursors for Fischer indole synthesis

Traditionally, hydrazines have been made by diazotisation of the corresponding aniline and reduction of the diazonium salt, or by reduction of the N-nitroso derivative as shown in **Scheme** 3.2[89]. However, the explosive hazards associated with the isolation of solid diazonium salts and the introduction of toxic elements by the reduction of the N-nitroso derivative, results in these methodologies not being ideal. Therefore, a safer and more reliable alternative to convert aryldiazonium salts into hydrazines has been found by using either elemental tin or tin(II) chloride in acidic media, or ascorbic acid[90, 91], a metal-free reductant. This procedure has been applied to the synthesis of eletriptan **(Scheme 3.3).**

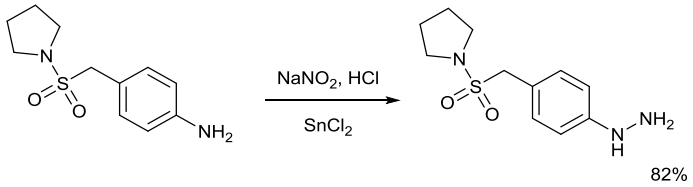

Scheme 3.2 Aryl hydrazines from reduction of N-nitrosoanilines

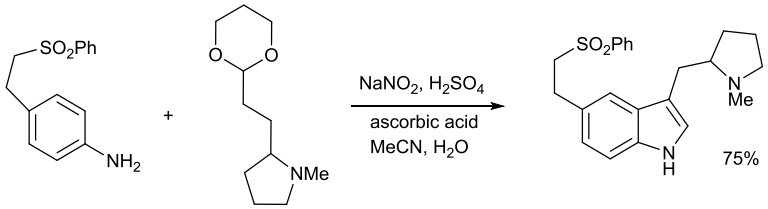

Scheme 3.3 Reduction of aryldiazonium salts with ascorbic acid, and Fischer indolisation of eletriptan[92] (use to treat migraines)

Use of the Japp-Klingemann reaction, involves the reaction of a diazonium salt with a β-ketoester under basic conditions **(Scheme 3.4).** First reported in 1887[93], it directly leads to hydrazones *via* the reaction. The scope of this procedure is currently limited to 2-substituted indoles only.

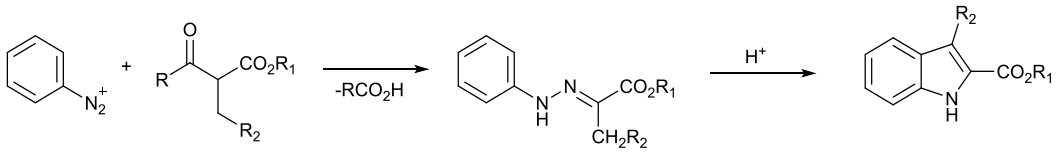

Scheme 3.4. The Japp-Kinglemann variation on the Fischer indole synthesis

An alternative approach to multi-substituted indoles, avoiding the need to isolate any intermediate, was reported by Buchwald *et al*.[94] and Hartwig **(Scheme 3.5).** The palladium-catalysed cross coupling reaction of aryl halides with hydrazine derivatives produces N-arylbenzophenone hydrazones, followed by its hydrolysis with enolisable ketones and subsequent Fischer indolisation.

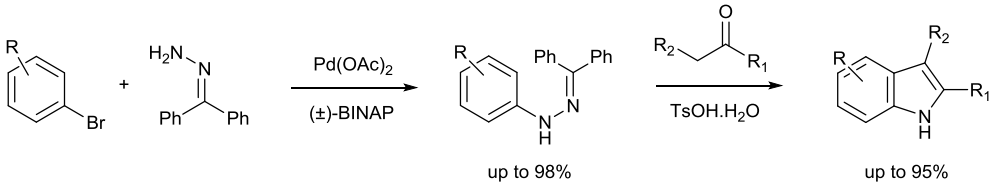

Scheme 3.5 Buchwald-Hartwig Pd-catalyzed arylation of benzophenone hydrazine in indole synthesis

3.2.1.2 Relevance of the acid choice for indole catalysis

The choice of acid catalyst is very important. Brønsted acids such as HCl, H_2SO_4, polyphosphoric acid and p-toluenesulfonic acid (p-TSA) have been used successfully. Lewis acids such as boron trifluoride, zinc chloride, iron chloride and aluminium chloride are also used as catalysts. The use of thionyl chloride was also explored for the synthesis of 3-(N-acylamino)-2-phenylindoles[95].

The importance of the acid-catalysts has been demonstrated for methoxy phenylhydrazines[96]. For instance, in the presence of catalytic amounts of $ZnCl_2$, an unexpected substitution between the methoxy group and chlorine takes place. Migration of the methoxy group has been observed in the presence of BF_3. In the presence of HCl, the expected product is only generated in very low yield along with other by-products ***(*Scheme 3.6)***[97].

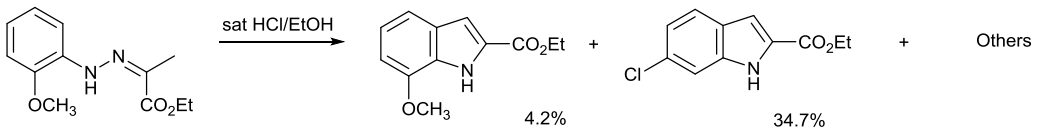

Scheme 3.6 Intent to synthesize 7-methoxy-2-propionyl-1H-indole

In recent years, alternative catalysts such as 2,4,6-trichloro-1,2,5-triazine (TCT) **(Scheme 3.7)**[98], rhodium complexes **(Scheme 3.8)**[99] or photoredox Pd-catalysed visible light[100] for C-H activation were developed for the synthesis of indoles.

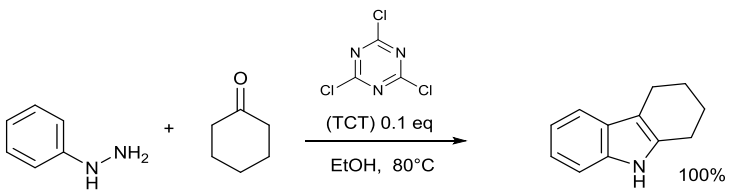

Scheme 3.7 Reaction of phenylhydrazine with cyclohexanone in the presence of TCT

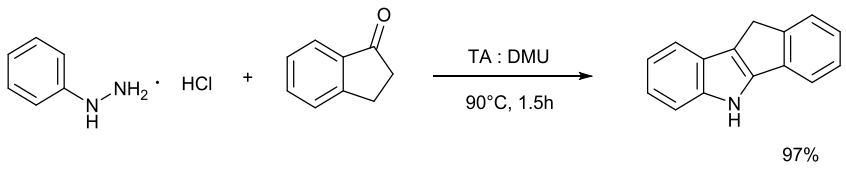

Scheme 3.8 Solvent free Fischer indole synthesis using low melting mixtures

Low melting L-(+)-tartaric acid-dimethyl urea mixture appears to be an alternative for the use of a solvent in Fischer synthesis. The melt plays the dual role of solvent as well as catalyst[101]. This reaction is an example of a redox neutral strategy for metal-catalysed C-H activation that has been developed in recent years[102-104]. The hydrazine generated acts as a directing group for regioselective insertion. At the same time, the hydrazine is acting as an internal oxidant for the regeneration of the catalyst for the next catalytic cycle without using an external oxidant (as commonly happens with metal-catalysed reactions) [94].

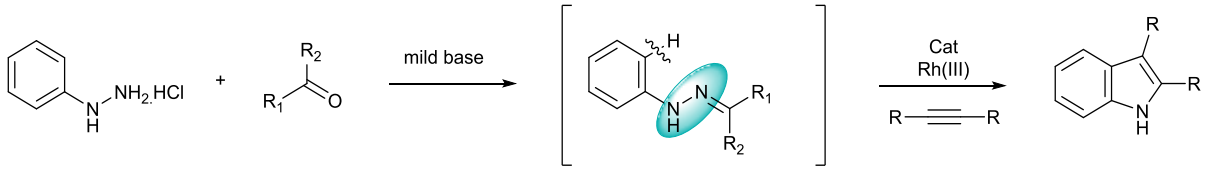

Scheme 3.9 Synthesis of indoles via Rhodium-Catalysed C-H activation directed by an in-situ generated redox-neutral group

3.3 Typical reactivity of indoles: C-2 *vs* C-3 position

Indoles are electron rich molecules and their chemistry is dominated by electrophilic substitution. There is a strong preference for electrophilic substitution in the five-membered ring, which is ~10^{13} times more reactive than benzene[105]. The attack at the nitrogen would destroy the aromaticity of the pyrrole ring hence there are two other remaining alternatives. The resonance structure A is favoured and explains the preference for the C-3 position due to the retention of benzenoid character of the bicycle, while B has perturbed this system **(Scheme** 3.10**)**. However electrophilic substitution can occur at C-2 if, for instance, the C-3 position is occupied by a substituent *via* attack at the C-3 position and rearrangement of 3,3-disubstituted indoles to 2,3-disubstituted indoles[82].

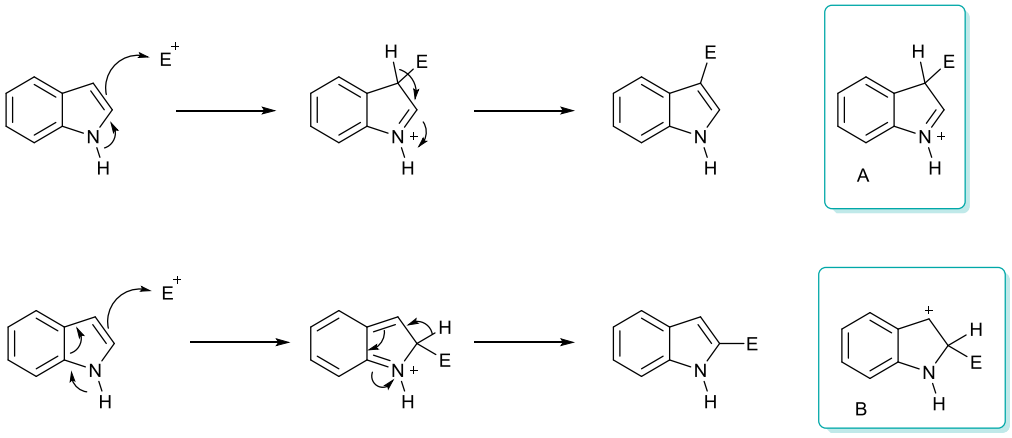

Scheme 3.10 Reactivity of indole

Terrier *et al*. have shown the effect of different substituents at the C-5 position of indole. The reactivity of these indoles upon 4,6-dinitrobenzofuroxan (DNBF), a neutral "superelectrophilic" heteroaromatic compound, increases with the indole basicity as shown in **Figure 3-3**. In addition, their studies have shown that the presence of a methyl group in the position adjacent to the electrophilic attack reduces the DNBF addition efficiency. This reduction in efficiency is attributed to a steric hindrance[105, 106].

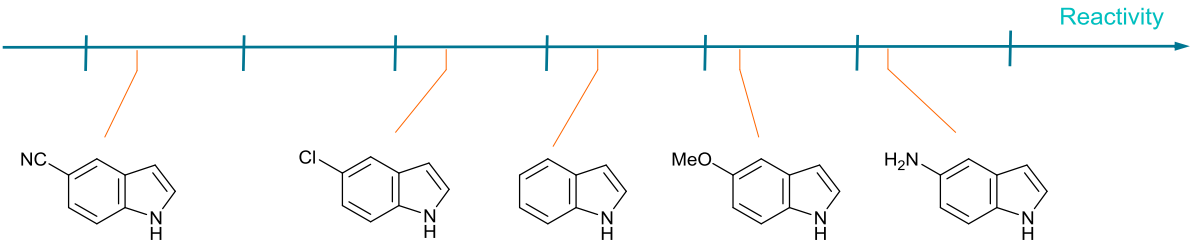

Figure 3-3 The reactivity ranking of some indoles

3.4 Functionalisation of indoles

3.4.1 Halogenation of indoles

The presence of functionalities is a requirement for metal catalysed cross-coupling reactions. Therefore, halogenated indoles are convenient intermediates that can undergo transmetalation or/and cross-coupling transformations.

The literature states different opinions regarding the halogenation of indoles. Two of the most controversial are remarked here; Sundberg says "*Halogenation follows the normal pattern of electrophilic substitution*" [107] whereas Li *et al*. say "*Synthesis of halogenated indoles is rare and difficult*"[108].

If the first statement published by researchers is correct and universal, then halogenation follows a traditional pattern of electrophilic substitution. The C-3 position is generally the preferred site of attack. If it is blocked, substitution occurs at the C-2 position. Therefore, halogenation of indoles could be done by one of the oldest reactions know in organic chemistry, electrophilic aromatic halogenation as a straight-forward step. However, additional factors such as electron-withdrawing or donating substituents may exercise directing influences[48].

There are other examples that are more in agreement with the second statement. In the presence of a strong electron withdrawing substituent at the C-3 position, substitution takes place in the benzene ring at the C-5 or C-6 position[107, 109]. Also, the presence of substituents in the six or five-membered ring along with the N-substituent decreases the chemo- and regioselectivity of halogenation in the indole[110]. Finally, an increased interest to this subject of regioselective halogenation over the past years shows the revalidation of the second statement over the first one[111].

Selective bromination of 3-bromoindole can be achieved by treating the indole with *n*-butyllithium, followed by the addition of trimethyltin chloride (Me_3SnCl) and titration with elemental bromine **Scheme 3.11**.

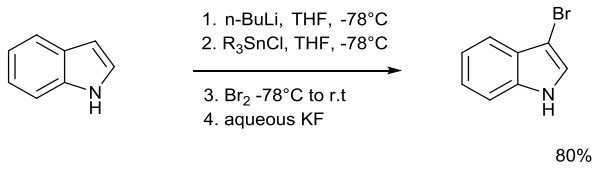

Scheme 3.11 Selective C-3 bromination of indole via metal-halogen exchange

Recent developments identified an efficient and inexpensive oxidative bromination and iodination protocol for arenes and heteroarenes, which can be used in kilogram-scale, reporting yields over 95%[112]. This mild oxidative system avoids the use of X_2 which are hazardous, toxic and corrosive[103], by using hydrogen halides which are readily available, easy to store and transport and inexpensive. Over the years, oxidative halogenation procedures[113, 114] have involved *in situ* formation of halogenating reagents, which requires the use of oxidants such as selectfluor, hydrogen peroxides, persulfates, *etc*. However, the generation and use *in situ* of the halogenating reagents has a number of limitations including limited substrate scope, potential explosiveness and limitation in heteroarenes. These drawbacks make reagents including N-halosuccinimides[115] and halogens[77, 116, 117], the most commonly used. However, reaction conditions using some of these reagents require highly acidic or basic media which have several

disadvantages including poor selectivity, multiple halogenation and narrow functional tolerance.

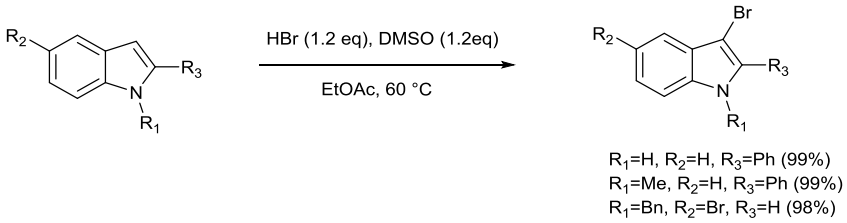

Scheme 3.12 Bromination using hydrogen halides

C-2 Functionalised indoles are a common moiety used for the synthesis of anticancer agents[118-120], compounds applied in fluorogenic probes[121, 122] or treatment of Parkinson's and depression[123]. This is why the introduction of a halogen at the C-2 position is very interesting in the synthesis of the target molecules. However, halogenation of substituted indoles at this position is rare and difficult[108] and remains a challenge. Sensitivity of 2-haloindoles and acid-catalysed hydrolysis of these compounds has been well documented[124, 125]. Also, the unpredictable reactivity depends strongly on the nature of the substituents in the indole.

A methodology for the synthesis of 2-halogenated indoles was first published by Bergman[126] making use of Katritzky[127] indole C-2 lithiation protocol. Carbon dioxide is used as an activating and easy N-removable protecting group. Despite a variety of electrophiles used, Bergman *et al* were the pioneers reporting the use of this as a halogenating reagent. Nowadays, the Bergman strategy is still in use[128].

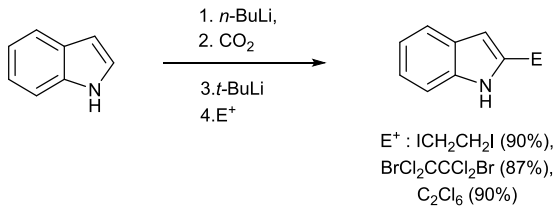

Scheme 3.13 Synthesis of 2-halogenated indoles

Cyclisation of *gem*-Dihaloofin[129]has attracted a lot of interest as an alternative to functionalise 2-bromo/chloro indole cores due to their high reactivity and easy availability[130]. In order to promote intramolecular cyclisation, different reagents such as Pd(0) and P(*t*Bu)$_3$ as ligand[131], Cs_2CO_3[108]or TBAF in THF[132] using microwave irradiation have been used as a catalyst **(Scheme 3.14)**.

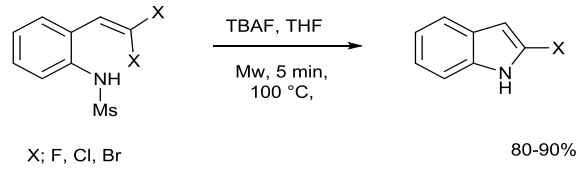

Scheme 3.14 Synthesis of 2-halogenated indoles using gem-Dihaloolefin in the presence of TBAF (metal free condition) to promote intramolecular cyclisation

Halogen functionalisation is still one of the most important key reactions, which continues to develop. Yeung *et al.*[133] reported a new type of bromination of sensitive lactones using indole as a catalyst. The reaction shown in **Scheme 3.15** is an example used to establish the electrophilicity of the intermediate-indole as a Br source.

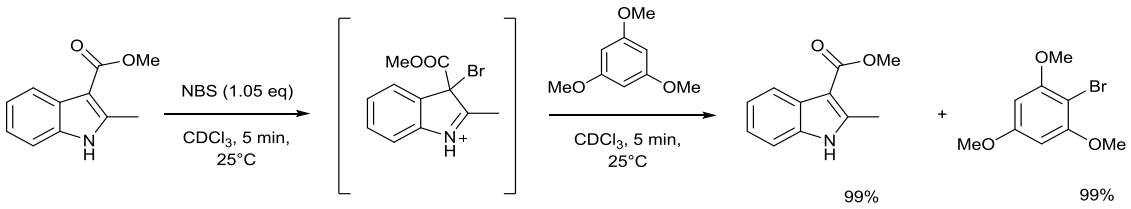

Scheme 3.15 Bromination of 1,3,5-trimethoxybenzene

3.4.2 Friedel-Crafts and Vilsmeier formylation reactions

Although the Friedel-Crafts reaction is one of the most important C-C bond forming reactions in organic chemistry, the synthesis of 3-acylindoles is often complicated by the competitive substitution at nitrogen. Acylation using acetic anhydride in acetic acid leads mainly to 1,3-diacetylindole. However, Gribble *et al.* were able to perform the regioselective acylation of N-protected indoles[134]. This acylation can even be used on indoles bearing an electron-withdrawing group at the C-2 position[135], although the yield is not as high as in the presence of an electron-withdrawing substituent **(Scheme 3.16).**

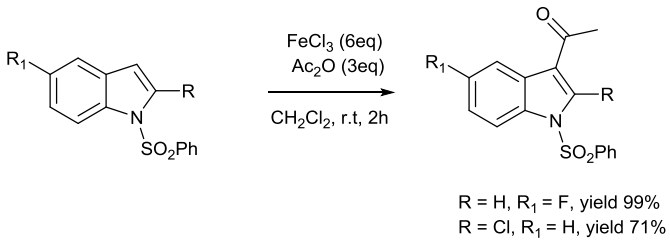

Scheme 3.16 C-3 Acylation of 5-fluoro-1-(phenylsulfonyl) indole and 2-chloro-1-(phenylsulfonyl) indole

These methods often suffer from side-reactions such as double acylation or polymerisation of indoles. There are many modified methods. For example, 1,5-diazabicyclo[4.3.0]non-5-ene has been used for regioselective organocatalytic C-3 acylation of N-protected indoles. However, acylation is influenced by substituents at the benzene ring **Scheme 3.17**.

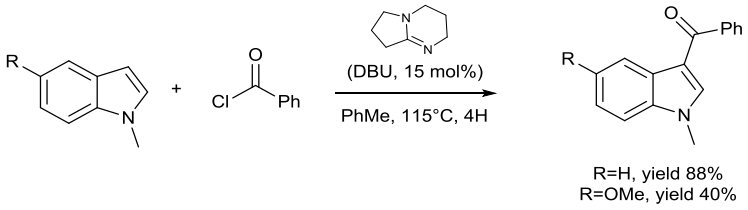

Scheme 3.17 C-3 Acylation of 5-substituted-N-protected indoles

Synthesis of a bridged indole-based dye *via* Friedel-Crafts alkylation[136, 137] employs sodium triphenylphosphine-*m*-sulfonate [133] which can be recovered (by precipitation) and re-used without a loss in its catalytic activity.

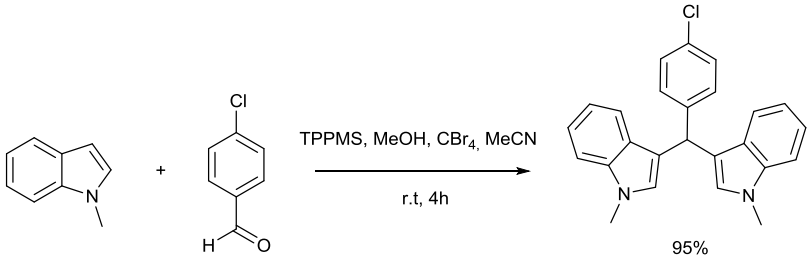

Scheme 3.18 Synthesis of 3,3'-(2-phenylethane-1,1-diyl)bis(1-methyl-1H-indole) *via* double C-3 alkylation of 1-methylindole[138]

Vilsmeier reaction can be an alternative to the Friedel-Crafts method, which generally requires a stoichiometric amount of Lewis acids or Brønsted acid, for the addition of carbonyl functionality at the C-3 position[139].

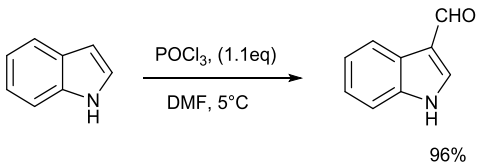

Scheme 3.19 Vilsmeier formylation of indole

3.4.3 Selective functionalization of indoles *via* metalation

Metalated indoles are extremely useful intermediates and they can be metalated at any position, by the use of direct *ortho* metalation or by halogen-metal exchange. Protection of the indole nitrogen plays a pivotal role in the reactivity of the indole.

The most widely used lithiating agents are alkyllithium or lithium amides. *n*-Butyllithium is a commonly used reagent, however, when stonger reagents are required *t*-butyllithium or *s*-butyllithium can be employed. As an alternative to RLi reagents, LDA is tolerable to many functional groups. It also has a greater selectivity for proton abstraction *vs* nucleophilic addition. Lithiating agents with varied steric hindrance, basicity and the potential for asymmetric deprotonations have been employed, for example, isopropylcyclohexylamide, dicyclohexylamide, bistrimethylsilylamide (LiHMDS), 2,2,6,6-tetramethylpiperidine (LiTMP).

For the compounds that can be deprotonated using either LDA or n-butyllithium, metalations with lithium amides are reversible. So, for efficient conversion the substrate must have a pK_a of two units lower than the base used.

The scope of the metalation reaction is expanded by the use of complexing and chelating reagents such as hexamethylphosphoric triamide (HMPA), N,N'-dimethylpropyleneurea (DMPU) and tetramethylethylenediamine (TMEDA) which increase the rate of metalation and the range of compounds which can be deprotonated.

3.4.3.1 Metalation directed by nitrogen functionality

3.4.3.2 Selective C-3 lithiation

The direct C3-lithiation of the indole ring has been observed with N-(trialkylsilyl)indoles[140, 141]. Although C-2 is more acidic than C-3 in N-substituted indoles the triisopropylsilyl-protecting group blocks reactivity at C-2 position. The N-triisopropylsilyl group is readily removed by TBAF.

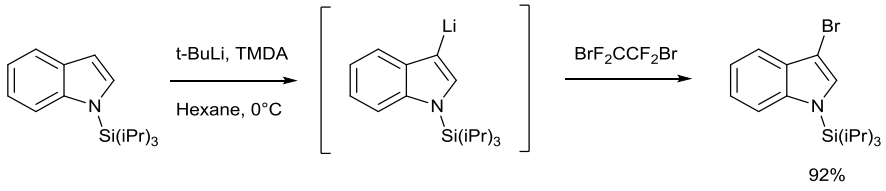

Scheme 3.20 C3-Lithiation of N-(trialkylsilyl)indoles

3.4.3.2.1 Selective C-2 lithiation of indole

The use of a removable N-protecting group would allow the preparation of 2-substituted N-unsubstituted indoles. An advantage of the benzenesulfonyl, as a common protecting group, is that it allows for the regioselective generation of 2-lithioindole derivatives containing methoxy groups and other potential directing groups in the benzenoid ring. Sundberg showed an absence of benzene ring lithiated products when phenylsulfonyl was used as a protecting group. Nevertheless, when the counterpart N-methyl indole was used, an activation of the benzene ring toward metalation was observed.[142]

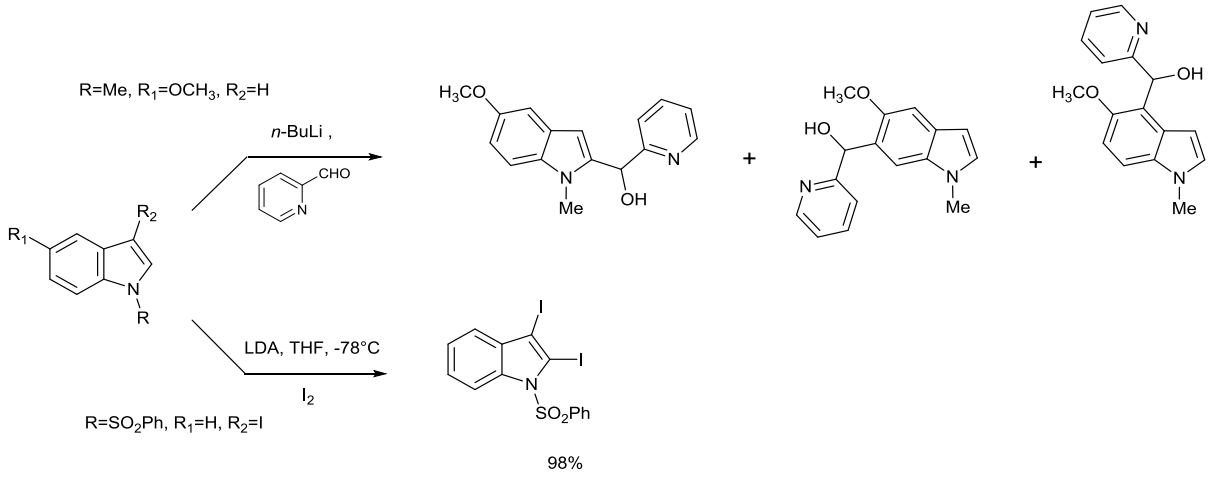

Scheme 3.21 C-2 Electrophilic substitution of indoles in the presence of LDA or *n*-BuLi

3.4.3.3 Directed *ortho* metalation

The intrinsic regioselectivity of metalation of a particular heterocycle can be overcome by the use of directing groups (inductive effect), chelation or a combination of both. The direct C-7, C-3 and C-2 lithiation of the indole can be achieved selectively using 1- (2,2- diethylbutanoyl)indole as a common substrate. These results are especially interesting because the regioselectivity is controlled essentially only by the effects of the ligands employed[143]. The DEB group can promote unprecedented C-7 lithiation under kinetically controlled conditions[144]. This unusual lithiation has been demonstrated to be useful for the synthesis of 3,7-disubstituted indoles which are not readily available by conventional synthetic methods.

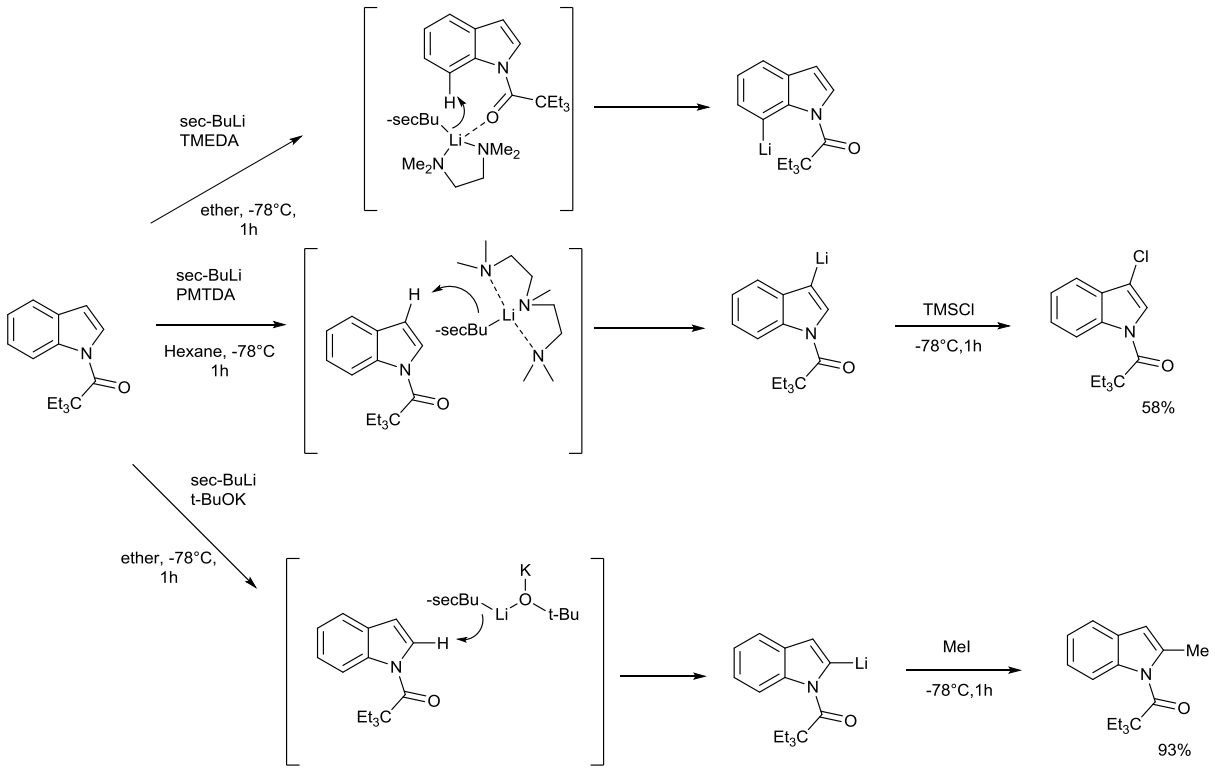

Scheme 3.22 Regioselective metalation of C-7, C-3, and C-2 position

3.4.3.4 Halogen–metal exchange in indole

3.4.3.4.1 Halogen–metal exchange at C-3 position of indole

Halogen–lithium exchange at the C-3 position has been explored by Gribble using 3-iodo-N-(phenylsulfonyl)indole as a substrate treated with *t*-BuLi. This leads to the formation of unstable 3-lithioindole at temperatures above -100 °C, which rearranges to the 2-lithioindole yielding 2-methyl-N-(phenylsulfonyl)indole upon quenching with 2-iodomethane[145].

However, in many cases, halogen–lithium exchange reactions proceed without side-reactions such as ring fragmentation or rearrangement to the corresponding 2-lithioindole intermediate (even at room temperature).

3.4.3.4.2 Halogen–metal exchange at C-2 possition of indole

N-(Substituted)indoles often undergo selective hydrogen-halogen exchange at C-2 assisted by a strong base. Hebert reported the formation of 1,2-bis metalated indoles treating 2-iodoindole with excess of *n*-butyllithium followed by quenching the lithiated species with different electrophiles yielding 2-substituted indoles[111] **(Scheme 3.23).**

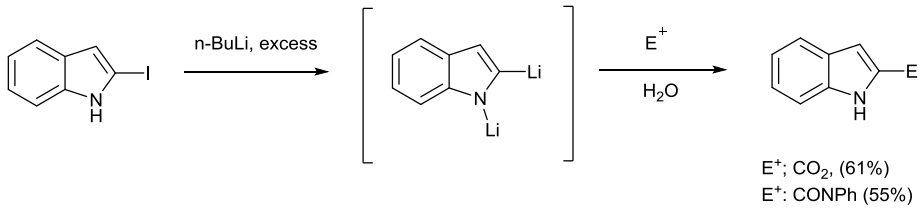

Scheme 3.23 Synthesis of 2-substituted indoles *via* 1,2-bismetalated indoles

Fifty years before, Shirley and Roussel failed in the attempt to introduce a second lithium atom using fourfold excess of the organometallic compound[146], contrasting with the carbazole[147] behaviour in which first the N-H bond can be replaced by an N-Li bond and the metalation in the *ortho* position takes place in a good yield. The stabilization of the anion, as shown in **Scheme 3.24**, would cause the lack in reactivity of N-lithioindole toward *n*-butyllithium.

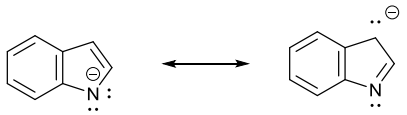

Scheme 3.24 Reactivity of N-lithioindole

3.5 Carbon-carbon bond formation

Formation of a carbon-carbon bond plays an important role in shaping chemical synthesis. Various strategies are available for the construction of the C-C bond including; carbonyl condensation (Aldol reaction), Diels-Alder cycloaddition or Wittig reaction. However, these processes are not very successful in the synthesis of complex frameworks. Cross-coupling reactions catalysed by transition-metals are an alternative approach, widely used in the last quarter of the 20th century.

3.5.1 Palladium catalyzed cross-coupling reactions

The significance of this useful synthetic strategy was shown when Heck, Negishi and Suzuki were awarded with the Nobel Prize in chemistry in 2010. There are many variations of

palladium catalyzed cross-coupling, in which the organometallic reagent varies on, which enables a wide range of substrates to be prepared **(Figure 3-4).**

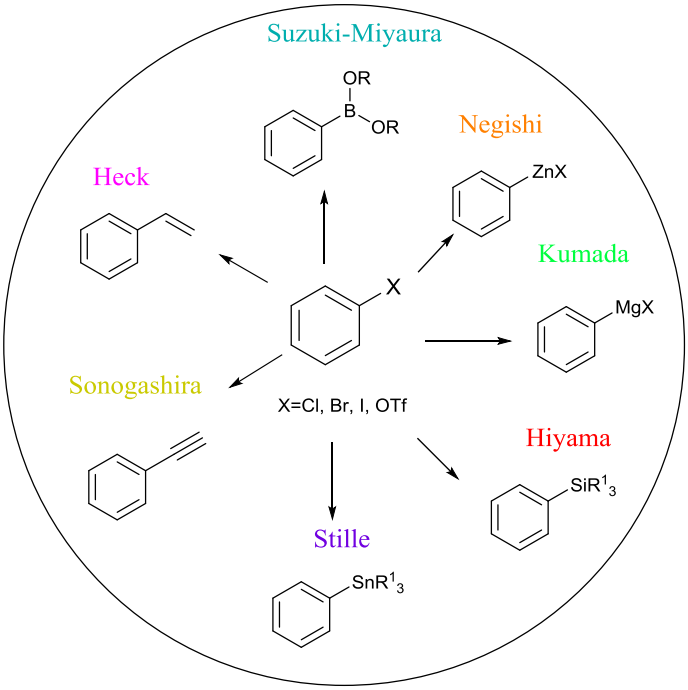

Figure 3-4 Palladium catalysed C-C reactions[84]

In essence all the reactions proceed by similar catalytic cycles. The majority of palladium cross-coupling reactions are catalyzed by Pd(0), Pd(II) or Pd(IV), however the zero-valent palladium catalyst is the most versatile. The cycle **(Scheme 3.25)** is initiated by the oxidative addition of the halide or pseudo halide to the $L_nPd(0)$, forming two new bonds and increasing the oxidation state of the palladium. At this stage, the processes diverge, in the Kumada, Negishi, Suzuki, Hiyama, Sonogashira and Stille coupling processes, oxidative addition is followed by transmetalation. This is the step that shows a difference between organometallic species used for the coupling with the generated Pd^{II} species. Subsequent reductive elimination results in C-C coupling regenerating the Pd^0 active species which re-enter the catalytic cycle. Alternatively, in the Heck process, the reaction progresses by coordination of Pd^{II} to an alkene followed by the *syn*- migration insertion that will undergo syn-β –hydride elimination to give the product assisted by a base.

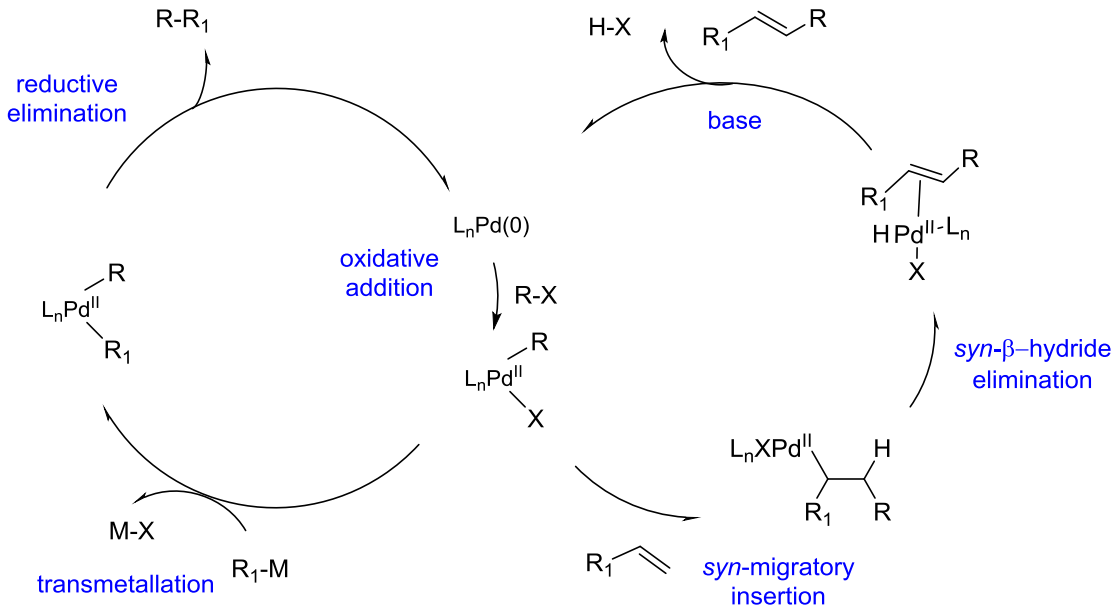

M = Zn (Negishi), B (Suzuki), Sn (Stille), Mg (Kumada), Si (Hiyama), Cu (Sonogashira)

Scheme 3.25 General mechanistic steps of cross-coupling reactions

3.5.2 Heck cross-coupling reaction

The Heck reaction is based on the alkenylation of organic electrophiles, although the first step is common to all cross-coupling reactions. Activation of the organic electrophile by oxidative addition to the active Pd(0) specie. There is no transmetalation and it follows a slightly different procedure. The C-C bond is formed by the insertion of the alkene followed by β-elimination leading preferentially to the E product formation.

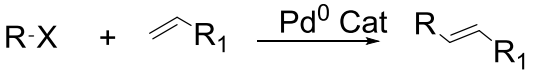

3.5.3 Sonogashira cross-coupling reaction

The Sonogashira reaction is based mainly on the coupling between organohalides with aryl or aliphatic alkynes. It is promoted by Cu(I) generating the alkynyl copper derivatives in presence of an amine as base (but copper-free variants of this C-C coupling are also well-established).

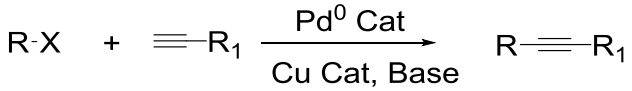

3.5.4 Kumada cross-coupling reaction

The Kumada reaction involves the coupling of organohalides with Grignard reagents. Due to the high reactivity of Grignard reagents, the reactions proceed quickly. However, the aggressive nature of the reagents limits its use due to intolerance to many functional groups.

$$R\text{-}X \quad + \; R_1\text{–}MgX \xrightarrow{Pd^0\ Cat} \quad R_1\text{–}R$$

3.5.5 Negishi cross-coupling reaction

The cross-coupling involving an organozinc reagent and organohalides (or equivalents) is known as the Negishi reaction. Despite the reduced reactivity compared to organomagnesium or organolithium reagents, the Negishi coupling is still regarded as a preferred option. This is due to a broader tolerance towards sensitive functional groups such as carbonyls and nitriles.

$$R\text{-}X \quad + \; R_1\text{–}ZnX \xrightarrow{Pd^0\ Cat} \quad R_1\text{–}R$$

3.5.6 Suzuki-Miyaura cross-coupling reaction

The Suzuki reaction involves the cross-coupling of organoboron reagents (boronic acids or esters) with organohalides (aryl or vinyl halides). A key step of the reaction involves transmetalation of organoboron reagents which require activation by base or fluoride, resulting in arylpalladium (II) halides. In the presence of (aqueous) base the reaction proceeds smoothly and offers a wide range of selective C-C bond formation, high tolerance to many functional groups and boron containing by-products are easily removable by alkali work-up.

$$R\text{-}X \quad + \; R_1\text{–}B(OR'')_2 \xrightarrow[Base]{Pd^0\ Cat} \quad R\text{-}R$$

3.5.7 Hiyama cross-coupling reaction

As in the Suzuki reaction, the activation by a base or fluoride is required for the transmetalation from organosilanes with organohalides (or their equivalents).

$$R'\text{–}X \quad + \quad RSiR''_3 \xrightarrow[Base]{Pd^0\ Cat} \quad R'\text{–}R$$

3.5.8 Stille cross-coupling reaction

The now named Stille reaction developed by John Stille and David Milstein in 1978, along with the Suzuki C-C coupling, are two of the most versatile palladium catalyzed cross-coupling

reactions. Due to its high stereospecificity and regioselectivity, the Stille reaction is preferred for the synthesis of highly functionalised molecules. More importantly, the reaction is tolerant to a wide variety of functional groups (amines, epoxides, carboxylic acids, alcohols) and organostannanes are relatively insensitive to moisture and oxygen. The main drawback is the toxicity of stannanes leading to the reaction not being adopted by industry, although the Stille reaction is popular at a small scale.

The Stille cross-coupling employs organostannanes to construct a new C-C bond.

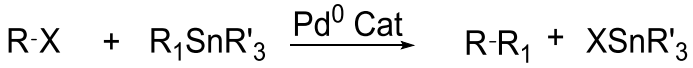

3.6 Bis(indolyl)pyridine as chelating ligands

Cyclometalated compounds with a variety of N-donor ligands (e.g., amines, azobenzenes, imines, hydrazones, oximes and N-centered heteroarenes) have been extensively investigated. Whereas, the chemistry of the analogous indole derivatives remains partially unexplored.

To the best of our knowledge, the synthesis of bis(indolyl)pyridine complexes is quite restricted and limited and is summarised in **Scheme 3.26**. In 2002 Tao, Wang *et al.*[148] published the synthesis of compounds Pd(BIP)Py, Pt(BIP)SMe_2 and Pt(BIP)Py. The synthesis of compound Pd(BIP)Py is the reaction of the corresponding salt Li_2BIP with $Pd(Py)_2Cl_2$. To ensure that the complex was formed in a reasonable yield, excess of the ligand in the ratio 3:1 was required (yield of 21% ratio 1:1). The same procedure was carried out for the synthesis of the platinum(II) complex. However, the reaction was unsuccessful and an alternative route was developed to yield Pt(BIP)Py *via* substitution of the labile dimethyl sulfoxide ligand from reaction of Pt(BIP)SMe_2 with pyridine in dichloromethane. The compound Pt(BIP)SMe_2 was obtained in yield of 21% from the reaction of H_2BIP with $Pt_2Me_4(SMe_2)_2$. To complete the coordination sphere of those divalent metals, a neutral ligand is required. In the case of the tetravalent complexes, two negatively charged ligands are required to saturate the coordination sphere of the metal centre yielding the neutral complexes.

It was not until one year later when Wang *et al.*[149] became interested in the synthesis of tetravalent complexes. Complexes Sn(BIP)Ph_2 and Pb(BIP)Ph_2 were synthesised from the corresponding salt Li_2BIP with the appropriate $M(Py)_2Cl_2$ in the yield of 68% and 64% respectively. The substitution reaction involves the replacement of Cl^- ions by the dianionic tridentate ligand forming cyclometalated complexes and LiCl as byproduct.

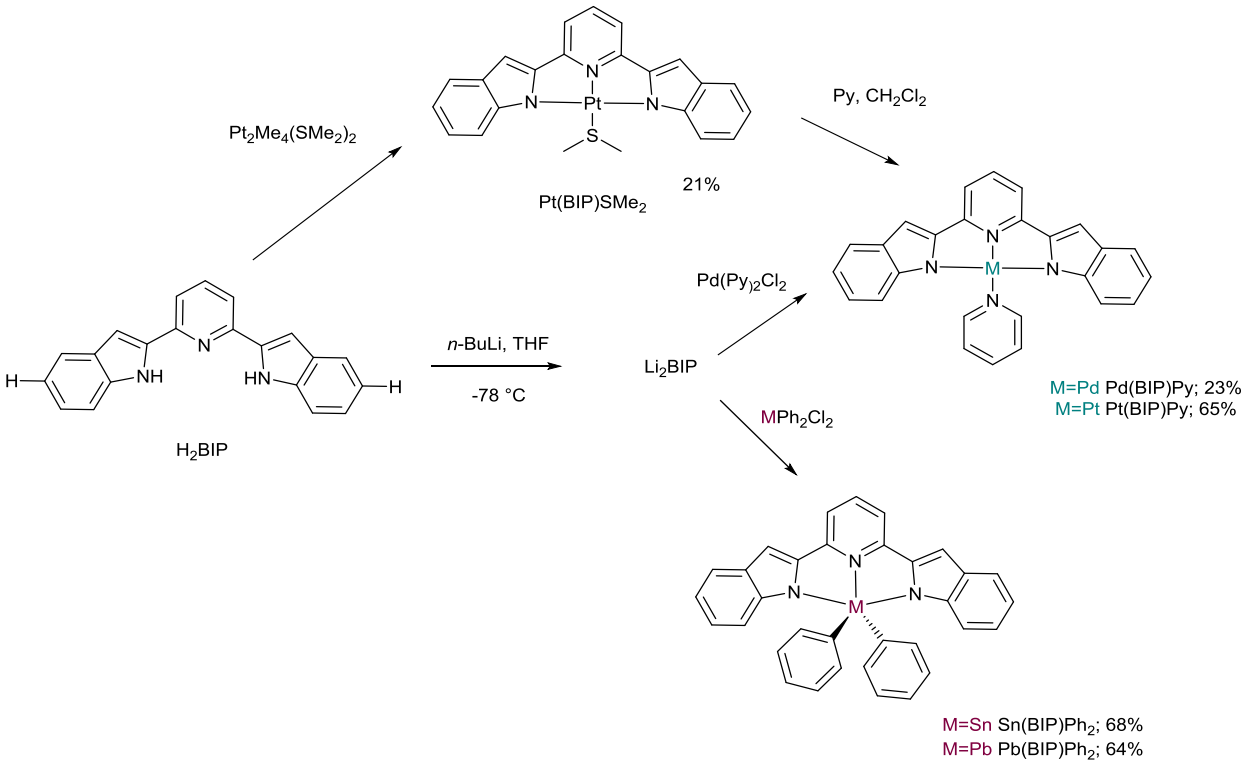

Scheme 3.26 Synthetic strategy towards H_2(BIP) metal complexes

These results show the need to use *n*-BuLi as a base to generate the dianionic ligand whereas other aromatic heterocyclic compounds do not require deprotonation **(Figure 3-5)** for complexation[150, 151,152, 153,154, 155]. Determination of pK_a is influenced by solvation effects, use of non-aqueous media, *etc*[156].

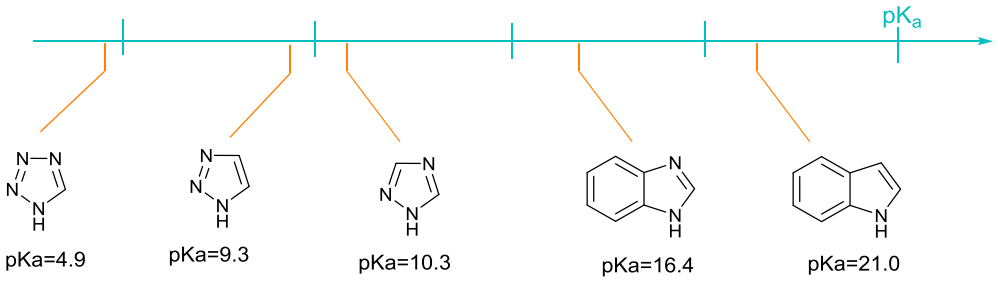

Figure 3-5 Calculated pK_a of different aromatic heterocycles[157]

3.7 Design and synthesis of bis(indolyl)derivatives

The functionalisation of the indole nucleus is still a fascinating area with a remarkable impact on organic synthesis[158]. Electrophilic substitution at the C-3 position is the natural reactivity pattern of indoles. Therefore, our goal is to access C-2 substituted derivatives. Furthermore,

the study aims to investigate how different functional groups affect the distribution of the electronic density and thus the photophysical properties. Structural alterations include: a) the residues that extend π -conjugation or inject/withdraw electrons in C-5 position **(3.1-3.3)**, b) the donor-acceptor strength of the linker **(3.3, 3.4-3.6)** and c) the conjugation of the aromatic system at the C-3 position **(3.3, 3.7-3.8)**.

1. Metal-free small organic molecules have rather limited π-conjugation, they can intrinsically display deep-blue emission as well as high fluorescence quantum yield (Φ). They have precise chemical structures, high purity and high thermal stability[159, 160].

2. Marginal structural modifications can lead to significant changes in the electronic distribution in the molecule tuning electronic spectra and the fluorescence quantum yields (Φ) without compromising their thermal stability.

3. These molecules are of particular interest because the pyridine and indole heterocyclic fragments are in juxtaposition. Thus, these synthetic scaffolds can potentially serve as dianionic terdentate ligands (N^N^N).

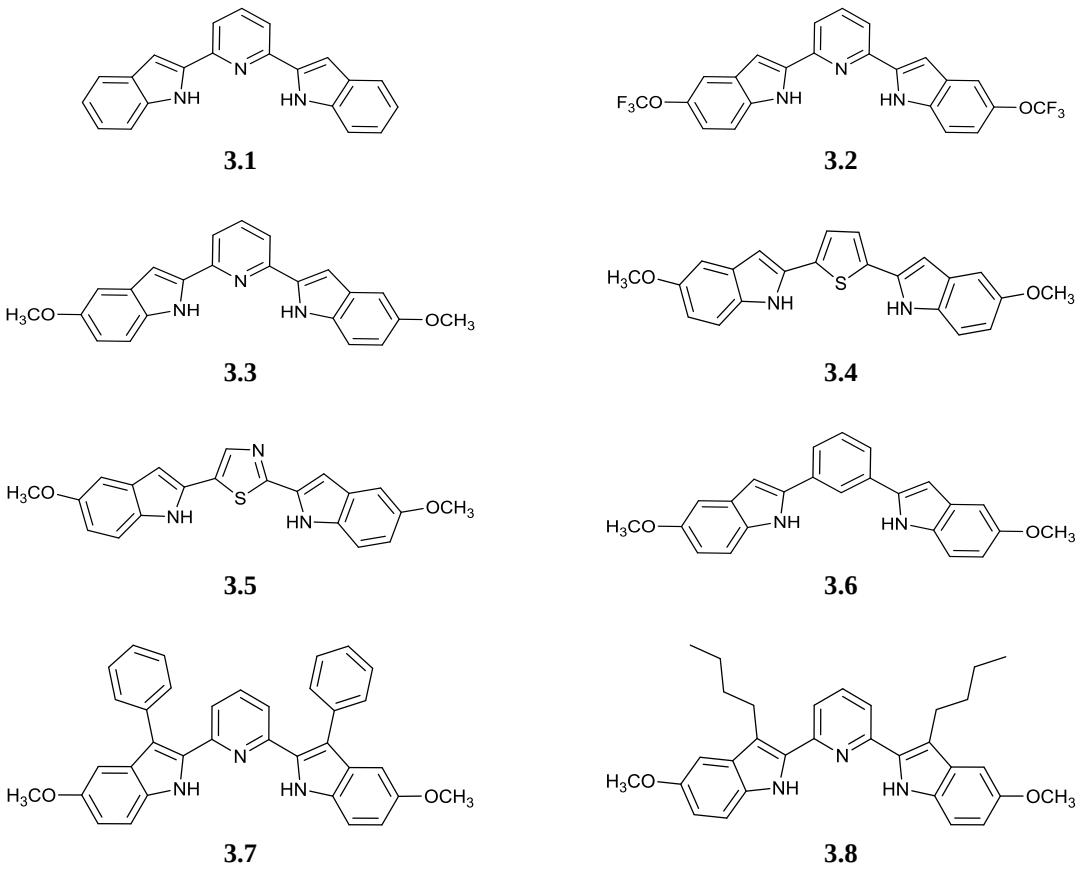

Figure 3-6. Structures of bis(indolyl)derivatives (3.1-3.8)

3.8 Synthesis of bis(indolyl)derivatives

3.8.1 Bis(indolyl)derivatives *via* Fischer synthesis

3.8.1.1 Synthesis of bis(phenylhydrazone)derivatives

Hydrazones have been widely used in organic synthesis, especially as intermediates for the preparation of heterocyclic compounds. The bis(phenylhydrazone)s can be used for a double Fischer reaction.

The synthesis of bis(phenylhydrazone)pyridines **(1-3)** and bis(phenylhydrazone)benzene **4** was accomplished using a condensation protocol[42, 46] by reacting an appropriate hydrazine with 2,6-diacetylpyridine or 1,3-diacetylbenzene, respectively **(Scheme 3.27)**.

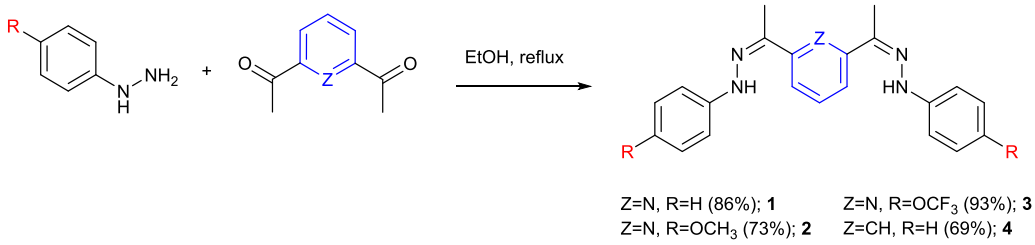

Scheme 3.27 Synthesis of bis(phenylhydrazone)derivatives

The synthesis of compounds **1-3** provides solids and results in yields of 73%-93%. But, the crude compounds **4-6** are very complex mixtures and thus more difficult to isolate. Compound **4** was obtained in a yield of 80% using solvent diffusion (EtOH:Ether) for the crystal growth. For compounds **5** and **6** repeated attempts at recrystallisation, precipitation or crystal growth using varying solvents proved unsuitable. In order to form **5** and **6** without the presence of the mono-condense product, the amount of hydrazine was increased. However this proved unsuccessful, as more complicated crude products were observed, along with unreacted starting materials.

3.8.2 Synthesis of bis(indolyl)derivatives *via* Fischer synthesis

In order to obtain only one regioisomer, indolisation requires the use of *p*-substituted phenylhydrazones. Phenyl rings with electron-donating substituents have been reported to enhance the rate of the indolisation. Whereas the presence of an electron-withdrawing group on the phenyl ring decreases the rate of cyclisation or the reaction will require harsher conditions[161, 162].

Through the synthesis of bis(phenylhydrazone)pyridines **(1-3)** we observed that the electronic effect of the studied substituents contradicts previously reported work[162, 163]. The indole-based molecules (Z=N and R=H, OCF_3) can be prepared by a PPA-catalysed cyclisation[164] of the bis(phenylhydrazone)derivatives. However, using the same procedure for [Z=N and R=OCH_3] and [Z=CH and R=H], the synthesis was unsuccessful.

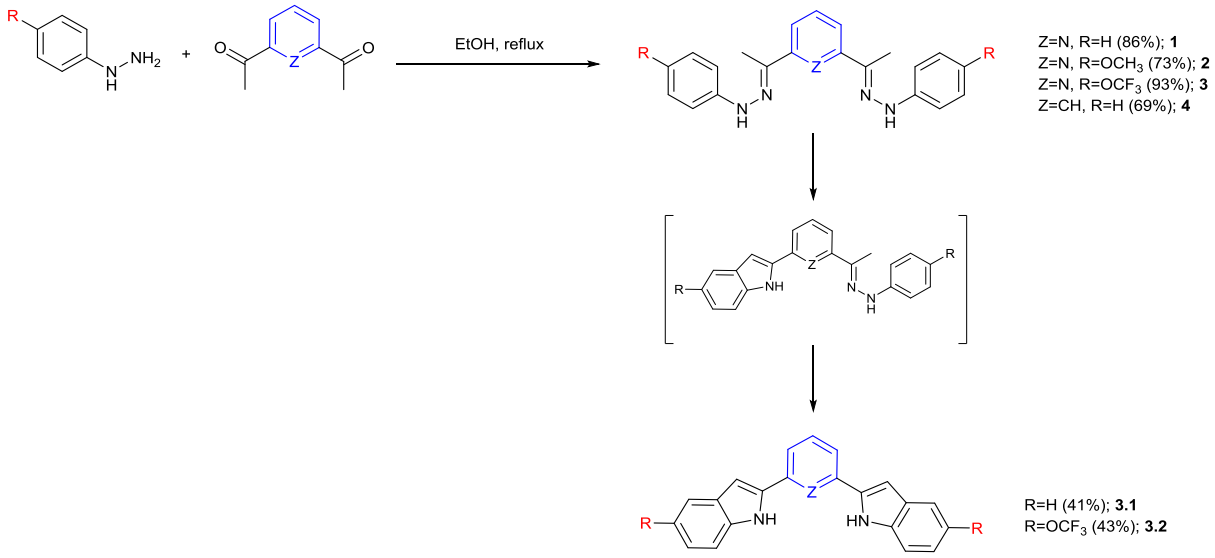

Scheme 3.28 Fischer synthesis of H_2BIP(R)

3.8.2.1 Synthesis of bis(4-methoxyphenylhydrazone)pyridine

The cyclisation behaviour of 2,6-diactetylpyridinebis(4-methoxyphenylhydrazone) shows that the situation is more complex than previously thought. The accepted mechanism for Fischer's synthesis **(Scheme 3.29)** was suggested by Robinson[86], although mechanistic details underlying the acid-promoted indolisation step remain yet unclear[165]. According to the Robinson mechanism, the phenylhydrazone **(M.1)** then rearranges to the ene-hydrazine **(M.2)**. Followed by the key [3,3]-sigmatropic rearrangement step, resulting in a diamine **(M.3)** and the loss of aromaticity. The intermediate diene **(M.2)** is stabilised by an electron-withdrawing group in the phenyl ring. Thus, the methoxy substituent is destabilised and should therefore be more reactive[162, 163]. The last step involves rearomatisation and ammonia elimination **(M.5)** to provide **M.6**.

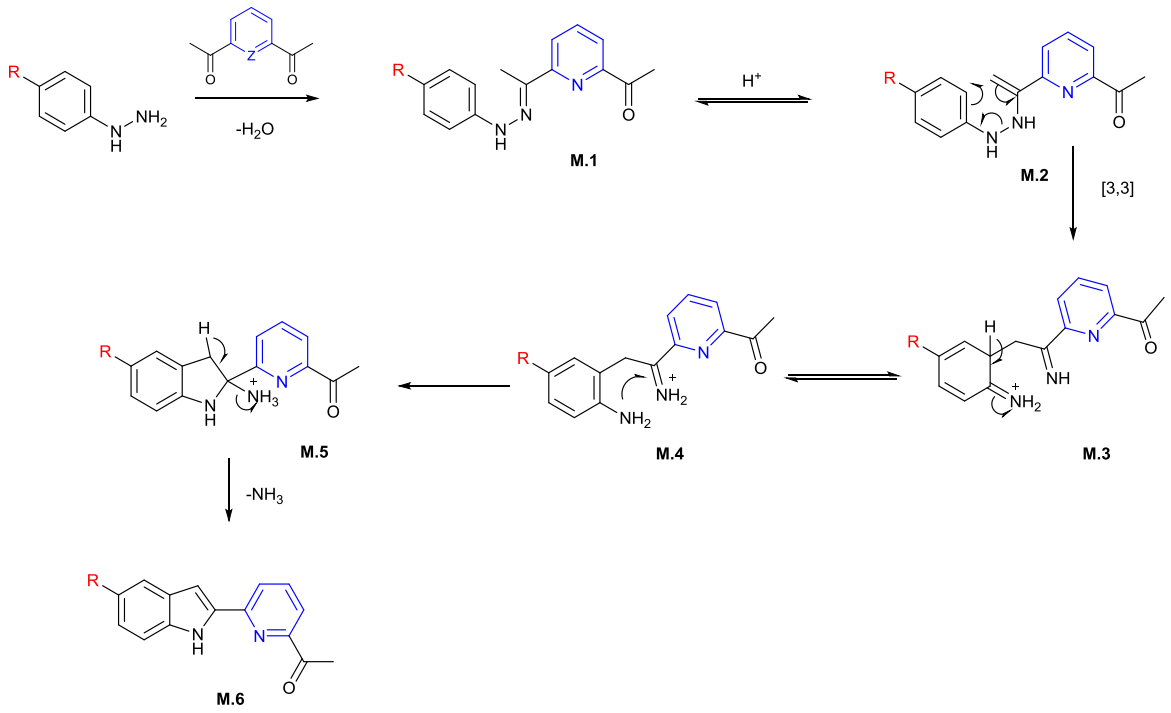

Scheme 3.29 Accepted mechanism for the Fischer indole synthesis

The methoxy substituent on the phenyl showed a dramatic effect on its reactivity in the Fischer cyclisation reaction. Varied conditions were investigated. When a mixture of NaOAc/CH_3COOH was used, the cyclisation step was unsuccessful and only starting materials were isolated. The use of Eaton's reagent (CH_3SO_3H/P_2O_5) favours the regiospecific formation of one product[166] which is not necessarily the most thermodynamically stable. The use of this reagent as an acid catalyst should overcome the energy barrier to form the bis(indolyl)pyridine derivative. However, the use of a co-solvent (DCM) and the Eaton's reagent only slightly enhanced the formation of the semi-cyclised intermediate (up to 19%) after the mixture was left to react overnight. Reaction conditions using ethanol as a solvent and *p*-TSA as a catalyst under microwave irradiation (MW) for 2.5 h at 120 °C provided the semi-cyclised intermediate and unreacted starting material.

Finally, in order to avoid the isolation of the hydrazone, a one-pot reaction using: i) low melting L-(+)-tartaric acid:dimethyl urea mixture and ii) microwave irradiation (2.5 h at 120 °C) was used to force the reaction to form the indole. The melt plays a dual role acting as solvent as well as catalyst[101]. However, the desired product was not obtained.

However, this strategy yielding **3.1** and **3.2** is rather limited by the availability of the biscarbonyl compounds. Additionally, the outcome of the reaction is strongly driven by the

electronic nature of substituents of the hydrazine reagents and the bridge unit.[163, 165] Thus, an alternative approach has been explored that can be used to access the target compounds.

3.8.3 Exploration of indole reactivity

3.8.3.1 Fischer synthesis of C-3 substituted indoles

Different approaches can be used for the synthesis of C3-substituted indoles; however, these procedures are undoubtedly more time consuming compared with the Fischer indole synthesis, which allows the generation of already functionalised indoles. Fischer indole synthesis is a convenient method allowing the attachment of different substituents at the C-2 and C-3 positions by using a variety of carbonyl compounds and hydrazine derivatives. Traditionally, the synthesis of indoles was carried out by isolating the unstable hydrazone and subsequent cyclisation with the appropriate acid. However, due to the instability of the intermediates, a one-pot synthesis proved a much better alternative **(Scheme 1-30)**. The acid choice and substituents on the arylhydrazone are of particular relevance as they determine the rate of the cyclisation and therefore, the formation of the products.

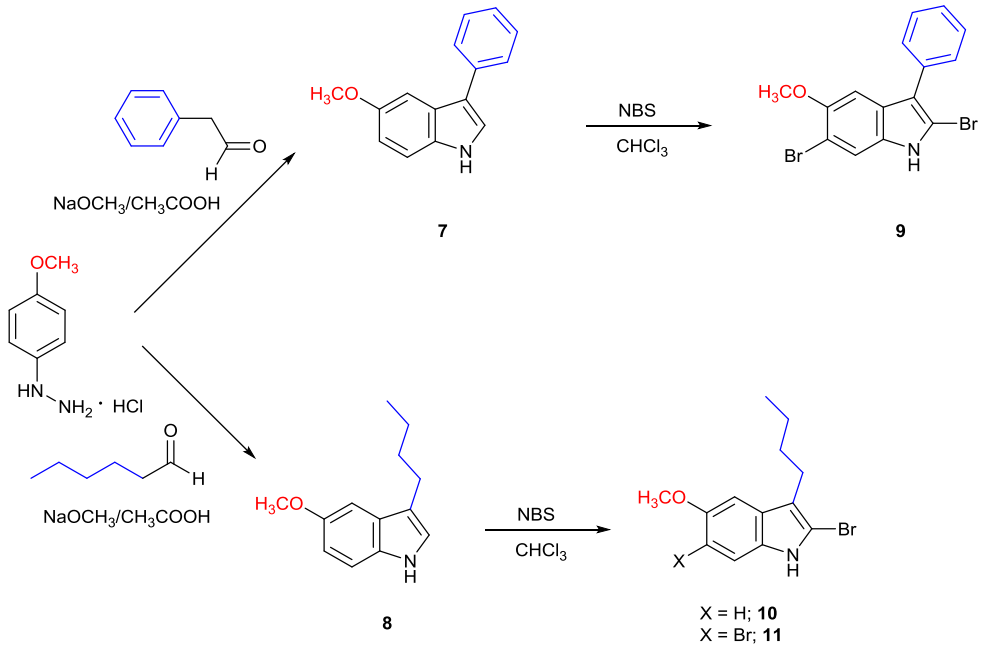

Scheme 3.30 One-pot Fischer synthesis of indole 7 and 8 and halogenation to obtain 9, 10 and 11

Different conditions were screened for the synthesis of compound **7**. The use of Brønsted acids AcOH and H_2SO_4 did not result in product formation, while 4% H_2SO_4 aqueous solution enabled indole formation in a 30% yield. The presence of sodium or ammonium acetate, which can act as a pH buffer during the reaction, seem to facilitate the cyclisation. Although,

formation of the indoles proceeds successfully (yield of 60%) under these reaction conditions, the purification step is a highly time-consuming procedure. To minimise the formation of side-products and to facilitate the isolation of the final molecules, it was decided to avoid strong acid media and alternative catalysts were sought. 2,4,6-Trichloro-1,2,5-triazine (TCT) is reported to be a suitable catalyst in the Fischer synthesis[98]. However, the results were not reproducible despite the amount of TCT being reduced from 0.5 eq to 0.1 eq and temperature was varied from 80°C to 65°C. It is believed that HCl generation in the reaction mixture and the peculiar reactivity of 4-methoxy phenyl hydrazine led to unwanted side products such as those resulting from hydrolysis of hydrazone. Alternatively, a use of the low melting mixture comprising from tartaric acid-dimethylurea as a free-solvent condition successfully resulted in 65% yield. However, the purification procedure has not been simplified and still remains a challenge.

After the best conditions were established ($NaOAc/CH_3COOH$), they were used for the synthesis of compound **8** resulting in 67% of yield.

3.8.3.2 Synthesis of 2-halogenated indoles

Although halogenated indoles are potential intermediates in C-C formation *via* transmetalation, particularly in cross-coupling reactions, the synthesis of 2-halogenated indole remains a challenge. Due to their hydrolysis, air sensitivity and thermal instability (they should be stored at T below -20 °C), these reactive intermediates should be utilised as soon as they are prepared. Generally, halogenation takes place at the C3-position, although the reaction can occur at the C2-position. These useful intermediates can be generated without N-protection of the indole by electrophilic substitution using NBS as a straight forward method.

This approach potentially, has the benefit of preparing several materials in "one pot". The most common bromination reaction involves the use of NBS (slight excess) in chloroform. In the case of compound **7**, it yields only the di-brominated indole **(9)** whose formation can be favoured by increasing the equivalents of NBS to give yields of 50% (from 1.2 to 2.2 eq). However, for compound **8**, the mixture of mono- **(10)** and di-brominated indole **(11)** can be controlled by adjusting the stoichiometric ratios of the reagents. Those resulting materials are sufficiently different in polarity to facilitate chromatography separation. However, due to the instability of compound **10**, which decomposes during the process, only the side product **11** is isolated (in the yield of 6%). Subsequently the amount of NBS was reduced to minimise the formation of **11** and compound **10** was not isolated but used straight away in the next step without further purification.

From the experimental results it can be concluded that the procedure for the synthesis of brominated indoles is dominated by the substituents present on the indole. Showing that the substituent at the C3-position causes a stronger effect compared with the C-5 position.

3.8.3.3 Synthesis of 3-butyl-5-methoxy-2-thiophene-1H-indole

Further investigations of the synthesised 2-bromo-3-butyl-5-methoxy-1H-indole **(10)** were focussed on a Stille cross-coupling reaction with 2-(tri-n-butylstannyl)thiophene. The brominated intermediate proved to be unstable, and so was used without further purification. A variety of catalysts were used, $Pd(PPh_3)_4$, $Pd(PPh_2)Cl_2$ and $Pd(dppf)Cl_2$, however, the reactions led to an intractable mixture. After column chromatography was carried out, the product isolated was not the desired compound. Thus, 2-halogenated indoles are not suitable intermediates.

3.8.3.4 Synthesis of 2-organostannyl indoles

In this section the synthetic approach for the preparation of 2-substituted-N-unsubstituted indoles is discussed. Organotin reagents possess several advantageous features such as air and moisture stability and tolerance to many functional groups. Stabilisation of the 1-indolyl anion is responsible for its lack of reactivity toward *n*-butyllithium for generation of 1,2-bismetalated indoles, thus protection should be carried out first. The phenylsulfonyl protecting group is one of the most commonly used, it directs *ortho* metalation through the stabilization of the C2-position by intramolecular interactions between a lone pair on the sulfonyl group with lithium **(Scheme 3.31)**. The synthesis of N-protected indoles **(13-15)** was achieved with an overall yield of 57-79% by following a two-step literature procedure. In the first step, indole was deprotonated with sodium hydride followed by electrophilic attack of benzenesulfonyl chloride. Compounds **14** and **15** were then reacted with *n*-BuLi or LDA as a base, followed by quenching with trimethyltin chloride. The sterically hindered LDA proved to be a better alternative than *n*-BuLi for the synthesis of the stannyl derivatives. The use of *n*-BuLi led to the formation of side-products due to the metalation of the *ortho* position of the phenylsulfonyl group. The organostannyl derivatives (**16** and **18**) were obtained in yields of 35% and 67% respectively.

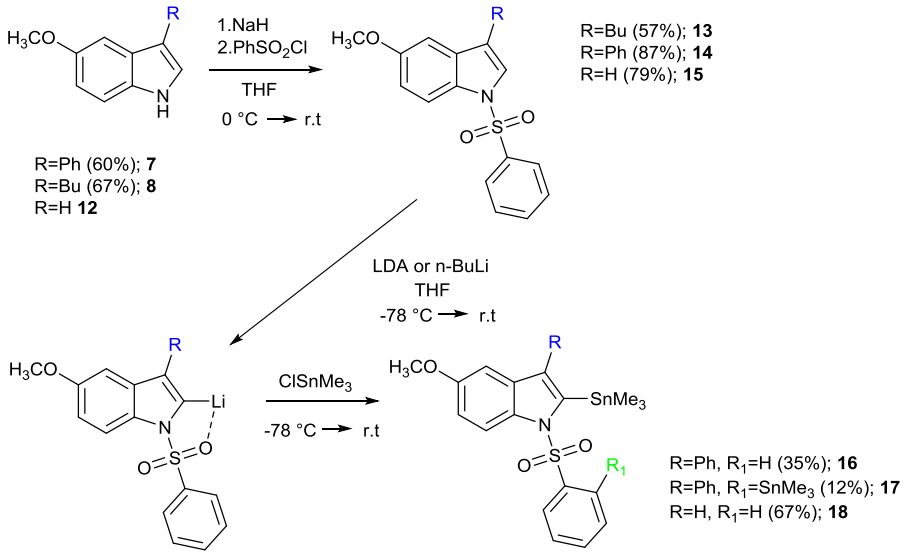

Scheme 3.31 Synthesis of N-protected indoles (13-15) and organnostanyl derivatives (16-18)

3.8.4 Synthesis of bis(indolyl)derivatives *via* one-pot double Stille cross-coupling

The preparation of such materials, where the functionalisation was carried out at the C2-position, was laborious due to low yields in the reaction sequence and highly time consuming purification processes. The one-pot double Stille reaction has such benefits as: a reduction in the number of steps, an increase in the yields and reduced time consumption.

3.8.4.1 Synthesis of 2,6-bis(5-methoxy-3-phenyl-1H-indole)pyridine (3.7)

The synthesis of compound **20** was performed by one-pot reaction of the two consecutive Stille cross-coupling processes. The reaction involved 5-methoxy-3-phenyl-1-phenylsulfonyl-2-trimethylstannylindole **(16)** and 2,6-dibromopyridine in the presence of $Pd(PPh_3)_4$ and CuI under refluxing THF for 4h **(Scheme 3.32)**. The formation of compound **14** proved that transmetalation occurred. However, the reductive elimination step leading to **19** did not take place. Several attempts to synthesise this product proved unsuccessful. Presumably the reaction process was sterically hindered due to the phenyl substituent at the C3-position. However, compound **20** was isolated in a yield of 84 % after column chromatography.

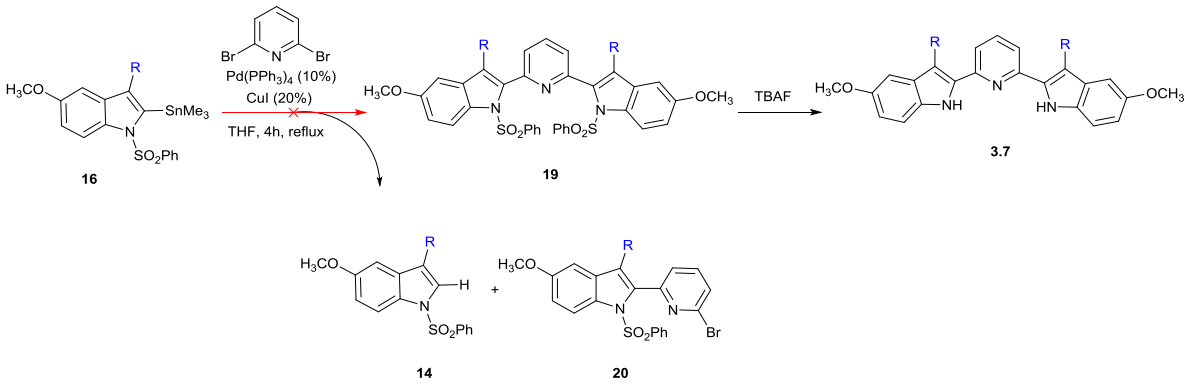

Scheme 3.32 Synthetic route to compounds 14, 19, 20 and 3.7

3.8.4.2 Synthesis of 2,6-bis(5-methoxy-1H-indole)pyridine (3.2) and 2,6-bis(5-methoxy-1H-indole)benzene (3.6)

The synthesis of compounds **3.2** and **3.6** can be achieved by following a two-step procedure. The initial step involved a one-pot double Stille cross-coupling reaction of 5-methoxy-3-phenyl-1-phenylsulfonyl-2-trimethylstannylindole **(18)** and 2,6-dibromopyridine or 1,3-dibromobenzene in the presence of $Pd(PPh_3)_4$ and CuI under reflux in THF for 24h **(Scheme 3.33)**. After work-up and purification by column chromatography the products **22** and **21** were isolated in the yields of 92% and 8%[2] respectively.

[2] As a consequence of the extremely low yield of compound **22,** mono-cross coupling product **30** was obtained in the yield of 18%. No further synthesis or analysis was carried out.

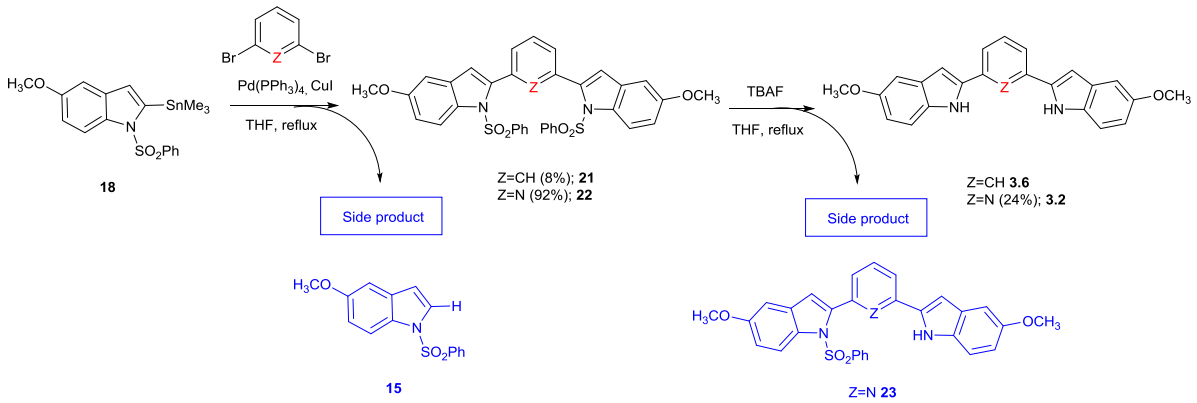

Scheme 3.33 Synthetic route to 2,6-bis(5-methoxy-1H-indole)pyridine (3.2) and 2,6-bis(5-methoxy-1H-indole)benzene (3.6)

From **Table 1**, it is clear that the most viable condition is using 10% of catalyst. Presumably due to the formation of compound **15**, the rate of transmetalation is greater than the reductive elimination step. Therefore by reducing the amount of catalyst the rate of the transmetalation step is reduced, avoiding complete consumption of **18** and transformation into **15**.

Table 3-1 Optimised conditions for the synthesis of 21 and 22

Z	$Pd(PPh_3)_4$	CuI	Yield
N	20%	20%	24%
N	10%	20%	92%
CH	20%	20%	5%
CH	10%	20%	8%

The second step involved the deprotection of compound **22** into compound **3.2** performed by the addition of the THF solution of TBAF. The presence of compound **23** can be excluded by controlling the stoichiometric amount of TBAF added (minimum of 3 eq). The chemical conversion for this step is 86%. After work-up and purification by column chromatography the product **3.2** was isolated only in a yield of 24% due to low solubility of crude mixture in most organic solvents. To overcome the solubility issues of the crude mixture, dry load was chosen.

3.8.4.3 Synthesis of 2,5-bis(5-methoxy-1H-indole)thiophene (3.4)

The synthesis of compound **3.4** was achieved by following a two-step procedure. The initial step involved a one-pot double Stille cross-coupling reaction of 5-methoxy-3-phenyl-1-phenylsulfonyl-2-trimethylstannylindole **(18)** and 2,5-dibromothiophene in the presence of $Pd(PPh_3)_4$ and CuI under reflux in THF for 24 h **(Scheme 3.34)**. After work-up and purification by column chromatography the product **24** was isolated in the yield of 89%.

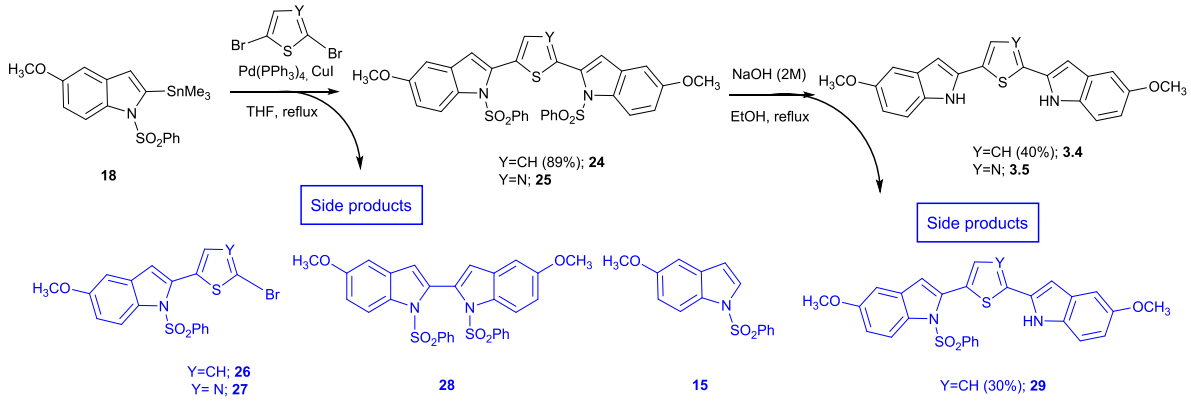

Scheme 3.34 Synthetic route to 2,5-bis(5-methoxy-1H-indole)thiophene (3.4) and 2,5-bis(5-methoxy-1H-indole)thiazole (3.5)

It is clear **(Table 3-2)** that the most viable condition was the one using 15% catalyst. The yields of individual side products can be controlled or even eliminated by controlling the amount of catalyst. The presence of co-catalyst was crucial, as in its absence only starting materials were obtained. An excess of $Pd(PPh_3)_4$ could involve the formation of undesired compounds, such us **15**, **26**, **27** and **28**. The use of 10% of catalyst significantly reduced the product yield and increased the presence of unreacted starting materials.

The second step involved the deprotection of compound **24** into compound **3.4** by adding TBAF solution in THF (5 equivalents). After work-up and purification by column chromatography the product **3.4** was isolated in the yield of 40% and compound **29** in the yield of 30 %.

Table 3-2 Optimised conditions for the synthesis of compound 24

Y	$Pd(PPh_3)_4$	CuI	Yield
CH	20%	-	-
CH	20%	20%	33%
CH	15%	20%	89%
CH	10%	20%	41%

3.8.4.4 Synthesis of 2,5-bis(5-methoxy-1-phenylsulphonyl-1H-indole)thiazole (25)

The synthesis of compound **3.5** can be achieved by following a two-step procedure. The initial step involved a one-pot double Stille cross-coupling reaction of 5-methoxy-3-phenyl-1-phenylsulfonyl-2-trimethylstannylindole **(18)** and 2,5-dibromothiazole in the presence of $Pd(PPh_3)_4$ and CuI under refluxing THF for 60 h **(Scheme 3.34)**.

The most viable condition for the synthesis of **25** required the use of 20% catalyst. The formation of some side-products such as **27** were eliminated by controlling the amount of catalyst. A decrease of the $Pd(PPh_3)_4$ catalyst below 10% did not lead to the product, but involved the formation of undesired compound **27** and the stannyl derivative **18**. Thus, the possibility for the double C-C coupling to proceed still remained. Nevertheless, longer reaction times did not lead to the formation of the desired compound **25**.

The second step to transform **25** to **3.5** could not be carried out because compound **25** undergoes slow decomposition in solution upon exposure to air and, as a result, complete characterization of **25** was not possible. However, both ^1H NMR (Figure 3-7) and LC-MS data (Found: 656.7, requires: 656.8) confirm the formation of 2,5-bis(5-methoxy-1-phenylsulphonyl-1H-indole)thiazole **(25)**.

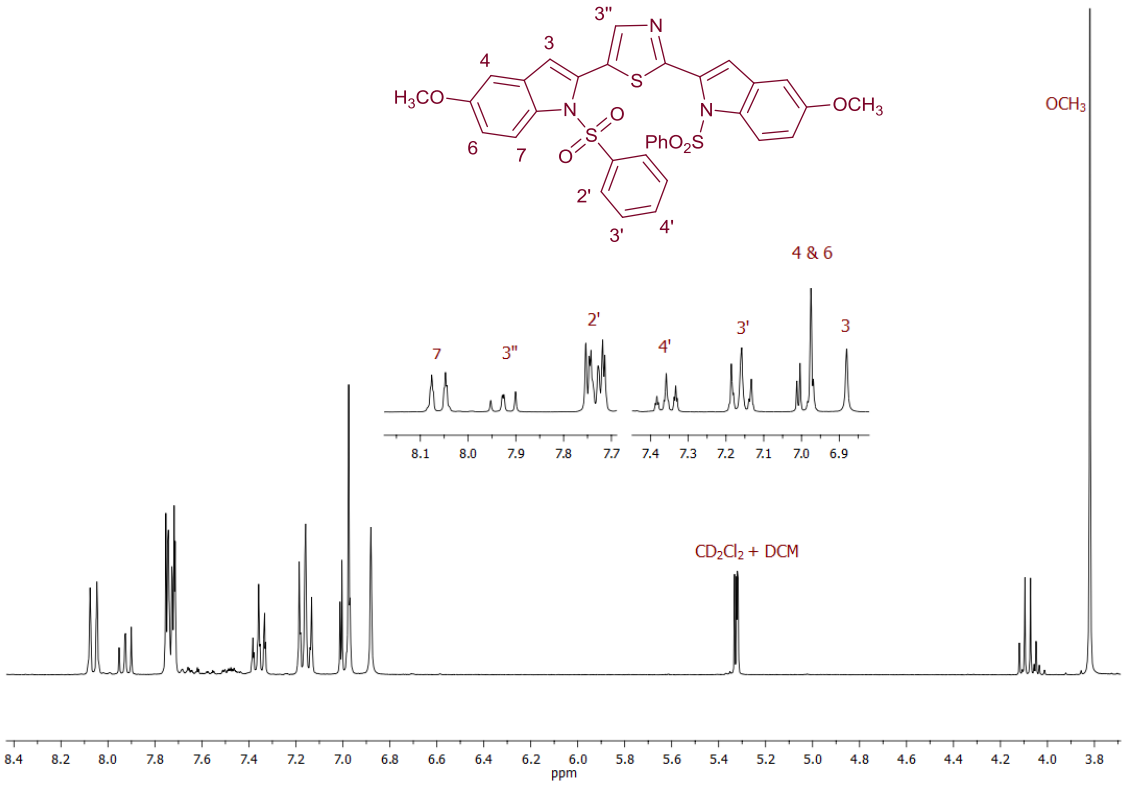

Figure 3-7 ^{1}HNMR spectrum of 2,5-bis(5-methoxy-1-phenylsulphonyl-1H-indole)thiazole (25)

3.9 Attempted synthesis of bis(indolyl)pyridine complexes

Coordination compounds are significant as metals constitute the bulk of the periodic table as well as the broad diversity of their properties. This comprises:

- different charge and coordination geometries depending of the environment,
- Lewis acid-character and therefore ligand interaction tuning their overall properties,
- redox activity and,
- partially fulfilled d-shell imparting interesting electronic and magnetic properties do transition metal complexes.

After the laborious preparation of the ligands, in theory, chelation can be achieved in two steps. The first one involves the generation of the dianionic ligand with *n*-BuLi followed by metal binding **(Scheme 3.35)**. Different stoichiometric base-ligand-metal ratios were screened for the bis(indolyl)pyridine derivatives **3.1-3.3**. Presumably, the pyridyl derivatives **3.1-3.3** may favour the chelation in comparison to the thiophenyl bisindole **3.4** due to a higher planarity of the bisindole framework of the former. The three nitrogen atoms are placed to act cooperatively in cation binding. The attempts to form gold complexes using the bis(indolyl)pyridines **(3.1-3.3)** as ligands were unsuccessful. Different conditions included the use of $KAuCl_4$ in the

presence of various bases (LDA, *n*-BuLi) with the different stoichiometric ratios of the ligands **3.1-3.3**. A metallic colour which seems to correspond to Au^0 was observed in the reactions. This can be explained by the dianionic tridentate ligand acting as a reducing agent. According to the literature, similar reactions of gold(III) chloride acid with amines acting as reducing agents in the formation of gold nanoparticles have been reported[167-169].

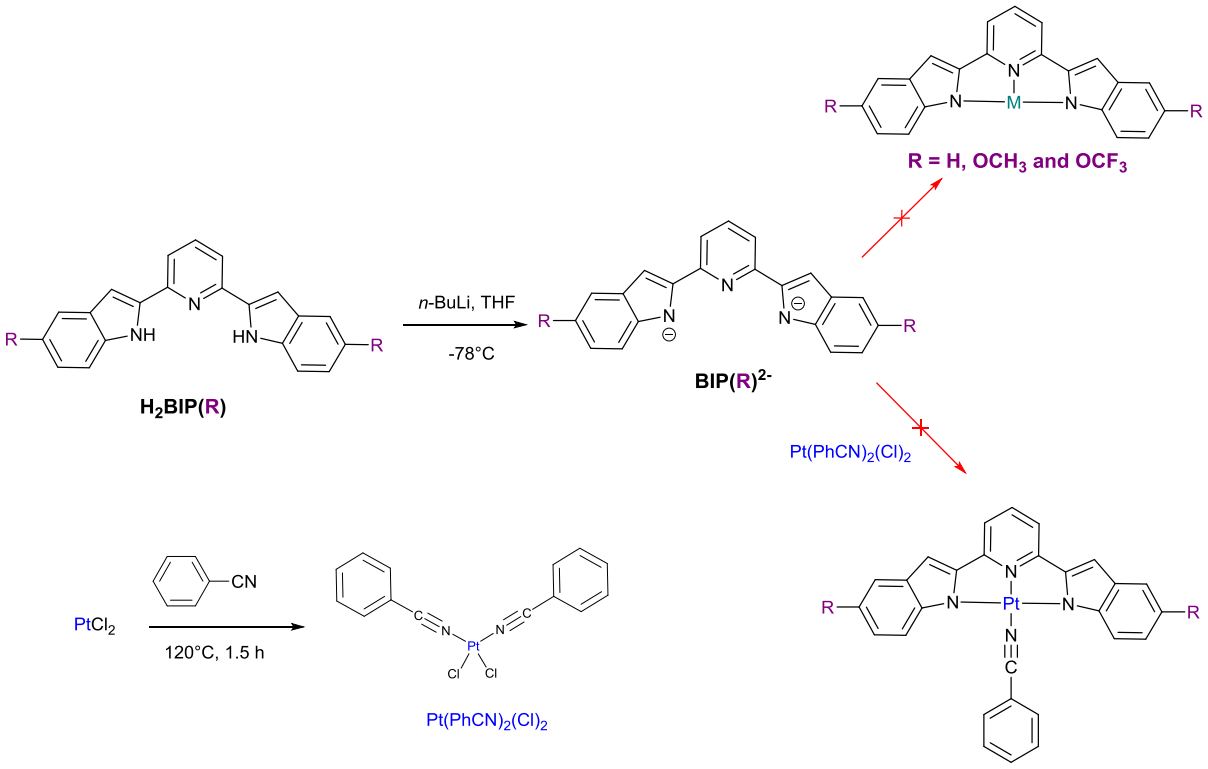

Scheme 3.35 Synthetic strategy for H_2BIP(R) complexes

In addition, attempts using different stoichiometric ratios of the ligands **3.1-3.3** and a variety of zinc and copper salts, $AgNO_3$[167], Ag_2O and bis(benzonitrile)dichloroplatinum(II) also proved unsuccessful. Here, is a summary of important factors that can affect the binding of the ligand and metal:

1. Following a synthetic route reported by Wang *et al.*, *n*-BuLi is required as a base. The first challenge is therefore the double deprotonation of the ligand. The deprotonated ligand provides two negative charges lowering the overall charge of the metal complex.
2. Orientation and proximity between the -NH and the electron lone pairs of the pyridine are crucial for intramolecular H-bonding. Indole is π-rich heterocycle, and in comparison to pyridine, is non-basic, being potentially a good H-bond donor. On the other hand, pyridine is π-deficient heterocycle but exhibits Lewis basicity (lone-pair) being a good H-bond acceptor.[170]

3. The bite angle (α) is smaller for 2-(2'-pyridyl)indole than 2-(2'-pyridyl)quinoline **(Figure 3-8)**. The bite angle of a bidentate ligand can be considered "the intersection of the linear axes containing the donor electrons". [164]A smaller angle is less preferred for an octahedral complexation due to a smaller approximation between the ligand and the metal. The presence of the five-membered ring of the indole causes a smaller angle.

Figure 3-8 The bite angle of 2-(2'-pyridyl)indole and 2-(2'-pyridyl)quinoline.

3.10 Photophysical properties of indole: experimental and theoretical

The importance to understand photophysical properties and electronic transitions of indole resides in its relation to the amino acid tryptophan, being its chromophore[171]. The luminescence of tryptophan is used when studying complex biological systems, protein structure and function [172].

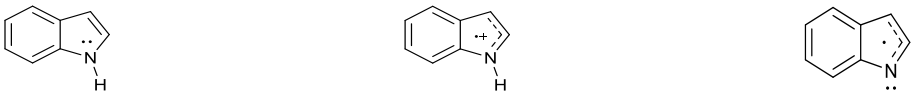

S.12 **S.13** **S.14**

Figure 3-9 Indole transients originated as consequence of photoexcitation

The theoretical interpretation of the absorption spectrum of indole is quite difficult[173, 174] due to a number of reactive intermediates besides the emitting singlet excited state. Also, it can include: the triplet of the indole **(S.12)**, the radical cation **(S.13)**, the neutral indolyl radical **(S.14)** and the solvated electron[175].

The π-deficient character of the pyridine and indole π-rich character can result in the H-bond donation from the indole to the pyridine. In the case of 2-(2'-pyridyl)indole, the intramolecular H-transfer can complicate the interpretation of the photophysical data. Potentially, this indole can exists as a tautomeric form **(Figure 3-10)**, although the disruption of the aromaticity makes such a process unfavourable. [176]

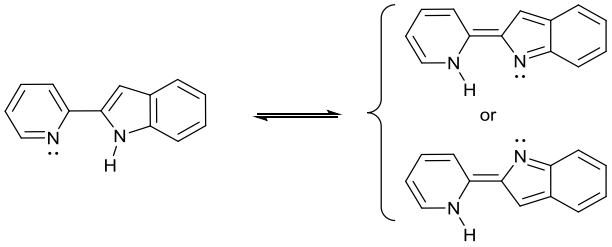

Figure 3-10 Intramolecular H-transfer in 2-(2'-pyridyl)indole

Introduction of new substituents, or the same substituents in a different position of the indole, causes changes not only to the geometry, but also to the electronic properties of the system. The magnitude and mainly direction of the permanent dipole moments alter the stability and may alter the order of the two lowest singlet excited states, which are responsible for the emission properties[177-179]. The singlet excited states can also be influenced by the solvent. Large solvatochromic effects have been observed in solutions of different polarities[172], which can be a consequence of exciplex formation[180-183].

It is known that the use of different solvents does not affect the ground state of indoles considerably (absorption spectra are little affected). However, due to the influence on the emission spectra, the excited state is highly polarised and depending of the solvent the transients could be more or less stabilised. Most likely the polarized forms **(Figure 3-11)** cause larger contributions to the excited state than to the ground state.[173]

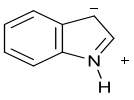

Figure 3-11 A polarised form of indole

3.10.1 Photophysical properties: absorption and emission profile of compound 3.1-3.4

The spectroscopic behaviour of compounds **3.1-3.3** in acetonitrile and **3.4** in toluene solutions were studied **(Figure 3-12)**. The absorption spectra of the pyridine-bridged series **3.1-3.3** display similarities in the near-blue region. This indicates that the indole-pyridine-indole core is the dominant feature of the main absorption between 280-380 nm attributed to π-π* transitions. However, the absorption profile of **3.1-3.3** is highly sensitive to changes in substitution of the indole nucleus. The presence of the electron-withdrawing substituent such as $–OCF_3$, or the electron-donating $–OCH_3$ groups influence the magnitude of the permanent dipole and therefore the energy of the electronic states.

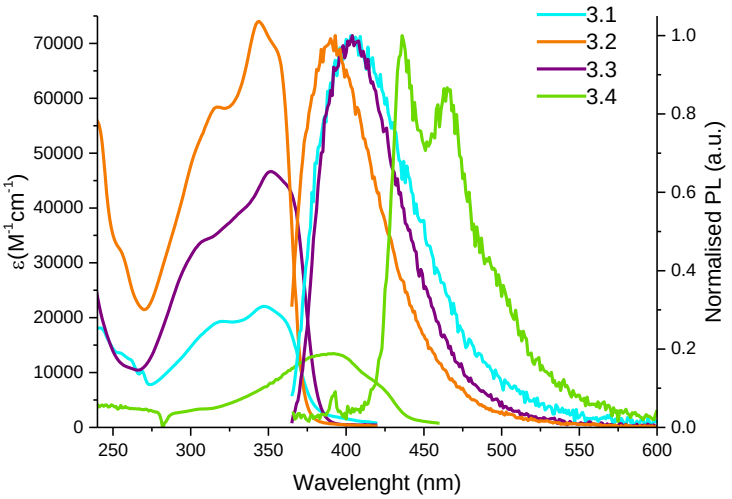

Figure 3-12 Absorption and normalised emission spectra of compounds 3.1-3.4

In comparison, compound **3.4** has a weaker absorption band at λ_{max}= 380 nm, which can be attributed to the changes in donor-acceptor character due to the use of thiophene as the bridging unit. Its band is red-shifted which is suggestive of the involvement of the sulfur atom lone pair in the electron delocalisation. There is a very small overlap between the absorption and emission spectra of compounds **3.1-3.3**. The emission profile of compound **3.1-3.3** consists of an asymmetric band with intensity maxima in the range of 393-404 nm, almost reassembling one another. However, for compound **3.4** the overlap is larger and the emission profile presents two bands with maxima at 435 and 465 nm. In the case of compound **3.4**, we can confirm that the different shape of the band compared with compounds **3.1-3.3**, is not a consequence of using toluene instead of acetonitrile. The efficiency of these novel compounds as emitters has been assessed by measuring the fluorescence quantum yield (Φ). Quantum yield values are obtained according to the literature method[184] using anthracene and 9,10-diphenylanthracene as cross-references. The photophysical properties of the compounds **3.1-3.4** are gathered in **Table 3-3**. Compounds **3.1**, **3.2** and **3.4** give very good quantum yields values of up to 55%. However, an impressive quantum yield of 92 % is achieved with compound **3.3** bearing an -– OCF_3 group. Deviations of the fluorescence quantum yields and extinction coefficients are a result of the structural modifications affecting conjugation, the bridging and peripheral units, planarity, etc. Overall, the difference in the photophysical behaviour of these materials demonstrates the capability of the peripheral groups to fine-tune the optical properties.

Table 3-3 Electronic and optical properties of bis(indolyl)derivatives 3.1-3.4

Z	Absorbance λ_{ab}/nm, ε/$M^{-1}cm^{-1}$	Emission λ_{em}/nm, Φ %	Bandgap, eV
$H_2BIP(H)$	320, 1.9 x 10^4 347, 2.2 x 10^4	403; 40	3.26
$H_2BIP(OCF_3)$	317, 5.8 x 10^4 344, 7.4 x 10^4	393; 92	3.36
$H_2BIP(OCH_3)$	352, 4.7 x 10^4	404; 55	3.15
$H_2BIT(OCH_3)$	380, 1.35 x 10^4	435, 465; 35	2.75

3.10.2 Density functional theory calculations[3]

3.10.2.1 Molecular orbitals

For a better understanding of the photophysical processes, it is crucial to understand the energy levels involved. Photoexcitation promotes the population of excited states with electrons from the ground state. Density functional theory (DFT) has been used to calculate electronic and optical properties of compounds **3.1-3.5**. The DFT has shown that in the case of H_2BIP **(3.1)** and $H_2BIP(OCF_3)$ **(3.2)** the HOMO is mainly localised on the indole, whereas the LUMO is mainly localised on the pyridine orbitals.

[3] In collaboration with Dr Natalia Martsinovich, Department of Chemistry, University of Sheffield

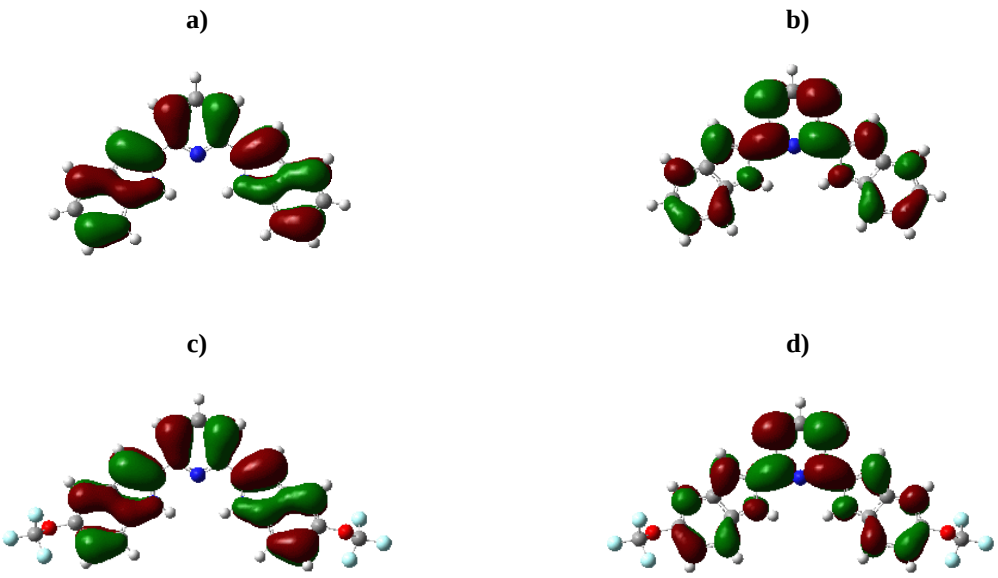

Figure 3-13 Frontier molecular orbitals of H_2BIP: a) HOMO and b) LUMO and $H_2BIP(OCF_3)$: c) HOMO and d) LUMO

In the case of $H_2BIP(OCH_3)$ **(3.3)** the HOMO is mainly localised on the indole with contributions from the orbitals localised on the methoxy group, whereas the LUMO is mainly localised on the pyridine. This different localization of the orbitals is expected leading to charge separation in the photo excited state.

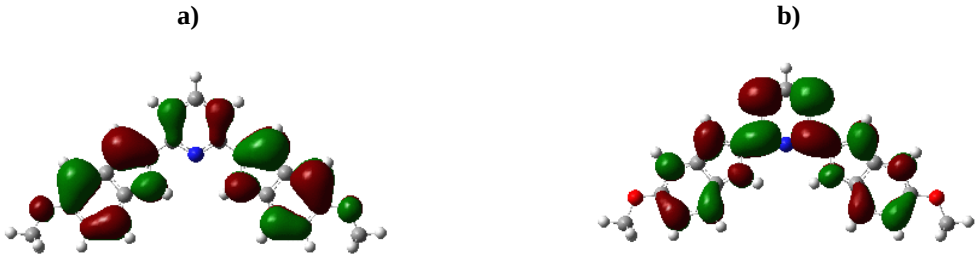

Figure 3-14 Frontier molecular orbitals of $H_2BIP(OCH_3)$: a) HOMO and b) LUMO

In the case of $H_2BIT(OCH_3)$ **(3.4)** and $H_2BIA(OCH_3)$ **(3.5),** the HOMO and LUMO are localised across the whole molecule. Therefore, the charge separation in these compounds is much less pronounced.

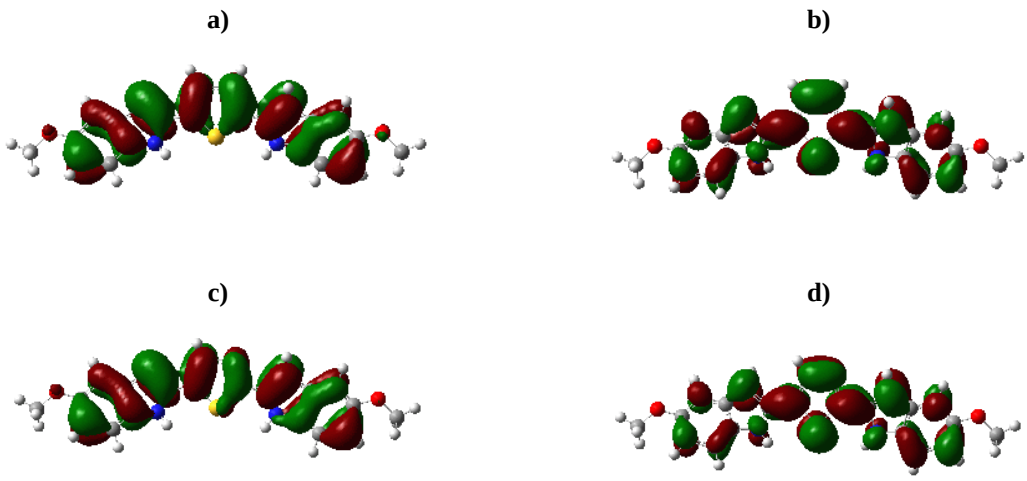

Figure 3-15. Frontier molecular orbitals of H_2BIT: a) HOMO, b) LUMO and H_2BIA: c) HOMO, b) LUMO

3.10.2.2 Electronic properties

The difference in energy between the HOMO and LUMO has been calculated in the solvent acetonitrile and are shown in **Figure 3-16**. The energy gaps are very similar (within 0.08 eV) for all three H_2BIP **3.1-3.3** molecules. There is 0.7-0.8 eV overestimation of the calculated HOMO-LUMO gaps compared to that which is determined by experimentation **(Table 3-3)**, because the calculated HOMO-LUMO gaps do not include exciton binding.[185] The gaps increase in the order H_2BIP(OCH_3)<H_2BIP(H)<H_2BIP(OCF_3), and in excellent agreement with experimental results. The lowest gap of H_2BIP(OCH_3) **3.3** can be attributed to delocalisation of its frontier orbitals onto the methoxy groups, while the higher gap of H_2BIP(OCF_3) **3.2** can be attributed to its non-planarity, and therefore lower conjugation in this molecule. H_2BIA(OCH_3) **(3.5)** and H_2BIT(OCH_3) **(3.4)** have the energy gap 0.5-0.6 eV smaller than the H_2BIP molecules, showing the significant effect of the central pyridine/thiophene/thiazole moiety. This change in the gap is mainly caused by the change in the LUMO energies **(Figure** 3-16**)**:

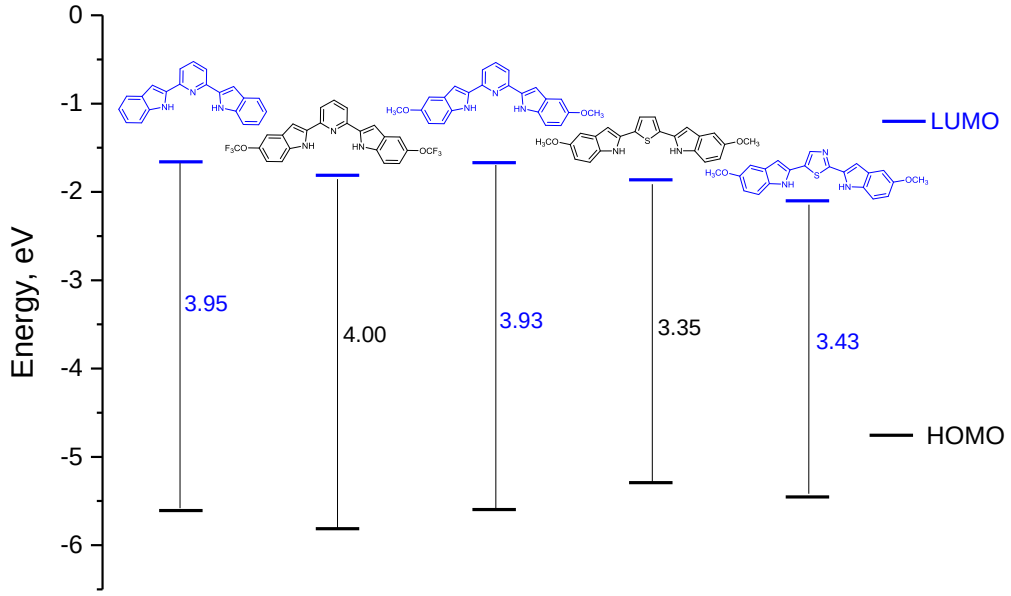

Figure 3-16 Energy of frontier molecular orbitals and band gap energies of compounds 3.1-3.5

3.10.2.3 Geometry

Density functional theory (DFT) calculations predict almost planar geometries for H_2BIP, H_2BIP(OCH_3) and H_2BIP(OCF_3) **(3.1-3.3)**. In comparison with them, the thiophene-based H_2BIT(OCH_3) **(3.4)** and the thiazole-based H_2BIA(OCH_3) **(3.5)** are non-planar. The degree of co-planarity was quantified by measuring the dihedral angles between the two indole groups **(Figure 3-17)**. All the compounds **3.1-3.3** have the dihedral angles of 4-7° in acetonitrile (7-14° in vacuum), H_2BIP(OCF_3) **(3.3)** is the less planar of the three H_2BIP compounds. While the dihedral angle for H_2BIT(OCH_3) **(3.4)** and H_2BIA(OCH_3) **(3.5)** are 38° (or 49° in vacuum) and 17° (or 34° in vacuum) respectively.

The higher planarity of H_2BIP molecules **(3.1-3.3)** can be explained by H-bonding formation between the π-rich indole with the π-deficient pyridine. Pyridine exhibits Lewis basicity , thus making it a good H acceptor[170] compared with the sulfur atom in the thiophene and thiazole heterocycles.

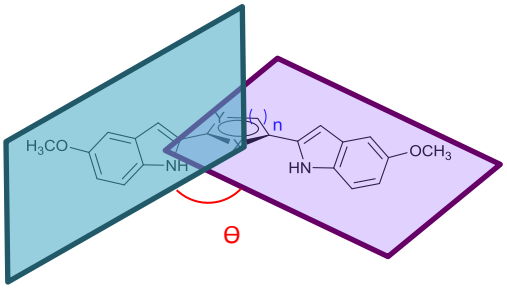

Figure 3-17 Dihedral angles between the planes of the two indole moieties

3.11 Conclusion

The synthesis of novel small π-conjugated materials was studied *via* double Fisher synthesis and Stille cross-coupling protocols. While double Fisher synthesis was limited by the availability of the biscarbonyl compounds and reactivity of the hydrazone intermediates, Stille cross-coupling was proved to be a more efficient method, allowing the synthesis of bis(indolyl)derivatives which are inaccessible *via* Fisher synthesis. The detailed investigation of both synthetic strategies gave a better understanding of the reactivity of the indole derivatives. However, despite several attempts, metalation of the bis(indolyl)derivatives was unsuccessful.

Analysis of these molecules using UV-vis spectroscopy showed the structural dependence of the photoluminescence properties. In addition, the donor-acceptor character of methoxy and trifluoromethoxy groups, together with π-bridging units, showed a dramatic effect on the photophysical properties of the final molecules. Shifts of **3.1-3.4** in absorption/emission spectra are defined by the nature of the linking groups. Also, the extinction coefficient and quantum yields can be controlled *via* the structural features of bisindoles. Compounds **3.1**, **3.2** and **3.4** prensented great quantum yields (up to 55%). However, compound **3.3** bearing OCF_3 group achieved an excellent quantum yield of 92%.

DFT calculations support the trends recorded in the experimental observations of these compounds, thus highlighting the reliability of the computational protocol for comparison of the related structures.

3.12 Experimental

3.12.1 General techniques

All chemicals were obtained from Sigma Aldrich, Alfa Aesar, VWR and Across and used without further purification. Anhydrous solvents were obtained from a PureSolv MD6 solvent purification system. ^{1}H NMR and ^{13}C NMR spectra were recorded on a Bruker Advanced 500 spectrometer. Chemical shifts (δ) are reported in parts per million (ppm) relative to the residual solvent peak and peaks are described as singlet (s), doublet (d), triplet (t), quartet (q), sextet (sex), multiplet (m), broad singlet (br) and coupling constants (J) are quoted in Hertz (Hz). Spectra were recorded in chloroform-d, dichloromethane-d_2 or deuterated DMSO-d_6 and were measured at room temperature unless otherwise stated. Where needed, two dimensional correlation spectroscopy (2D-COSY), heteronuclear single quantum coherence spectroscopy (HSQC) and heteronuclear multiple bond correlation spectroscopy (HMBC) were used in order to aid assignment. The progress of reactions was monitored by TLC and purified by column chromatography using silica gel 60 (40-63μm). High resolution mass spectrometry (HRMS) was performed on Bruker MaXis Impact (EI+) by positive and negative electrospray ionisation. The accepted experimental error was <4 ppm. High performance liquid chromatography (HPLC) was performed on an Agilent 1100 Infinity Series equipped with a UV detector and Ascentis Express C_{18} reverse phase column, using MeCN/water (50-95%) containing 0.1% TFA, at a flow rate of 0.5 mL min^{-1} over a period of 12 minutes. Infrared spectra (IR) were recorded in solid phase on a Bruker Alpha Platinum ATR FTIR spectrometer with vibrational frequencies given in cm^{-1}. Melting points were measured on a Stuart SMP30. The electronic absorption spectra were recorded on a Cary 100 UV-vis scanning spectrometer. The fluorescence spectra were recorded on a FluoroMax-3 spectrofluorimeter. Quantum yields of fluorescence were measured by the relative method using optically dilute solutions.

3.12.2 Experiments

Synthesis of hydrazones **1-4** is discussed in the **Chapter 2**; and full characterisation is given for the new materials in **2.6.2**.

3.12.2.1 2,6-Bis(1H-indol-2-yl)pyridine (3.1)[164]

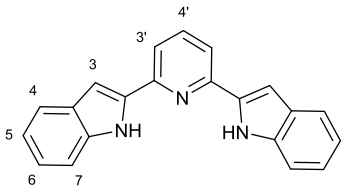

A solution of compound **1** (175 mg, 0.51 mmol) in 1 g of polyphosphoric acid (PPA) was heated at 100°C overnight. The reaction mixture was cooled to room temperature, neutralised with 10% NaOH aqueous solution and extracted with DCM (3 × 75 mL). The combined organic phases were washed with water and dried over anhydrous Na_2S0_4. The solvents were removed under reduced pressure to yield compound **3.1** as a yellow-camel solid (64.3 mg, 41%). **^{1}H NMR** (300 MHz, $CDCl_3$) δ ppm 9.65 (s, 2H, NH), 7.73 (m, 1H, 4'-H), 7.65 (m, 4H, 4-H and 7-H), 7.50 (d, *J* = 8.1 Hz, 2H, 3'-H), 7.25-7.13 (m, 4H, 5-Hand 6-H), 7.07 (s, 2H, 3-H); **m/z (ES+):** Found: 310.1366, requires: 310.1266; **IR ν_{max}/cm^{-1} (solid):** 3433, 3047, 1595, 1564, 1449, 1334, 1300, 786, 743, 612; **M.pt:** 248 °C.

3.12.2.2 2,6-Bis[(5-trifluoromethoxy)-1H-indol-2-yl]pyridine (3.2)

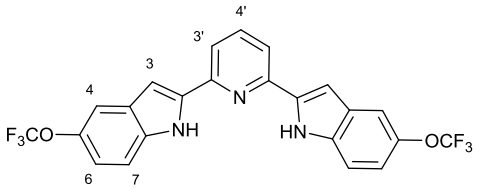

The same procedure as described for compound **3.1** starting from compound **3** (1.13 g, 2.2 mmol) dissolved in 1 g of polyphosphoric acid (PPA) heated at 100 °C overnight. Compound **3.2** was isolated as a yellow solid (446 mg, 43%).**^{1}H NMR** (500 MHz, $CDCl_3$) δ ppm 9.56 (s, 2H, NH), 7.80 (dd, *J* = 8.4, 7.2 Hz, 1H, 4'-H), 7.71 (dd, *J* = 7.2 Hz, 0.6 Hz, 2H, 3'-H), 7.53 (s, 2H, 4-H), 7.48 (d, *J* = 8.8 Hz, 2H, 7-H), 7.14 (dd, *J* = 8.8, 1.4 Hz, 2H, 6-H), 7.08 (d, *J* = 1.4 Hz, 2H, 3-H). **^{13}C NMR** (125 MHz, $CDCl_3$) δ ppm 149.5, 143.6, 138.1, 137.7, 134.9, 129.3, 121.0 (q, J_{F-C} = 255.6 Hz), 119.1, 117.6, 113.7, 112.1, 101.7; **m/z (ES+):** Found: 495.1254 [M+NH_4^+], requires: 495.1250; **IR ν_{max}/cm^{-1} (solid):** 3465, 3314, 1693, 1595, 1564, 1453, 1252, 1191, 1131, 868, 782; **M.pt:** 226 °C.

3.12.2.3 2,6-Bis[(5-methoxy)-1H-indol-2-yl]pyridine (3.3)

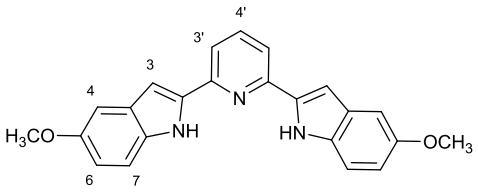

To a solution of **22** (400 mg, 0.61 mmol) in dry THF (20 mL), 1.83 mL of 1M TBAF in THF (1.9 mmol) was added. The reaction was refluxed for 2.5 h. The reaction mixture was hydrolysed with water (15 mL) and extracted with ethyl acetate (3 × 25 mL). The combined organic layers were washed with brine, dried over Na_2SO_4. The solvents were removed under reduced pressure. Compound **3.3** was purified by column chromatography on Silica (Hex-EtOAc with a gradient from 9:3 to 7:3) yielding a yellow solid (54 mg, 24%). **^{1}H NMR** (500 MHz, CD_2Cl_2) δ ppm 9.68 (s, 2H, NH), 7.78 (dd, *J* = 8.2, 7.1 Hz, 1H, 4'-H), 7.69 (dd, *J* = 8.2, 0.7 Hz, 2H, 3'-H), 7.43 (d, *J* = 8.8 Hz, 2H, 7-H), 7.11 (d, *J* = 2.5 Hz, 2H, 4-H), 7.02 (dd, *J* = 2.0, 0.7 Hz, 2H, 3-H), 6.90 (dd, *J* = 8.8, 2.5 Hz, 2H, 6-H), 3.86 (s, 6H, OCH_3); **^{13}C NMR** (125 MHz, CD_2Cl_2) δ ppm 155.1, 150.3, 137.7, 137.6, 132.3, 130.0, 118.4, 114.4, 112.6, 102.7, 101.1, 56.1; **m/z (ES+):** Found: 370.1561, requires 370.1550; **IR ν_{max}/ cm^{-1} (solid):** 3430, 3446, 2922, 2853, 1623, 1594, 1562, 1540, 1450, 1211, 781; **M.pt:** 295 °C.

3.12.2.4 2,5-Bis[(5-methoxy)-1H-indol-2-yl]thiophene (3.4)

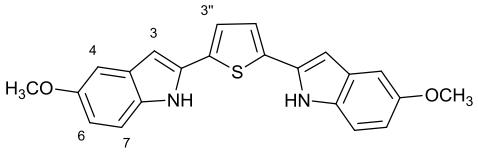

The same procedure as described for compound **3.3**, starting from compound **25** (223 mg, 0.34 mmol) and TBAF (1.7 mmol, 1M in THF). Compound **3.4** was purified by column chromatography (Hex-EtOAc, 7:3) and isolated as a green solid (51 mg, 40%). **^{1}H NMR** (400 MHz, CD_3CN) δ ppm 9.78 (s, 2H, N-H), 7.33 (s, 2H, 3''-H), 7.28 (dt, *J* = 8.8, 0.7 Hz, 2H, 7-H), 7.05 (d, *J* = 2.5 Hz, 2H, 4-H), 6.80 (dd, *J* = 8.8, 2.5 Hz, 2H, 6-H), 6.65 (dd, *J* = 2.2, 0.8 Hz, 2H, 3-H), 3.80 (s, 6H, OCH_3); **^{13}C NMR** (125 MHz, CD_2Cl_2) δ ppm 155.2, 134.9, 133.0, 132.3, 130.0, 123.9, 113.4, 112.0, 102.4, 101.0, 56.1; **m/z (ES+):** Found: 375.1159 [M+H], requires: 375.1162; **IR ν_{max}/cm^{-1} (solid):** 3448, 3409, 3064, 2916, 2848, 1699, 1450, 1437, 1220, 1028, 779; **M.pt:** 251 °C.

3.12.2.5 5-Methoxy-3-phenyl-1H-indole (7)[186]

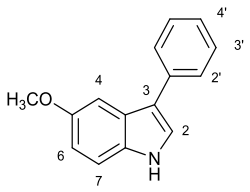

4-Methoxyphenylhydrazine hydrochloride (980 mg, 5.6 mmol) was dissolved in a heated solution of sodium acetate (1.18 g, 14.4 mmol) in glacial acetic under a nitrogen atmosphere. Phenylacetaldehyde (1.00 mL, 8.6 mmol) was added dropwise. The reaction mixture was stirred overnight at 75°C, then after cooling was poured into water (20 mL) and extracted with diethyl ether (3 × 25 mL). The combined organic layers were washed with a saturated solution of $NaHCO_3$ (3 × 30 mL) until the pH was adjusted to 7 and dried over Na_2SO_4. The solvents were removed under reduced pressure, the residue was passed through a silica plug and purified by column chromatography on Silica (Hexane-Diethyl ether, 1:7) to yield compound **7** as a yellow solid (0.81 g, 60%). **^{1}H NMR** (500 MHz, $CDCl_3$) δ ppm 8.15 (br s, 1H, NH), 7.65 (dd, *J* = 7, 1.2 Hz, 2H, 2'-H), 7.46 (t, *J* = 7.0 Hz, 2H, 3'-H), 7.38 (d, *J* = 2.4 Hz, 1H, 4-H), 7.36 – 7.28 (m, 3H, 2-H and 7-H), 6.92 (dd, *J* = 8.8, 2.4 Hz, 1H, 6-H), 3.87 (s, 3H, OCH_3); **^{13}C NMR** (125 MHz, $CDCl_3$) δ ppm 154.8, 135.9, 132.0, 128.9, 127.4, 126.2, 126.0, 122.8, 118.2, 112.7, 112.3, 101.7, 56.1; **m/z (ES+):** Found: 224.1069 [M+H], requires 224.1075; **IRν_{max}/cm^{-1}:** 3402, 3006, 2956, 2827, 1613, 1598, 1580, 1537; **M.pt:** 69.8-70.8 °C.

3.12.2.6 3-*n*-Butyl-5-methoxy-1H-indole (8)[187]

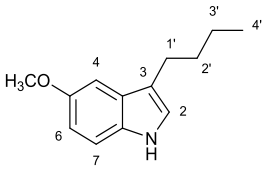

The same procedure as described for compound **7** using hexanal (2 mL, 16.7 mmol), NaOAc (3 g, 36.14 mmol) and 4-methoxyphenylhydrazine hydrochloride (2.43 g, 13.9 mmol). The residue was passed through a silica plug and then purified by column chromatography on Silica (Hexane-DCM, 1:9) to yield the compound **8** as a yellow oil (2.00 g, 67%). **^{1}H NMR** (500 MHz, $CDCl_3$) δ ppm 7.78 (br s, 1H, NH), 7.24 (d, *J* = 8.8 Hz, 1H, 7-H), 7.05 (d, *J* = 2.5 Hz, 1H, 4-H), 6.95 (d, *J* = 2.2 Hz, 1H, 2-H), 6.85 (dd, *J* = 8.8, 2.5 Hz, 1H, 6-H), 3.88 (s, 3H, OCH_3), 2.72 (t, *J* = 7.4 Hz, 2H, 1'-H), 1.69 (dt, *J* = 15.3, 7.4 Hz, 2H, 2'-H), 1.43 (sex, *J* = 7.4 Hz, 2H, 3'-H), 0.96 (t, *J* = 7.4 Hz, 3H, 4'-H); **^{13}C NMR** (125 MHz, $CDCl_3$) δ ppm 154.0, 131.7, 128.2, 122.0, 117.1, 112.1, 111.8, 101.2, 56.2, 32.3, 25.0, 22.8, 14.2; **m/z (ES+):** Found:

204.1390 [M+H], requires 204.1310; **IRν_{max}/cm^{-1}(liquid):** 3414, 2954, 2926, 2855, 1623, 1582, 1482.

3.12.2.7 2-Bromo-3-*n*-butyl-5-methoxy-1H-indole (10)

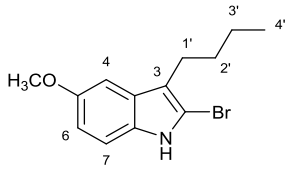

N-bromosuccinimide (415 mg, 2.5 mmol) in small portions was added to an ice cooled solution of compound **8** (515 mg, 2.5 mmol) in chloroform (80 mL). The reaction was wrapped with foil and allowed to react for 1h at room temperature. The reaction mixture was diluted in DCM (20 mL) and washed with water (3 × 20 mL). The combined organic layers were washed with brine, dried over Na_2SO_4 and the solvents were evaporated under reduced pressure yielding compound **10**. **^{1}H NMR** (300 MHz, $CDCl_3$) δ ppm 7.80 (s, 1H, NH), 7.17 (d, *J* = 8.8 Hz, 1H, 6-H), 6.97 (d, *J* = 2.5 Hz, 1H, 4-H), 6.82 (dd, *J* = 8.8, 2.5 Hz, 1H, 7-H), 3.86 (s, 3H, OCH_3), 2.68 (t, *J* = 7.5 Hz, 2H, 1'-H), 1.64 (dt, *J* = 14.7, 7.5 Hz, 2H, 2'-H), 1.39 (td, *J* = 14.7, 7.5 Hz, 2H, 3'-H), 0.94 (t, *J* = 7.5 Hz, 3H, 4'-H); **m/z (ES+):** Found: 282.0480 [M+H], requires 282.0415.

3.12.2.8 2,6-Dibromo-3-*n*-butyl-5-methoxy-1H-indole (11)

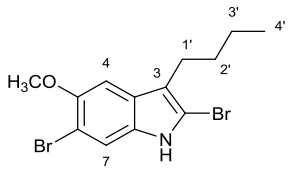

The same procedure as described for compound **10** using N-bromosuccinimide (111 mg, 0.67 mmol) and compound **8** (126 mg, 0.61 mmol). Compound **11** was purified by column chromatography on Silica (Hex-DCM, 4:3) and isolated as a brown oil (13 mg, 5.8%). **^{1}H NMR** (500 MHz, $CDCl_3$) δ ppm 7.81 (s, 1H, NH), 7.47 (s, 1H, 7-H), 6.97 (s, 1H, 4-H), 3.93 (s, 3H, OCH_3) 2.67 (t, *J* = 7.5 Hz, 2H, 1'-H), 1.61 (dt, *J* = 14.7, 7.5 Hz, 2H, 2'-H), 1.38 (dq, *J* = 14.7, 7.5 Hz, 2H, 3'-H), 0.94 (d, *J* = 7.5 Hz, 3H, 4'-H).

3.12.2.9 3-*n*-Butyl-5-methoxy-1-phenylsulfonylindole (13)

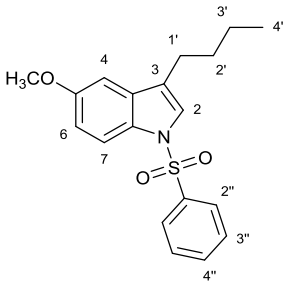

NaH (240 mg, 5.9 mmol, 60% dispersion in oil) was charged with nitrogen, washed with 2 mL of Hexane twice before being dissolved in THF (7 mL) and then, a solution of compound **8** (401 mg, 2.0 mmol) in THF (4 mL) was added dropwise at 0°C. The reaction mixture was left to stir for 1h at room temperature. Benzenesulfonyl chloride (0.50 mL, 3.9 mmol) was added dropwise at the same temperature and the reaction was stirred for 7h. The reaction mixture was hydrolysed with water (10 mL) and extracted with diethyl ether (3 × 25 mL). The combined organic layers were washed with brine and dried over Na_2SO_4. The solvents were evaporated under reduced pressure. Compound **13** was purified by column chromatography on Silica (Hex-DCM, 1:3) yielding a rose-white solid (230 mg, 57%).**^{1}H NMR** (500 MHz, CD_2Cl_2) δ ppm 7.86 (dd, *J* = 8.1, 1.5 Hz, 1H, 7-H), 7.81 (dd, *J* = 7.5, 1.2 Hz, 2H, 2’’-H), 7.53 (t, *J* = 7.5 Hz, 1H, 4’’-H), 7.42 (t, *J* = 7.5 Hz, 2H, 3’’-H), 7.28 (s, 1H, 2-H), 6.91 (d, *J* = 8.1, 1H, 6-H) 6.89 (s, 1H, 4-H), 3.81 (s, 3H, OCH_3), 2.61 (t, *J* = 7.5 Hz, 2H, 1’-H), 1.64 (dt, *J* = 14.7, 7.4 Hz, 2H, 2’-H), 1.39 (dq, *J* = 14.7, 7.4 Hz, 2H, 3’-H), 0.94 (t, *J* = 7.4 Hz, 3H, 4’-H); **^{13}C NMR** (125 MHz, CD_2Cl_2) δ ppm 156.9, 138.4, 134.0, 132.9, 130.5, 129.5, 127.0, 124.8, 123.9, 115.0, 113.7, 102.7, 56.0, 31.3, 24.9, 22.8, 14.0; **m/z (ES+)**: Found: 344.1317 [M+H], requires 344.1242; **IRν_{max}/cm^{-1}(solid)**: 3005, 2955, 2928, 2869, 2833, 1609, 1446, 1251; **M.pt**: 77.1-77.8 °C.

3.12.2.10 5-Methoxy-3-phenyl-1-phenylsulfonylindole (14)[188]

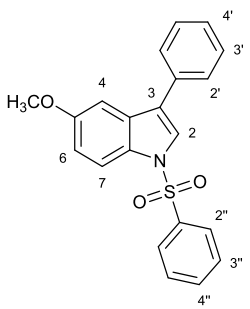

NaH (160 mg, 3.8 mmol, 57-63% dispersion in oil) was charged with nitrogen, washed with 2 mL of Hexane twice before being dissolved in THF (5 mL) and then, a solution of solution

of compound **7** (573 mg, 2.6 mmol) in THF (7 mL) was added dropwise at 0°C. The reaction mixture was left to stir for 1h at room temperature. Benzenesulfonyl chloride (0.36 mL, 2.8 mmol) was added dropwise at the same temperature and the reaction was stirred for 45 min. The reaction mixture was hydrolysed with water (10 mL) and extracted with diethyl ether (3 × 25 mL). The combined organic layers were washed with brine, dried over Na_2SO_4. The solvents were evaporated under reduced pressure. Compound **14** was purified by column chromatography on Silica (Hex-DCM, 1:13) yielding a white solid (808 mg, 87%). **^{1}H NMR** (500 MHz, $CDCl_3$) δ ppm 7.96 (d, *J* = 9.0 Hz, 1H, 7-H), 7.89 (dd, *J* = 8.3, 0.9 Hz, 2H, 2''-H), 7.64 (s, 1H, 2-H), 7.60 – 7.56 (m, 2H, 2'-H), 7.56 – 7.51 (m, 1H, 4''-H), 7.45 (m, 4H, 3'-H and 3''-H), 7.40 – 7.34 (m, 1H, 4'-H), 7.20 (d, *J* = 2.5 Hz, 1H, 4-H), 6.98 (dd, *J* = 9.0, 2.5 Hz, 1H, 6-H), 3.82 (s, 3H, OCH_3); **^{13}C NMR** (125 MHz, $CDCl_3$) δ ppm 198.0, 157.0, 155.6, 138.3, 134.0, 133.2, 129.4, 129.1, 128.0, 127.7, 126.9, 124.5, 123.9, 114.9, 114.1, 103.2, 55.9; **m/z (ES+):** Found 364.1006 [M+H]**,** requires 364.0929; **IRν_{max}/cm^{-1} (solid):** 3135, 3061, 2920, 1611, 1471, 1364; **M.pt:** 127.5-128.0 °C.

3.12.2.11 5-Methoxy-1-phenylsulfonylindole (15)[189]

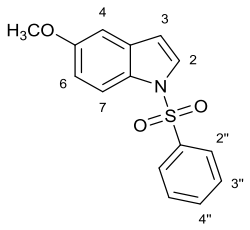

To a solution of compound **9** (4.12 g, 27.9 mmol) in dry THF (20 mL) under nitrogen was added dropwise a solution of NaH (1.53 g, 36.4 mmol) in dry THF (250 mL) at 0 °C. The reaction mixture was warmed to room temperature and reacted for 1h. The mixture was cooled to 0 °C before the addition of benzenesulfonyl chloride (3.6 mL, 28.0 mmol). The reaction mixture reacted overnight. Once completed, the reaction mixture was hydrolysed with water (15 mL) and extracted with ethyl acetate (3 × 25 mL). The combined organic phases were washed with brine and dried over Na_2SO_4. The solvents were removed under reduced pressure. Compound **15** was recrystallised from EtOH and isolated as an off-white crystalline (6.34 g, 79%). **^{1}H NMR** (500 MHz, $CDCl_3$) δ ppm 7.88 (d, *J* = 9.0 Hz, 1H, 7-H), 7.84 (dd, *J* = 8.5, 1.2 Hz, 2H, 2''-H), 7.54 – 7.50 (m, 2H, 2-H and 4''-H), 7.42 (t, *J* = 7.8 Hz, 2H, 3''-H), 6.97 (d, *J* = 2.5 Hz, 1H, 4-H), 6.92 (dd, *J* = 9.0, 2.5 Hz, 1H, 6-H), 6.59 (dd, *J* = 3.6, 0.6 Hz, 1H, 3-H), 3.81 (s, 3H, OCH_3); **^{13}C NMR** (125 MHz, $CDCl_3$) δ ppm 133.9, 129.4, 127.3, 126.8, 114.6, 113.9, 109.5, 103.9, 55.8; **m/z (ES+):** Found: 288.0693 [M+H], requires 288.0690;

IR ν_{max}/cm^{-1} (solid): 3136, 3103, 3000, 2949, 2839, 15832, 1445, 1436, 1370, 1141, 1120, 1090, 994; **M.pt:** 95-97 °C.

3.12.2.12 5-Methoxy-3-phenyl-1-phenylsulfonyl-2-trimethylstannylindole (16)

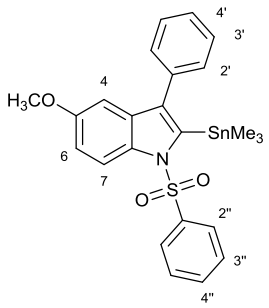

To a solution of compound **14** (1.64 g, 4.5 mmol) in THF (30 mL) was added 1.6 M hexane solution of *n*BuLi (4.48 mL, 7.2 mmol) at -78°C within 45 min. The orange solution was allowed to reach room temperature and was left sitting for 1 h. Trimethyltin chloride (7.48 mL, 7.2 mmol, 1M in THF) was added dropwise at -78°C and the reaction was left for 2h. The reaction mixture was hydrolysed with water (15 mL) and extracted with ethyl acetate (3 × 25 mL). The combined organic layers were washed with a saturated solution of KF, dried over Na_2SO_4 and the solvents were evaporated under reduced pressure. Compound **15** was purified by column chromatography on Silica (Hex-EtOAc, 9:1) yielding a white solid (210 mg, 35%). **^{1}H NMR** (500 MHz, C_2D_6O) δ ppm 7.77 (d, *J* = 9.0 Hz, 1H, 7-H), 7.70 (d, *J* = 7.3 Hz, 2H, 2''-H), 7.63 (t, *J* = 7.3 Hz, 1H, 4''-H), 7.58 – 7.49 (m, 4H, 3''-H and 3'-H), 7.47 (d, *J* = 7.3 Hz, 1H, 4'-H), 7.44 (dd, *J* = 6.7, 1.5 2H, 2'-H), 6.91 (dd, *J* = 9.0, 2.5 Hz, 1H, 6-H), 6.71 (d, *J* = 2.5 Hz, 1H, 4-H), 3.66 (s, 3H, OCH_3), 0.09 (9H, $SnMe_3$); **^{13}C NMR** (125 MHz, C_2D_6O) δ ppm 156.5, 141.8, 138.2, 136.7, 134.2, 134.1, 132.9, 132.6, 129.8, 129.5, 128.8, 128.2, 126.2, 115.1, 113.7, 101.3, 55.3, -5.2; **m/z (ES+):** Found: 528.0655 [M+H], requires 528.0577; **IRν_{max}/cm^{-1} (solid):** 3060, 2991, 2921, 1768, 1525, 1360, 1216; **M.pt:** 112.4-113.6 °C.

3.12.2.13 5-Methoxy-3-phenyl-1-[(2'-trimethylstannyl)phenylsulfonyl]-2-trimethylstannylindole (17)

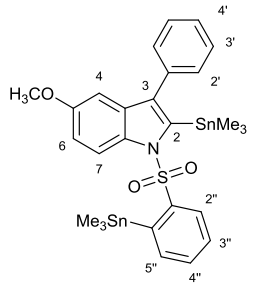

The same procedure as described for compound **16**. Compound **17** was isolated as a violet solid (216 mg, 7%). **^{1}H NMR** (500MHz, C_2D_6O) δ ppm 7.79 (dd, *J* = 7.7, 1.1 Hz, 1H, 2''-H), 7.60 – 7.49 (m, 7H,2'-4'H and 3''-H), 7.43 (td, *J* = 7.7, 1.1 Hz, 1H, 4''-H), 7.40 (d, *J* = 9.0 Hz, 1H, 7-H), 6.96 (dd, *J* = 7.7, 1.1 Hz, 1H, 5''-H), 6.87 (dd, *J* = 9.0, 2.5 Hz, 1H, 6-H), 6.79 (d, *J* = 2.5 Hz, 1H, 4-H), 3.70 (s, 3H, OCH_3), 0.47 (s, 9H, $SnMe_3$), 0.01 (s, 9H, $SnMe_3$); **^{13}C NMR** (125 MHz, C_2D_6O) δ ppm 156.2, 145.2, 141.9, 141.9, 137.5, 135.8, 134.2, 132.6, 132.6, 132.4, 130.1, 129.7, 128.7, 128.0, 124.5, 114.0, 113.5, 101.5, 55.3, -5.2, -5.2; **m/z (ES+):** Found: 692.0279 [M+H], requires 692.0225; **IRν_{max}/cm^{-1} (solid):** 3053, 2957, 2918, 1738, 1606, 1487, 1431, 1345; **M.pt:** 58.2-59.0 °C.

3.12.2.14 5-Methoxy-1-phenylsulfonyl-2-trimethylstannylindole (18)

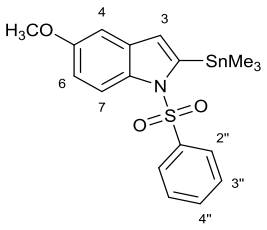

To a solution of compound **15** (3.94 g, 13.7 mmol) in THF (30 mL) was added 2M THF solution of LDA (10.3 mL, 20.5 mmol) at -20°C dropwise. The orange solution was allowed to reach room temperature and was left sitting for 1 h. Trimethyltin chloride (21.3 mL, 20.5 mmol, 1M in THF) was added dropwise at -78°C and the reaction was left for 2h. The reaction mixture was hydrolysed with water (15 mL) and extracted with ethyl acetate (3 × 25 mL). The combined organic layers were washed with a saturated solution of KF, dried over Na2SO4 and the solvents were evaporated under reduced pressure. Compound **18** was purified by column chromatography on Silica (Hex-DCM, 1:1) yielding a white solid (4.10 g, 67%). **^{1}H NMR** (500 MHz, $CDCl_3$) δ ppm 7.74 (d, *J* = 9.0 Hz, 1H, 7-H), 7.65 (dd, *J* = 7.9 Hz, 1.0 Hz, 2H, 2''-H), 7.49 (t, *J* = 7.9 Hz, 1H, 4''-H), 7.39 (t, *J* = 7.9 Hz, 2H, 3''-H), 6.49 (d, *J* = 2.5

Hz, 1H, 4-H), 6.82 (dd, *J* = 9.0 Hz, 2.5Hz, 1H, 6-H), 6.77 (d, *J* = 2.5 Hz, 1H, 4-H), 3.80 (s, 3H, OCH_3), 0.42 (s, 9H, $SnMe_3$); **^{13}C NMR** (100 MHz, $CDCl_3$) δ ppm 156.4, 144.6, 139.1, 133.5, 133.2, 133.0, 129.2, 126.4, 120.5, 114.5, 113.3, 102.7, 55.7, -6.6; **m/z (ES+):** Found: 474.0155 [M+Na], requires: 474.0158; **IR ν_{max}/cm^{-1} (solid):** 3068, 2972, 2913, 2833, 1586, 1506, 1586, 1506, 1448, 1422, 1362 1145, 1108, 1089; **M.pt:** 64-65°C.

3.12.2.15 6-(5-Methoxy-3-phenyl-1-phenylsulfonylindol-2-yl)-2-bromopyridine (20)

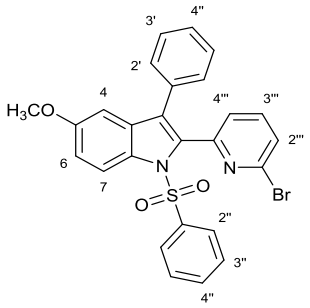

A solution of 2,6-dibromopyridine (27 mg, 0.11 mmol), compound **16** (139 mg, 0.26 mmol) and CuI (2 mg, 10%) in THF (5 mL) was degassed and bubbled with nitrogen for 30 min. Then, $Pd(PPh_3)_4$ (13.3 mg, 10%) dissolved in THF (2 mL) was added. The reaction mixture was transferred to a pre-heated hot-plate at 65 °C and refluxed for 4h. The reaction mixture was hydrolysed with 10 mL of water and extracted with ethyl acetate (3 x 15 mL). The combined organic layers were washed with brine, dried over Na_2SO_4 and the solvents were removed under reduced pressure. Compound **20** was purified by column chromatography on Silica (Hex-EtAcO, 7:3) and/or HPLC (50:95+Formic acid 0.1%) to yield the compound as a yellow-orange solid (160 mg, 84%). **^{1}H NMR** (500 MHz, DMSO) δ ppm 8.05 (d, *J* = 9.2 Hz, 1H, 7-H), 7.95 (dd, *J* = 7.8, 1.1 Hz, 2H, 2''-H), 7.75 (t, *J* = 7.4 Hz, 1H, 3'''-H), 7.71 (m, 2H, 4''-H and 4'''-H), 7.61 (t, *J* = 7.8 Hz, 2H, 3''-H), 7.52 (dd, *J* = 7.4, 0.8 Hz, 1H, 2'''-H), 7.35 (t, *J* = 7.2 Hz, 2H, 3'-H), 7.30 (t, *J* = 7.2 Hz, 1H, 4'-H), 7.22 (dd, *J* = 7.2, 1.4 Hz, 2H, 2'-H), 7.10 (dd, *J* = 9.2, 2.5 Hz, 1H, 6-H), 6.88 (d, *J* = 2.5 Hz, 1H, 4-H), 3.72 (s, 3H, OCH_3); **^{13}C NMR** (125 MHz, DMSO) δ ppm 156.8, 151.2, 140.0, 140.0, 136.9, 134.6, 134.1, 131.0, 130.0, 129.9, 129.5, 129.5, 128.6, 127.9, 127.8, 126.9, 126.3, 125.1, 115.9, 115.0, 102.4, 55.4; **m/z (ES+):** Found: 519.0383 [M+H], requires 519.0300; **IRν_{max}/cm^{-1} (solid):** 3052, 2917, 2849, 1606, 1541, 1495, 1448, 1334; **M.pt:** 161.0-161.9°C.

3.12.2.16 1,3-bis(5-Methoxy-1-(phenylsulfonyl)-1H-indol-2-yl)benzene (21)

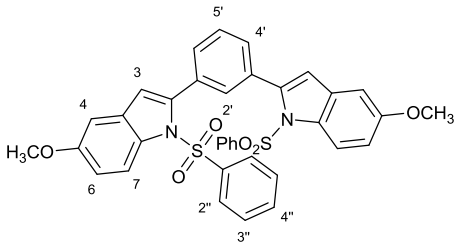

The same procedure as described from compound **20** starting from compound **18** (1.07 g, 2.35 mmol), 1,3-dibromobenzene (0.13 mL, 1.08 mmol), CuI (41 mg, 20%) and $Pd(PPh_3)_4$ (124 mg, 20%). Compound **21** was purified by column chromatography on Silica (Hex-EtOAc, gradient from 4:1) and isolated as a brown solid (56 mg, 8.0%).**^{1}H NMR** (400 MHz, $CDCl_3$) δ ppm 8.20 (d, *J* = 9.1 Hz, 2H, 7-H), 7.81 (s, 1H, 2'-H), 7.57 (d, *J* = 7.8 Hz, 2H, 4''-H), 7.47 (d, *J* = 7.8 Hz, 5H, 3''-H and 5'-H), 7.42 (t, *J* = 7.6 Hz, 2H, 4'-H), 7.29 (t, *J* = 7.8 Hz, 4H, 2''-H), 6.97 (dd, *J* = 9.1, 2.6 Hz, 2H, 6-H), 6.89 (d, *J* = 2.6 Hz, 2H, 4-H), 6.60 (s, 2H, 3-H), 3.83 (s, 6H, OCH_3); **^{13}C NMR** (100 MHz, $CDCl_3$) δ ppm 157.4, 142.9, 136.9, 133.7, 133.1, 132.0, 132.0, 131.6, 130.5, 128.8, 127.1, 126.9, 118.0, 114.9, 113.8, 103.4, 55.7; **m/z (ES+):** Found: 671.1279 [M+Na], requires: 671.1281; **IR ν_{max}/cm^{-1} (solid):** 3072, 2995, 2921, 2851, 2832, 1609, 1585, 1477, 1462, 1448, 1368, 1260, 1424; **M.pt:** 177-179 °C.

3.12.2.17 2,6-Bis(5-methoxy-1-phenylsulfonylindol-2-yl)pyridine (22)

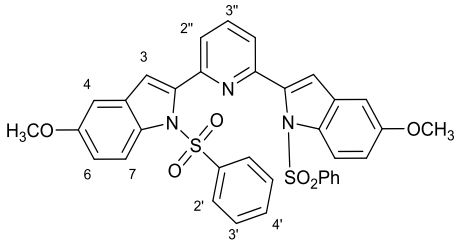

The same procedure as described for compound **20** starting from compound **18** (1.13g, 2.5 mmol), 2,6-dibromopyridine (270 mg, 1.2 mmol), CuI (40 mg, 20%), and $Pd(PPh_3)_4$ (133 mg, 10%) refluxed overnight at 90 °C. Compound **22** was purified by column chromatography (Hex-EtOAc, 7:3) and isolated as a white solid (0.70 g, 92%). **^{1}H NMR** (500 MHz, CD_2Cl_2) δ ppm 8.06 (d, *J* = 8.9 Hz, 2H, 7-H), 7.92 (dd, *J* = 8.1, 7.5 Hz, 1H, 4''-H), 7.75 – 7.71 (m, 6H, 2'-H and 3''-H), 7.36 (t, *J* = 7.4, 1.2 Hz, 2H, 4'-H), 7.16 (dd, *J* = 8.4, 7.4 Hz, 4H, 3'-H), 7.00-6.98 (m, 4H, 4-H and 6-H), 6.87 (d, *J* = 0.7 Hz, 2H, 3-H), 3.82 (s, 6H, OCH_3); **^{13}C NMR** (125 MHz, CD_2Cl_2) δ ppm 157.7, 151.0, 142.1, 137.5, 135.8, 133.9, 133.1, 131.9, 129.0, 127.7, 125.2, 117.5, 116.0, 114.7, 104.1, 56.0; **m/z (ES+):** Found: 650.1434 [M+H], requires:

650.1414; **IR ν_{max}/cm^{-1} (solid):** 3060, 2999, 2954, 2837, 1606, 1563, 1474, 1448, 1427, 1366, 1359, 1177, 1143, 601, 570; **M.pt:** 197-200°C.

3.12.2.18 2,5-Bis(5-methoxy-1-phenylsulfonylindol-2-yl)thiophene (24)

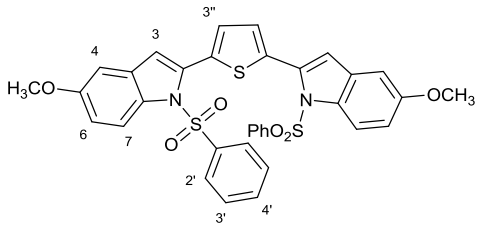

The same procedure as described from compound **20** starting from compound **18** (900 mg, 2.0 mmol), 2,5-dibromothiophene (220 mg, 0.91 mmol), CuI (35 mg, 20%) and $Pd(PPh_3)_4$ (158 mg, 15%). Compound **24** was purified by column chromatography on Silica (Hex-EtOAc, gradient from 4:1 to 7:3) and isolated as a green solid (515 mg, 89%). **^{1}H NMR** (500 MHz, $CDCl_3$) δ ppm 8.23 (d, *J* = 9.2 Hz, 2H, 7-H), 7.53 (dd, *J* = 8.4, 1.1 Hz, 4H, 2'-H), 7.47 (t, *J* = 7.6 Hz, 2H, 4'-H), 7.32 (dd, *J* = 8.4, 7.6 Hz, 4H, 3'-H), 7.27 (s, 2H, 3''-H), 7.00 (dd, *J* = 9.2, 2.6 Hz, 2H, 6-H), 6.90 (d, *J* = 2.6 Hz, 2H, 4-H), 6.63 (s, 2H, 3-H), 3.84 (s, 6H, OCH_3); **^{13}C NMR** (125 MHz, $CDCl_3$) δ ppm 157.3, 137.4, 134.6, 134.2, 133.9, 133.2, 131.3, 130.3, 129.0, 127.1, 117.8, 115.2, 114.4, 103.3, 55.8; **m/z (ES+):** Found: 655.1029 [M+H], requires: 655.1026; **IR ν_{max}/cm^{-1} (solid):** 3073, 3000, 2920, 2834, 1585, 1464, 1447, 1434, 1370, 1207, 1174, 1144, 600, 569; **M.pt:** 152-156 °C.

3.12.2.19 2,5-Bis(5-methoxy-1-phenylsulfonylindol-2-yl)thiazole (25)

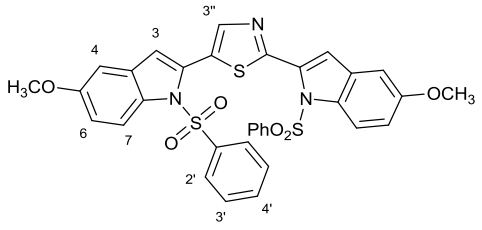

Same procedure as described from compound **20** starting from compound **18** (0.58 mmol, 2.2 equiv), 2,5-dibromothiazole (0.26 mmol), CuI (20%) and $Pd(PPh_3)_4$ (20%). Chemical conversion is quantitative; however, compound **25** rapidly decomposes. **^{1}H NMR** (300 MHz, CD_2Cl_2) δ 8.06 (d, *J* = 8.6 Hz, 2H, 7-H), 7.93 (dd, *J* = 8.3, 7.3 Hz, 1H, 3''-H), 7.77 – 7.69 (m, 4H, 2'-H), 7.40 – 7.32 (m, 4H, 4'-H), 7.16 (t, *J* = 7.9 Hz, 4H, 3'H), 6.99 (m, 4H, 4-H and 6- H), 6.88 (s, 2H, 3-H), 3.82 (s, 6H, OCH_3).

3.12.2.20 Bis(5-methoxy-1-phenylsulfonylindol-2-yl) (28)

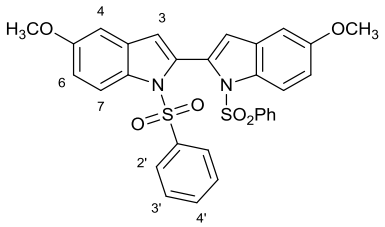

The same procedure as described for compound **20** starting from compound **18** (392 mg, 0.87 mmol), 2,5-dibromothiophene (97 mg, 0.40 mmol), CuI (15.2 mg, 20%) and $Pd(PPh_3)_4$ (92.5 mg, 20%). Compound **28** was purified by column chromatography on Silica (Hex-EtOAc, 7:3). **^{1}H NMR** (400 MHz, $CDCl_3$) δ ppm 8.16 (d, *J* = 9.0 Hz, 2H, 7-H), 7.63 (d, *J* = 7.4 Hz, 2H, 2'-H), 7.49 (t, *J* = 7.4 Hz, 2H, 4'-H), 7.35 (t, *J* = 7.8 Hz, 4H, 3'-H), 7.04 (dd, *J* = 9.2, 2.4 Hz, 2H, 6-H), 6.99 (d, *J* = 2.1 Hz, 2H, 4-H), 6.51 (s, 2H, 3-H), 3.86 (s, 6H, OCH_3); **m/z (ES+):** Found: 595.0979 [M+Na], requires 595.0968.

3.12.2.21 2-(5-Methoxy-1-phenylsulfonylindol-2yl)-5-(5-methoxy-1H-indol-2-yl)thiophene (29)

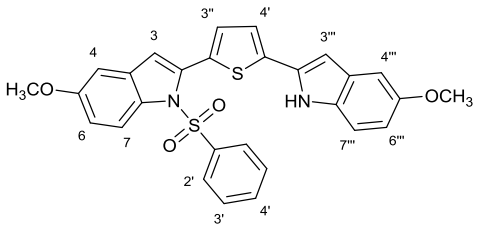

Compound **29** was isolated as the 2nd product following the procedure for the compound **2.4**. Green solid (52 mg, 30%). **^{1}H NMR** (500 MHz, $CDCl_3$) δ ppm 8.21 (d, *J* = 9.2 Hz, 2H, 7-H and NH), 7.48 – 7.38 (m, 3H, PG), 7.31 (d, *J* = 3.8 Hz, 1H, 3''-H), 7.28 – 7.21 (m, 3H, 7-H and PG), 7.24 (d, *J* = 3.8 Hz, 1H, 4''-H), 7.06 (d, *J* = 2.5 Hz, 1H, 4'''-H), 6.99 (dd, *J* = 9.2, 2.6 Hz, 1H, 6-H), 6.88 (dd, *J* = 8.7, 2.5 Hz, 2H, 4-H and 6'''-H), 6.69 (dd, *J* = 2.1, 0.8 Hz, 1H, 3'''-H), 6.60 (d, *J* = 0.6 Hz, 1H, 3-H), 3.86 (s, 3H, OCH_3'''), 3.83 (s, 3H, OCH_3); **^{13}C NMR** (125 MHz, $CDCl_3$) δ ppm 157.4, 154.9, 137.4, 137.1, 134.8, 133.8, 133.2, 132.6, 132.1, 131.4, 131.4, 131.3, 129.7, 128.9, 126.9, 122.9, 117.9, 114.9, 114.3, 113.3, 111.8, 103.2, 102.3, 101.0, 56.0, 55.8; **m/z (ES+):** Found: 515.1098 [M+H], requires: 515.1094; **IR ν_{max}/cm^{-1} (solid):** 3365, 3065, 2925, 2830, 1719, 1609, 1365, 1293, 1202, 1171, 1025; **M.pt:** 103-106 °C.

3.12.2.22 6-(5-Methoxy-3-phenyl-1-phenylsulfonylindol-2-yl)-2-bromobencene (30)

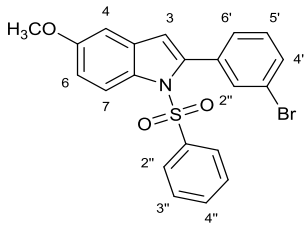

Compound **30** was isolated as the 2nd product following the procedure for the compound **21**. Brown solid (124 mg, 18 %). **^{1}H NMR** (400 MHz, $CDCl_3$) δ ppm 8.10 (d, *J* = 9.1 Hz, 1H, 7-H), 7.47 (d, *J* = 1.0 Hz, 2H), 7.36 (dd, *J* = 13.1, 7.4 Hz, 2H), 7.27 (dd, *J* = 8.4, 1.2 Hz, 2H), 7.19 (dd, *J* = 16.5, 9.0 Hz, 3H), 6.89 (dd, *J* = 9.1, 2.6 Hz, 1H, 6-H), 6.79 (d, *J* = 2.6 Hz, 1H, 4-H), 6.40 (s, 1H, 3-H), 3.73 (s, 3H, OCH_3); **^{13}C NMR** (101 MHz, $CDCl_3$) δ ppm 157.3, 141.3, 137.2, 134.4, 133.8, 133.0, 132.8, 129.2, 128.8, 126.8, 121.6, 117.8, 114.7, 114.11, 103.4, 55.7. **m/z (ES+):** Found: 442.0105 [M+Na], requires: 442.0034; **IR ν_{max}/cm^{-1} (solid):** 3065, 2997, 2960, 2933, 2829, 1736, 1480, 1461, 1365, 1329, 1176, 1148, 1061, 1034, 995; **M.pt:** 152-154 °C.

Chapter 4 Synthesis and Characterisation of Phenanthroline Derivatives and their Iridium(III) Complexes

The following chapter covers the synthesis of five novel phenanthroline-based ligands and a detailed study of their photophysical properties. To improve the applicability of the 1,10-phenanthroline (Phen) derivatives, it is very important to understand the driving factors that allow the tuning of their photophysical properties. Three strategies to tune the photophysical properties of phenanthroline, are described in this chapter.

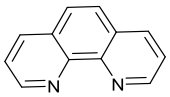

Phen (S.15)

The first strategy is to increase π-system through a structural modification of 5,6- positions without compromising the solubility of the molecule.

A second less exploited, however fruitful, strategy involves the protonation of the phenanthroline-nitrogen atoms. The spectrophotometric studies provide a better understanding of the acid forms, showing that protonation induces stabilisation of the electronic transitions (red-shift). Also, a detailed ^{1}H NMR analysis provides further insights on the protonation of the modified phenanthrolines.

The third strategy involves taking advantage of phenanthroline structural features as a classic chelating agent. This chapter therefore covers the synthesis of the five phenanthroline-based iridium cationic complexes. 2-Phenylpyridine and phenanthroline are utilised as cyclometalating (C^N) and ancillary (N^N) ligands, respectively. The use of different ancillary ligands can show their effect in the photophysical properties of the resulting complexes. Also, in addition to the mononuclear iridium complexes, the di-nuclear complex is synthesised an characterised.

4.1 Introduction

4.1.1 Phenanthroline derivatives

1,10-Phenanthroline (Phen) is a versatile starting material for organic, inorganic and supramolecular chemistry synthesis, which has been used extensively for decades. Due to the unique structural features of Phen, e.g. aromaticity, basicity, co-planarity, rigidity and chelating capability (two nitrogen atoms in juxtaposition)[190]. Its properties are exploited for the

construction of efficient luminescent materials[191], in molecular recognition[192] and sensing[193], binding/cleaving reagent for DNA and RNA[194], catalysis[195], photodynamic therapy[196] and cancer research[197].

Various methodologies are known for the synthesis of 1,10-phenanthrolines, including the classical Skraup[198, 199] and Friedlander reactions. The Shkraup reaction, first discovered in 1880, can be applied to 8-aminoquinolines for the construction of 1,10-phenanthrolines. For the derivatisation of the wide use[130] of 1,10-phenanthroline, the previously mentioned methods are not necessarily useful in the case of substrates bearing sensitive functionalities. These methods usually require strong acidic or basic conditions and high temperatures[200]. Thus, substituted 1,10-phenanthrolines are normally synthesised by modifying the existing framework using nucleophilic or electrophilic aromatic substitutions, or by construction of the heterocycles incorporating the substituents onto the parent nucleus.

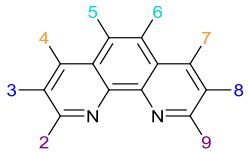

Figure 4-1 Reactive positions of phenanthroline

Phen is an excellent building block for the synthesis of highly luminescent materials **(Figure 4-1)**. The 2,9- and 4,7-positions are the most active sites of Phen towards nucleophilic reagents; while positions 5,6- or 3,8-, with a higher electronic density, are preferred by electrophilic reagents[201, 202].

Phenanthroline-halides are important starting materials; however, direct halogenation is difficult and non-selective, which is typical for π-deficient heterocyclic compounds. Generally, for the compounds containing the electron withdrawing imine nitrogen (C=N-), the electrophilic substitution with halogens requires harsh reaction conditions[203] and yields are fairly satisfactory[204, 205]. Substitution of the aromatic system at the positions 2,9-[206] and 4,7-[207, 208] is the favoured strategy[209, 210]. Whereas, manipulation of 3,8- and 5,6-positions of the phenanthroline core is more difficult with a lesser number of synthetic approaches available[190].

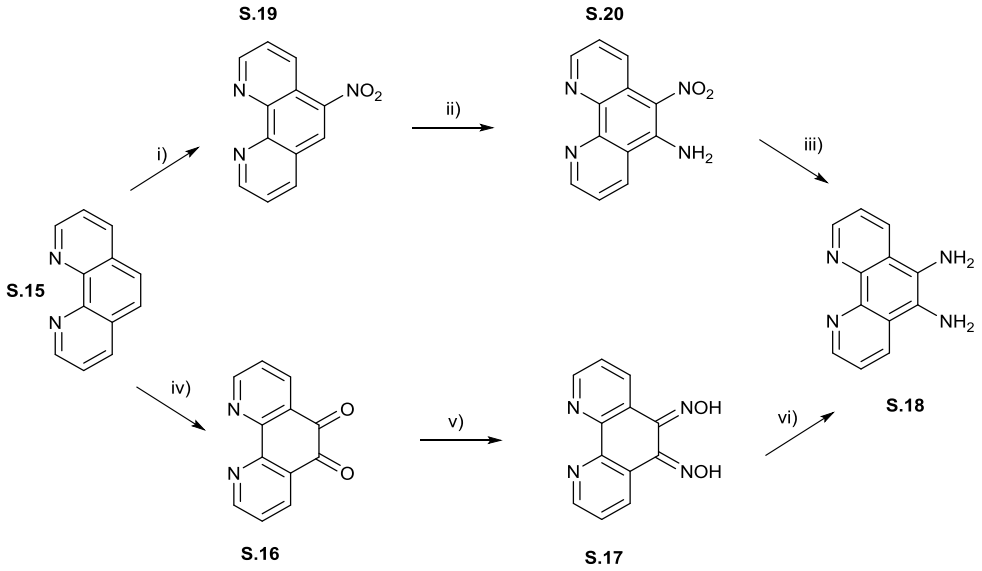

Scheme 4.1 Synthetic route to two useful synthons (S.16 and S.18): i) HNO_3;ii) NH_2OH HCl·, base, EtOH ;iii)N_2H_4, Pd/C(10%) MeOH; iv) H_2SO_4/HNO3, KBr v) NH_2OH HCl·, base, EtOH, N_2H_4, Pd/C(10%) MeOH

The synthetically viable synthons for the useful derivatisation of the 5,6-positions are 5,6-diamino-1,10-phenanthroline (phen-diamine) **(S.18)** and 5,6-dione-1,10-phenanthroline (phen-dione) **(S.16)**. Two main procedures are reported in the literature for the synthesis of compound **S.18**[211-213], which are very similar comprising of two general stages[212, 214] **(Scheme 4.1)**: 1) amination and 2) the formation of the dioxime and its consequent reduction.

1) 5-Nitro-1,10-phenanthroline **(S.19)** is formed by nitration of compound **S.15**, followed by amination with either hydroxylamine under strong basic conditions or with liquid ammonia. The reduction of 5-nitro-6-amino-1,10-phenanthroline **(S.20)** yield the corresponding **S.18**.

2) Phen (**S.15)** was easily oxidised to phenanthroline-5,6-dione **(S.16)** followed by the transformation of **S.16**[215-218] to the dioxime derivative **S.17**. This product is converted by catalytic reduction into the corresponding **S.18**.

Phen-diamine **(S.18)** and Phen-dione **(S.16)** can be condensed with a variety of ortho-quinones to form additional derivatives. The two most widely used are pyrazino[2,3-f][1,10]phenanthroline **(S.22)** [219-222] and 1H-Imidazo[4,5-f][1,10]phenanthroline **(S.21)**[223-225].

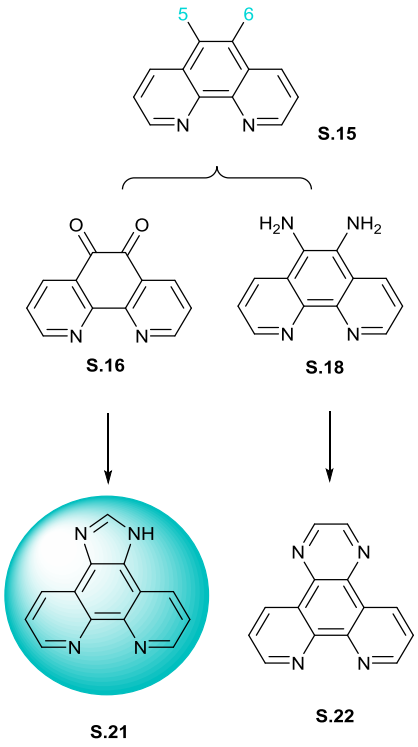

Figure 4-2 Versatile building blocks: 1H-Imidazo[4,5-f][1,10]phenanthroline (S.21) and Pyrazino[2,3-f][1,10]phenanthroline (S.22) *via* modification of 5,6- positions

4.1.2 1,10-Phenanthroline as ancillary ligand for Ir(III) complexes

N-Containing heterocycles with electron-withdrawing imine nitrogen(s) (C=N-), have attracted interest for their ability to form metal complexes[40]. 2-2'-Bipyridyl (ppy, **S.23**) systems are the most commonly used. However, Phen **(S.15)** has several distinct features compared with its analogue 2,2'-bypiridine (bpy, **S.1**). Co-planarity of the two nitrogen atoms in juxtaposition[190] causes a strong entropically favoured Phen-metal binding. The similar disposition of the nitrogen atoms in bpy is disrupted by the free rotation on the bond that links the heterocycles.[190] In addition, cyclometalation upon C-3 was observed between the iridium centre and bpy ligand **(S.9)**[226]. This observation is explanatory of the extensive popularity of 2-phenylpyridine as a cyclometalating ligand (ppy)[227, 228]. Where the carbon atom has a negative charge and the Ir-C bond is strong enough to be comparable to covalent bonds.

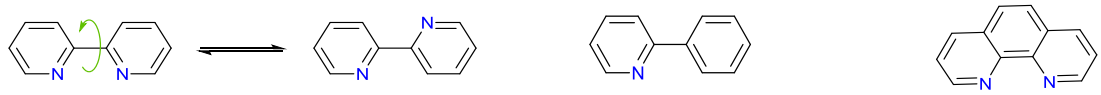

Bpy (S.1) **Ppy (S.23)** **Phen (S.15)**

Figure 4-3 Examples of bidental ligands

Another feature of this class of chelating agents, in particular Phen, is their low σ-donor nitrogen ability. Phen presents a weak basicity (pK_a 4.95 in water)[190]. Comparing Phen with aliphatic diamines such as ethylenediamine (en) (pK_a 10.65 and 8.04 for successive addition of proton to en)[229] its basicity is remarkably lower[230, 231]. In agreement with the electron-deficiency of the heteroaromatic rings and therefore low σ-donating ability of the nitrogen atoms. Although the entropic contribution is larger than en for the stability of the complex formed (nitrogen atoms placed to act cooperatively in cation binding). The σ-donating ability of these heterocyclic nitrogen atoms is poor, but is overcome by the ability of Phen to act as a π-acceptor[231]. In addition, their σ-electron deficiency, makes them excellent acceptors capable of stabilising metal ions in lower oxidation states.[190]

4.1.3 Cyclometalated iridium(III) complexes

Over the last two decades heavy metal complexes[232], in particular Ir(III) complexes, have attracted considerable attention[66, 233, 234] due to their photophysical and photochemical properties. While cyclometalated Ir(III) complexes have been widely exploited as organic light-emitting diodes (OLEDs)[235], light emitting electrochemical cells (LEECs)[236, 237] and photocatalysts, very few iridium complexes were employed in living cells and therefore as biological labelling reagents[238-240]. In the search to overcome the optical shortcomings present in fluorescent probes based in organic dyes: (i) poor water solubility, (ii) poor photostability, (iii) high toxicity to living cells, (iv) tissue damaged due to the radiation (UV) required for the excitation and small Stokes shifts[241]. The development of new d^8-metal Pt complexes, d^{10}-metal Zn(II) complexes or d^6-metal complexes (Ru, Re, Os), Ir in particular, has been one of the main research focuses.

Ir(III) complexes have been thoroughly investigated for better understanding of the excited state and the electron transfer processes to optimise the potential for practical applications. The iridium(III) complexes possess several useful properties such as good stability, high photoluminescent quantum yields (which can be modulated through synthetic modifications) and their efficient spin-orbit coupling. Photoinduced energy and electron transfer processes are

frequently observed in Ir(III) cyclometalated complexes. Cyclometalated iridium(III) complexes have one of the largest spin–orbit coupling constants known (3909 cm^{-1})[242], resulting in an efficient intersystem crossing (ISC) in these systems.[243]The efficiency of this process leads to the mixed singlet and triplet metal-to-ligand charge-transfer processes that allows the otherwise forbidden S_0 to T_1 transitions[244]. It is also apparent that incorporation of additional metal centres facilitates the spin-orbit coupling, enhancing the radiative rate constant and thus the efficiency of phosphorescence. In addition, polynuclear complexes possess enhanced extinction coefficients as compared to mononuclear analogues[245]. In iridium(III) polynuclear complexes the role of the metal centre has often been ignored, in most of the literature reported there is only one metal centre.[246] Extensive literature searches show there are few reports of di- metal d^6 (Ru(II)[247-249], Os(II)[250], Rh(III)[251]) complexes and even of tetra-nuclear Ru(II) complexes[252]. However, little published data containing ppy-Phen di-nuclear iridium complexes[253-255] was found.

4.1.4 General synthesis of mononuclear Ir(III) complexes with bidentate ligands

In 1991, during the preparation of $[Ir(bpy)_3]^{3+}$, Watts noticed spontaneous cyclometalation, which occurred at C-3 in one of the bpy ligands[226]. This led to an extensive use of ppy as a cyclometalating ligand.

Ir(III) complexes containing cyclometalated ligands hold a pseudo-octahedral coordination. The iridium atom usually has six coordination sites, occupied by three monoanionic bidentate ligands[256]. Cyclometalated Ir(III) complexes are commonly synthesised *via* a standard two step procedure. The first step involves the preparation of a bis µ-chloro dinuclear Ir(III) dimer $[Ir(C\hat{}N)_2(\mu\text{-}Cl)]_2$, Nonoyama reaction[257], by reacting $IrCl_3{\cdot}nH_2O$ and a cyclometalating pro-ligand HC^N. In the second step a third ligand can substitute the chlorides in the Ir(III) dimer. Depending on whether all the ligands are identical to each other, the iridium complexes can be classified either as homoleptic $[Ir(C\hat{}N)_3]$ if C^N ligands are identical or heteroleptic $[Ir(C\hat{}N)_2(C'\hat{}N')$, if a different C'^N' is used[258]. Homoleptic iridium complexes possess two geometric isomers, facial (*fac*) and meridional (*mer*), which have N,N-*cis* and N,N-*trans* configurations respectively **(Scheme 4.2)**. The coexistence of both isomers is quite common. However, both isomers present distinctly different photophysical properties[227, 259], which are very important for a variety of applications[237, 259]. The kinetic isomer *mer* can be thermally or photochemically isomerised to the thermodynamic *fac* isomer[259]. In contrast, heteroleptic Ir(III) complexes have a strong preference for N,N-*trans* configurations, avoiding isomeric contamination.

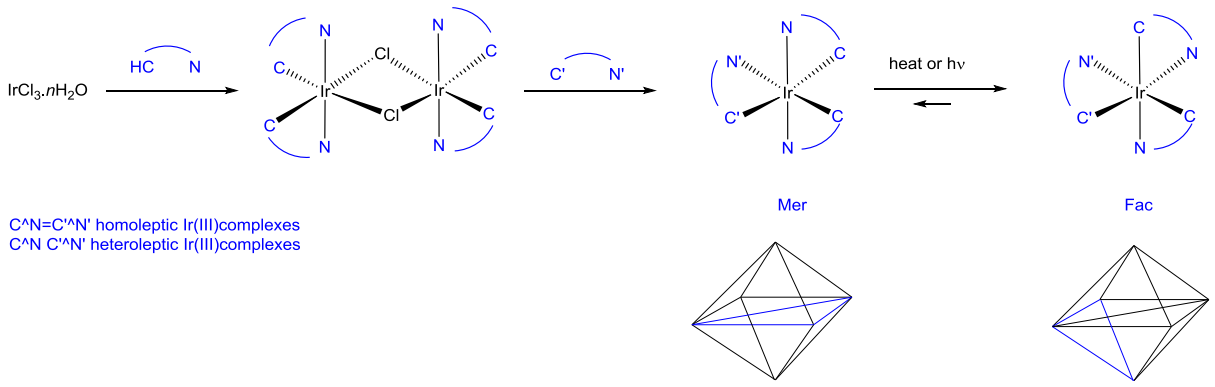

Scheme 4.2 General synthetic route to cyclometalated Ir(III) complexes *via* Nonoyama reaction

Following this synthetic strategy, neutral and ionic (mono-, bis- and tris-) cyclometalated Ir(III) complexes have been synthesised. With the choice of an appropriate third ligand the charges on the iridium complexes can be controlled. In contrast to neutral iridium complexes, cationic iridium complexes can be synthesised and isolated more easily, getting closer to theoretical yields[260, 261].

4.1.5 Cyclometalated iridium complexes: octahedral coordination & photophysics

The electronic configuration of iridium(III) centre is a $5d^6$. The octahedral crystal field of the ligands splits the five degenerate d-orbitals into two sets: a triply degenerate level, t_{2g}, and a doubly degenerate level, e_g[262]. The splitting pattern and magnitude (Δ_0) are both dependent on the metal nature and the crystal field strength of the ligand, specifically: i) the type of ligands and ii) the different spatial orientations and arrangement, and thus electrostatic interactions. The electron distribution between the t_{2g} and e_g levels is defined by Δ_0. In accordance with Hund's rule, in a strong field system (where Δ_0 is large) it is energetically favourable to pair electrons in the t_{2g} level (a low spin complex). Whereas, a low field system (where Δ_0 is smaller than the pairing energy) results in a high spin configuration with the maximum number of unpaired electrons distributed across the t_{2g} and e levels).

Three types of excited states can be identified for metal complexes. They are classified based on the origin and destination of the orbitals: i) metal centred states (MC) from the promotion of an electron from t_{2g} to e_g orbitals; ii) ligand centred states (LC) that are mainly π-π* transition amd iii) metal-to-ligand charge-transfer transitions (MLCT) **(Figure 4-4)**.

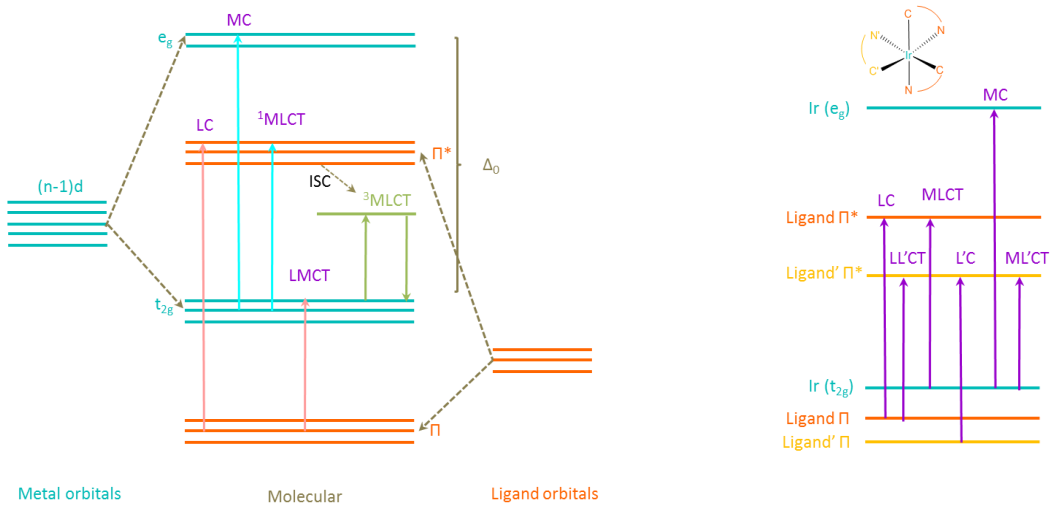

Figure 4-4 Simplified diagram of molecular orbitals for an octahedral d^6 complex involving 2-phenylpyridine (left). Diagram of a heteroleptic Ir complex, where the use of a third ligand (L') enables additional transitions (right).

For better understanding of the photophysical processes associated with the d^6 metal complexes, it is crucial to understand the electronic transitions involved **(Figure 4-4)**. Photoexcitation promotes the population of excited states. In the case of the *fac*-[Ir(C^N)$_3$] complex, density functional theory (DFT) calculations[263, 264] showed, that the HOMO **(Figure 4-5a)** is delocalised over the t_{2g} of Ir and π orbitals of the 2-phenylpyridine, whereas the LUMO **(Figure 4-5b)** only involves the π* orbital of the 2-phenylpyridine. It shows that, there are at least two types of electronic transitions occurring: LC transitions involving π-π* orbitals of the ligand and MLCT involving the iridium electrons from the t_{2g} orbitals. In addition, the strong spin–orbit coupling (SOC) in iridium facilities the triplet ^{3}MLCT and ^{3}LC transitions. Consequently, the four electronic excited states: the singlets (^{1}MLCT and ^{1}LC) and triplets (^{3}MLCT and ^{3}LC) have become available. In reality in cyclometaletd Ir(III) complexes, the triplet excited state (^{3}MLCT) is a result of combined LC and MLCT transitions[265]. Generally, ^{1}LC transitions are higher in energy than ^{1}MLCT. Since, the energy difference between singlet and triplet states ($E_{singlet}$-$E_{triplet}$) of a LC transition is usually higher than that of a MLCT, the ^{3}MLCT transition energy is higher than ^{3}LC.[256] Hence, the transitions ^{3}MLCT and ^{3}LC are rarely distinguished as a consequence of their small molar absorptivity and featureless band patterns.[227]

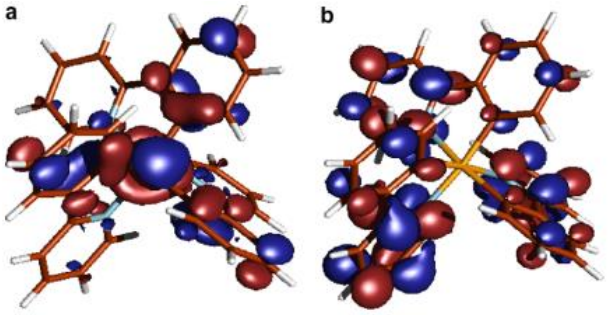

Figure 4-5 Frontier molecular orbitals of $Ir(ppy)_3$ at S_0 optimized geometry: (a) HOMO and (b) LUMO. Taken from (Jansson et al., 2007)[263]

Generally, emission arises from the lowest excited state. Particularly, emission from phosphorescent iridium(III) complexes mainly arises from ^{3}MLCT or a mixture of ^{3}MLCT and ^{3}LC transitions[266]. Altering the structure of the ligands can have a significant effect on the luminescence properties observed[242, 267]. First, by the functionalisation of the C^N and/or by the use of ancillary ligands, other transitions, such as intraligand-charge-transfer (ILCT), in addition to LC and MLCT states can occur depending on the energy of states **(Figure 4-4)**. Those transitions are localised on the ligand. A use of these strategies shows tangled photophysics. Despite its complexity, these approaches are used to modulate the luminescent properties[232, 262, 265, 268] because the energy is mainly determined by a "global" LUMO energy. Extending the π-conjugation of either a cyclometalating or an ancillary ligand decreases the band gap producing a bathochromic shift in the emission spectra[269].

4.2 Design and synthesis of 1,10-phenanthroline derivatives

Based on previous statements, the possibility of varying the substitution pattern directly at the imidazole-precursor was investigated for use as a building block. The structural features were carefully selected to increase the lying between π-π* and n-π* electronic states by increasing the conjugation of the aromatic system through modification of the 5,6-positions, enhancing the PL quantum yield of the material.

1. Phenanthroline derivative ligands have poor solubility in most organic solvents[270]. To overcome this issue and prevent intermolecular π-π stacking, bulky branched chains were incorporated into the structures. The substantial increase in the steric bulk of the ligand facilitates the solubility of the compound. Although, the synthesis is not trivial and thermal stability may be comprised.

2. Substitution at the imidazole-nitrogen (-NH) can potentially alter the electron distribution in the molecule and therefore the electronic properties. However, the substitution can also lead to a reduction of the planarity of the molecule.
3. Structural modification of **4.1-4.5** can modify the energies of π-π* and n-π* electronic transitions and enhance the PL quantum yield of the material.

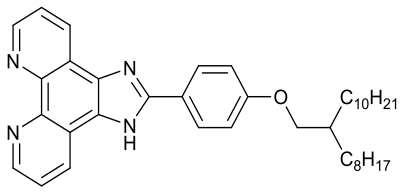

4.1

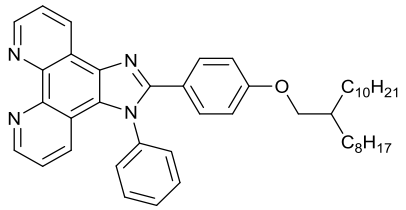

4.2

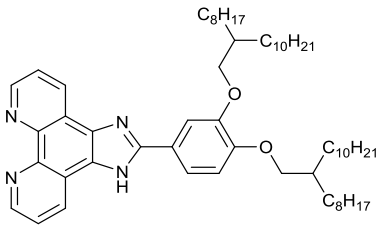

4.3

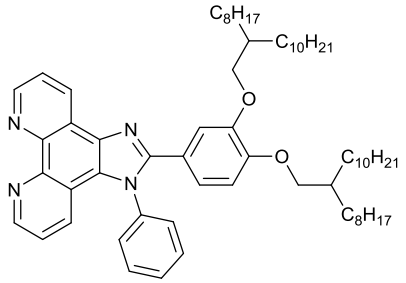

4.4

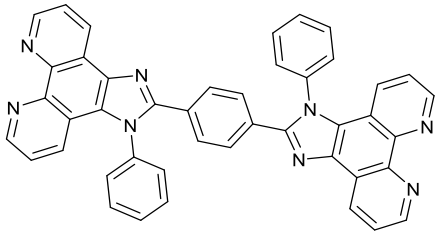

4.5

Figure 4-6 Structures of phenanthroline ligands (4.1-4.5)

4.2.1 Synthesis of 1,10-phenanthroline derivatives

Two synthetic routes towards the synthesis of 2-{4-[(2-octyldodecyl)oxy]phenyl}-1H-imidazo[4,5-f][1,10]phenanthroline **(4.1)** and 2-{4-[(2-octyldodecyl)oxy]phenyl}-1-phenyl-1H-imidazo[4,5-f][1,10]phenanthroline **(4.2)** have been investigated and are discussed in **section 4.2.1.1**.

4.2.1.1 Synthesis of 2-{4-[(2-octyldodecyl)oxy]phenyl}-1H-imidazo[4,5-f][1,10]phenanthroline

The imidazole-containing phenanthroline derivative 4-(1H-imidazo[4,5-f][1,10]phenanthrolin-2-yl)phenol **(31)** and 4-(1H-imidazo[4,5-f][1,10]phenanthrolin-2-yl)benzene-1,2-diol **(32)**[271] were synthesised according to the methods reported in literature with an overall yield of 90% and 93%, respectively. Oxidation of 1,10-phenanthroline **(S.15)** with NaBr and the mixture of concentrated acids (H_2SO_4 and HNO_3) led to 1,10-phenanthroline-5,6-dione **(S.16)**.[194] A subsequent reaction of **S.16** with either 4-hydroxybenzaldehyde **(S.24)** or 2,4-dihydroxybenzaldehyde in glacial acetic acid and ammonium acetate resulted in the formation of compounds **(31)** and **(32)**, respectively. An attempt to alkylate compound **31** with 9-(iodomethyl)nonadecane **(33)** gave compound **4.1**. However, since the isolation of **4.1** in a pure form proved to be difficult, an alternative synthetic route was used to access compound **4.1**.

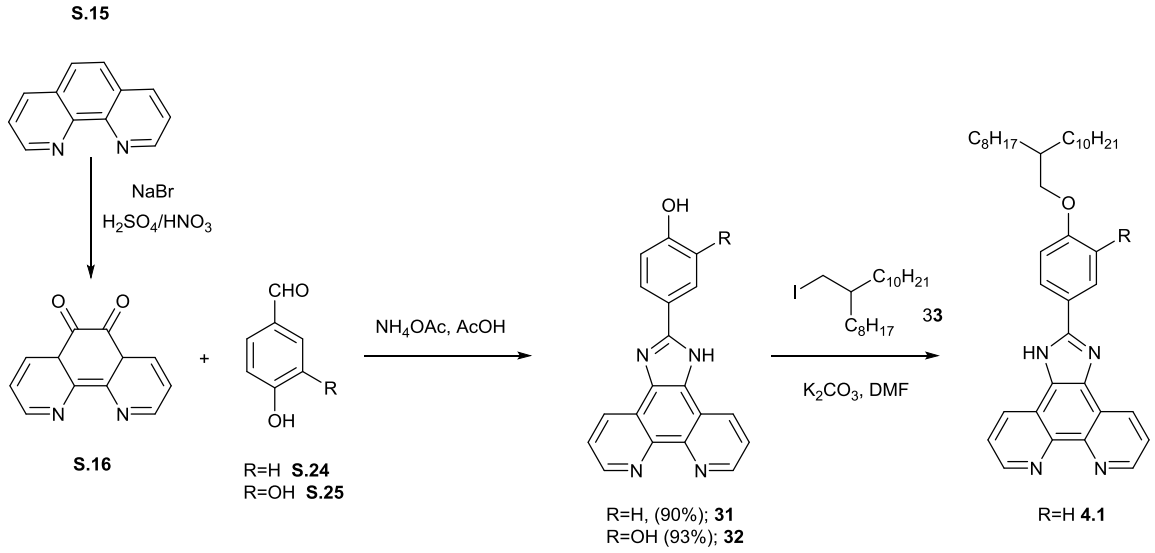

Scheme 4.3 Synthesis 2-{4-[(2-octyldodecyl)oxy]phenyl}-1H-imidazo[4,5-f][1,10]phenanthroline (4.1)

Having in mind difficulties associated with the purification, an alternative approach was developed for the synthesis of compounds **4.1** and **4.3**. Firstly, 9-(iodomethyl)nonadecane **(33)** was synthesised according to the methods reported in literature[272]. **S.26** was converted to the corresponding iodide **(33)** with the yield of 93%, using triphenylphosphine, imidazole and iodine. The alkyl iodide was subsequently used in excess with a mild base for the alkylation of **S.24** to achieve **34** in 63% of yield.

The first attempt to synthesise compounds **35** and **36**, using 2 molar equivalents of potassium carbonate and 2.2 molar equivalents of alkyl iodide **(33)** led to the formation of products in very poor yields of 15% and 29%, respectively. The low yields of the desired compounds promoted further investigations into the molar ratios of base and the corresponding iodide. A slight increase in the amount of base (2.5 eq), while the concentration of alkyl iodide remained constant, did not show any improvement. When 2.5 molar equivalents of base and 3.2 molar equivalents of the iodide compound were used, compound **35** was obtained in a 45% yield. In addition, a side product, **36**, was present. Finally, 4 molar equivalents of base and 3.2 molar equivalents of the iodide resulted in a yield of 51% for compound **35**. However, in all cases, due to the appearance of compound **36**, it was considered that the second alkylation was not as effective due to the steric effect.

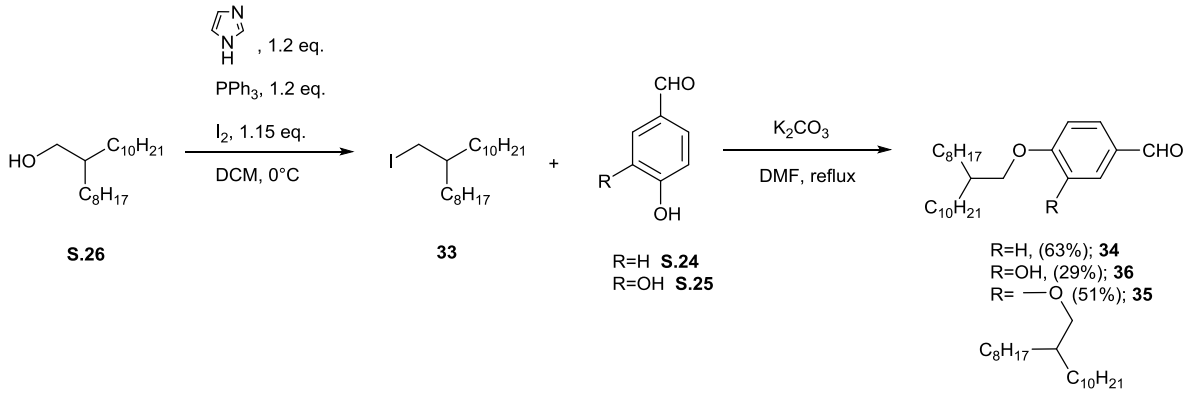

Scheme 4.4 Synthesis of 9-(iodomethyl)nonadecane

Imidazole-containing phenanthroline derivatives were then synthesised by reacting **S.16** with the appropriate aldehyde (**34** and **35**) to obtain compounds **4.1** and **4.3 (Scheme 4.5)** in yields of 22% and 15%, respectively.

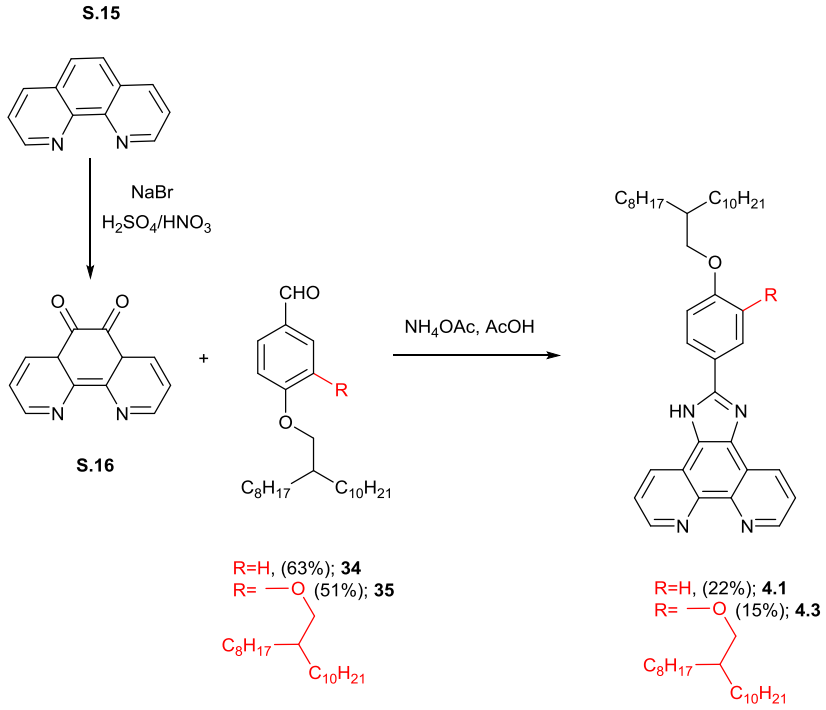

Scheme 4.5 Synthesis of 2-{4-[(2-octyldodecyl)oxy]phenyl}-1H-imidazo[4,5-f][1,10]phenanthroline (4.1) and 2-{3,4-bis[(2-octyldodecyl)oxy]phenyl}-1H-imidazo[4,5-f][1,10]phenanthroline (4.3)

4.2.1.2 Synthesis of 2-{4-[(2-octyldodecyl)oxy]phenyl}-1-phenyl-1H-imidazo[4,5-f][1,10]phenanthroline (4.2) and 2-{3,4-bis[(2-octyldodecyl)oxy]phenyl}-1-phenyl-1H-imidazo[4,5-f][1,10]phenanthroline (4.4)

The synthesis of compounds **4.2** and **4.4** was carried out according to the approach depicted in **Scheme 4.6**. Through a one-step reaction, **4.2** and **4.4** were prepared by refluxing **34** or **35** with 9,10-phenanthreequinone **(S.16)**, with commercially available aniline. Firstly, for the synthesis of compound **4.2**, the ratio of the reagents Phen:aldehyde:aniline was 1:1:1.2. Although the conversion rate was quite high, the purification process proved to be more difficult due to the remaining aldehyde. A ratio of 1.3:1:1.2 provided up to 81% yield. However, the yield of compound **4.4**, using Phen:aldehyde:aniline in the ratio of 1:1:1.2, was only 48%.

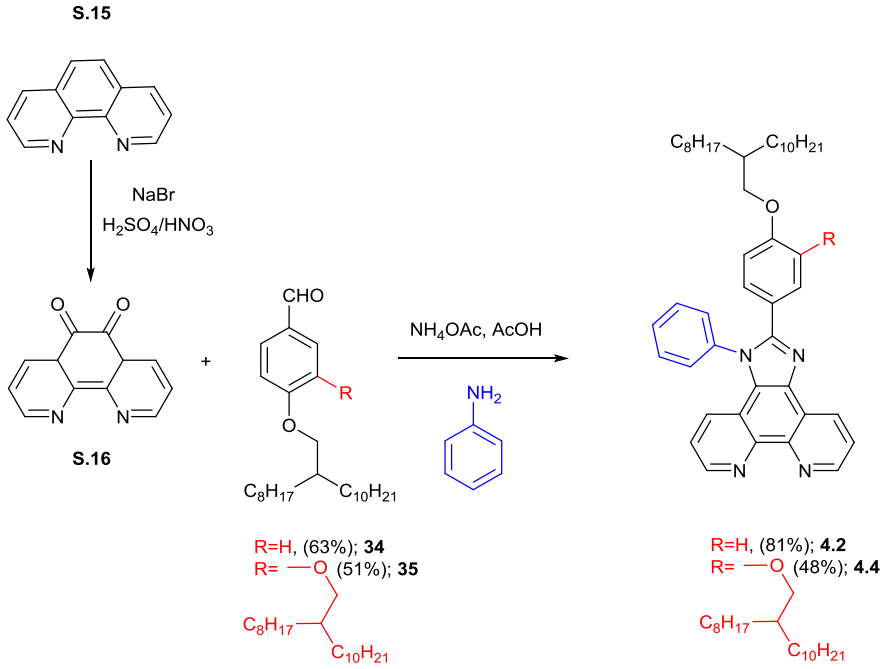

Scheme 4.6 Synthesis of 2-{4-[(2-octyldodecyl)oxy]phenyl}s1-phenyl-1H-imidazo[4,5-f][1,10]phenanthroline (4.2) and 2-{3,4-bis[(2-octyldodecyl)oxy]phenyl}-1-phenyl-1H-imidazo[4,5-f][1,10]phenanthroline (4.4)

4.2.1.3 Synthesis of 1,4-bis(1-phenyl-1H-imidazo[4,5-f][1,10]phenanthrolin-2-yl)benzene (4.5)

The synthesis of 1,4-bis(1-phenyl-1H-imidazo[4,5-f][1,10]phenanthrolin-2-yl)benzene **(4.5)** was accomplished as described in Scheme 4.7. Compound **4.5** was synthesised *via* the condensation of 1,10-phenanthroline-5,6-dione **(S.16)**, terephtaldehyde **(S.27)**, aniline and ammonium acetate in refluxing glacial acetic acid in the yield of 85%.

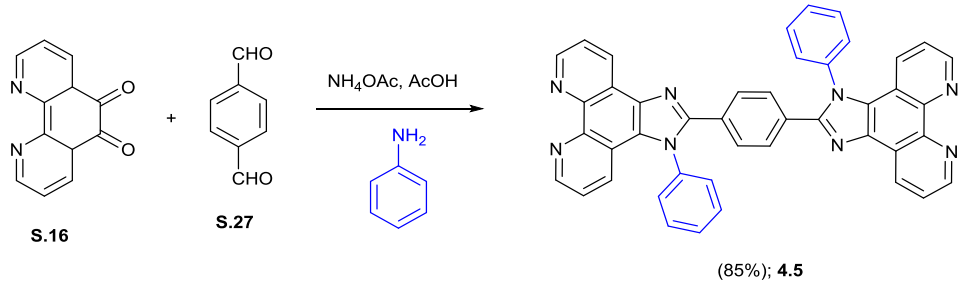

Scheme 4.7 Synthesis of 1,4-bis(1-phenyl-1H-imidazo[4,5-f][1,10]phenanthrolin-2-yl)benzene (4.5)

4.3 Synthesis of Ir(III) phenanthroline complexes

Iridium(III) complexes can be synthesised *via* preparation of the μ-dichloro-bridged Ir dimer, followed by cleavage of the dimer in the presence of a N^N ligand. Synthesis of heteroliptic Ir(III) complexes generally avoids isomeric contamination and requires mild reaction conditions enabling the use of a wide range of ligands[256].

One of the factors hampering the applicability of cationic iridium complexes is their low solubility in many ordinary organic solvents such as dichloromethane, toluene and chlorobenzene[273]. It has been noted that the use of long chains like alkyls is beneficial to improve the solubility[273-275]. Altering the ligands can have a significant effect on the luminescence properties too[242] and this strategy has been used to modulate the luminescent properties. In addition, the quasi-octahedral-geometry of iridium allows introduction of ligands in a specific manner.

The design of cationic iridium complexes is as follows:

1. To alter electronic properties of cationic iridium complexes **Ir.4.1-Ir.4.5**, modified phenanthrolines **4.1-4.5** as ancillary ligands are used.
2. To improve the solubility beyond strong polar solvents, substitution at the imidazole nitrogen can be used (although, it can lead to distortion of planarity of the phenan-imidazole unit).
3. To access cationic heteroliptic complexes with yields closer to theoretical values and of high purity, the synthesis based on the μ-dichloro-bridged Ir dimer as (C^N) starting material is used.[260, 261]

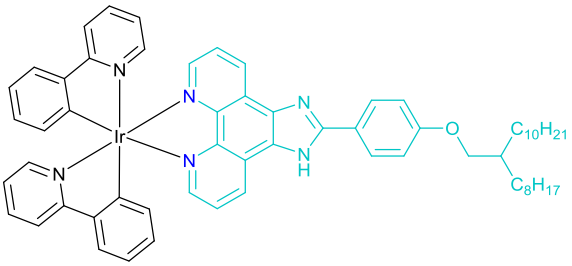

Ir.4.1

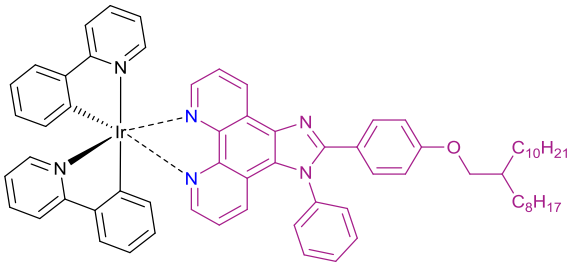

Ir.4.2

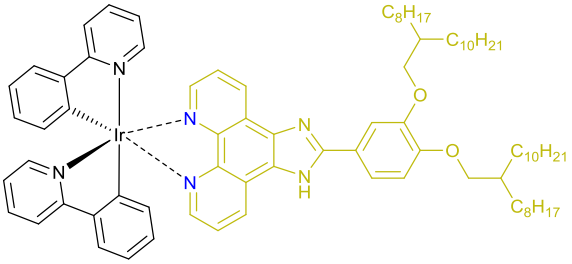

Ir.4.3

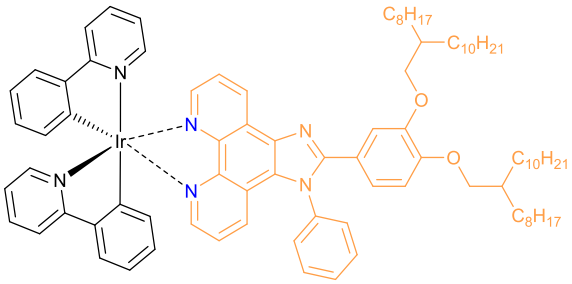

Ir.4.4

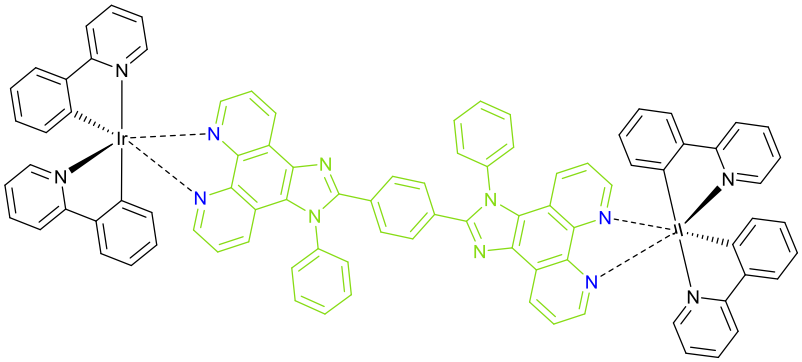

Ir.4.5

Figure 4-7 Synthetic targets for Ir(III)-phenanthroline complexes (Ir.4.1-Ir.4.5)

4.3.1 Synthesis of complexes Ir.4.1-Ir.4.5

The Ir(III) complexes **Ir.4.1-Ir.4.5** were prepared using the most popular synthetic protocol **(Scheme 4.8** and **Scheme 4.9)**. The first step was the isolation of the μ-dichloro-bridged Ir dimer **(37)**, followed by cleavage of the dimer in the presence of a N^N ligand.

4.3.1.1 Synthesis of cationic Ir(III) complexes

The synthesis of four mononuclear **(Ir.4.1-Ir.4.4)** and di-nuclear **(4.5)** Ir(III) complexes was performed as shown in **Scheme 4.8** and **Scheme 4.9**. The complexes were prepared in yields up to 98%.

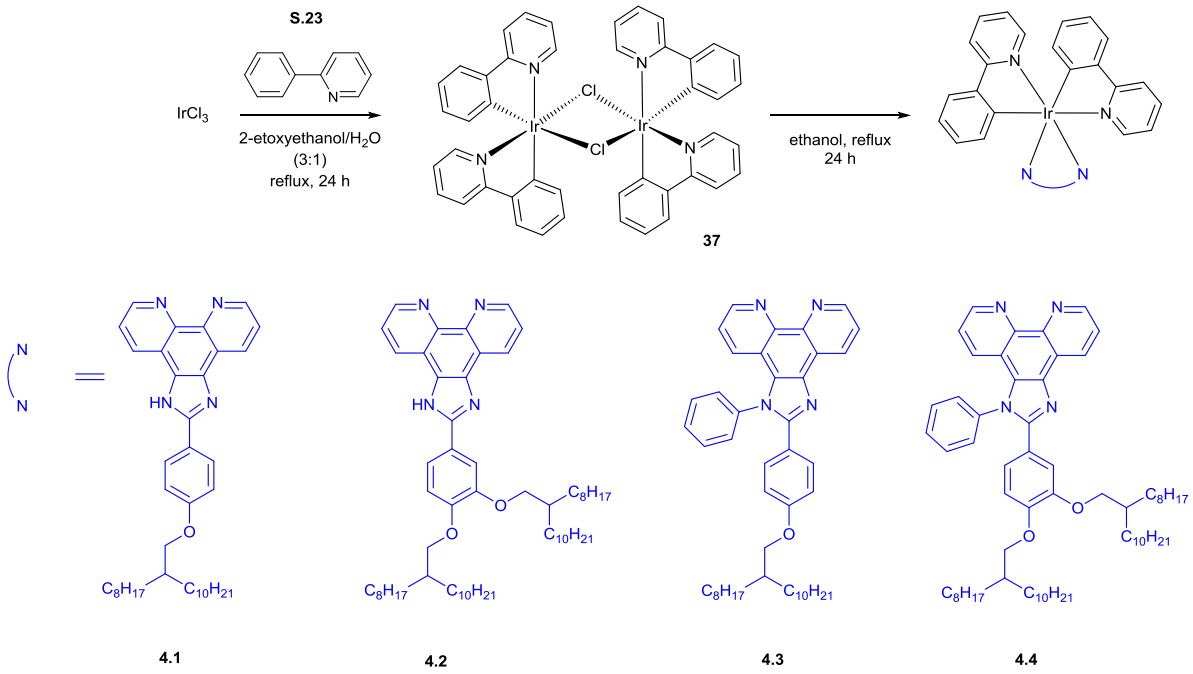

Scheme 4.8 Synthesis of mononuclear Ir(III) complexes 4.1-4.4

4.3.1.2 Synthesis of di-nuclear Ir(III) complex

Scheme 4.9 shows a simple and effective way to obtain the dinuclear cyclometalated iridium(III) complex **(Ir.4.5)** by using a bis-N^C-coordinating ligand **(4.5)**. The ligand was synthesised through the condensation of 1,10-phenanthroline-5,6-dione **(S.16)**, terephthalaldehyde, aniline and ammonium acetate in refluxing glacial acetic acid. The Ir(III) complex **4.5** was obtained in a yield of 25% by the direct reaction of the μ-dichloro-bridged Ir dimer **(37)** in dry ethanol in the presence of the ligand (N^N) **4.5** in the ratio 1.5:1, respectively.

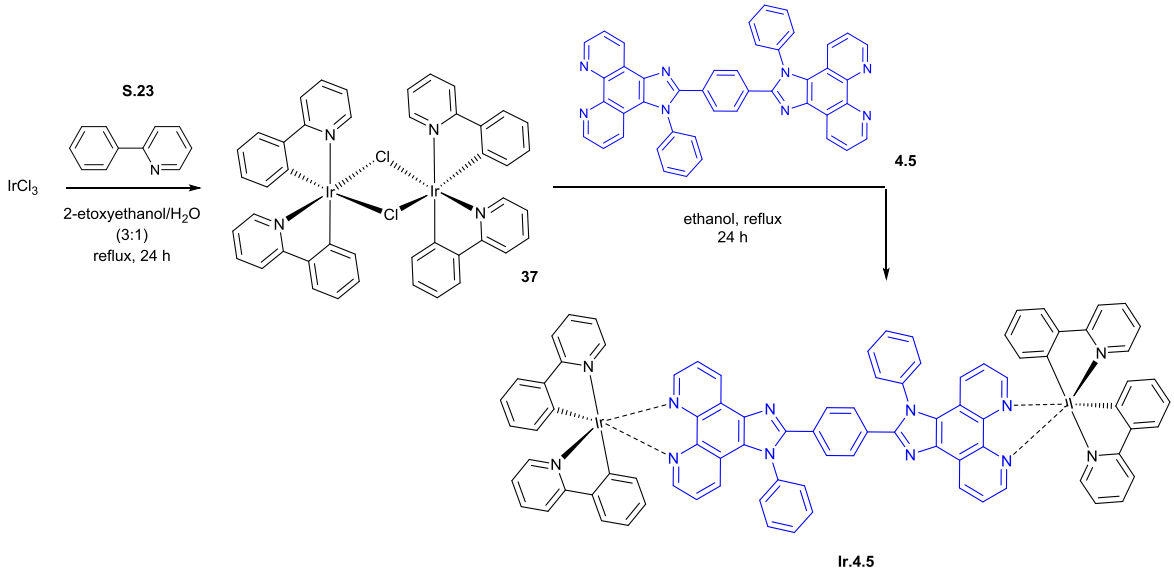

Scheme 4.9 Synthesis of di-nuclear Ir(III) complex Ir.4.5

4.4 Analysis of 1,10-phenanthroline derivatives

4.4.1 Photophysical properties

Photophysical properties of 1,10-phenanthroline **(Scheme 4.8)** have been studied since the fifties and curiously, unmodified Phen is a weakly emissive compound (Φ =0.0087)[276]. More detailed discussion in literature has suggested that Phen and phenanthrene have very similar absorption spectra and therefore the lowest energy band can be assigned to allowed π-π* transitions[277, 278]. Although emission is mainly originated from π-π* transitions, Phen has close lying π-π* and n-π* electronic states. Deactivation *via* non-radiative pathways are usually observed in n-π*, causing a small fluorescence quantum yield[279]. Several strategies are available to increase the band gap and obtain a wide range of highly luminescent compounds with emission bands from the UV to NIR. This includes functionalisation at the various ring positions, complexation with transition metals and lanthanides or protonation of the phenanthroline nitrogen atoms[278]. The latter is a fruitful but less exploited strategy[276] that has been studied in **Section 4.4.2**.

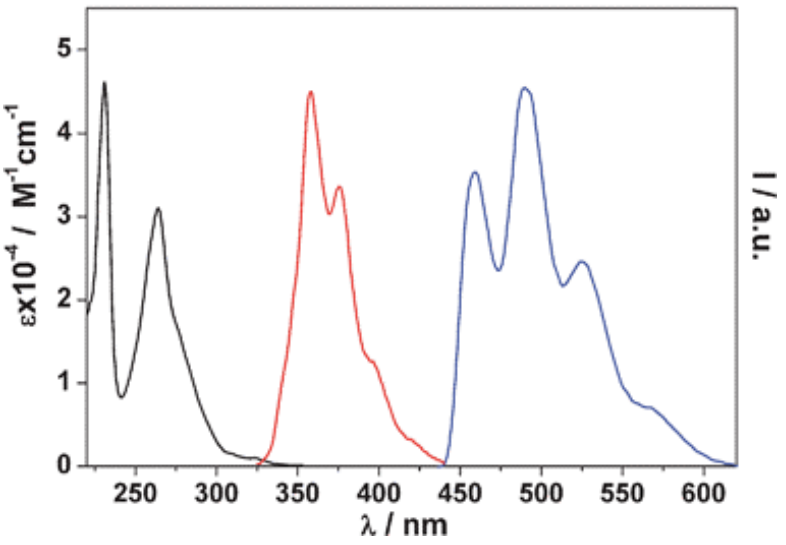

Figure 4-8 1,10-Phenanthroline spectra (in DCM) from left to right: absorption, fluorescence and 77 K phosphorescence emission intensities are normalised. Taken from (Accorsi *et al.*, 2009)[276]

4.4.1.1 Absorption and emission properties of compounds 4.1-4.5

The absorption spectra of the series display similarities in the near-blue region. This indicates that the 2-phenyl-1H-imidazo-phenanthroline core is a dominant feature of the main absorption between 275-285 nm. Compound **4.1** has low solubility in common organic solvents and to simplify the analysis, it was excluded. **Figure 4-9** shows the absorption spectra of compounds **4.2-4.5** in dichloromethane as a function of the molar absorptivity. It shows a red-shift of the absorption maximum going from Phen, **4.2<4.3<4.4<4.5**. This red shift indicates an increase in the conjugation of the molecules. As can be seen in **Figure 4-9** comparing **4.3** and **4.4**, the substitution of the hydrogen at the imidazole ring reduces the absorption intensity and leads to a loss of the band at 329 nm. The molar absorptivity of **4.2-4.5** increases in the following order **4.2<4.4<4.5<4.3**. Photoluminescence spectra of **4.2-4.5** in dichloromethane **(Figure 4-9)** consists of broad, featureless and asymmetric bands with a maximum intensity in the range of 404-437 nm, resembling one another for **4.3** and **4.4**. The photophysical data is gathered in **Table 1**.

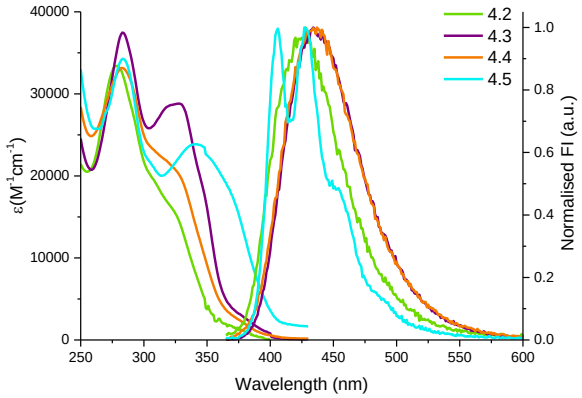

Figure 4-9 The absorption and normalised emission spectra of compounds 4.2-4.5 in dichloromethane (energy of excitation 350 nm)

The quantum yields were calculated according to the literature method using anthracene and 9,10-diphenyl anthracene as cross-references[184]. The efforts to increase the quantum yields of **4.1-4.5** by extending π-conjugation of Phen was successful. Being a less common synthetic strategy, a substitution at the 5,6-positions of the aromatic system in Phen was found to be effective, with a 20% improvement in the quantum yield as summarised in **Table 4-1**. Moreover, by linking two Phen aromatic moieties in compound **4.5**, an impressive quantum yield of 68% is achieved.

Table 4-1 Photophysical properties of compounds 4.1-4.5

Compound	Absorbance λ_{max} (nm), ε ($M^{-1}cm^{-1}$)	Emission λ_{em} (nm), Φ (%)	
4.1	286, 1.8 x 10^2 332, 1.3 x 10^2	494	NA
4.2	278, 3.3 x 10^4 308, 1.9 x 10^4	426	20
4.3	283, 3.7 x 10^4 329, 2.9 x 10^4	437	19
4.4	283, 3.3 x 10^4 327, 2.0 x 10^4	437	16
4.5	284, 3.4 x 10^4 341, 2.4 x 10^4	404, 427, 453,	68

4.4.2 Acidochromism: UV-Vis and ^{1}H NMR titrations

1,10-Phenathroline (Phen) has been identified as a luminescent heterocyclic system in the last 50 years[280]. Phen itself and its derivatives have been versatile ligands in coordination chemistry. However, some intrinsic properties of this class of ligands (luminescence, rigidity, two aromatic nitrogen atoms, *etc*.) also make them appealing as analytical probes for proton and cation sensing[281].

The spectrophotometric and ^{1}H NMR behaviour of Phen **4.1-4.5** upon addition of trifluoroacetic acid (TFA) was investigated. In the case of compounds **4.1-4.5**, protonation can occur at the Phen-nitrogen atoms (pKa=4.95)[190], and either at the benzimidazole-nitrogen (pKa=5.48)[282] or 1-phenyl-1H-benzimidazole (predicted pKa=5.48)[4].

[4] Calculated using Advanced Chemistry Development (ACD/Labs) Software V11.02 (© 1994-2017 ACD/Labs)

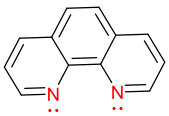

pKa 4.95

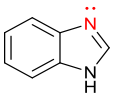

pKa 5.48

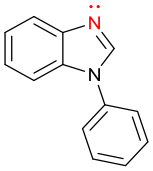

pKa 4.42

Figure 4-10 Phenanthroline, benzimidazole and 1-Phenyl-1H-benzimidazole

4.4.2.1 Spectrophotometric titrations

The absorption and emission profile of compounds **4.1-4.5** in dichloromethane (2×10^{-5}M) underwent spectral changes in the presence of TFA (2.6×10^{-2} M). The corresponding spectra are shown in **Figure 4-11**, **Figure 4-12**, **Figure 4-14**, **Figure 4-16** and **Figure 4-18**. The attenuation of the absorption band of the neutral compounds **4.2-4.5** and the appearance of a new band are observed with an increase in TFA concentration. Generally, the red-shifted absorption peak upon addition of TFA is represented as positive acidochromism[281]. The presence of isosbestic points suggests that a chemical reaction occurs e.g. the protonation of the phenanthroline-derivatives nitrogen atoms. The protonated species are responsible for a red-shifted band [283] in the Phen derivatives **4.1-4.5 (Scheme 4.10)**. The fluorescence in the emission spectra of **4.2-4.5** is completely quenched upon the addition of acid. When considering Phen, inversion between the strongly emissive π-π* and emissive n-π* states is possible. Protonation can stabilise the n-π* state relative to the π-π* state and therefore decrease the emission[284].

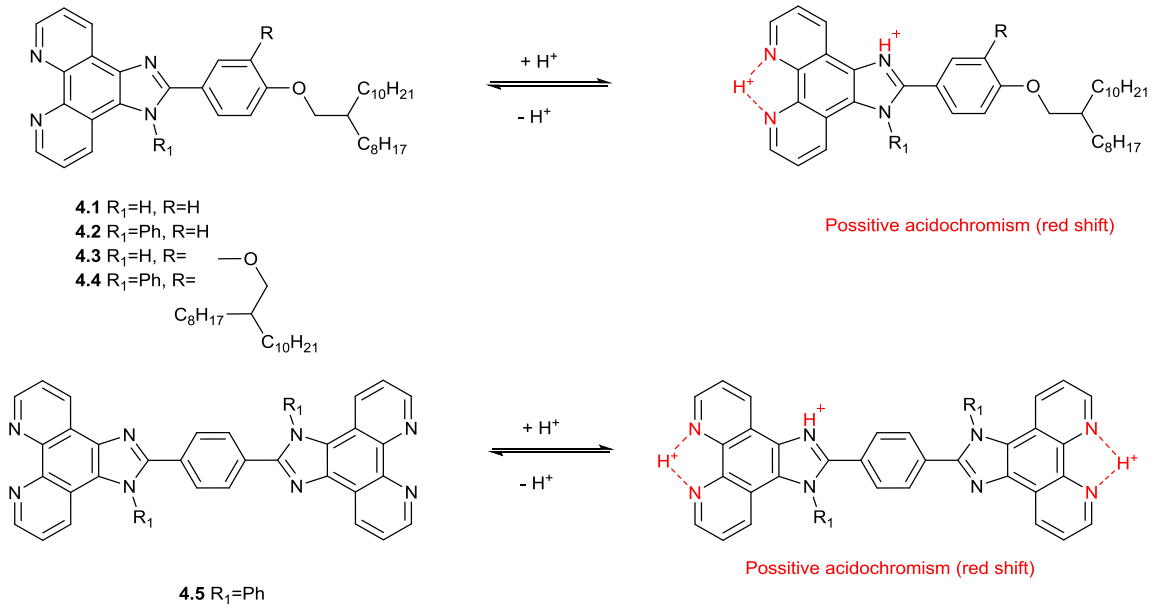

Scheme 4.10 Protonation-deprotonation mechanism in compounds 4.1-4.5 in the presence of TFA

4.4.2.1.1 Acidochromism in compound 4.1

Compound **4.1** has really low solubility. It shows a weak absorption in the UV spectral region between 286-332 nm ($\varepsilon \sim 10^2\ M^{-1}cm^{-1}$) **(Figure 4-11a)** and emission at 494 nm **(Figure 4-11b)**. Upon the addition of TFA, there is a noticeable increase in the extinction coefficient and emission intensity. This could be a result of the increased solubility of the protonated species.

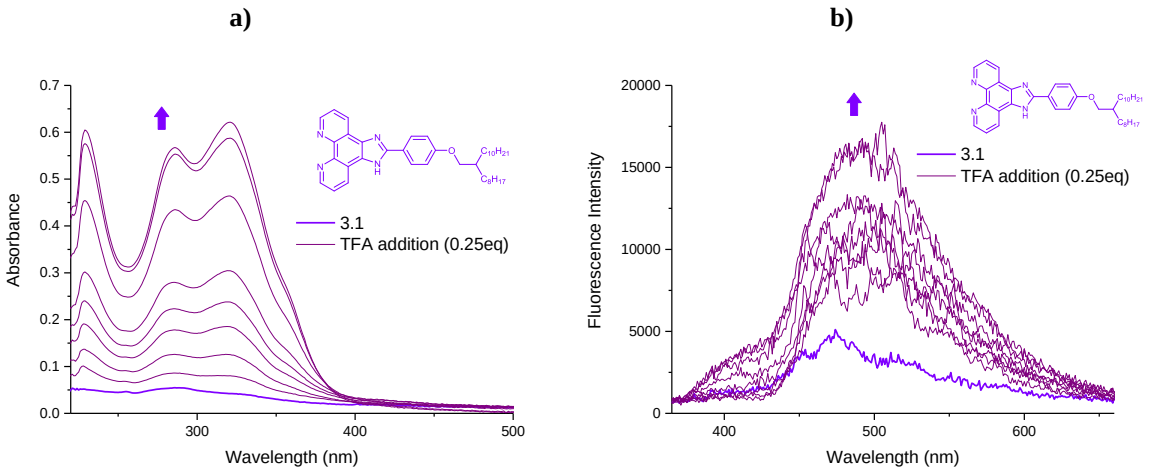

Figure 4-11 Spectrophotometric titration of compound 4.1 (1.6×10^{-6} M) with TFA (2.6×10^{-2} M) in DCM: a) absorption; b) emission (energy of excitation 350 nm)

4.4.2.1.2 Acidochromism in compound 4.2

Compound **4.2** shows a strong featureless absorption band in the ultraviolet spectral region at λ_{max}=278 nm (ε=3.3 x 10^4 $M^{-1}cm^{-1}$) and λ_{max}=308 nm (ε=1.9 x 10^4 $M^{-1}cm^{-1}$) **(Figure 4-12a)**, and it has a blue emission at λ_{em}=426 nm **(Figure 4-12b)**. Upon the addition of TFA (2 equivalents), strong spectral changes are observed that can be attributed to protonation of the imidazo-phenanthroline unit. The presence of isosbestic point at 294 nm suggests the coexistence of the species associated with the protonation process of the imidazo-phen nitrogen atoms. No more changes in the absorption spectrum of **4.2** are observed after 2 equivalents of TFA are added. The new band at λ_{max}=308 nm can be assigned to the protonated species.

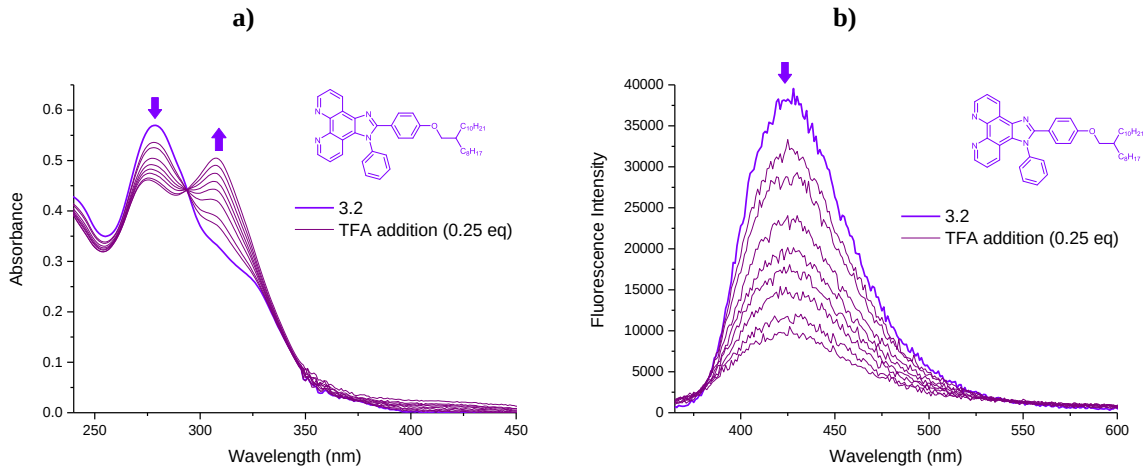

Figure 4-12 Spectrophotometric titration of compound 4.2 (2.3×10^{-5} M) with TFA (2.6×10^{-2} M) in DCM: a) absorption; b) emission (energy of excitation 350 nm)

Figure 4-13 shows a plot of the normalised absorption and emission variation as a function of the number of TFA equivalents, which correspond to the decrease in absorbance intensity of **Phen 4.2** (at 276 nm) along with the protonation of the imidazo-phen unit (at 308 nm) and the decrease of emission intensity (at 426 nm). The emission decrease follows a similar pattern to the decrease observed for absorption at 276 nm upon the addition of TFA.

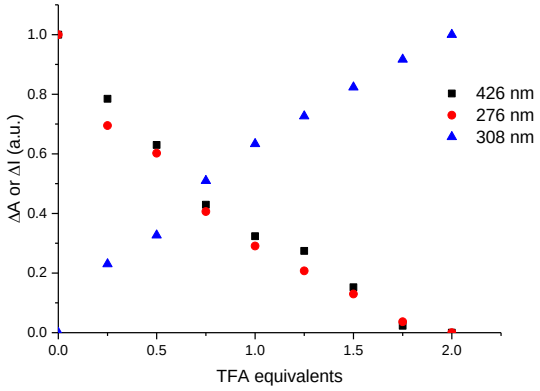

Figure 4-13 Normalised absorption (276 nm and 308 nm) and emission (426 nm) of compound 4.2 (2.3×10^{-5} M) in a DCM solution as function of the number of equivalents of trifluoroacetic acid added (2eq).

4.4.2.1.3 Acidochromism in compound 4.3

Compound **4.3** shows a strong structured absorption band in the UV spectral region at λ_{max}=283 nm (ε=3.7 x 10^4 $M^{-1}cm^{-1}$) and λ_{max}=329 nm (ε=2.9 x 10^4 $M^{-1}cm^{-1}$) **(Figure 4-14a)**, and a blue emission at λ_{em}=437 nm **(Figure 4-14b)**. Upon addition of TFA, strong spectral changes are observed that can be attributed to protonation of the imidazo-phenanthroline unit. The presence of only one isosbestic point at 302 nm suggests the coexistence of the species associated with the protonation of the phenanthroline nitrogen atoms. The absorption changes are complete after addition of 2.0 equivalents of acid.

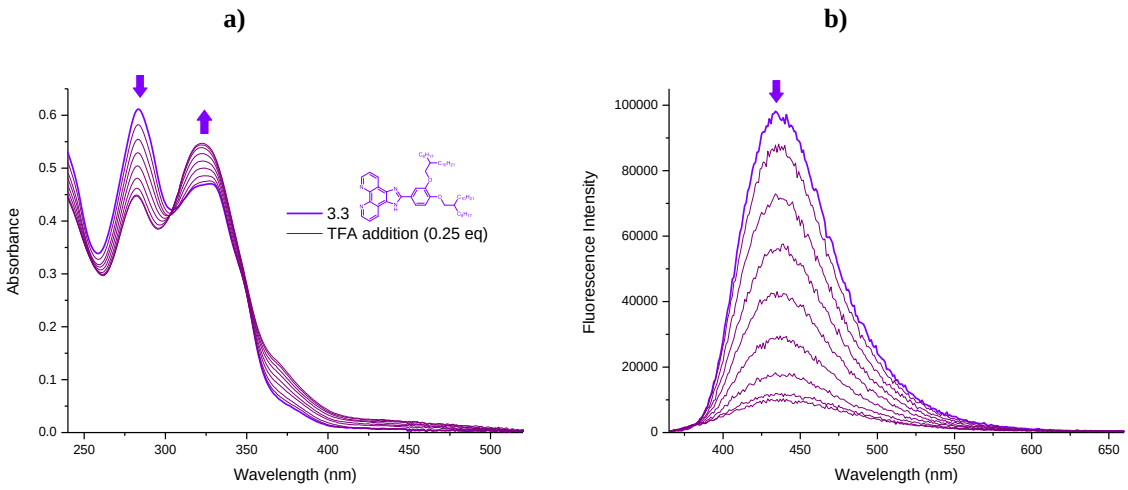

Figure 4-14 Spectrophotometric titration of compound 4.3 (1.6×10^{-5} M) with TFA (2.6×10^{-2} M) in DCM: a) absorption; b) emission (energy of excitation 350 nm)

Figure 4-15 shows a plot of the normalised absorption and emission variation as a function of the number of TFA equivalents. There is an absorbance decrease of the band associated with **Phen 4.3** (at 437 nm) along with an increase in the band which correspond to the protonated imidazo-phen unit (at 329 nm) and a decrease of emission intensity (at 437 nm). The emission of Phen was quenched by the addition of TFA.

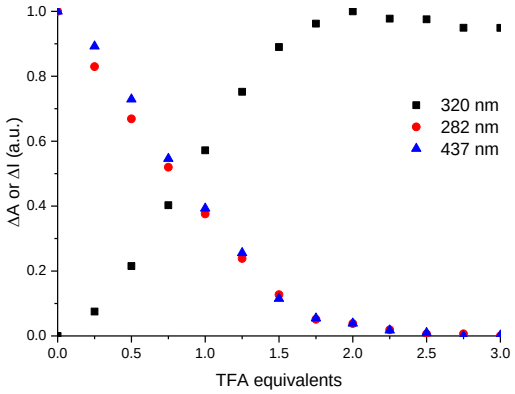

Figure 4-15 Normalised absorption (282 nm and 329 nm) and emission (437 nm) of compound 4.3 (1.6×10^{-5} M) in a DCM solution as function of the number of equivalents of trifluoroacetic acid added (3 eq).

4.4.2.1.4 Acidochromism in compound 4.4

Compound **4.4** shows a strong structured absorption band in the UV spectral region at λ_{max}=283 nm (ε=3.3 x 10^4 $M^{-1}cm^{-1}$) and λ_{max}=327 nm (ε=2.0 x 10^4 $M^{-1}cm^{-1}$) **(Figure 4-16a)**, and a blue emission at λ_{max}=437 nm **(Figure 4-16b)**. Upon addition of TFA, strong spectral changes are observed that can be attributed to the protonation of the imidazo-phen unit at λ_{max}=309 nm. The presence of only one isosbestic point at 297 nm suggests the coexistence of two species associated with the protonation of the phenanthroline nitrogen atoms. The titration is complete after 3 equivalents of the TFA are added and the band at λ_{max}=309 nm is assigned to the protonated species.

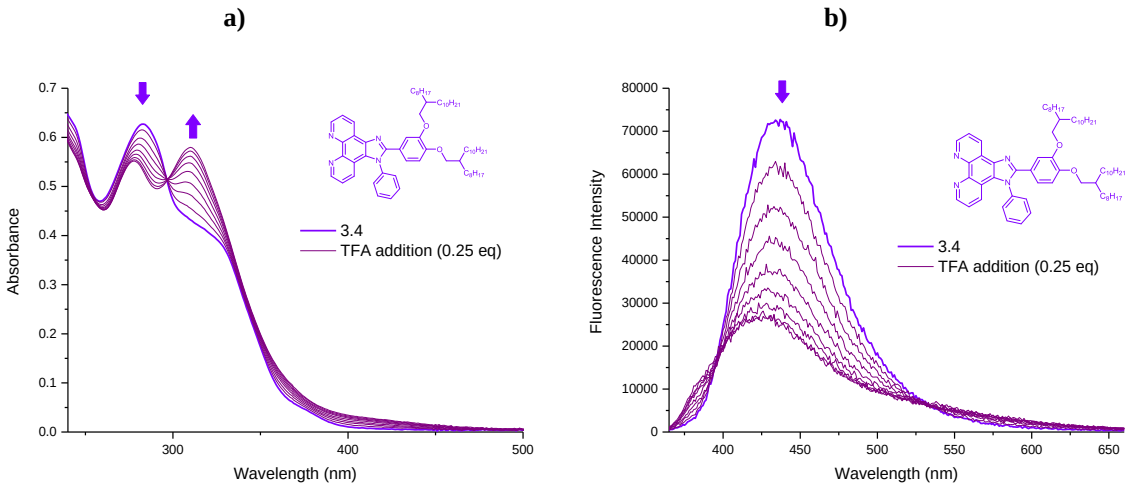

Figure 4-16 Spectrophotometric titration of compound 4.4 (1.9×10^{-5} M) with TFA (2.6×10^{-2} M) in DCM: a) absorption; b) emission (energy of excitation 350 nm)

Figure 4-17 shows a plot of the normalised absorption and emission variation as a function of the number of TFA equivalents, which correspond to the decrease in absorbance intensity of **Phen 4.4** (437 nm) with the protonation of the imidazo-phen unit (309 nm) and the decrease of emission intensity (437 nm). The emission is quenched by the addition of TFA and the decrease is parallel to the decrease observed for the absorption at 283 nm.

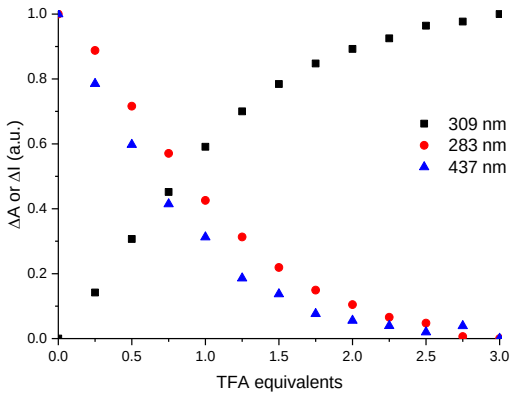

Figure 4-17 Normalised absorption (283 nm and 309 nm) and emission (437 nm) of compound 4.4 (1.9×10^{-5} M) in a DCM solution as function of the number of equivalents of trifluoroacetic acid added (3 eq).

4.4.2.1.5 Acidochromism in compound 4.5

Compound **4.5** shows a strong structured absorption band in the UV spectral region at λ_{max}=284 nm (ε=3.4 x 10^4 $M^{-1}cm^{-1}$) and λ_{max}=341 nm (ε=2.4 x 10^4 $M^{-1}cm^{-1}$) **(Figure 4-18a)**, and a blue emission at λ_{em}=404 nm, λ_{em}=427 nm, λ_{em}=453 nm and λ_{em}=490 nm **(Figure 4-18b)**. Upon addition of trifluoracetic acid, strong spectral changes are observed and can be attributed to protonation of the imidazo-phen unit. The absorption spectra now shows the presence of two well-defined isosbestic points and an "artificial" one which is the product of the dilutions. These two isosbestic points at 291 nm and 384 nm are indicative of the coexistence of different species in equilibrium, as a consequence of two imidazo-phenan units (four nitrogen atoms). The titration is complete after 4 equivalents of TFA are added, absorption bands at λ_{max}=303 nm and λ_{max}=330 nm are assigned to the protonated species.

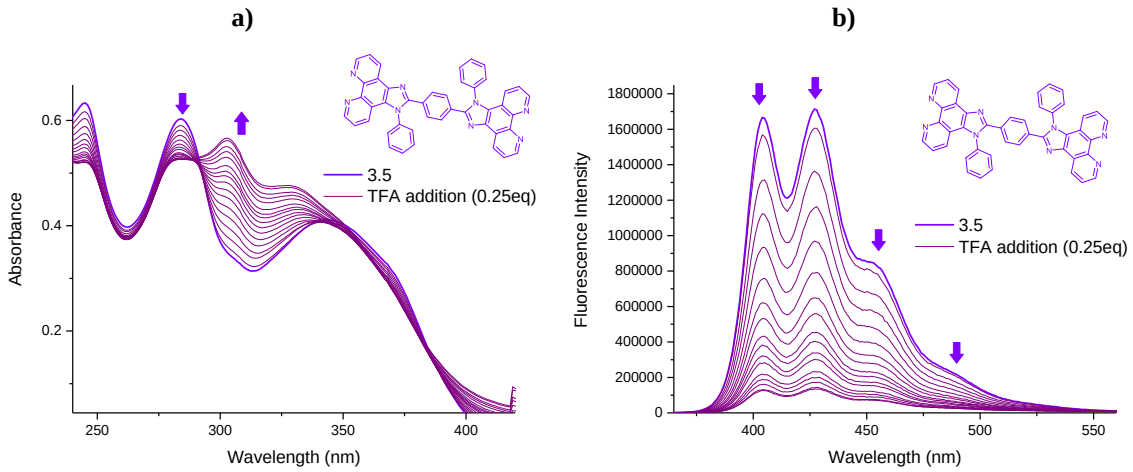

Figure 4-18 Spectrophotometric titration of compound 4.5 (1.6×10^{-6} M) with TFA (2.6×10^{-2} M) in DCM: a) absorptio; b) emission (energy of excitation 350 nm)

Figure 4-19 shows a plot of the normalised absorption and emission variation as a function of the number of TFA equivalents, which correspond to the absorbance intensity decrease of **Phen 4.5** (309 nm) with the protonation of the imidazo-phen unit (at 437 nm) and the decrease of emission intensity (at 404 nm, 427 nm, 453 nm and 490 nm). Emission of Phen is quenched by the addition of TFA.

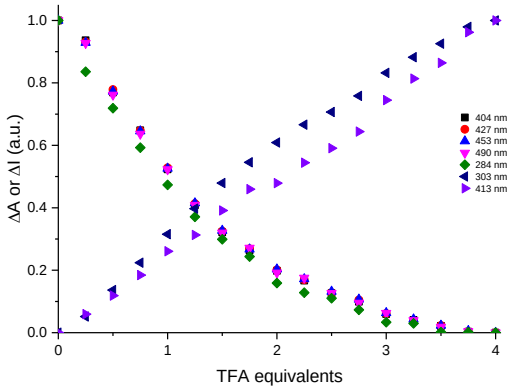

Figure 4-19 Normalised absorption (284 nm, 303 nm and 413 nm) and emission (404 nm, 427 nm, 453nm and 490 nm) of compound 3.5 (1.6×10^{-6} M) in a DCM solution as function of the number of equivalents of trifluoroacetic acid added (4 eq).

4.4.3 ^{1}H NMR titrations

The response of phenanthrolines **4.2-4.5** in $CDCl_3$ (0.3-0.4 mM) to acid was tested using TFA (1.3×10^{-6} M). In general on addition of TFA, there was a downfield shift of the hydrogens of the Phen core. Preferential location in the case of unsymmetrical N-Ph substituted phenanthrolines was observed due to steric and electronic effects[285]. While for compound **4.3** the proton was shared between the Phen nitrogen atoms, when the molecule became symmetric after the imidazole was protonated.

The asymmetric Phen derivative **4.2** displayed a distinct downfield shift in the signals of the protons belonging to the Phen unit 1-H, 3-H, 2-H, 1'-H and 3'-H upon addition of TFA **(Figure 4-20)**. Addition of 2.0 equivalents of TFA did not lead to substantial changes, indicating the completion of the protonation event. There was a preferential protonation to N **(Figure 4-21)**, however the shuttling of the proton between both nitrogen atoms (N and N) was fast on the NMR time scale. Therefore, the NMR spectra represented an average of the adduct shown in **Figure 4-20**. There was no significant shift in the signals of protons 4-H, 5-H, 2''-H, 3''-H and 4''-H **(Figure 4-20)**. This suggested that under experimental conditions there was not a second protonation event occurring in the benzoimidazole in $CDCl_3$.

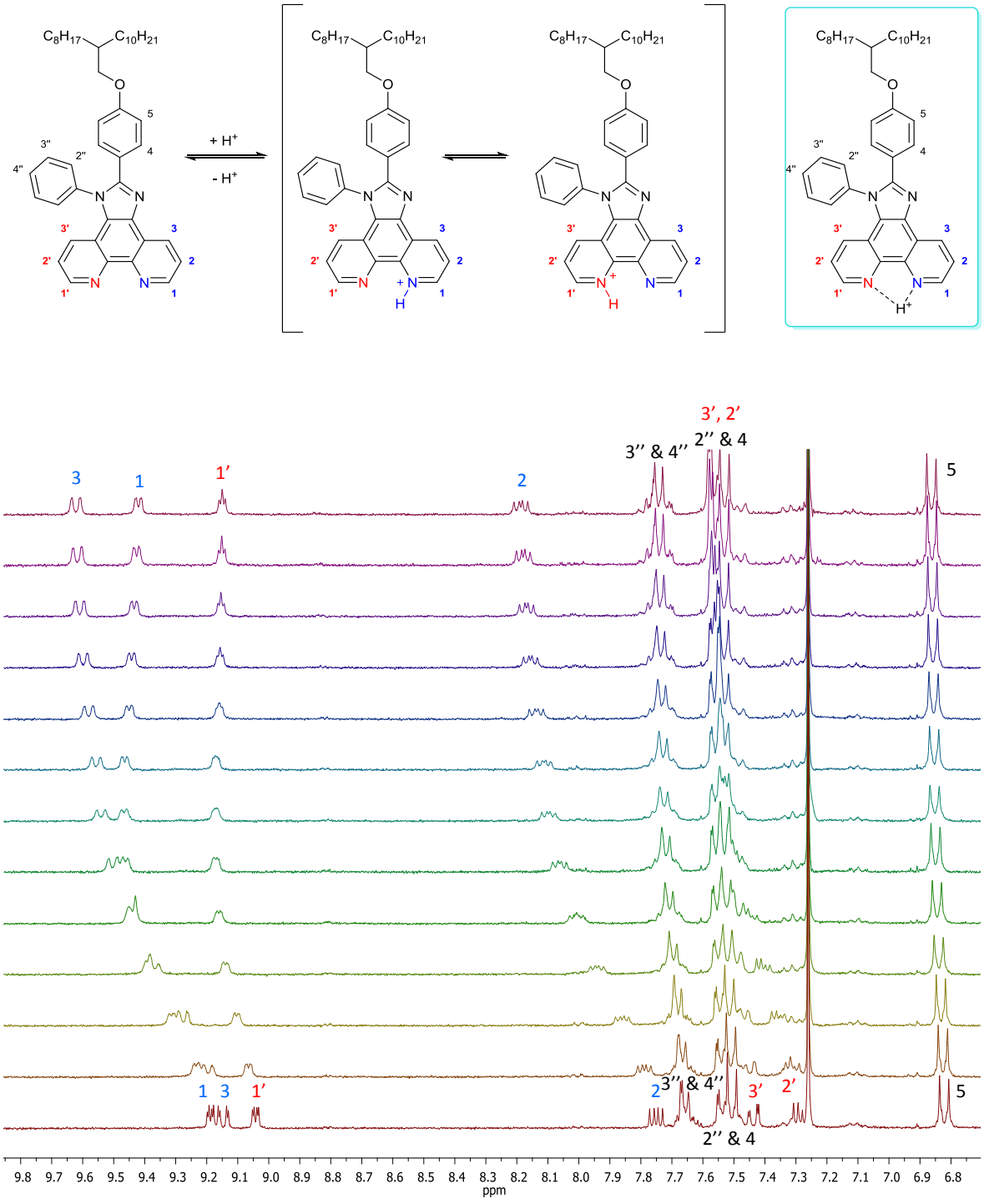

Figure 4-20 ^{1}H NMR titration of phenanthroline 4.2 (0.45 mM) in $CDCl_3$ with TFA addition: from 0 to 3 eq, with a consecutive aliquot of 0.25 eq (from bottom to the top)

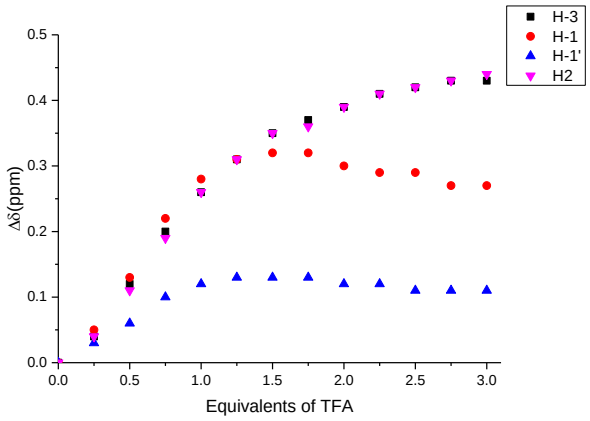

Figure 4-21 ^{1}H NMR proton shift upon titration of a phenanthroline 4.2 (0.45 mM) against TFA in $CDCl_3$

^{1}H NMR investigation of compound **4.3** shows broad signals. The broadness of the signals could be due to the concentration of the sample or dynamic exchange behaviour of the molecule (e.g. rotamers, proton exchange). The ^{1}H NMR was attempted using different concentrations and at a higher temperature. Lower concentrations were inconsistent with the integration values of expected protons, and could be a consequence of slow spin relaxation. Another experiment at high temperature (333 K) was performed to improve the signal resolution, however there were no changes. The H signals became more defined after addition of 2.5 equivalents of TFA **(Figure 4-22)**. The pK_a values of phenanthroline (4.95) and benzimidazole (5.48) are very similar indicating that protonation can occur simultaneously at the imidazole and phenanthroline unit. Most likely, protonation of the imidazole takes place due to the shifts of protons 4-H, 6-H being more affected than 5-H **(Figure 4-22)**.

The 1-H, 3-H, 2-H, 1'-H and 3'-H protons of asymmetric Phen derivative **4.4** displayed a distinct downfield shift upon the addition of TFA **(Figure 4-23)**. Addition of 2.25 equivalents of TFA did not lead to substantial changes indicating the completion of the protonation event. There was a preferential protonation to N **(Figure 4-24)**, however the shuttling of the proton between both nitrogen atoms (N and N) was fast. Therefore, the NMR spectra was an average of the adduct shown in **Figure 4-23**. There is no significant shift in the signals of protons 4-H, 5-H, 6-H, 2''-H, 3''-H and 4''-H **(Figure 4-23)**. This suggested that under experimental conditions there was not a second protonation event occurring in the benzoimidazole.

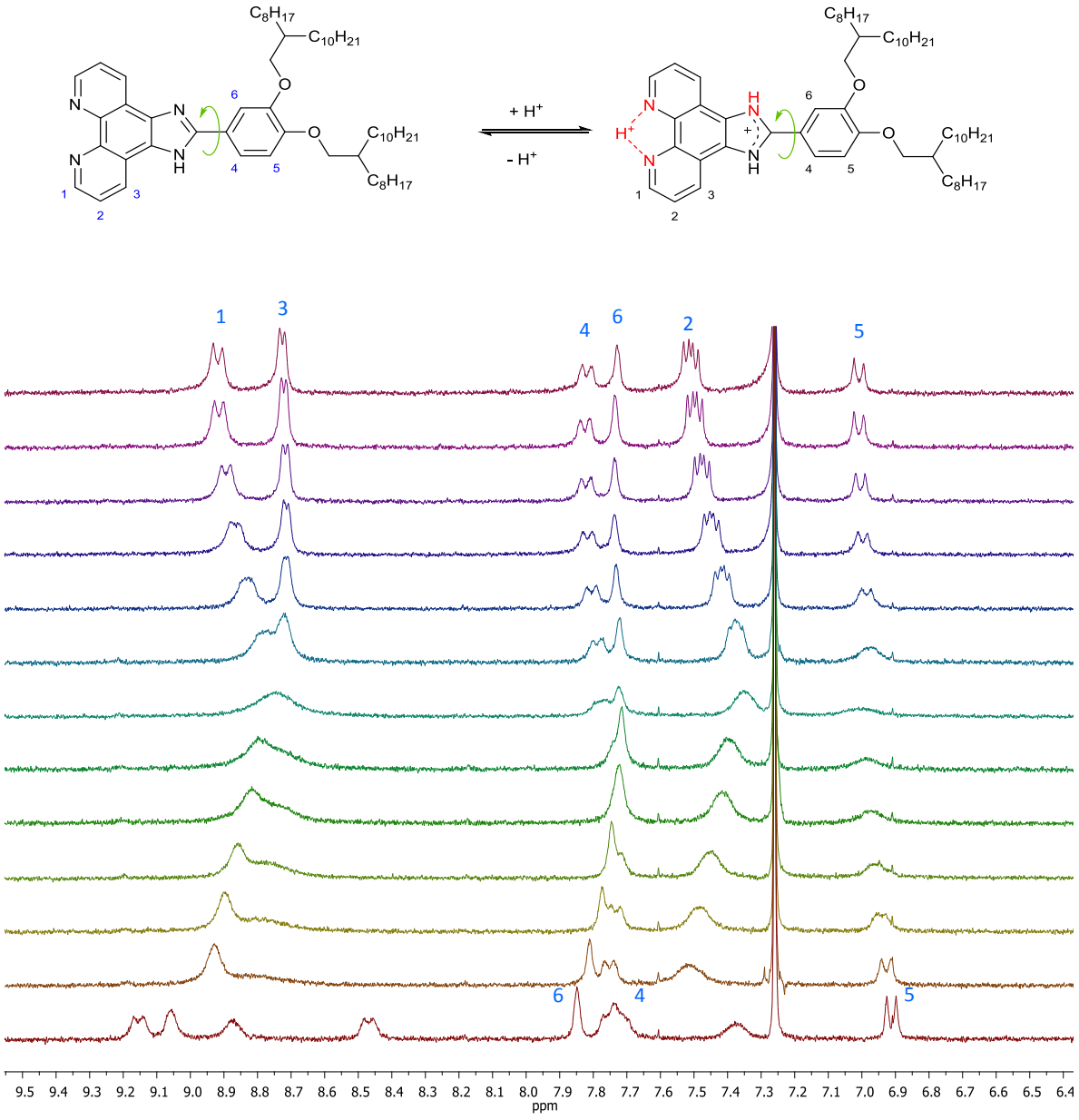

Figure 4-22 ^{1}H NMR titration of a phenanthroline 4.3 (0.32 mM) in $CDCl_3$ with TFA addition: from 0 to 3 eq, with a consecutive aliquot of 0.25 eq (from bottom to the top)

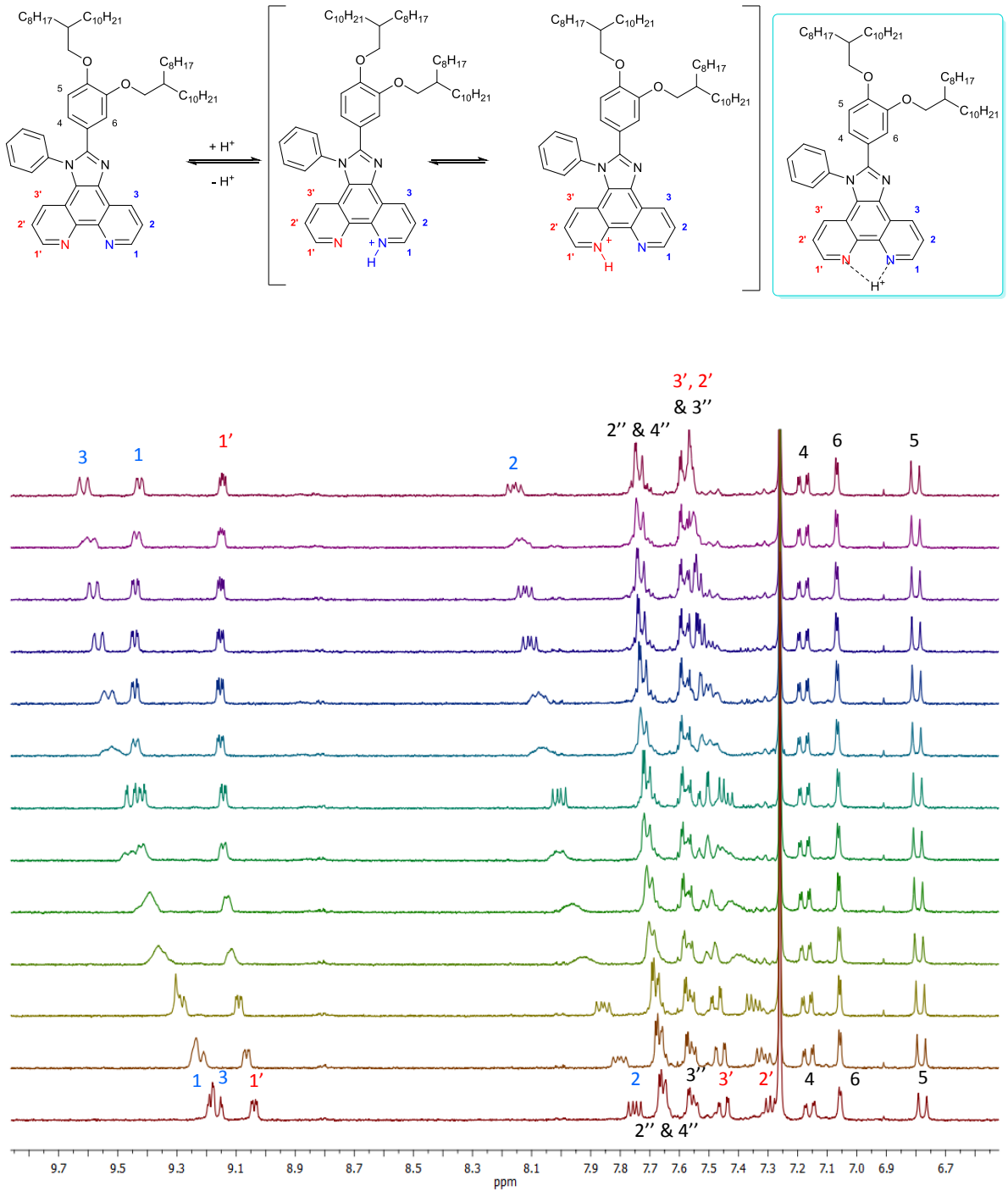

Figure 4-23 ^{1}H NMR titration of a phenanthroline 4.4 (0.30 mM) in $CDCl_3$ with TFA addition: from 0 to 3 eq, with a consecutive aliquot of 0.25 eq (from bottom to the top)

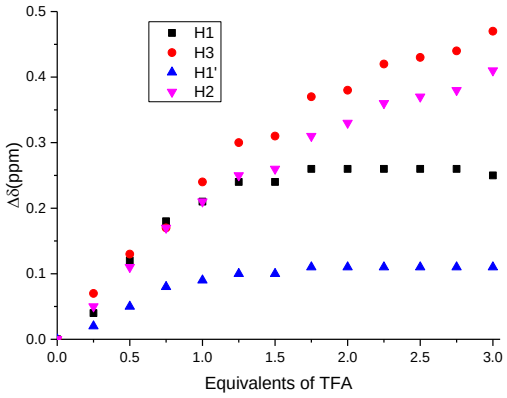

Figure 4-24 ^{1}H NMR proton shift upon titration of a phenanthroline 4.4 (0.30 mM) against TFA in $CDCl_3$

The asymmetric Phen derivative **4.5** displayed a distinct downfield shift in the signals of the protons belonging to the Phen structure, such as 1-H, 3-H, 2-H, 1'-H and 3'-H upon addition of TFA **(Figure 4-25)**. Between addition of 1.0 equivalent and 2.0 equivalents there was no substantial shift in the signals of the aforementioned protons. As can be seen from **Figure 4-26**, the gradients of the first process and second process are very similar. This indicates a sequential protonation process of the equivalent phenanthroline hydrogens. Here too, there was a preferential protonation to N. The NMR spectra was an average of the adduct shown in **Figure 4-25** due to the fast shuttling of the proton between both nitrogen atoms (N and N). There was no significant shift in the signals of protons 4-H, 5-H, 6-H, 2''-H, 3''-H and 4''-H **(Figure 4-25)**. This suggested that under experimental conditions there was not a second protonation event occurring in the benzoimidazole.

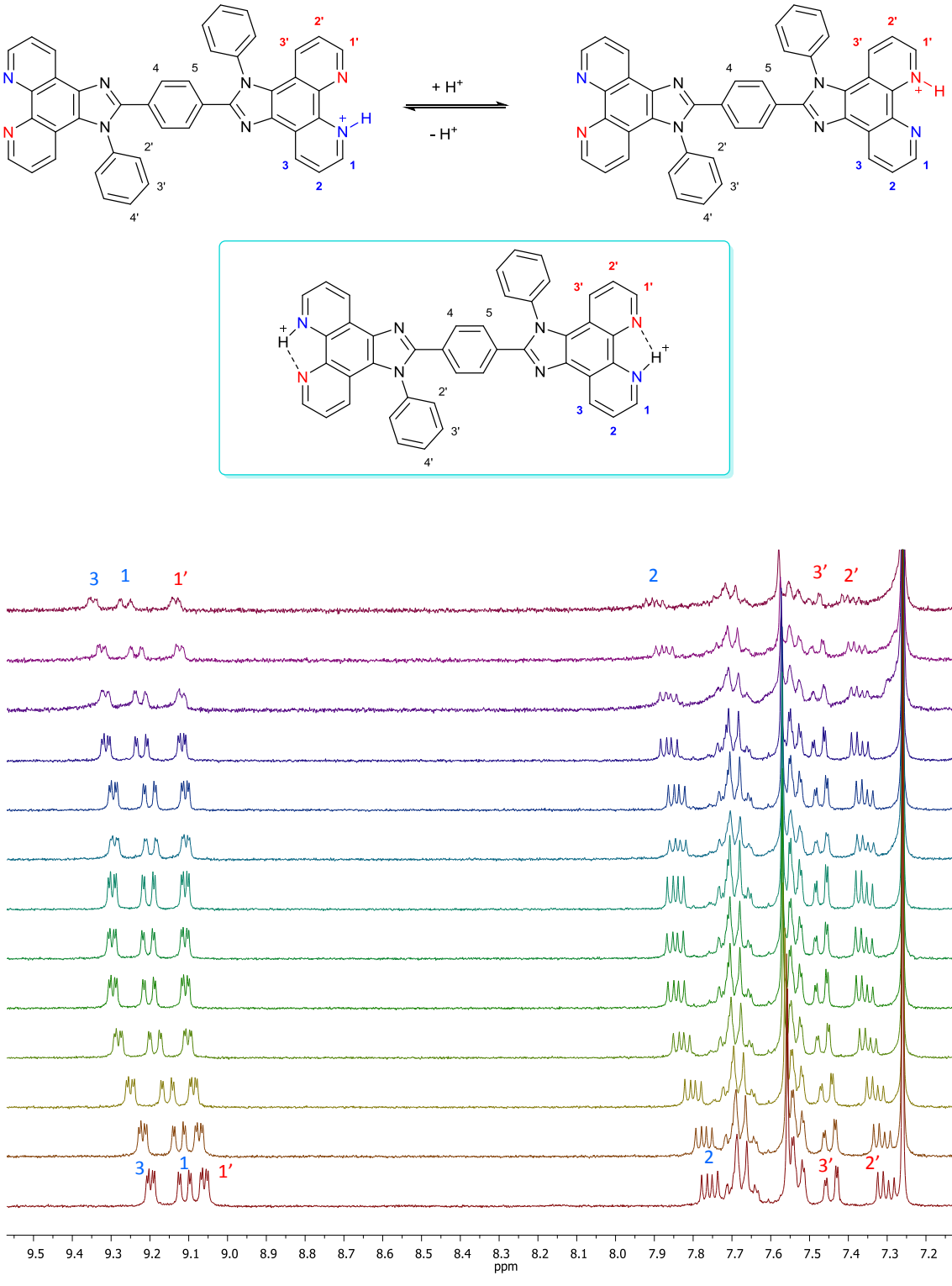

Figure 4-25 ^{1}H NMR titration of a phenanthroline 4.5 (0.36 mM) in $CDCl_3$ with TFA addition: from 0 to 3 eq, with a consecutive aliquot of 0.25 eq (from bottom to the top)

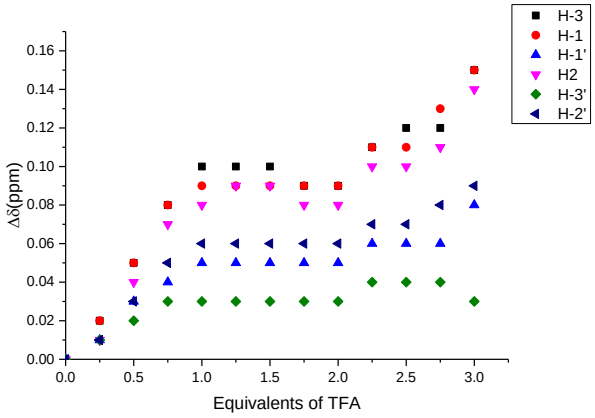

Figure 4-26 ^{1}H NMR proton shift upon titration of a phenanthroline 4.5 (0.36 mM) against TFA in $CDCl_3$

4.5 Analysis of Ir(III)-phenanthroline complexes

4.5.1 Photophysical properties of compounds Ir.4.1-Ir.4.5

In cyclometalated iridium complexes, fluorescence is mostly absent as a result of spin–orbit coupling from the metal; which accelerates intersystem crossing to the triplet state[265].

Figure 4-27 shows the spectroscopic behaviour of *fac*-[Ir(C^N)$_3$] in dichloromethane solution. *Fac*-Ir (ppy)$_3$ shows an intense ultraviolet absorption band (250-320 nm) associated to ^{1}LC (π-π* absorption of the free ppy ligand). The weaker absorption bands on the visible region (320-510 nm) are assigned to MLCT transitions[235, 286]. The band with a maximum at 385 nm is typically assigned to ^{1}MLCT, whereas the weaker shoulder that appears at longer wavelengths (450-510 nm) is assigned to ^{3}MLCT[287]. *Fac*-Ir (ppy)$_3$ in dichloromethane solution shows an asymmetric emission band at 515 nm. This broad band is associated with phosphorescence from ^{3}MLCT[288-290].

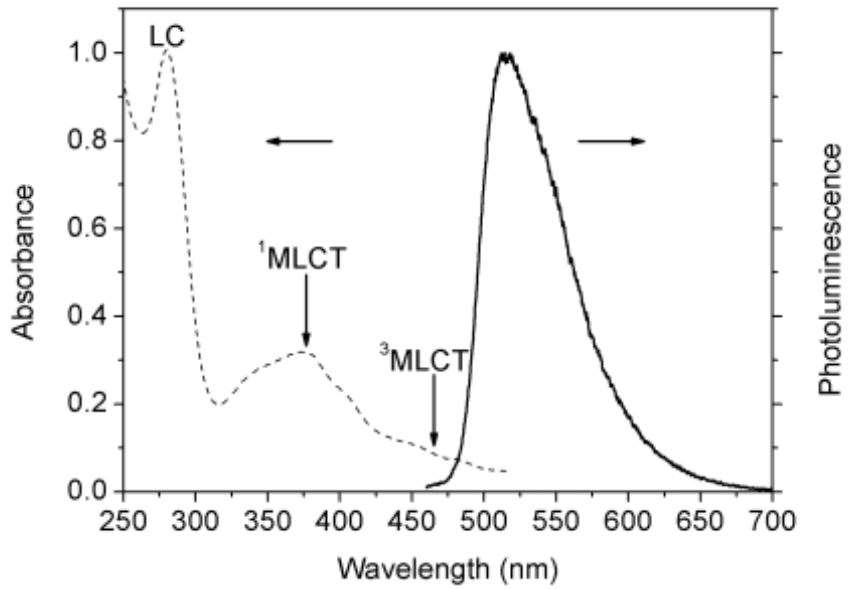

Figure 4-27 Normalised absorption (dashed line) and photoluminescence (solid line) spectra of $Ir(ppy)_3$ in dichloromethane. Taken from (Wang *et al.*, 2009)[287]

4.5.1.1 Absorption and emission properties of compounds Ir.4.1-Ir.4.5

The spectroscopic behaviour of five cationic iridium(III) complexes in dichloromethane solution were studied. Due to the presence of the same cyclometalated ligand 2-phenylpyridine and different Phen derivatives as auxiliary ligands, the absorption spectra of compounds **Ir.4.1-Ir.4.4** displayed high similarities **(Figure 4-28)**. However, the polynuclear complex **Ir.4.5** possesses an enhanced extinction coefficient (10^5 $M^{-1}cm^{-1}$ *vs* 10^4 $M^{-1}cm^{-1}$). Photoluminescence spectra of complexes **Ir.4.1-Ir.4.5** in dichloromethane **(Figure 4-28)** consist of broad, featureless and asymmetric bands with a maximum intensity in the range of 567-574 nm, almost resembling one another. These bands can be assigned to MLCT transitions. The photophysical data of the target iridium(III) complexes are summarised in **Table 4-2**.

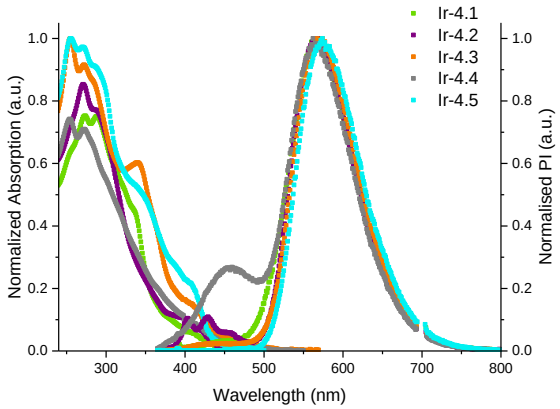

Figure 4-28 Normalised absorption and photoluminiscence spectra of complexes Ir.4.1-Ir.4.5 in DCM at room temperature (excitation energy: 350 nm)

Table 4-2 Optical properties of compounds Ir.4.1-Ir.4.5

Compound	Absorbance λ_{max} (nm), $\varepsilon(M^{-1}cm^{-1})$	Emission λ_{em} (nm), Φ_{PL}	
Ir. 4.1	273, 5.3 x 10^4; 288, 5.3 x 10^4	570	0.069
Ir.4.2	271, 5.8 x 10^4; 287, 5.2 x 10^4	567	0.028
Ir.4.3	255, 6.2 x 10^4 ; 272, 5.7 x 10^4; 340, 3.7 x 10^4; 415, 8.2 x 10^4; 470, 2.2 x 10^4	571	0.057
Ir.4.4	254, 6.7 x 10^4; 272, 6.4 x 10^4	465, 567	0.054
Ir.4.5	255, 7.1 x 10^5 ; 270, 6.9 x 10^5; 296, 6.1 x 10^5; 348, 3.6 x 10^5; 412, 1.5 x 10^5; 469, 2.4 x 10^4	574	0.054

4.5.1.1.1 Compound Ir.4.1

The absorption behaviour of compound **Ir.4.1** in DCM (8.87 x 10^{-6} M) at room temperature was studied. Similar to published data, the observed bands at λ_{max} =273 nm (ε=5.3 x 10^4 $M^{-1}cm^{-1}$) and λ_{max} =272 nm (ε=5.3 x 10^4 $M^{-1}cm^{-1}$) can be assigned to π-π^* (spin-allowed) transitions, these intense bands in the UV region closely resemble the ones of free ppy[287] and phen **4.1** free ligands. There is another band at around 339 nm (ε=3.0 x 10^4 $M^{-1}cm^{-1}$) and also

a weaker absorption band extended to the visible region with a maximum at around 400 nm (ε=4.7 x 10^3 $M^{-1}cm^{-1}$). The latter can be due to ^{1}MLCT or ^{3}MLCT transitions. The photoluminescence spectrum of **Ir.4.1** in dichloromethane solution shows an asymmetric emission band. This major peak at 570 nm is responsible for the orange emission upon excitation with light at 350 nm.

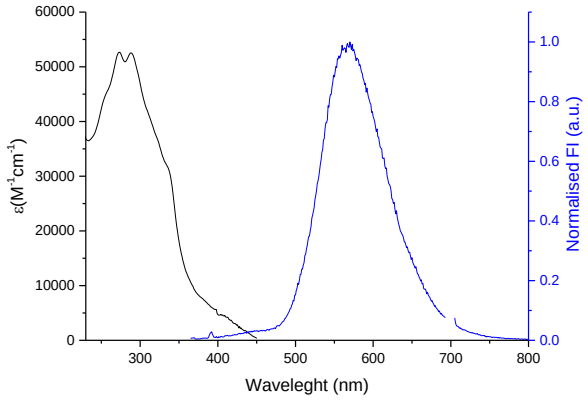

Figure 4-29 Absorption spectra of compound Ir.4.1 and normalised photoluminescence in dichloromethane (excitation energy: 350 nm)

4.5.1.1.2 Compound Ir.4.2

The absorption behaviour of compound **Ir.4.2** in DCM (1.08 x 10^{-5} M) at room temperature was studied. Similar to published data, the observed bands with λ_{max}=271 nm (ε=5.8 x 10^4 $M^{-1}cm^{-1}$) and λ_{max}=287 nm (ε=5.2 x 10^4 $M^{-1}cm^{-1}$) can be assigned to π-π* (spin-allowed) transitions, these intense bands in the UV region closely resemble the ones of the free ppy[287] and phen **4.2** ligands. The weaker absorption band, extended to the visible region, observed at around 406 nm (ε=5.5 x 10^3 $M^{-1}cm^{-1}$) can be due to ^{1}MLCT or ^{3}MLCT transitions. The photoluminescence spectrum of **Ir.4.2** in dichloromethane solution shows four bands; three weaker bands at 403 nm, 429 nm and 456 nm and a major peak at 567nm. Excitation performed at 350 nm caused orange emission associated with the prime peak at 567 nm.

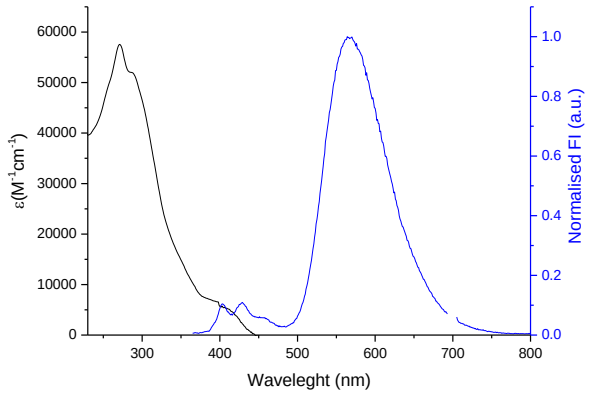

Figure 4-30 Absorption spectra of compound Ir.4.2 and normalised photoluminescence in dichloromethane (excitation energy: 350 nm)

4.5.1.1.3 Compound Ir.4.3

The absorption behaviour of compound **Ir.4.3** in DCM (9.5 x 10^{-6} M) at room temperature was studied. Similar to published data, the observed bands with λ_{max} =255 nm (ε=6.2 x 10^4 $M^{-1}cm^{-1}$) and λ_{max} =272 nm (ε=5.7 x 10^4 $M^{-1}cm^{-1}$) can be assigned to the π-π* (spin-allowed) transitions, these intense bands in the UV region closely resemble the ones of the ppy[287] and phen **4.3** free ligands. The weaker absorption band with a maximum at λ_{max} =340 nm (ε = 3.7 x 10^4 $M^{-1}cm^{-1}$) could be due to ^{1}MLCT, whereas the weaker shoulder that appears between 415-470 nm, with vibrational satellites could be due to ^{3}MLCT transitions. The photoluminescence spectrum of **Ir.4.3** in dichloromethane solution shows a major band associated with ^{3}MLCT transition. This major peak at 571 nm is responsible for the orange emission upon excitation with light at 350 nm.

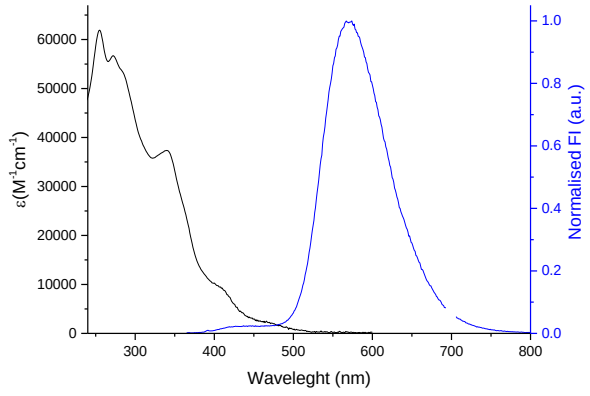

Figure 4-31 Absorption spectra of compound Ir.4.3 and normalised photoluminescence in dichloromethane (excitation energy: 350 nm)

4.5.1.1.4 Compound Ir.4.4

The absorption behaviour of compound **Ir.4.4** in DCM (7.94 x 10^{-6} M) at room temperature was studied. Similar to published data, the observed bands with λ_{max} =254 (ε=6.7 x 10^4 $M^{-1}cm^{-1}$) and 272 nm (ε=6.4 x 10^4 $M^{-1}cm^{-1}$) can be assigned to π-π* (spin-allowed) transitions, these intense bands in the UV region closely resemble the ones of ppy[287] and phen **4.4** free ligands. The weaker absorption band, extended to the visible region, observed at around 400 nm can be due to ^{1}MLCT or ^{3}MLCT transitions. The photoluminescence spectrum of **Ir.4.4** in dichloromethane solution shows two bands. A weaker band with its intensity at 465 nm and a major peak. The orange emission upon excitation with light at 350 nm is a consequence of the peak at 567 nm.

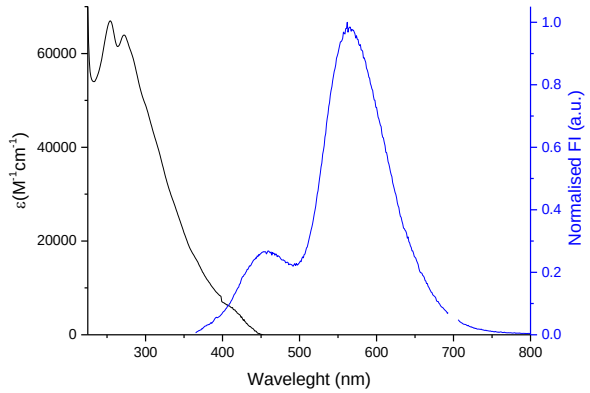

Figure 4-32 Absorption spectra of compound Ir.4.4 and normalised photoluminescence in dichloromethane (excitation energy: 350 nm)

4.5.1.1.5 Compound Ir.4.5

The absorption behaviour of compound **Ir.4.5** in DCM (5.71 x 10^{-6} M) at room temperature was studied. Similar to published data, the observed bands with λ_{max} =at 255, 270 and 296 nm can be allocated to the π-π* transitions ($\varepsilon \approx 10^5$ $M^{-1}cm^{-1}$), these three intense ultraviolet bands closely resemble the ones of free ppy[287] and phen **4.4** free ligands. The weaker absorption band, extended to the visible region, observed at between 400-500 nm can be due to ^{1}MLCT or ^{3}MLCT (metal-to-ligand charge-transfer transitions). The photoluminescence spectrum of **Ir.4.5** in dichloromethane solution consists of a featureless and asymmetric bands with intensity maximum at 571 nm. This prime peak is responsible for the orange emission upon excitation with light at 350 nm.

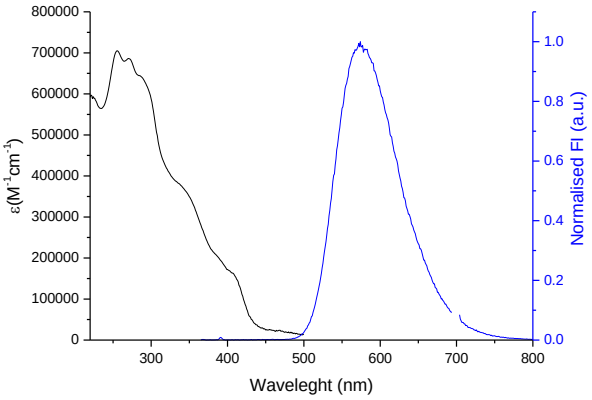

Figure 4-33 Absorption spectra of compound Ir.4.5 and normalised photoluminescence in dichloromethane (excitation energy: 350 nm)

4.6 Conclusions

This chapter describes effective ways to tune the photophysical properties and to improve the emission efficiency of phenanthroline derivatives. Two different strategies were investigated for the synthesis of 1H-imidazo[4,5-f][1,10]phenanthroline derivatives. A small library of five novel structures **4.1-4.5** was prepared.

One of the main issues of phenanthroline derivatives is their low solubility in most organic solvents. Therefore, an important goal was to increase the solubility by using a bulky branched chain and the substitution of the –NH with a phenyl group. The latter has proven to be more efficient than addition of a second 4-[(2-octyldodecyl)oxyl] substituent.

Notice that the racemic mixture of 2-octyl-dodecanol was used to develop the synthetic strategy. There are four possible diastereoisomers for the molecules **35**, **4.3** and **4.4** which have two chiral centers. There was no observation of any optical activity $[\alpha]_{598}^{20}$ for compounds 33-36 and 4.1-4.4.

Analysis of these molecules using UV-vis spectroscopy showed the dependence of the photoluminescence properties from the structure of the phen-based derivatives. This strategy allowed improvement of the quantum yields of compounds **4.2-4.4** compared with unmodified phen emission (Φ=0.0087). Emission of compound **4.5** was proven to be the most effective (Φ=0.68).

The response of the phen derivatives to acid was tested using UV-vis spectroscopy studies which confirm that protonation induced stabilisation of the electronic transitions with a positive acidochromism (red-shift). In addition, ^{1}H NMR titrations supported that basicity in **4.1-4.5** was influenced by the -NH substitution.

The UV-vis spectroscopy and ^{1}HNMR analysis of all the novel compounds helped to give a deeper understanding of the photophysical properties of the molecules, along with their potential as sensors.

The synthesis of four mononuclear **Ir.4.1-Ir.4.4** and one of the di-nuclear **Ir.4.5** novel iridium(III) complexes was successfully carried out. The UV-vis absorption spectra of the cationic iridium(III) complexes **Ir.4.1-Ir.4.5** displayed common features. These small differences were a result of the use of the different phenanthrolines **4.1-4.5** as ancillary ligand (N^N). However, the polynuclear complex **(Ir.4.5)** possessed enhanced extinction coefficient in comparison to the mononuclear analogues. Moreover, the use of the same cyclometalated ligand along with modified phenanthrolines in mononuclear complexes did not show a substantial change on the emission. Emission maximum was not very sensitive to the type of ancillary ligand used. Interestingly, the di-nuclear Ir(III) complex **(Ir.4.5)** has a very similar emission pattern to the synthesised mononuclear Ir(III) complexes. The photoluminescence quantum yields in dichloromethane solutions were moderated (Φ_{PL}<0.1).

4.7 Experimental

4.7.1 General techniques

All chemicals were obtained from Sigma Aldrich, Alfa Aesar, VWR and Across and used without further purification. Anhydrous solvents were obtained from a PureSolv MD6 solvent purification system. ^{1}H NMR and ^{13}C NMR spectra were recorded on a Bruker Advanced 500 spectrometer. Chemical shifts (δ) are reported in parts per million (ppm) relative to the residual solvent peak and peaks are described as singlet (s), doublet (d), triplet (t), quartet (q), sextet (sex), multiplet (m), broad singlet (br) and coupling constants (J) are quoted in Hertz (Hz). Spectra were recorded in chloroform-d, dichloromethane-d_2 or deuterated DMSO-d_6 and were measured at room temperature unless otherwise stated. Where needed, two dimensional correlation spectroscopy (2D-COSY), heteronuclear single quantum coherence spectroscopy (HSQC) and heteronuclear multiple bond correlation spectroscopy (HMBC) were used in order to aid assignment. The progress of reactions was monitored by TLC and purified by column

chromatography using silica gel 60 (40-63µm). High resolution mass spectrometry (HRMS) was performed on Bruker MaXis Impact (EI+) by positive and negative electrospray ionisation. The accepted experimental error was <4 ppm. High performance liquid chromatography (HPLC) was performed on an Agilent 1100 Infinity Series equipped with a UV detector and Ascentis Express C_{18} reverse phase column, using MeCN/water (50-95%) containing 0.1% TFA, at a flow rate of 0.5 mL min^{-1} over a period of 12 minutes. Infrared spectra (IR) were recorded in solid phase on a Bruker Alpha Platinum ATR FTIR spectrometer with vibrational frequencies given in cm^{-1}. Melting points were measured on a Stuart SMP30. The electronic absorption spectra were recorded on a Cary 100 UV-vis scanning spectrometer. The fluorescence spectra were recorded on a FluoroMax-3 spectrofluorimeter. Quantum yields of fluorescence were measured by the relative method using optically dilute solutions.

4.7.2 Experiments

4.7.2.1 1,10-Phenanthroline-5,6-dione (S.16)[194]

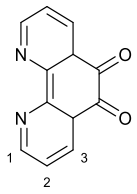

The compound 1,10-phenanthroline-5,6-dione **(S.16)** was prepared from a modification of literature method. Dropwise concentrated H_2SO_4 (35 mL) was added to 1,10-phenanthroline **(S.15)** (2.51 g, 13.9 mmol), in an ice bath. To this solution NaBr (4.54 g, 44.1 mmol) was added, followed by the dropwise addition of concentrated HNO_3 (17.5 mL). The mixture was stirred at room temperature for 20 min and then refluxed for 1h. After being allowed to cool to room temperature, crushed ice was added and the solution was neutralised 30% (v/v) NaOH. The filtrate (dissolved in hot water) and the filtered waters were extracted with DCM. The organic layers were collected and, after removal of the solvent under pressure, the title compound was obtained as yellow solid (1.53 g, 52%). **^{1}H NMR** (400 MHz, $CDCl_3$) δ ppm 9.12 (dd, *J* = 4.7, 1.7 Hz, 2H, 1-H), 8.51 (dd, *J* = 7.9, 1.7 Hz, 2H), 2-H, 7.59 (dd, *J* = 7.9, 4.7 Hz, 2H, 3-H); **m/z (ES+):** Found: 213.0650 [M+H], requires: 213.0659

4.7.2.2 (±)-9-(Iodomethyl)nonadecane (33)[272]

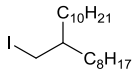

To a stirred solution of 2-octyl-dodecanol (11.08 g, mmol) in of dichloromethane at 0 °C triphenylphosphine (13.11 g, 50 mmol) and imidazole (3.4 g, 50 mmol) were added. The mixture was stirred for 15 minutes before iodine (12.1 g, 48 mmol) was added in small portions. The reaction was allowed to warm to room temperature over 2 h before the addition of 5 mL of saturated Na_2SO_3. The bright yellow reaction mixture was concentrated *in vacuo*, diluted with pentane (50 mL) and washed with water (3 × 100 mL) and brine (100 mL). The resulting pentane solution was passed through a silica plug, eluting with pentane and concentrated *in vacuo* to yield the product as a colorless oil (14.15 g, 93%). **^{1}H NMR** (500 MHz, $CDCl_3$) δ ppm 3.27 (d, *J* = 4.6 Hz, 2H, I-CH_2), 1.53 (s, 1H, -CH) 1.27 (m, 32H, -CH_2), 0.88 (m, 6H, -CH_3); **m/z (ES+):** iodide too labile.

4.7.2.3 4-(1H-imidazo[4,5-f][1,10]phenanthrolin-2-yl)phenol (31)[291]

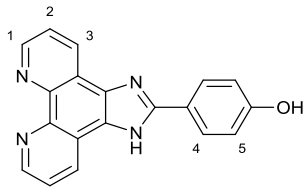

A mixture of 1,10-phenanthroline-5,6-dione **(S.16)** (704 mg, 3.32 mmol), 4-hydroxybenzaldehyde **(S.24)** (446 mg, 3.65 mmol) and ammonium acetate (5.1 g, 66.3 mmol) in glacial acetic acid (15 mL) was refluxed under nitrogen for 3.5 h. The reaction was allowed to reach room temperature and filtered, then washed with copious amounts of acetone and ether. The title compound was obtained as a yellow solid after being *vacuum* dried (927 mg, 90%).**^{1}H NMR** (300 MHz, DMSO) δ ppm 9.02 (dd, *J* = 4.3, 1.7 Hz, 2H, 1-H), 8.91 (d, *J* = 8.2 Hz, 2H, 3-H), 8.12 (d, *J* = 8.7 Hz, 2H, 5-H), 7.83 (bs, 2H, 2-H), 6.99 (d, *J* = 8.7 Hz, 2H, 4-H); **m/z (ES+):** Found: 335.0904 [M+Na], requires: 335.0903.

4.7.2.4 4-(1H-imidazo[4,5-f][1,10]phenanthrolin-2-yl)benzene-1,2-diol (32)[271]

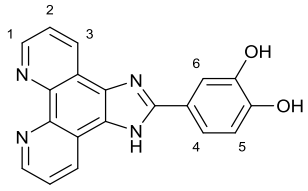

A mixture of 1,10-phenanthroline-5,6-dione **(S.16)** (426 mg, 2.01 mmol), 3,4-dihydroxybenzaldehyde **(S.25)** (305 mg, 2.21 mmol) and ammonium acetate (3.1g, 40.2 mmol) in glacial acetic acid (9 mL) was refluxed under nitrogen for 2 h and 20 min. The reaction was allowed to reach room temperature, then poured into water and treated with ammonia solution (35%) until neutral pH. The precipitate was filtered off and washed with

abundant water to obtain the title compound as a brownish solid (614 mg, 93%). **^{1}H NMR** (300 MHz, DMSO) δ ppm 9.02 (d, *J* = 4.1 Hz, 2H, 1-H), 8.91 (dd, *J* = 14.4, 7.6 Hz, 2H, 3-H), 7.87 – 7.77 (m, 2H, 2-H), 7.74 (d, *J* = 2.1 Hz, 1H, 5-H), 7.60 (dd, *J* = 8.2, 2.1 Hz, 1H, 4-H), 6.95 (d, *J* = 8.2 Hz, 1H, 5-H); **m/z (ES+):** Found: 351.0850 [M+Na], requires: 351.0852.

4.7.2.5 (±)-4-[(2-octyldodecyl)oxy]benzaldehyde (34)

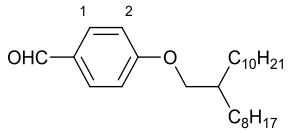

To a solution of 4-hydroxybenzaldehyde **(S.24)** (995 mg, 8.2 mol), and potassium carbonate (1.13 g, 9.8 mmol) in DMF (10 mL) dropwise 9-(iodomethyl)nonadecane **(33)** (4.0 g, 9.8 mmol) was added. The mixture was refluxed under nitrogen for 24 h. The reaction was allowed to reach room temperature, poured onto water and then extracted with DCM. The combined organic layers were dried over $MgSO_4$ and the solvents were evaporated under reduced pressure. The residue was purified by silica gel column chromatography (Hexane-DCM, 1:2) to provide a colourless oil (2.1 g, 63%). **^{1}H NMR** (400 MHz, $CDCl_3$) δ ppm 9.88 (s, 1H, -CHO), 7.82 (d, *J* = 8.7 Hz, 1H, 2-H), 6.99 (d, *J* = 8.7 Hz, 1H, 1-H), 3.91 (d, *J* = 5.8 Hz, 2H, -OCH_2), 1.80 (dt, *J* = 12.0, 5.8 Hz, 1H, -CH), 1.26 (s, 33H, -CH_2), 0.88 (t, *J* = 6.8 Hz, 6H, -CH_3); **^{13}C NMR** (100 MHz, $CDCl_3$) δ ppm 190.9, 164.7, 132.1, 129.9, 114.9, 38.0, 31.4, 30.1, 29.8, 29.8, 29.8, 29.7, 29.5, 29.5, 27.0, 14.3; **m/z (ES+):** Found: 425.3391 [M+Na], requires: 425.3390; **IR ν_{max}/cm^{-1} (liquid):** 2921, 2852, 1693, 1600, 1577, 1509, 1466, 1391, 1377, 1310, 1254, 1214, 1157, 1019.

4.7.2.6 Diastereoisomers of 3,4-bis[(2-octyldodecyl)oxy]benzaldehyde (35)

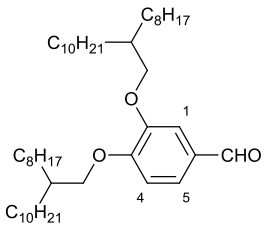

To a solution of 3,4-dihydroxybenzaldehyde **(S.25)** (1.03 g, 7.5 mmol) and potassium carbonate (4.1 g, 29.8 mmol) in DMF (30 mL) was added dropwise 9-(iodomethyl)nonadecane **(33)** (9.3 g, 22.7 mmol). The mixture was refluxed under nitrogen for 24 h. The reaction was cooled to room temperature, poured onto water and then extracted with DCM. The combined organic layers were dried over $MgSO_4$ and the solvents were evaporated under reduced pressure. The residue was purified by silica gel column chromatography (Hexane-DCM, 2:1)

to provide a brown oil (2.7 g, 51%). **^{1}H NMR** (400 MHz, $CDCl_3$) δ ppm 9.83 (s, 1H, -CHO), 7.40 (dd, *J* = 8.1, 1.8 Hz, 1H,5-H), 7.37 (d, *J* = 1.8 Hz, 1H, 1-H), 6.93 (d, *J* = 8.1 Hz, 1H, 4-H), 3.92 (dd, *J* = 11.8, 5.7 Hz, 4H, -OCH_2), 1.83 (dq, *J* = 11.8, 5.7 Hz, 2H, -CH), 1.26 (s, 64H, -CH_2), 0.88 (t, *J* = 6.8 Hz, 12H, -CH_3); **^{13}C NMR** (100 MHz, $CDCl_3$) δ ppm 191.2, 155.3, 150.0, 129.9, 126.7, 111.7, 110.7, 71.8, 38.2, 32.1, 31.5, 31.5, 30.3, 30.2, 29.9, 29.8, 29.8, 29.5, 27.1, 22.9, 14.3; **m/z (ES+):** Found: 699.6663 [M+H], requires: 699.6650; **IR ν_{max}/cm^{-1} (liquid):** 2921, 2852, 1691, 1594, 1584, 1509, 1465, 1435, 1378, 1340, 1266, 1237, 1164, 1020.

4.7.2.7 (±)-3-hydroxy-4-[(2-octyldodecyl)oxy]benzaldehyde (36)

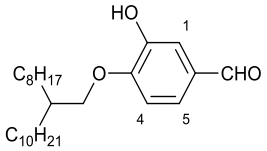

To a solution of 3,4-dihydroxybenzaldehyde **(S.25)** (370 mg, 2.68 mmol), and potassium carbonate (778 mg, 5.63 mmol) in DMF (10 mL) dropwise 9-(iodomethyl)nonadecane **(33)** (2.4 g, 5.9 mmol) was added. The mixture was refluxed under nitrogen for 24 h. The reaction was cooled to room temperature, poured onto water and then extracted with DCM. The combined organic layers were dried over $MgSO_4$ and the solvents were evaporated under reduced pressure. The residue was purified by silica gel column chromatography (Hexane-DCM, 1:2) to provide a brown oil (318 mg, 28%). **^{1}H NMR** (400 MHz, $CDCl_3$) δ ppm 9.84 (s, 1H, -CHO), 7.45 (d, *J* = 1.9 Hz, 1H, 1-H), 7.42 (dd, *J* = 8.2, 1.9 Hz, 1H, 5-H), 6.96 (d, *J* = 8.2 Hz, 1H, 4-H), 5.69 (s, 1H, -OH), 4.01 (d, *J* = 5.8 Hz, 2H, -OCH_2), 1.86 (dt, *J* = 12.1, 5.8 Hz, 1H, -CH), 1.48 – 1.15 (m, 35H, -CH_2), 0.88 (t, *J* = 6.8 Hz, 6H, -CH_3); **^{13}C NMR** (100 MHz, $CDCl_3$) δ ppm 191.1, 151.5, 146.4, 130.6, 124.6, 114.2, 111.0, 72.3, 38.0, 32.1, 32.0, 31.5, 30.1, 29.8, 29.8, 29.7, 29.7, 29.5, 29.4, 27.0, 22.8, 22.8, 14.3; **m/z (ES+):** Found: 441.3340 [M+Na], requires: 441.3339; **IR ν_{max}/cm^{-1} (liquid):** 3549, 3368, 2921, 2852, 1686, 1610, 1585, 1507, 1459, 1377, 1343, 1272, 1244, 1199, 1124, 1012.

4.7.2.8 (±)-2-{4-[(2-octyldodecyl)oxy]phenyl}-1H-imidazo[4,5-f][1,10]phenanthroline (4.1)

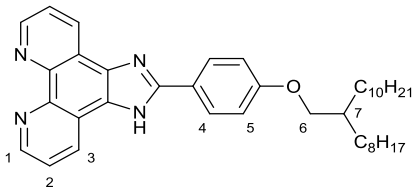

A mixture of 1,10-phenanthroline-5,6-dione **(S.16)** (988 mg, 4.66 mmol), of 4-[(2-octyldodecyl)oxy]benzaldehyde **(34)** (1.7 g, 4.2 mmol) and ammonium acetate (6.5 g, 84.6 mmol) in glacial acetic acid (28 mL) was refluxed under nitrogen for 24 h. The reaction mixture was poured into water and treated with ammonia solution (35%) until neutral pH. The precipitate was filtered off and washed with abundant water. The compound was dissolved in DCM and washed with water. The combined organic layers were dried over $MgSO_4$ and the solvents were evaporated under reduced pressure. The residue was purified by silica gel column chromatography (DCM-EtOH to pure EtOH) to obtained the title compound as a yellow solid (560 mg ,22%). **^{1}H NMR** (400 MHz, $CDCl_3$) δ ppm 8.87 (s, 2H, 1-H), 8.75 (s, 2H, 3-H), 8.27 (d, *J* = 8.5 Hz, 2H, 5-H), 7.35 (s, 2H, 2-H), 6.76 (d, *J* = 8.5 Hz, 2H, 4-H), 3.72 (d, *J* = 5.3 Hz, 2H, 6-H), 1.69 (s, 1H, 7-H), 1.22 (s, 36H, -CH_2), 0.84 (m, 6H, CH_3); **^{13}C NMR** (100 MHz, $CDCl_3$) δ ppm 160.7, 152.6, 147.2, 143.8, 130.9, 128.5, 123.3, 122.8, 114.8, 71.1, 38.0, 32.0, 32.0, 31.4, 30.1, 29.8, 29.7, 29.7, 29.5, 29.4, 26.9, 22.8, 22.8, 14.2; **m/z (ES+):** Found: 593.4227 [M+H], requires: 593.4214; **ν_{max}/cm^{-1} (solid):** 3072, 2920, 1610, 1579, 1525, 1483, 1455, 1401, 1360, 1333, 1291, 1246; **M.pt**: >350 °C.

4.7.2.9 (±)-2-{4-[(2-octyldodecyl)oxy]phenyl}-1-phenyl-1H-imidazo[4,5-f][1,10]phenanthroline (4.2)

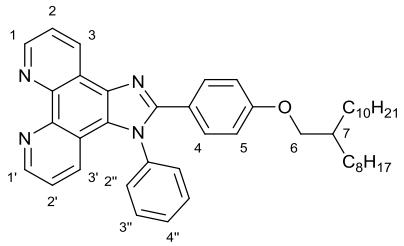

A mixture of 1,10-phenanthroline-5,6-dione **(S.16)** (1.5 g, 6.9 mmol), of 4-[(2-octyldodecyl)oxy]benzaldehyde **(34)** (2.30 g, 5.71 mmol), aniline (0.63 mL, 6.85 mmol) and ammonium acetate (4.40 g, 57.1 mmol) in glacial acetic acid (25 mL) was refluxed under nitrogen for 24 h. The reation mixture was poured into water and treated with ammonia solution (35%) until neutral pH, then poured onto water and then extracted with DCM. The combined

organic layers were dried over $MgSO_4$ and the solvents were evaporated under reduced pressure The residue was purified by silica gel column chromatography (DCM-EtOH, 10:1 to pure EtOH) to obtain the title compound as a brown solid (3.1 g, 81 %). **^{1}H NMR (**400 MHz, $CDCl_3$) δ ppm 9.19 (dd, *J* = 4.4, 1.7 Hz, 1H, 1-H), 9.14 (dd, *J* = 8.1, 1.7 Hz, 1H, 3-H), 9.04 (dd, *J* = 4.3, 1.5 Hz, 1H, 1'-H), 7.75 (dd, *J* = 8.1, 4.4 Hz, 1H, 2-H), 7.65 (dt, *J* = 8.9, 4.4 Hz, 3H, 3''-H and 4''-H), 7.54 (dd, *J* = 7.9, 1.6 Hz, 2H, 2''-H), 7.50 (d, *J* = 8.9 Hz, 2H, 4-H), 7.43 (dd, *J* = 8.4, 1.5 Hz, 1H, 3'-H), 7.28 (dd, *J* = 8.4, 4.3 Hz, 1H, 2'-H), 6.82 (d, *J* = 8.9 Hz, 2H, 5-H), 3.81 (d, *J* = 5.8 Hz, 2H, 6-H), 1.75 (dd, *J* = 11.5, 5.8 Hz, 1H, 7-H), 1.26 (s, 38H, -CH_2), 0.88 (t, *J* = 6.7 Hz, 6H, CH_3); **^{13}C NMR** (100 MHz, $CDCl_3$) δ ppm 160.4 (s), 152.5 (s), 149.1 (s), 147.9 (s), 145.0 (s), 144.5 (s), 138.4 (s), 136.3 (s), 130.8 (s), 130.7 (s), 130.3 (s), 129.0 (s), 128.0 (s), 126.9 (s), 124.2 (s), 123.6 (s), 122.2 (s), 122.1 (s), 120.0 (s), 120.0 (s), 114.6 (s), 71.2 (s), 38.0 (s), 32.1 (s), 32.1 (s), 31.5 (s), 30.2 (s), 29.8 (s), 29.8 (s), 29.7 (s), 29.5 (s), 29.5 (s), 27.0 (s), 22.8 (s), 14.3 (s); **m/z (ES+):** Found: 670.4534 [M+H], requires: 670.4516; **ν_{max}/cm^{-1} (solid):** 2348, 3064, 2921, 2852, 1686, 1608, 1498, 1465, 1442, 1377, 1296, 1250; **M.pt**: 178-180 °C.

4.7.2.10 Diastereoisomers of 2-{3,4-bis[(2-octyldodecyl)oxy]phenyl}-1H-imidazo[4,5-f][1,10]phenanthroline (4.3)

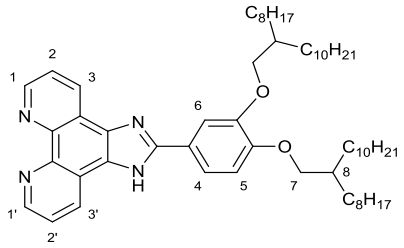

A mixture of 1,10-phenanthroline-5,6-dione **(S.16)** (0.75 g, 3.54 mmol), 3,4-bis[(2-octyldodecyl)oxy]benzaldehyde **(35)** (1.7 g, 2.4 mmol) and ammonium acetate (3.6 g, 47.2 mmol) in glacial acetic acid (20 mL) was refluxed under nitrogen for 24 h. The reaction mixture was poured into water and treated with ammonia solution (35%) until neutral pH. The precipitate was filtered off and washed with abundant water. The compound was dissolved in DCM and washed with water. The combined organic layers were dried over $MgSO_4$ and the solvents were evaporated under reduced pressure. The residue was purified by silica gel column chromatography (DCM-EtOH to pure EtOH) to obtain the title compound as an orange crystalline solid (227 mg, 14 %). **^{1}H NMR** (400 MHz, $CDCl_3$+TFA) δ ppm 9.32 (d, *J* = 8.2 Hz, 2H, 1-H), 9.03 (d, *J* = 4.7 Hz, 2H, 3-H), 7.94 (dd, *J* = 8.2, 4.7 Hz, 2H, 2-H), 7.73 (d, *J* = 8.5 Hz, 1H, 4-H), 7.65 (s, 1H, 6-H), 6.90 (d, *J* = 8.5 Hz, 1H, 5-H), 3.94 (d, *J* = 4.8 Hz, 2H, 7-H), 1.96 – 1.75 (m, 1H, 8-H), 1.59 – 1.11 (m, 34H, -CH_2), 0.99 – 0.71 (m, 12H, -CH_3); **^{13}C NMR**

(100 MHz, $CDCl_3$+TFA) δ ppm 155.1, 152.0, 150.6, 146.6, 136.5, 135.6, 126.4, 125.8, 122.3, 119.9, 119.8, 116.9, 114.1, 113.1, 112.7, 111.2, 110.8, 72.2, 72.0, 38.4, 38.2, 32.1, 31.4, 30.3, 29.9, 29.9, 29.9, 29.8, 29.8, 29.6, 29.6, 27.1, 22.9, 14.2; **m/z (ES+):** Found: 889.7298 [M+H], requires: 889.7293; **ν_{max}/cm^{-1} (solid):** 3084, 2954, 2920, 2851, 1605, 1564, 1522, 1489, 1394, 1260, 1218, 1133, 1068, 1029, 806, 739; **M.pt**: 85-87 °C.

4.7.2.11 Diastereoisomers of 2-{3,4-bis[(2-octyldodecyl)oxy]phenyl}-1-phenyl-1H-imidazo[4,5-f][1,10]phenanthroline (4.4)

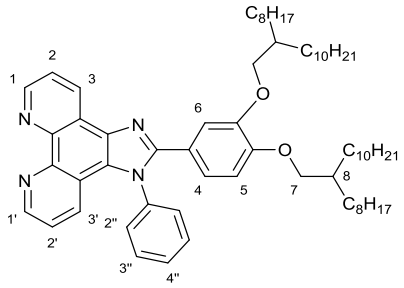

A mixture of 1,10-phenanthroline-5,6-dione **(S.16)** (685 mg, 3.22 mmol), 3,4-bis[(2-octyldodecyl)oxy]benzaldehyde **(35)** (2.3 g, 3.2 mmol), aniline (0.35 mL) and ammonium acetate (2.49 g, 32.2 mmol) in glacial acetic acid (14 mL) was refluxed under nitrogen for 24 h. The reaction mixture was then cooled to room temperature. The reaction mixture was poured into water and treated with ammonia solution (35%) until neutral pH and then extracted with DCM. The combined organic layers were dried over $MgSO_4$ and the solvents were evaporated under reduced pressure. The residue was purified by silica gel column chromatography (DCM-EtOH to pure EtOH) to obtain the title compound as a red crystalline solid/glue (1.50 g, 48%). **^{1}H NMR (400 MHz, $CDCl_3$)** δ ppm 9.16 (m, 2H, 1-H and 3-H), 9.03 (dd, *J* = 4.3, 1.5 Hz, 1H, 1'-H), 7.75 (dd, *J* = 8.1, 4.4 Hz, 1H, 2-H), 7.70 – 7.61 (m, 3H, 2''-H and 4''-H), 7.56 (dd, *J* = 6.5, 3.0 Hz, 2H, 3''-H), 7.44 (dd, *J* = 8.4, 1.5 Hz, 1H, 3'-H), 7.32 – 7.27 (m, 1H, 2'-H), 7.16 (dd, *J* = 8.4, 2.0 Hz, 1H, 4-H), 7.05 (d, *J* = 2.0 Hz, 1H, 6-H), 6.77 (d, *J* = 8.5 Hz, 1H, 5-H), 3.83 (d, *J* = 5.6 Hz, 2H, 7-H), 3.61 (d, *J* = 5.6 Hz, 2H, 7-H), 1.76 (m, 2H, 8-H), 1.36 (m, 64H, -CH_2), 0.93 – 0.81 (m, 12H, CH_3); **^{13}C NMR (100 MHz, $CDCl_3$)** δ ppm 152.6, 150.7, 149.2, 149.2, 148.0, 145.0, 144.6, 138.8, 136.3, 130.8, 130.8, 130.4, 129.2, 128.1, 126.9, 124.2, 123.7, 122.5, 122.3, 122.3, 120.1, 120.1, 114.3, 113.0, 72.0, 71.8, 38.3, 38.3, 32.2, 31.6, 30.0, 30.0, 30.0, 29.9, 29.7, 29.6, 27.2, 22.9, 14.4; **m/z (ES+):** Found: 965.7606 [M+H], requires: 975.7606; **ν_{max}/cm^{-1} (solid/glue):** 3263, 3136, 3054, 2954, 2921, 2852, 1691, 1670, 1599, 1498, 1464, 1443, 1316, 1257, 1223; **M.pt**: 56-58 °C.

4.7.2.12 1,4-Bis(1-phenyl-1H-imidazo[4,5-f][1,10]phenanthrolin-2-yl)benzene (4.5)

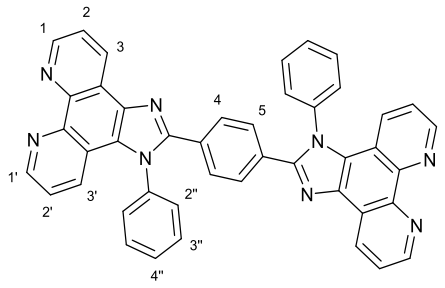

A mixture of 1,10-phenanthroline-5,6-dione **(S.16)** (639 mg, 3.01 mmol), terephtaldehyde **(S.27)** (202 mg, 1.51 mmol), aniline (0.28 mL, 3.01 mmol) and ammonium acetate (4.6 g, 60.2 mmol) in glacial acetic acid (4 mL) was refluxed under nitrogen for 24 h. The reaction mixture was then cooled to room temperature before the amount of glacial acetic acid was reduced under vacuum. The resulting clay was poured into water and neutralised with ammonia solution (35%). The precipitate was obtained using centrifuge and washed with water and diethyl ether. The yellow product was dried using the freeze dryer to give the title compound as a white powder (0.85 g, 85%). **^{1}H NMR** (400 MHz, $CDCl_3$) δ ppm 9.19 (dd, *J* = 4.3, 1.6 Hz, 2H, 1-H), 9.11 (dd, *J* = 8.1, 1.6 Hz, 2H, 3-H), 9.05 (dd, *J* = 4.2, 1.5 Hz, 2H, 1'-H), 7.76 (dd, *J* = 8.1, 4.4 Hz, 2H, 2-H), 7.72 – 7.62 (m, 6H, Ph), 7.58 – 7.50 (m, 4H, Ph), 7.44 (dd, *J* = 8.4, 1.4 Hz, 2H, 3'-H), 7.30 (dd, *J* = 8.4, 4.3 Hz, 2H, 2'-H); **^{13}C NMR (101 MHz, $CDCl_3$)** δ ppm 151.4, 149.3, 148.3, 145.2, 144.7, 137.9, 136.4, 130.9, 130.7, 130.7, 130.6, 129.4, 128.7, 128.2, 127.3, 124.0, 123.7, 122.4, 119.9; **m/z (ES+):** Found: 667.2353 [M+H], requires: 667.2353; **ν_{max}/cm^{-1} (solid):** 3286, 3078, 3056, 1651, 1597, 1564, 1514, 1497, 1465, 1455, 1440, 1425, 1155, 831; **M.pt**: > 350 °C.

4.7.2.13 μ-Dichloro-bridged iridium dimer [Ir(ppy)$_4$Cl$_2$] (37)

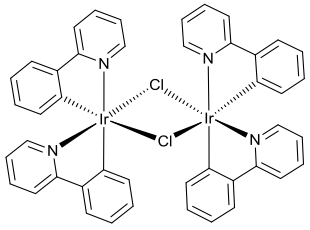

$IrCl_3$ (202 mg, 0.68 mmol) with 2-phenylpyridine **(S.23)** (0.21 mL, 1.49 mmol, 2.2 equivalents) in a mixture of 2-ethoxyethanol and water (3:1) was refluxing at 110 °C overnight. The solid product was filtered through a sinter funnel and washed with water, hexane and diethyl ether. The yellow μ-dichloro-bridged Ir dimer **(37)** was directly used after dried under vacuum without further purification (260 mg, 65%). **^{1}H NMR** (300 MHz, $CDCl_3$) δ ppm 9.24 (dd, *J* =

5.8, 0.6 Hz, 1H), 7.87 (d, *J* = 7.7 Hz, 1H), 7.73 (td, *J* = 7.9, 1.5 Hz, 1H), 7.48 (dd, *J* = 7.6, 1.0 Hz, 1H), 6.85 – 6.67 (m, 2H), 6.56 (td, *J* = 7.6, 1.3 Hz, 1H), 5.93 (d, *J* = 7.3 Hz, 1H); **m/z (ES+):** Found: 501.0941 [M/2-Cl^+], requires: 501.0943.

4.7.2.14 Synthesis of the cationic iridium complexes

All iridium(III) complexes were prepared by the same procedure. Herein, only the synthesis of **4.1** is described in detail.

4.7.2.14.1 $[Ir(ppy)_2(4.1)]^+$(Ir.4.1)

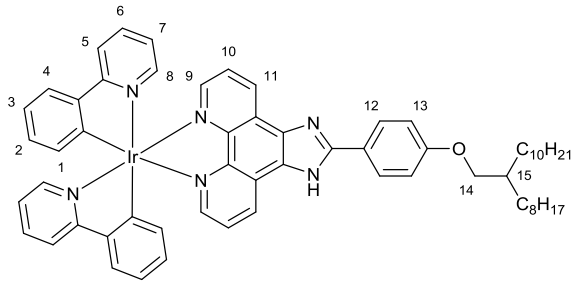

To a solution of 2-{4-[(2-octyldodecyl)oxy]phenyl}-1H-imidazo[4,5-f][1,10]phenanthroline **(4.1)** (96 mg, 0.16 mmol) in ethanol (40 mL) was added an ethanoic solution of µ-dichloro-bridged Ir dimer **(37)** (79 mg, 0.07 mmol). The resulting mixture was refluxed for 24 h. Upon cooling, diethyl ether was added to the reaction mixture and filtered through a sinter funnel. After dried under vacuum the title compound was obtained as a bright yellow crystalline solid (150 mg, 86%). **^{1}H NMR (400 MHz, $CDCl_3$)** δ ppm 8.67 (d, *J* = 8.3 Hz, 2H, 9-H), 8.12 (s, 2H), 7.93 (d, *J* = 8.1 Hz, 2H), 7.71 (m, 7H, 4-H and 11-H), 7.36 (d, *J* = 5.9 Hz, 2H), 7.03 (m, 7H, 3-H), 6.84 (t, *J* = 6.3 Hz, 2H, 2-H), 6.42 (d, *J* = 7.5 Hz, 2H, 1-H), 3.88 (d, *J* = 5.6 Hz, 2H, 14-H), 1.87 – 1.76 (m, 1H, 15-H), 1.31 (m, 32H, -CH_2), 0.87 (m, 6H, -CH_3); **^{13}C NMR (100 MHz, $CDCl_3$)** δ ppm 168.17 (s), 161.16 (s), 155.05 (s), 150.69 (s), 148.68 (s), 147.85 (s), 143.73 (s), 138.02 (s), 132.00 (s), 130.94 (s), 129.38 (s), 124.91 (s), 123.22 (s), 122.77 (s), 121.96 (s), 119.65 (s), 114.91 (s), 71.08 (s), 38.03 (s), 32.03 (s), 31.45 (s), 30.16 (s), 29.81 (s), 29.76 (s), 29.71 (s), 29.46 (s), 26.98 (s), 26.96 (s), 22.79 (s), 14.23 (s); **m/z (ES+):** Found: 1093.5093 [M^+], requires: 1093.5093; **ν_{max}/cm^{-1} (solid):** 3348, 3047, 2920, 2850, 1606, 1583, 1465, 1452, 1362, 1248, 1075, 808, 757, 727.

4.7.2.14.2 [Ir(ppy)$_2$(4.2)]$^+$(Ir.4.2)

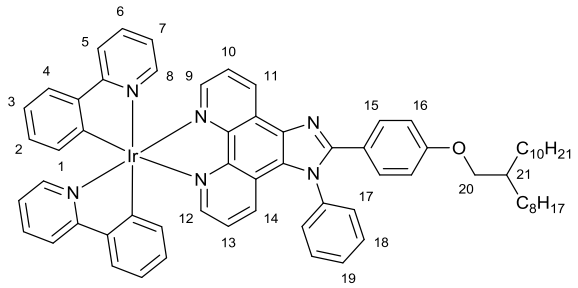

With 0.37 mmol 2-{4-[(2-octyldodecyl)oxy]phenyl}-1-phenyl-1H-imidazo[4,5-f][1,10]phenanthroline **(3.2)** in place of **4.1**, this complex was obtained by a procedure similar to that described for **4.1**. Yield: 42 mg, 98%, gold crystalline solid.**^{1}H NMR (400 MHz, CDCl$_3$)** δ ppm 9.31 (dd, *J* = 8.3, 1.3 Hz, 1H, 9-H), 8.24 (dd, *J* = 5.0, 1.2 Hz, 1H, 11-H), 8.14 (dd, *J* = 5.0, 1.2 Hz, 1H, 12-H), 7.87 (m, 3H, 10-H), 7.78 – 7.58 (m, 10H), 7.49 (m, 4H), 7.34 (dd, *J* = 31.6, 5.3 Hz, 2H), 7.12 – 6.96 (m, 4H), 6.92 (m, 3H, 2-H), 6.81 (d, *J* = 8.9 Hz, 2H), 6.36 (t, *J* = 7.0 Hz, 2H, 1-H), 3.79 (d, *J* = 5.6 Hz, 2H, 20-H), 1.73 (m, 21-H), 1.27 (m, 32H, -CH$_2$), 0.85 (t, *J* = 6.7 Hz, 6H, -CH$_3$); **^{13}C NMR (100 MHz, CDCl$_3$)** δ ppm 168.0, 167.8, 161.1, 155.1, 150.3, 149.9, 149.5, 148.8, 148.8, 148.7, 148.4, 144.8, 144.8, 143.8, 143.7, 138.6, 138.6, 137.2, 137.1, 133.1, 132.0, 132.0, 131.5, 131.4, 131.3, 131.1, 131.0, 130.9, 130.4, 128.9, 128.5, 127.8, 126.9, 126.7, 126.4, 125.1, 125.0, 123.9, 123.6, 123.0, 122.7, 121.0, 120.2, 120.0, 119.9, 114.8, 71.3, 38.0, 32.1, 32.0, 31.4, 30.1, 29.8, 29.8, 29.7, 29.5, 29.5, 27.0, 22.8, 14.3; **m/z (ES+):** Found: 1169.5420 [M$^+$], requires: 1169.5397; **ν_{max}/cm^{-1} (solid):** 3371, 3046, 2920, 2851, 1680, 1605, 1582, 1562, 1439, 1400, 1248, 1176, 1125, 726, 693.

4.7.2.14.3 [Ir(ppy)$_2$(4.3)]$^+$(Ir.4.3)

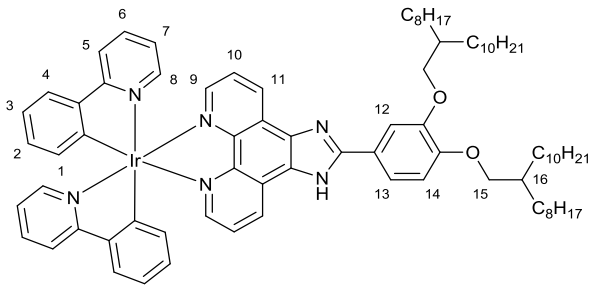

With 0.09 mmol 2-{3,4-bis[(2-octyldodecyl)oxy]phenyl}-1H-imidazo[4,5-f][1,10]phenanthroline **(4.3)** in place of **4.1**, this complex was obtained by a procedure similar to that described for **4.1**. Yield: 93 mg, 98%., orange crystalline solid. **^{1}H NMR** (400 MHz, CDCl$_3$) δ ppm 8.22 (m, 3H), 7.91 (d, *J* = 8.1 Hz, 2H), 7.70 (m, 6H), 7.37 (s, 2H), 6.99 (m, 8H), 6.40 (d, *J* = 7.4 Hz, 2H, 1-H), 4.13 (d, *J* = 5.3 Hz, 2H, 15-H), 3.86 (d, *J* = 5.0 Hz, 2H, 15-H),

1.84 (s, 4H, 16-H), 1.27 (m,64 H, -CH_2), 0.86 (m, 12H, -CH_3); **^{13}C NMR** (101 MHz, $CDCl_3$) δ ppm 168.2, 155.3, 151.5, 150.6, 149.8, 147.9, 143.7, 138.0, 132.0, 131.0, 124.9, 123.2, 122.8, 121.1, 119.7, 113.2, 112.3, 72.2, 71.8, 38.4, 38.2, 32.1, 31.6, 31.5, 30.3, 30.3, 29.9, 29.9, 29.8, 29.6, 29.6, 29.6, 29.5, 29.5, 27.2, 27.1, 22.8, 14.2; **m/z (ES+):** Found: 1389.8179 [M^+], requires: 1389.8163; **ν_{max}/cm^{-1} (solid):** 3046, 2920, 2851, 1737, 1606, 1477, 1455, 1261, 1062, 809, 758, 728.

4.7.2.14.4 [Ir(ppy)$_2$(4.4)]$^+$(Ir.4.4)

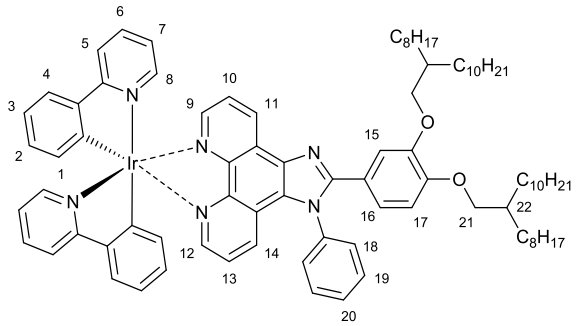

With 0.21 mmol 2-{3,4-bis[(2-octyldodecyl)oxy]phenyl}-1-phenyl-1H-imidazo[4,5-f][1,10]phenanthroline **(4.4)** in place of **4.1**, this complex was obtained by a procedure similar to that described for **4.1**. Yield: 296 mg, 98%, orange crystalline solid. **^{1}H NMR (400 MHz, $CDCl_3$)** δ ppm 9.37 (d, *J* = 7.9 Hz, 1H, 9-H), 8.27 (d, *J* = 4.7 Hz, 1H, 11-H), 8.18 (s, 1H, 12-H), 7.97 – 7.85 (m, 3H, 10-H), 7.73 (m, 9H), 7.58 – 7.47 (m, 3H, 13-H and 14-H), 7.38 – 7.29 (m, 1H), 7.17 (d, *J* = 8.9 Hz, 1H, 16-H), 7.08 (dd, *J* = 16.2, 8.2 Hz, 4H), 7.02 – 6.92 (m, 3H, 2-H), 6.78 (d, *J* = 8.4 Hz, 1H, 17-H), 6.41 – 6.32 (m, 2H, 1-H), 3.84 (d, *J* = 5.6 Hz, 2H, 21-H), 3.59 (d, *J* = 5.4 Hz, 2H, 21-H), 1.87 – 1.72 (m, 2H, 22-H), 1.27 (d, *J* = 8.6 Hz, 64H, -CH_2), 0.97-0.74 (m, 12H, -CH_3); **^{13}C NMR (100 MHz, $CDCl_3$)** δ ppm 168.0, 167.8, 155.0, 151.3, 150.1, 149.7, 149.4, 149.2, 148.7, 148.3, 144.8, 144.7, 143.7, 143.6, 138.5, 138.5, 137.3, 137.1, 133.1, 131.9, 131.9, 131.4, 131.2, 131.0, 130.9, 130.2, 128.8, 128.5, 128.4, 127.7, 126.8, 126.6, 126.3, 125.0, 124.9, 123.7, 123.4, 123.1, 122.9, 122.7, 122.5, 120.8, 120.1, 119.9, 119.8, 113.9, 112.7, 71.8, 71.7, 38.1, 38.1, 32.0, 31.4, 30.2, 30.2, 29.8, 29.8, 29.8, 29.7, 29.5, 29.4, 27.0, 27.0, 24.7, 22.8, 14.2: **m/z (ES+):** Found: 1465.8488 [M^+], requires: 1465.8476; **ν_{max}/cm^{-1} (solid):** 3367, 3044, 2920, 2851, 1681, 1605, 1477, 1440, 1259, 1141, 1030, 1007, 757, 725.

4.7.2.14.5 $[Ir(ppy)_2(4.5)]^+$(Ir.4.5)

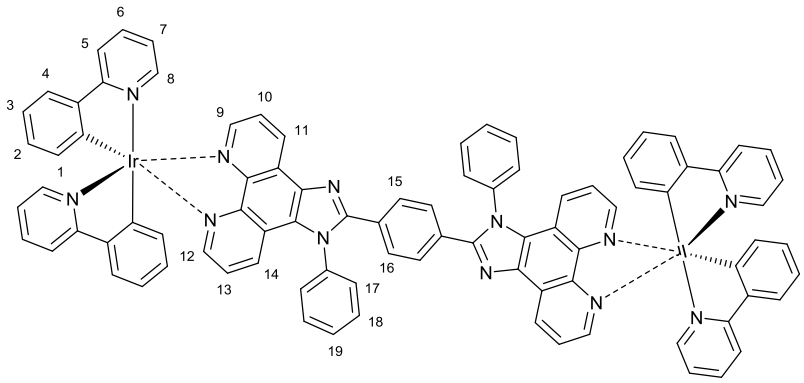

With 0.14 mmol 1,4-bis(1-phenyl-1H-imidazo[4,5-f][1,10]phenanthrolin-2-yl)benzene **(4.5)** in place of **4.1**, this complex was obtained by a procedure similar to that described for **4.1**. Yield: 60 mg, 27%, brown crystalline solid. **^{1}H NMR** (400 MHz, $CDCl_3$) δ ppm 9.31 (dd, *J* = 8.2, 1.2 Hz, 2H, 9-H), 8.27 (dd, *J* = 5.1, 1.3 Hz, 2H, 10-H), 8.16 (dd, *J* = 5.1, 1.2 Hz, 2H, 12-H), 7.96 – 7.82 (m, 6H, 11-H and 8-H), 7.81 – 7.62 (m, 18H), 7.59 (s, 4H), 7.52 (dd, *J* = 8.6, 5.1 Hz, 4H, 13-H), 7.41 (d, *J* = 5.9 Hz, 2H), 7.35 (d, *J* = 5.9 Hz, 2H), 7.06 (m, 6H,3-H), 6.95 (m, 6H, 2-H), 6.46 – 6.30 (m, 4H, 1-H); **m/z (ES+):** Found: 834.2086 [$M/2^{+2}$], requires: 834.2083; **ν_{max}/cm^{-1} (solid):** 3323, 3041, 1604, 1581, 1475, 1377, 1157, 756, 720.

Bibliography

1. E. Wassennan, E. Flapan, O. Kahn, L. Ouahab, C. Mathonière and H. O. Stumpf, 1999.
2. A. Nada, *J. Chem. Educ*, 1983, **60**, 451.
3. V. Ramamurthy and N. Turro, *Chemical Reviews*, 1993, **93**, 585-586.
4. G. S. Hammond and N. J. Turro, *Science*, 1963, **142**, 1541-1553.
5. *The Egyptian God Ra | Sun God of Egypt | Eye of Ra*, http://www.ancient-egypt-online.com/egyptian-god-ra.html, Accessed Mon Nov 27 2017 12:58:45 GMT+0000 (GMT Standard Time.
6. V. Balzani, P. Ceroni and A. Juris, *Photochemistry and photophysics: concepts, research, applications*, John Wiley & Sons, 2014.
7. E. V. Anslyn and D. A. Dougherty, *Modern Physical Organic Chemistry*, University Science Books, 2006.
8. L. E. Kreno, K. Leong, O. K. Farha, M. Allendorf, R. P. Van Duyne and J. T. Hupp, *Chemical Reviews*, 2011, **112**, 1105-1125.
9. P. Atkins, P. W. Atkins and J. de Paula, *Atkins' Physical Chemistry*, OUP Oxford, 2014.
10. F. Ahmed, *Journal of Chemical Education*, 1987, **64**, 427.
11. M. Sauer and J. Hofkens, *Handbook of fluorescence spectroscopy and imaging: from ensemble to single molecules*, John Wiley & Sons, 2010.
12. B. K. Swavey S, *Comprehensive Coordination Chemistry II*, 2nd Edition edn., Pergamon Press, Oxford 2004.
13. P. J. Steel, *Coordination Chemistry Reviews*, 1990, **106**, 227-265.
14. C. Kaes, A. Katz and M. W. Hosseini, *Chemical Reviews*, 2000, **100**, 3553-3590.
15. N. Belskaya, A. Eliseeva and V. A. Bakulev, *Russian Chemical Reviews*, 2015, **84**, 1226.
16. L. Popov, V. Orekhovskii, Y. V. Revinskii, E. Shepelenko, S. Borodkin and I. Koretskii, *Russian Journal of General Chemistry*, 2017, **87**, 945-951.
17. M. Katyal and Y. Dutt, *Talanta*, 1975, **22**, 151-166.
18. S. L. Buchwald, C. Mauger, G. Mignani and U. Scholz, *Advanced Synthesis & Catalysis*, 2006, **348**, 23-39.
19. R. Brehme, D. Enders, R. Fernandez and J. M. Lassaletta, *European Journal of Organic Chemistry*, 2007, **2007**, 5629-5660.
20. N. P. Belskaya, W. Dehaen and V. A. Bakulev, *Arkivoc*, 2010, **1**, 275-332.
21. J. D. Ranford, J. J. Vittal and Y. M. Wang, *Inorganic chemistry*, 1998, **37**, 1226-1231.
22. U. Salgın-Gökşen, N. Gökhan-Kelekçi, Ö. Göktaş, Y. Köysal, E. Kılıç, Ş. Işık, G. Aktay and M. Özalp, *Bioorganic & Medicinal Chemistry*, 2007, **15**, 5738-5751.
23. J.-m. Yu, G.-P. Lu and C. Cai, *Chemical Communications*, 2017, **53**, 5342-5345.
24. W. Wei, Z. Wang, X. Yang, W. Yu and J. Chang, *Advanced Synthesis & Catalysis*, 2017.
25. P. Xu, G. Wang, Z. Wu and C. Zhu, *Chemical Science*, 2017, **8**, 1303-1308.

26. T. Mistri, M. Dolai, D. Chakraborty, A. R. Khuda-Bukhsh, K. K. Das and M. Ali, *Organic & Biomolecular Chemistry*, 2012, **10**, 2380-2384.

27. L. N. Suvarapu, Y. K. Seo, S.-O. Baek and V. R. Ammireddy, *Journal of Chemistry*, 2012, **9**, 1288-1304.

28. K. Padmini, P. J. Preethi, M. Divya, P. Rohini, M. Lohita, K. Swetha and P. Kaladar, *International Journal of Pharmaceutical Sciences Review and Research* 2013, **2**, 43-58.

29. S. Rollas and S. Küçükgüzel, *Molecules*, 2007, **12**, 1910.

30. L. Savini, L. Chiasserini, A. Gaeta and C. Pellerano, *Bioorganic & Medicinal Chemistry*, 2002, **10**, 2193-2198.

31. C. Jayabalakrishnan and K. Natarajan, *Synthesis and Reactivity in Inorganic and Metal-Organic Chemistry*, 2001, **31**, 983-995.

32. Z. Haghighijoo, O. Firuzi, B. Hemmateenejad, S. Emami, N. Edraki and R. Miri, *Bioorganic Chemistry*, 2017, **74**, 126-133.

33. S. Rollas, N. Gulerman and H. Erdeniz, *Il Farmaco*, 2002, **57**, 171-174.

34. M. C. Rodríguez-Argüelles, S. Mosquera-Vázquez, P. Touron-Touceda, J. Sanmartín-Matalobos, A. M. García-Deibe, M. Belicchi-Ferrari, G. Pelosi, C. Pelizzi and F. Zani, *Journal of Inorganic Biochemistry*, 2007, **101**, 138-147.

35. J. Sayer, B. Pinsky, A. Schonbrunn and W. Washtien, *Journal of the American Chemical Society*, 1974, **96**, 7998-8009.

36. H. C. Yao and P. Resnick, *Journal of the American Chemical Society*, 1962, **84**, 3514-3517.

37. V. Atlan, L. El Kaim and C. Supiot, *Chemical Communications*, 2000, 1385-1386.

38. A. S. Guram, R. A. Rennels and S. L. Buchwald, *Angewandte Chemie International Edition*, 1995, **34**, 1348-1350.

39. J. Louie and J. F. Hartwig, *Tetrahedron Letters*, 1995, **36**, 3609-3612.

40. T. Yasuda and T. Yamamoto, *Macromolecules*, 2003, **36**, 7513-7519.

41. R. C. Stoufer and D. H. Busch, *Journal of the American Chemical Society*, 1956, **78**, 6016-6019.

42. J. D. Curry, M. A. Robinson and D. H. Busch, *Inorganic Chemistry*, 1967, **6**, 1570-1574.

43. E. Fischer and F. Jourdan, *Chem. Ber*, 1883, **16**, 2241.

44. A. M. Garrote Cañas, N. Martsinovich and N. N. Sergeeva, *ChemistrySelect*, 2017, **2**, 2433-2438.

45. S. Wagaw, B. H. Yang and S. L. Buchwald, *Journal of the American Chemical Society*, 1999, **121**, 10251-10263.

46. G. J. Britovsek, V. C. Gibson, B. S. Kimberley, S. Mastroianni, C. Redshaw, G. A. Solan, A. J. White and D. J. Williams, *Journal of the Chemical Society, Dalton Transactions*, 2001, 1639-1644.

47. R. Ali, Z. Mirza, G. M. Ashraf, M. A. Kamal, S. A. Ansari, G. A. Damanhouri, A. M. Abuzenadah, A. G. Chaudhary and I. A. Sheikh, *Anticancer research*, 2012, **32**, 2999-3005.

48. P. Boyle, *The Lancet*, 2006, **368**, 629-630.

49. S. Dasari and P. B. Tchounwou, *European Journal of Pharmacology*, 2014, **740**, 364-378.

50. K. R. Harrap, M. Jones, C. R. Wilkinson, H. M. Clink, S. Sparrow, B. C. Mitchley, S. Clarke and A. Veasey, in *Cisplatin*, Elsevier, Editon edn., 1980, pp. 193-212.

51. W. Han Ang and P. J. Dyson, *European Journal of Inorganic Chemistry*, 2006, **2006**, 4003-4018.

52. N. Busto, J. Valladolid, C. Aliende, F. A. Jalon, B. R. Manzano, A. M. Rodríguez, J. F. Gaspar, C. Martins, T. Biver and G. Espino, *Chemistry–An Asian Journal*, 2012, **7**, 788-801.

53. M. Selvaganapathy and N. Raman, 2016.

54. C. Marzano, M. Pellei, F. Tisato and C. Santini, *Anti-Cancer Agents in Medicinal Chemistry (Formerly Current Medicinal Chemistry-Anti-Cancer Agents)*, 2009, **9**, 185-211.

55. K. Pothiraj, T. Baskaran and N. Raman, *Journal of Coordination Chemistry*, 2012, **65**, 2110-2126.

56. N. E. Chayen, *Journal of Applied Crystallography*, 1997, **30**, 198-202.

57. S. M. Mobin, A. K. Srivastava, P. Mathur and G. K. Lahiri, *Inorganic Chemistry*, 2009, **48**, 4652-4654.

58. G. Hänggi, H. Schmalle and E. Dubler, *Inorganica Chimica Acta*, 1992, **197**, 135-140.

59. J. X. Hu, Y. F. Hu, X. Xiao, Y. Q. Zhang, Z. Tao, S. F. Xue, J. X. Liu and Q. J. Zhu, *European Journal of Inorganic Chemistry*, 2013, **2013**, 3632-3640.

60. N. Leesakul, W. Runrueng, S. Saithong and C. Pakawatchai, *Acta Crystallographica Section E: Structure Reports Online*, 2012, **68**, m837-m837.

61. M. Homocianu, *Journal of Advanced Research in Physics*, 2011, **2**.

62. D. W. Domaille, E. L. Que and C. J. Chang, *Nature Chemical Biology*, 2008, **4**, 168-175.

63. J. Wan, W. Duan, K. Chen, Y. Tao, J. Dang, K. Zeng, Y. Ge, J. Wu and D. Liu, *Sensors and Actuators B: Chemical*, 2018, **255**, 49-56.

64. D. Cheng, X. Liu, H. Yang, T. Zhang, A. Han and L. Zang, *Sensors*, 2016, **17**, 35.

65. A. Trapaidze, C. Hureau, W. Bal, M. Winterhalter and P. Faller, *JBIC Journal of Biological Inorganic Chemistry*, 2012, **17**, 37-47.

66. H. Kozlowski, M. Luczkowski, M. Remelli and D. Valensin, *Coordination Chemistry Reviews*, 2012, **256**, 2129-2141.

67. M. Lovell, J. Robertson, W. Teesdale, J. Campbell and W. Markesbery, *Journal of the Neurological Sciences*, 1998, **158**, 47-52.

68. K. J. Barnham and A. I. Bush, *Current opinion in chemical biology*, 2008, **12**, 222-228.

69. M. Bost, S. Houdart, M. Oberli, E. Kalonji, J.-F. Huneau and I. Margaritis, *Journal of Trace Elements in Medicine and Biology*, 2016, **35**, 107-115.

70. A. Baeyer, *European Journal of Organic Chemistry*, 1866, **140**, 295-296.

71. D. E. Nichols and C. D. Nichols, *Chemical Reviews*, 2008, **108**, 1614-1641.

72. T. M. Khan, N. Benaich, C. F. Malone, R. L. Bernardos, A. R. Russell, G. B. Downes, M. J. Barresi and L. D. Hutson, *Journal of the Peripheral Nervous System*, 2012, **17**, 76-89.

73. G. H. Svoboda, N. Neuss and M. Gorman, *Journal of Pharmaceutical Sciences*, 1959, **48**, 659-666.

74. T. Kishi, T. Goto, Y. Hirata, O. Shimomura and F. H. Johnson, *Tetrahedron Letters*, 1966, **7**, 3427-3436.

75. D. Sain, C. Kumari, A. Kumar and S. Dey, *Supramolecular Chemistry*, 2016, **28**, 239-248.

76. D. Jeyanthi, M. Iniya, K. Krishnaveni and D. Chellappa, *Spectrochimica Acta Part A: Molecular and Biomolecular Spectroscopy*, 2015, **136**, 1269-1274.

77. L. Khurana, H. I. Ali, T. Olszewska, K. H. Ahn, A. Damaraju, D. A. Kendall and D. Lu, *Journal of Medicinal Chemistry*, 2014, **57**, 3040-3052.

78. D. E. Beck, K. Agama, C. Marchand, A. Chergui, Y. Pommier and M. Cushman, *Journal of Medicinal Chemistry*, 2014, **57**, 1495-1512.

79. J. Shi, G. Zhao, X. Wang, H. E. Xu and W. Yi, *Organic & biomolecular chemistry*, 2014, **12**, 6831-6836.

80. M. Inman and C. J. Moody, *Chemical Science*, 2013, **4**, 29-41.

81. G. R. Humphrey and J. T. Kuethe, *Chemical Reviews*, 2006, **106**, 2875-2911.

82. A. H. Jackson and P. P. Lynch, *Journal of the Chemical Society, Perkin Transactions 2*, 1987, 1215-1219.

83. E. Vedejs and S. D. Monahan, *The Journal of Organic Chemistry*, 1997, **62**, 4763-4769.

84. D. F. Taber and P. K. Tirunahari, *Tetrahedron*, 2011, **67**, 7195-7210.

85. S. G. Dawande, V. Kanchupalli, J. Kalepu, H. Chennamsetti, B. S. Lad and S. Katukojvala, *Angewandte Chemie International Edition*, 2014, **53**, 4076-4080.

86. B. Robinson, *Chemical Reviews*, 1963, **63**, 373-401.

87. S. Garrod, M. E. Bollard, A. W. Nicholls, S. C. Connor, J. Connelly, J. K. Nicholson and E. Holmes, *Chemical research in toxicology*, 2005, **18**, 115-122.

88. E. Sotaniemi, J. Hirvonen, H. Isomäki, J. Takkunen and J. Kaila, *Annals of clinical research*, 1971, **3**, 30-33.

89. J. Bosch, T. Roca, M. Armengol and D. Fernández-Forner, *Tetrahedron*, 2001, **57**, 1041-1048.

90. M. Marinozzi, G. Marcelli, A. Carotti and B. Natalini, *RSC Advances*, 2014, **4**, 7019-7023.

91. T. Norris, C. Bezze, S. Z. Franz and M. Stivanello, *Organic Process Research & Development*, 2008, **13**, 354-357.

92. C. P. Ashcroft, P. Hellier, A. Pettman and S. Watkinson, *Organic Process Research & Development*, 2010, **15**, 98-103.

93. F. R. Japp and F. Klingemann, *European Journal of Inorganic Chemistry*, 1887, **20**, 2942-2944.

94. S. Wagaw, B. H. Yang and S. L. Buchwald, *Journal of the American Chemical Society*, 1998, **120**, 6621-6622.

95. N. Przheval'skii, N. Skvortsova and I. Magedov, *Chemistry of Heterocyclic Compounds*, 2002, **38**, 1055-1061.

96. F. R. Leroux, B. Manteau, J.-P. Vors and S. Pazenok, *Beilstein Journal of Organic Chemistry*, 2008, **4**.

97. Y. Murakami, *Proceedings of the Japan Academy, Series B*, 2012, **88**, 1-17.

98. E. Siddalingamurthy, K. M. Mahadevan, J. N. Masagalli and H. N. Harishkumar, *Tetrahedron Letters*, 2013, **54**, 5591-5596.

99. K. Muralirajan and C. H. Cheng, *Advanced Synthesis & Catalysis*, 2014, **356**, 1571-1576.

100. J. Zoller, D. C. Fabry, M. A. Ronge and M. Rueping, *Angewandte Chemie International Edition*, 2014, **53**, 13264-13268.

101. S. Gore, S. Baskaran and B. König, *Organic Letters*, 2012, **14**, 4568-4571.

102. Y. Lian, R. G. Bergman, L. D. Lavis and J. A. Ellman, *J. Am. Chem. Soc*, 2013, **135**, 7122-7125.

103. L. Ping, D. S. Chung, J. Bouffard and S.-g. Lee, *Chemical Society Reviews*, 2017.

104. K. Muralirajan, R. Haridharan, S. Prakash and C. H. Cheng, *Advanced Synthesis & Catalysis*, 2015, **357**, 761-766.

105. S. Lakhdar, M. Westermaier, F. Terrier, R. Goumont, T. Boubaker, A. R. Ofial and H. Mayr, *The Journal of Organic Chemistry*, 2006, **71**, 9088-9095.

106. F. Terrier, M.-J. Pouet, J.-C. Halle, S. Hunt, J. R. Jones and E. Buncel, *Journal of the Chemical Society, Perkin Transactions 2*, 1993, 1665-1672.

107. R. Sundberg, *The Chemistry of Indoles*, Elsevier Science, 2012.

108. P. Li, Y. Ji, W. Chen, X. Zhang and L. Wang, *RSC Advances*, 2013, **3**, 73-78.

109. A. Da Settimo and E. Nannipieri, *The Journal of Organic Chemistry*, 1970, **35**, 2546-2551.

110. T. B. Parsons, C. Ghellamallah, L. Male, N. Spencer and R. S. Grainger, *Organic & Biomolecular Chemistry*, 2011, **9**, 5021-5023.

111. B. Jiang, K. Tao, W. Shen and J. Zhang, *Tetrahedron Letters*, 2010, **51**, 6342-6344.

112. S. Song, X. Sun, X. Li, Y. Yuan and N. Jiao, *Organic Letters*, 2015, **17**, 2886-2889.

113. L. Shi, D. Zhang, R. Lin, C. Zhang, X. Li and N. Jiao, *Tetrahedron Letters*, 2014, **55**, 2243-2245.

114. L. Bedrač and J. Iskra, *Advanced Synthesis & Catalysis*, 2013, **355**, 1243-1248.

115. S. Soto, E. Vaz, C. Dell'Aversana, R. Álvarez, L. Altucci and Á. R. de Lera, *Organic & biomolecular chemistry*, 2012, **10**, 2101-2112.

116. A. M. Bunker, J. J. Edmunds, K. A. Berryman, D. M. Walker, M. A. Flynn, K. M. Welch and A. M. Doherty, *Bioorganic & Medicinal Chemistry Letters*, 1996, **6**, 1061-1066.

117. J. D. Williams, J. J. Chen, J. C. Drach and L. B. Townsend, *Journal of Medicinal Chemistry*, 2004, **47**, 5753-5765.

118. U. Jacquemard, N. Dias, A. Lansiaux, C. Bailly, C. Logé, J.-M. Robert, O. Lozach, L. Meijer, J.-Y. Mérour and S. Routier, *Bioorganic & Medicinal chemistry*, 2008, **16**, 4932-4953.

119. Y.-X. Gong, Q. Wu, H.-H. Zhang, Q.-N. Zhu and F. Shi, *Organic & biomolecular chemistry*, 2015, **13**, 7993-8000.

120. A. Paterna, P. M. Borralho, S. E. Gomes, S. Mulhovo, C. M. Rodrigues and M.-J. U. Ferreira, *Bioorganic & Medicinal Chemistry Letters*, 2015, **25**, 3556-3559.

121. C. Zhao, Y. Zhou, Q. Lin, L. Zhu, P. Feng, Y. Zhang and J. Cao, *The Journal of Physical Chemistry B*, 2010, **115**, 642-647.

122. L.-Y. Niu, Y.-Z. Chen, H.-R. Zheng, L.-Z. Wu, C.-H. Tung and Q.-Z. Yang, *Chemical Society Reviews*, 2015, **44**, 6143-6160.

123. Z. V. Chirkova, M. V. Kabanova, S. I. Filimonov, I. G. Abramov, A. Petzer, J. P. Petzer, S. I. Firgang and K. Y. Suponitsky, *Bioorganic & Medicinal Chemistry Letters*, 2015, **25**, 1206-1211.

124. R. S. Phillips and L. A. Cohen, *Journal of the American Chemical Society*, 1986, **108**, 2023-2030.

125. W. B. Lawson, A. Patchornik and B. Witkop, *Journal of the American Chemical Society*, 1960, **82**, 5918-5923.

126. J. Bergman and L. Venemalm, *The Journal of Organic Chemistry*, 1992, **57**, 2495-2497.

127. A. R. Katritzky and K. Akutagawa, *Tetrahedron Letters*, 1985, **26**, 5935-5938.

128. C. Merlic and Y. You, *Tetrahedron*, 2001, **57**, 5199-5212.

129. S. Cacchi and G. Fabrizi, *Chemical Reviews*, 2011, **111**, PR215-PR283.

130. G. Chelucci and R. P. Thummel, *Chemical Reviews*, 2002, **102**, 3129-3170.

131. S. G. Newman and M. Lautens, *Journal of the American Chemical Society*, 2010, **132**, 11416-11417.

132. M. Wang, P. Li, W. Chen and L. Wang, *RSC Advances*, 2014, **4**, 26918-26923.

133. T. Chen, T. J. Y. Foo and Y.-Y. Yeung, *ACS Catalysis*, 2015, **5**, 4751-4755.

134. D. M. Ketcha and G. W. Gribble, *The Journal of Organic Chemistry*, 1985, **50**, 5451-5457.

135. D. M. Ketcha, B. A. Lieurance, D. F. Homan and G. W. Gribble, *The Journal of Organic Chemistry*, 1989, **54**, 4350-4356.

136. Q. Xing, P. Li, H. Lv, R. Lang, C. Xia and F. Li, *Chemical Communications*, 2014, **50**, 12181-12184.

137. C. Huo and T. H. Chan, *Advanced Synthesis & Catalysis*, 2009, **351**, 1933-1938.

138. C. Huo, C. Sun, C. Wang, X. Jia and W. Chang, *ACS Sustainable Chemistry & Engineering*, 2013, **1**, 549-553.

139. G. Smith, *Journal of the Chemical Society (Resumed)*, 1954, 3842-3846.

140. U. Klingebiel, W. Lüttke, M. Noltemeyer and H. G. Schmidt, *Journal of Organometallic Chemistry*, 1993, **456**, 41-44.

141. M. Matsuzono, T. Fukuda and M. Iwao, *Tetrahedron Letters*, 2001, **42**, 7621-7623.

142. R. J. Sundberg and R. L. Parton, *The Journal of Organic Chemistry*, 1976, **41**, 163-165.

143. T. Fukuda, Y. Mine and M. Iwao, *Tetrahedron*, 2001, **57**, 975-979.

144. T. Fukuda, R. Maeda and M. Iwao, *Tetrahedron*, 1999, **55**, 9151-9162.

145. M. G. Saulnier and G. W. Gribble, *The Journal of Organic Chemistry*, 1982, **47**, 757-761.

146. D. A. Shirley and P. A. Roussel, *Journal of the American Chemical Society*, 1953, **75**, 375-378.

147. H. GILMAN and R. H. KIRBY, *The Journal of Organic Chemistry*, 1936, **1**, 146-153.

148. Q. Liu, L. Thorne, I. Kozin, D. Song, C. Seward, M. D'Iorio, Y. Tao and S. Wang, *Journal of the Chemical Society, Dalton Transactions*, 2002, 3234-3240.

149. W.-L. Jia, Q.-D. Liu, R. Wang and S. Wang, *Organometallics*, 2003, **22**, 4070-4078.

150. Q.-D. Liu, M. S. Mudadu, R. Thummel, Y. Tao and S. Wang, *Advanced Functional Materials*, 2005, **15**, 143-154.

151. S.-F. Liu, Q. Wu, H. L. Schmider, H. Aziz, N.-X. Hu, Z. Popović and S. Wang, *Journal of the American Chemical Society*, 2000, **122**, 3671-3678.

152. X. Liu, W. Sun, L. Zou, Z. Xie, X. Li, C. Lu, L. Wang and Y. Cheng, *Dalton Transactions*, 2012, **41**, 1312-1319.

153. L. Li, Y.-S. Wong, T. Chen, C. Fan and W. Zheng, *Dalton Transactions*, 2012, **41**, 1138-1141.

154. T. Zou, C. T. Lum, S. S. Y. Chui and C. M. Che, *Angewandte Chemie International Edition*, 2013, **52**, 2930-2933.

155. E. S. Andreiadis, D. Imbert, J. Pécaut, R. Demadrille and M. Mazzanti, *Dalton Transactions*, 2012, **41**, 1268-1277.

156. K. Shen, Y. Fu, J.-N. Li, L. Liu and Q.-X. Guo, *Tetrahedron*, 2007, **63**, 1568-1576.

157. J. F. Robyt, *Essentials of carbohydrate chemistry*, Springer Science & Business Media, 2012.

158. R. Dalpozzo, *Chemical Society Reviews*, 2015, **44**, 742-778.

159. L. Duan, L. Hou, T.-W. Lee, J. Qiao, D. Zhang, G. Dong, L. Wang and Y. Qiu, *Journal of Materials Chemistry*, 2010, **20**, 6392-6407.

160. X. Yang, X. Xu and G. Zhou, *Journal of Materials Chemistry C*, 2015, **3**, 913-944.

161. C. J. Cramer, *Theoretical Chemistry Accounts: Theory, Computation, and Modeling (Theoretica Chimica Acta)*, 2002, **108**, 366-366.

162. S. Sajjadifar, H. Vahedi, A. Massoudi and O. Louie, *Molecules*, 2010, **15**, 2491-2498.

163. Q. Liu, M. S. Mudadu, H. Schmider, R. Thummel, Y. Tao and S. Wang, *Organometallics*, 2002, **21**, 4743-4749.

164. R. P. Thummel and V. Hegde, *The Journal of Organic Chemistry*, 1989, **54**, 1720-1725.

165. N. Çelebi-Ölçüm, B. W. Boal, A. D. Huters, N. K. Garg and K. Houk, *Journal of the American Chemical Society*, 2011, **133**, 5752-5755.

166. D. Zhao, D. L. Hughes, D. R. Bender, A. M. DeMarco and P. J. Reider, *The Journal of Organic Chemistry*, 1991, **56**, 3001-3006.

167. S. R. Tetgure, A. U. Borse, B. R. Sankapal, V. J. Garole and D. J. Garole, *Amino acids*, 2015, **47**, 757-765.

168. T. Maruyama, Y. Fujimoto and T. Maekawa, *Journal of Colloid and Interface Science*, 2015, **447**, 254-257.

169. J. Newman and G. Blanchard, *Langmuir*, 2006, **22**, 5882-5887.

170. F. Wu, C. M. Chamchoumis and R. P. Thummel, *Inorganic Chemistry*, 2000, **39**, 584-590.

171. E. Jalviste and N. Ohta, *The Journal of Chemical Physics*, 2004, **121**, 4730-4739.

172. M. J. Tubergen and D. H. Levy, *The Journal of Physical Chemistry*, 1991, **95**, 2175-2181.

173. G. Cravotto, F. Demartin, G. Palmisano, A. Penoni, T. Radice and S. Tollari, *Journal of Organometallic Chemistry*, 2005, **690**, 2017-2026.

174. C. Brand, J. Küpper, D. W. Pratt, W. L. Meerts, D. Krügler, J. Tatchen and M. Schmitt, *Physical Chemistry Chemical Physics*, 2010, **12**, 4968-4979.

175. E. Evleth, O. Chalvet and P. Bamiere, *The Journal of Physical Chemistry*, 1977, **81**, 1913-1917.

176. F. Wu, J. Hardesty and R. P. Thummel, *The Journal of Organic Chemistry*, 1998, **63**, 4055-4061.

177. J. Wilke, M. Wilke, C. Brand, J. D. Spiegel, C. M. Marian and M. Schmitt, *The Journal of Physical Chemistry A*, 2017, **121**, 1597-1606.

178. M. Martinaud and A. Kadiri, *Chemical Physics*, 1978, **28**, 473-485.

179. O. Oeltermann, C. Brand, B. Engels, J. Tatchen and M. Schmitt, *Physical Chemistry Chemical Physics*, 2012, **14**, 10266-10270.

180. M. S. Walker, T. W. Bednar and R. Lumry, *The Journal of Chemical Physics*, 1967, **47**, 1020-1028.

181. J. P. Dinnocenzo, A. M. Feinberg and S. Farid, *The Journal of Physical Chemistry A*, 2017.

182. C. D. Borsarelli, S. G. Bertolotti and C. M. Previtali, *Photochemistry and Photobiology*, 2001, **73**, 97-104.

183. U. Bhattacharjee, C. Beck, A. Winter, C. Wells and J. W. Petrich, *The Journal of Physical Chemistry B*, 2014, **118**, 8471-8477.

184. R. Steiner, Academic Press Inc Jnl-Comp Subscriptions 525 B ST, STE 1900, San Diego, CA 92101-4495, Editon edn., 1984.

185. E. Baerends, O. Gritsenko and R. Van Meer, *Physical Chemistry Chemical Physics*, 2013, **15**, 16408-16425.

186. Z. Zhang, Z. Hu, Z. Yu, P. Lei, H. Chi, Y. Wang and R. He, *Tetrahedron Letters*, 2007, **48**, 2415-2419.

187. J.-B. Baudin, M.-G. Comménil, S. A. Julia, R. Lorne and L. Mauclaire, *Bulletin de la Société chimique de France*, 1996, **4**, 329-350.

188. A. N. Campbell, E. B. Meyer and S. S. Stahl, *Chemical Communications*, 2011, **47**, 10257-10259.

189. I. R. Greig, G. L. Baillie, M. Abdelrahman, L. Trembleau and R. A. Ross, *Bioorganic & Medicinal Chemistry Letters*, 2016, **26**, 4403-4407.

190. A. Bencini and V. Lippolis, *Coordination Chemistry Reviews*, 2010, **254**, 2096-2180.

191. C.-J. Kuo, T.-Y. Li, C.-C. Lien, C.-H. Liu, F.-I. Wu and M.-J. Huang, *Journal of Materials Chemistry*, 2009, **19**, 1865-1871.

192. H.-J. Zhong, W. Wang, T.-S. Kang, H. Yan, Y. Yang, L. Xu, Y. Wang, D.-L. Ma and C.-H. Leung, *Journal of Medicinal Chemistry*, 2017, **60**, 497-503.

193. K. Qiu, Y. Liu, H. Huang, C. Liu, H. Zhu, Y. Chen, L. Ji and H. Chao, *Dalton Transactions*, 2016, **45**, 16144-16147.

194. Y. Sun, D. A. Lutterman and C. Turro, *Inorganic chemistry*, 2008, **47**, 6427-6434.

195. S. K. Seth, S. Mandal, P. Purkayastha and P. Gupta, *Polyhedron*, 2015, **95**, 14-23.

196. J. Liu, Y. Chen, G. Li, P. Zhang, C. Jin, L. Zeng, L. Ji and H. Chao, *Biomaterials*, 2015, **56**, 140-153.

197. T. Chen, Y. Liu, W.-J. Zheng, J. Liu and Y.-S. Wong, *Inorganic Chemistry*, 2010, **49**, 6366-6368.

198. H. Saggadi, D. Luart, N. Thiebault, I. Polaert, L. Estel and C. Len, *RSC Advances*, 2014, **4**, 21456-21464.

199. C. Lüdtke, A. Haupt, M. Wozniak and N. Kulak, *Journal of Fluorine Chemistry*, 2017, **193**, 98-105.

200. A. Takahashi, Y. Hirose, H. Kusama and N. Iwasawa, *Chemical Communications*, 2008, 609-611.

201. P. Alreja and N. Kaur, *RSC Advances*, 2016, **6**, 23169-23217.

202. A. Schilt, Oxford, Editon edn., 1969.

203. V. Dénes and R. Chira, *Advanced Synthesis & Catalysis*, 1978, **320**, 172-175.

204. Y. Saitoh, T.-a. Koizumi, K. Osakada and T. Yamamoto, *Canadian Journal of Chemistry*, 1997, **75**, 1336-1339.

205. F. H. Case, *The Journal of Organic Chemistry*, 1951, **16**, 941-945.

206. C. J. Chandler, L. W. Deady and J. A. Reiss, *Journal of Heterocyclic Chemistry*, 1981, **18**, 599-601.

207. M. Schmittel and H. Ammon, *European Journal of Organic Chemistry*, 1998, **1998**, 785-792.

208. A. R. Katritzky, Q.-H. Long, N. Malhotra, T. A. Ramanarayanan and H. Vedage, *Synthesis*, 1992, **1992**, 911-913.

209. Y.-Z. Hu, Q. Xiang and R. P. Thummel, *Inorganic Chemistry*, 2002, **41**, 3423-3428.

210. K. De, J. Legros, B. Crousse, S. Chandrasekaran and D. Bonnet-Delpon, *Organic & Biomolecular Chemistry*, 2011, **9**, 347-350.

211. S. Bodige and F. M. MacDonnell, *Tetrahedron Letters*, 1997, **38**, 8159-8160.

212. J. Bolger, A. Gourdon, E. Ishow and J.-P. Launay, *Inorganic Chemistry*, 1996, **35**, 2937-2944.

213. S. Oh, J. R. Gallagher, J. T. Miller and Y. Surendranath, *Journal of the American Chemical Society*, 2016, **138**, 1820-1823.

214. H. Camren, M.-Y. Chang, L. Zeng and M. E. McGuire, *Synthetic communications*, 1996, **26**, 1247-1252.

215. J.-F. Lefebvre, D. Saadallah, P. Traber, S. Kupfer, S. Gräfe, B. Dietzek, I. Baussanne, J. De Winter, P. Gerbaux and C. Moucheron, *Dalton Transactions*, 2016, **45**, 16298-16308.

216. R. Satapathy, H. Padhy, Y. H. Wu and H. C. Lin, *Chemistry-A European Journal*, 2012, **18**, 16061-16072.

217. A. Patel, S. Y. Sharp, K. Hall, W. Lewis, M. F. Stevens, P. Workman and C. J. Moody, *Organic & biomolecular chemistry*, 2016, **14**, 3889-3905.

218. C. Zhong, H. Huang, A. He and H. Zhang, *Dyes and Pigments*, 2008, **77**, 578-583.

219. D. Cortés-Arriagada, L. Sanhueza, I. González, P. Dreyse and A. Toro-Labbé, *Physical Chemistry Chemical Physics*, 2016, **18**, 726-734.

220. S. K. Tripathy, U. De, N. Dehury, P. Laha, M. K. Panda, H. S. Kim and S. Patra, *Dalton Transactions*, 2016, **45**, 15122-15136.

221. G. Li, L. Sun, L. Ji and H. Chao, *Dalton Transactions*, 2016, **45**, 13261-13276.

222. L.-P. Zhang, K.-J. Jiang, Q. Chen, G. Li and L.-M. Yang, *RSC Advances*, 2015, **5**, 46206-46209.

223. T. Cardinaels, J. Ramaekers, P. Nockemann, K. Driesen, K. Van Hecke, L. Van Meervelt, S. Lei, S. De Feyter, D. Guillon and B. Donnio, *Chemistry of Materials*, 2008, **20**, 1278-1291.

224. M. Q. Granato, D. de Souza Gonçalves, S. H. Seabra, M. McCann, M. Devereux, A. L. S. dos Santos and L. F. Kneipp, *Frontiers in microbiology*, 2017, **8**.

225. P. Ren, R. Wang, S. Pu, G. Liu and C. Fan, *Journal of Physical Organic Chemistry*, 2014, **27**, 183-190.

226. R. J. Watts, *Comments on Inorganic Chemistry*, 1991, **11**, 303-337.

227. Y. You and S. Y. Park, *Dalton Transactions*, 2009, 1267-1282.

228. A. Kapturkiewicz, *Analytical and Bioanalytical Chemistry*, 2016, **408**, 7013-7033.

229. P. Paoletti, *Pure and Applied Chemistry*, 1984, **56**, 491-522.

230. G. Anderegg, *Helvetica Chimica Acta*, 1963, **46**, 2813-2822.

231. G. Anderegg, *Helvetica Chimica Acta*, 1963, **46**, 2397-2410.

232. M. K. Nazeeruddin, R. Humphry-Baker, D. Berner, S. Rivier, L. Zuppiroli and M. Graetzel, *Journal of the American Chemical Society*, 2003, **125**, 8790-8797.

233. A. Juris, V. Balzani, F. Barigelletti, S. Campagna, P. l. Belser and A. Von Zelewsky, *Coordination Chemistry Reviews*, 1988, **84**, 85-277.

234. K. K.-W. Lo and K. K.-S. Tso, *Inorganic Chemistry Frontiers*, 2015, **2**, 510-524.

235. S. Lamansky, P. Djurovich, D. Murphy, F. Abdel-Razzaq, H.-E. Lee, C. Adachi, P. E. Burrows, S. R. Forrest and M. E. Thompson, *J. Am. Chem. Soc*, 2001, **123**, 4304-4312.

236. C. E. Housecroft and E. C. Constable, *Coordination Chemistry Reviews*, 2017.

237. E. Zysman-Colman, Wiley Online Library, Editon edn., 2017.

238. X. Chen, L. Sun, Y. Chen, X. Cheng, W. Wu, L. Ji and H. Chao, *Biomaterials*, 2015, **58**, 72-81.

239. C. Wang, L. Lystrom, H. Yin, M. Hetu, S. Kilina, S. A. McFarland and W. Sun, *Dalton Transactions*, 2016, **45**, 16366-16378.

240. K. K.-W. Lo, M.-W. Louie and K. Y. Zhang, *Coordination Chemistry Reviews*, 2010, **254**, 2603-2622.

241. W. Xu, J. Zuo, L. Wang, L. Ji and H. Chao, *Chemical Communications*, 2014, **50**, 2123-2125.

242. S. Campagna, F. Puntoriero, F. Nastasi, G. Bergamini and V. Balzani, in *Photochemistry and Photophysics of Coordination Compounds II*, Springer, Editon edn., 2007, vol. 281, pp. 143-203.

243. M. Vijayakumar and M. Gopinathan, *Journal of Molecular Structure: THEOCHEM*, 1996, **361**, 15-19.

244. Q. Zhao, S. Liu, M. Shi, C. Wang, M. Yu, L. Li, F. Li, T. Yi and C. Huang, *Inorganic chemistry*, 2006, **45**, 6152-6160.

245. L. Hammarström, F. Barigelletti, L. Flamigni, M. T. Indelli, N. Armaroli, G. Calogero, M. Guardigli, A. Sour, J.-P. Collin and J.-P. Sauvage, *The Journal of Physical Chemistry A*, 1997, **101**, 9061-9069.

246. X. Yang, X. Xu, J.-s. Dang, G. Zhou, C.-L. Ho and W.-Y. Wong, *Inorganic chemistry*, 2016, **55**, 1720-1727.

247. P. Srinivasan, R. Mason, J. MacNeil and B. MacLean, *Inorganica Chimica Acta*, 2011, **366**, 116-121.

248. F. Gao, H. Chao, F. Zhou, B. Peng and L.-N. Ji, *Inorganic Chemistry Communications*, 2007, **10**, 170-173.

249. L. Wang, H. Yin, P. Cui, M. Hetu, C. Wang, S. Monro, R. D. Schaller, C. G. Cameron, B. Liu and S. Kilina, *Dalton Transactions*, 2017.

250. E. Coronado, P. Gaviña, S. Tatay, R. Groarke and J. G. Vos, *Inorganic Chemistry*, 2010, **49**, 6897-6903.

251. Y. Ohsawa, S. Sprouse, K. King, M. DeArmond, K. Hanck and R. Watts, *Journal of Physical Chemistry*, 1987, **91**, 1047-1054.

252. H. Chao, R.-H. Li, C.-W. Jiang, H. Li, L.-N. Ji and X.-Y. Li, *Journal of the Chemical Society, Dalton Transactions*, 2001, 1920-1926.

253. S. K. Seth, S. Mandal, K. Srikanth, P. Purkayastha and P. Gupta, *European Journal of Inorganic Chemistry*, 2017, **2017**, 873-880.

254. Y. E. Begantsova and L. Bochkarev, *Russian Journal of General Chemistry*, 2017, **87**, 1198-1203.

255. S. K. Seth, P. Gupta and P. Purkayastha, *New Journal of Chemistry*, 2017.

256. Y. You and W. Nam, *Chemical Society Reviews*, 2012, **41**, 7061-7084.

257. M. Nonoyama, *Bulletin of the Chemical Society of Japan*, 1974, **47**, 767-768.

258. W.-Y. Wong, *Organometallics and related molecules for energy conversion*, Springer, 2015.

259. A. B. Tamayo, B. D. Alleyne, P. I. Djurovich, S. Lamansky, I. Tsyba, N. N. Ho, R. Bau and M. E. Thompson, *Journal of the American Chemical Society*, 2003, **125**, 7377-7387.

260. H.-C. Su, H.-F. Chen, F.-C. Fang, C.-C. Liu, C.-C. Wu, K.-T. Wong, Y.-H. Liu and S.-M. Peng, *Journal of the American Chemical Society*, 2008, **130**, 3413-3419.

261. R. D. Costa, E. Ortí, H. J. Bolink, S. Graber, C. E. Housecroft and E. C. Constable, *Advanced Functional Materials*, 2010, **20**, 1511-1520.

262. H. J. Emeléus and A. G. Sharpe, *Advances in inorganic chemistry and radiochemistry*, Academic Press, 1968.

263. E. Jansson, B. Minaev, S. Schrader and H. Ågren, *Chemical Physics*, 2007, **333**, 157-167.

264. P. J. Hay, *The Journal of Physical Chemistry A*, 2002, **106**, 1634-1641.

265. J. Demas and B. DeGraff, *Coordination Chemistry Reviews*, 2001, **211**, 317-351.

266. M. Reddy and K. Bejoymohandas, *Journal of Photochemistry and Photobiology C: Photochemistry Reviews*, 2016, **29**, 29-47.

267. M. S. Lowry and S. Bernhard, *Chemistry-A European Journal*, 2006, **12**, 7970-7977.

268. J. Li, P. I. Djurovich, B. D. Alleyne, M. Yousufuddin, N. N. Ho, J. C. Thomas, J. C. Peters, R. Bau and M. E. Thompson, *Inorganic Chemistry*, 2005, **44**, 1713-1727.

269. Ł. Skórka, M. Filapek, L. Zur, J. G. Małecki, W. Pisarski, M. Olejnik, W. Danikiewicz and S. Krompiec, *The Journal of Physical Chemistry C*, 2016, **120**, 7284-7294.

270. Q. Zhao, S. Liu, M. Shi, F. Li, H. Jing, T. Yi and C. Huang, *Organometallics*, 2007, **26**, 5922-5930.

271. Q.-L. Zhang, J.-H. Liu, X.-Z. Ren, H. Xu, Y. Huang, J.-Z. Liu and L.-N. Ji, *Journal of Inorganic Biochemistry*, 2003, **95**, 194-198.

272. R. Di Pietro, T. Erdmann, N. Wang, X. Liu, D. Gräfe, J. Lenz, J. Brandt, D. Kasemann, K. Leo and M. Al-Hussein, *Journal of Materials Chemistry C*, 2016, **4**, 10827-10838.

273. H. Tang, Y. Li, B. Zhao, W. Yang, H. Wu and Y. Cao, *Organic Electronics*, 2012, **13**, 3211-3219.

274. R. Wang, D. Liu, H. Ren, T. Zhang, H. Yin, G. Liu and J. Li, *Advanced Materials*, 2011, **23**, 2823-2827.

275. H. Tang, Z. Chen, L. Wei, J. Miao, G. Meng, Y. He and H. Wu, *Dyes and Pigments*, 2016, **131**, 340-348.

276. G. Accorsi, A. Listorti, K. Yoosaf and N. Armaroli, *Chemical Society Reviews*, 2009, **38**, 1690-1700.

277. M. S. Henry and M. Z. Hoffman, *Journal of Physical Chemistry*, 1979, **83**, 618-625.

278. L. Cola, *Journal of the Chemical Society, Faraday Transactions*, 1992, **88**, 553-556.

279. B. N. Bandyopadhyay and A. Harriman, *Journal of the Chemical Society, Faraday Transactions 1: Physical Chemistry in Condensed Phases*, 1977, **73**, 663-674.

280. A. Listorti, A. Degli Esposti, R. S. Kishore, V. Kalsani, M. Schmittel and N. Armaroli, *The Journal of Physical Chemistry A*, 2007, **111**, 7707-7718.

281. S. Kothavale and N. Sekar, *Dyes and Pigments*, 2017, **136**, 31-45.

282. T. N. Brown and N. Mora-Diez, *The Journal of Physical Chemistry B*, 2006, **110**, 20546-20554.

283. P. Singh, A. Baheti and K. J. Thomas, *The Journal of Organic Chemistry*, 2011, **76**, 6134-6145.

284. F. Pina, M. A. Bernardo and E. García-España, *European Journal of Inorganic Chemistry*, 2000, **2000**, 2143-2157.

285. J.-P. Sauvage and C. Dietrich-Buchecker, *Molecular catenanes, rotaxanes and knots: a journey through the world of molecular topology*, John Wiley & Sons, 2008.

286. T. Tsuboi and N. Aljaroudi, *Optical Materials*, 2005, **27**, 1859-1863.

287. H. Wang, Q. Liao, H. Fu, Y. Zeng, Z. Jiang, J. Ma and J. Yao, *Journal of Materials Chemistry*, 2009, **19**, 89-96.

288. W. Stampor and J. Mężyk, *Chemical Physics*, 2007, **337**, 151-160.

289. T. Matsushita, T. Asada and S. Koseki, *The Journal of Physical Chemistry C*, 2007, **111**, 6897-6903.

290. K. Goushi, Y. Kawamura, H. Sasabe and C. Adachi, *Japanese Journal of Applied Physics*, 2004, **43**, L937.

291. J.-Q. Wang, X.-J. Hou, H.-B. Bo and Q.-z. Chen, *Inorganic Chemistry Communications*, 2015, **61**, 31-34.

Appendix

^{1}HNMR and ^{13}C NMR data of novel compounds

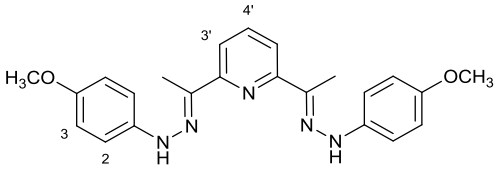

2

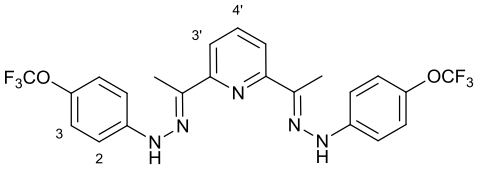

3

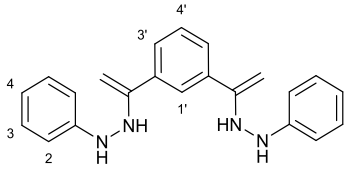

4

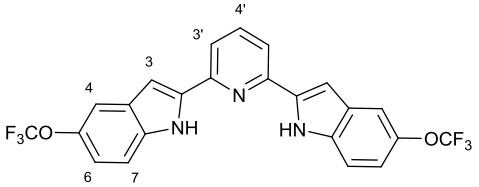

3.2

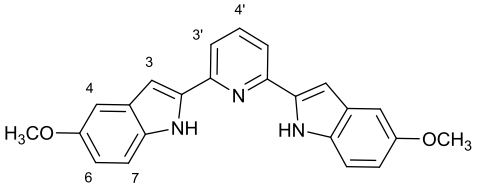

3.3

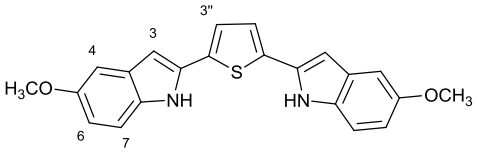

3.4

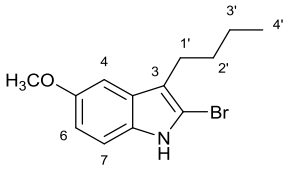

10

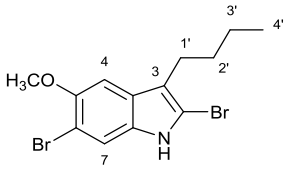

11

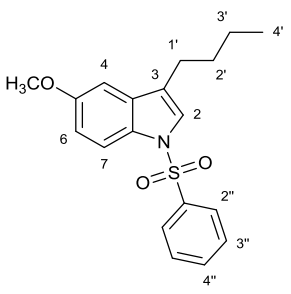

13

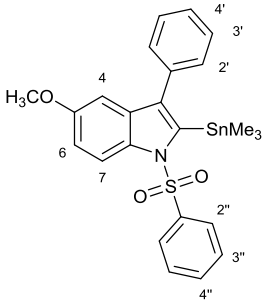

16

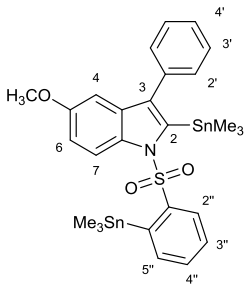

17

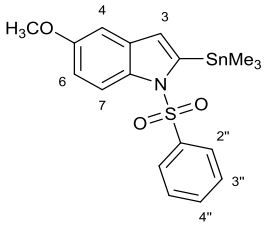

18

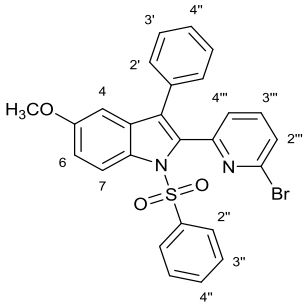

20

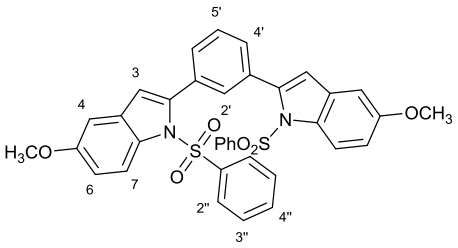

21

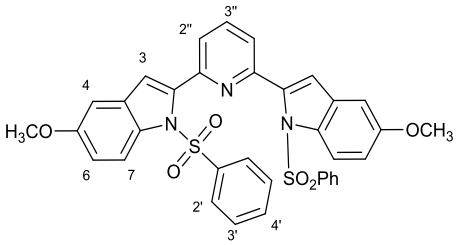

22

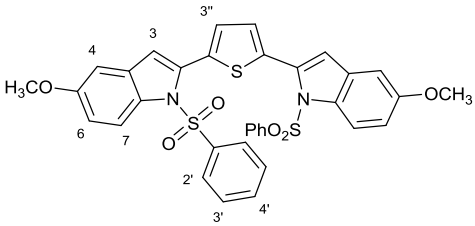

24

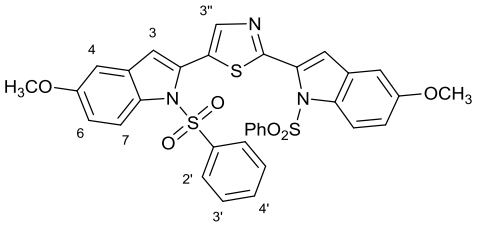

25

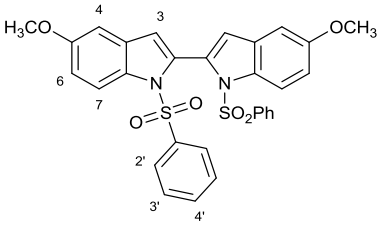

28

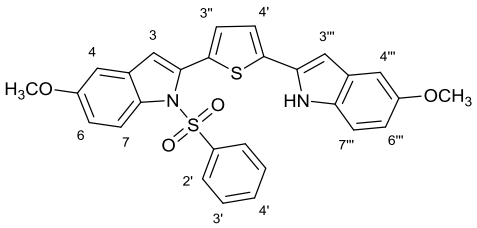

29

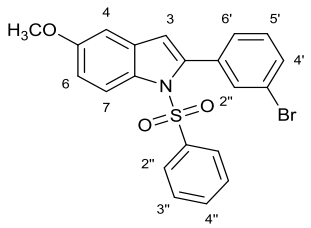

30

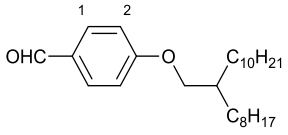

34

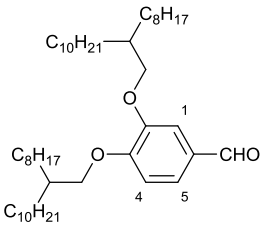

35

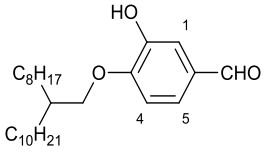

36

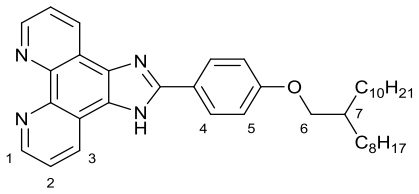

4.1

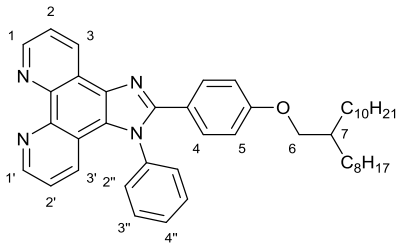

4.2

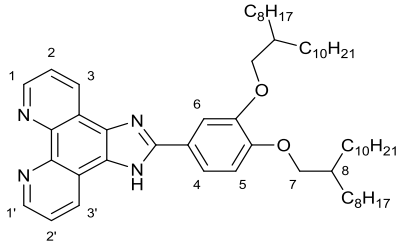

4.3

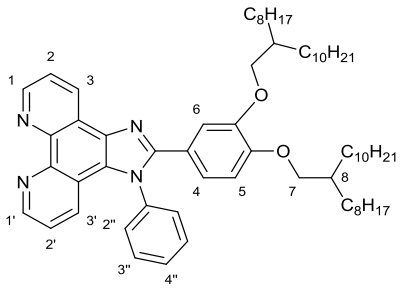

4.4

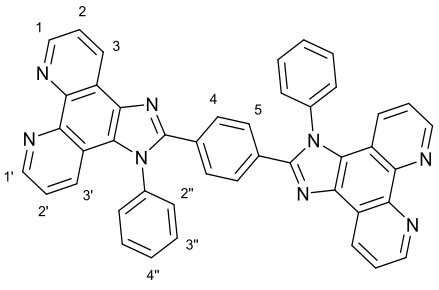

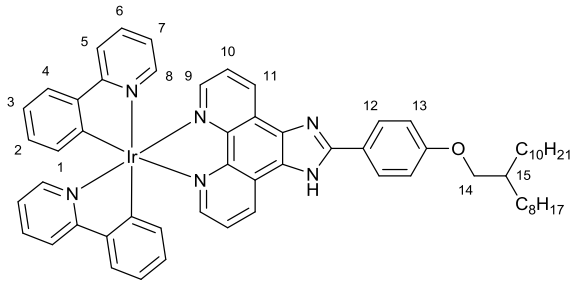

4.5

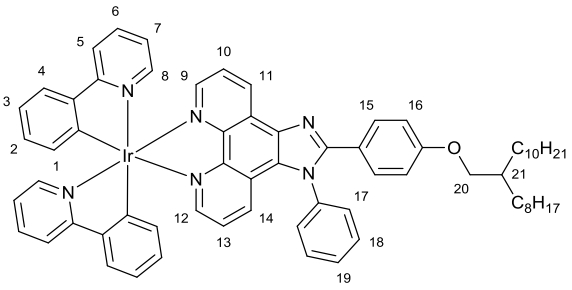

Ir.4.1

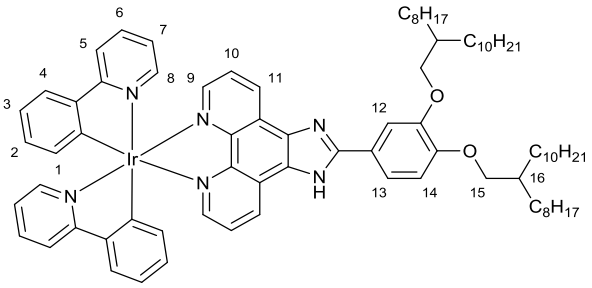

Ir.4.2

Ir.4.3

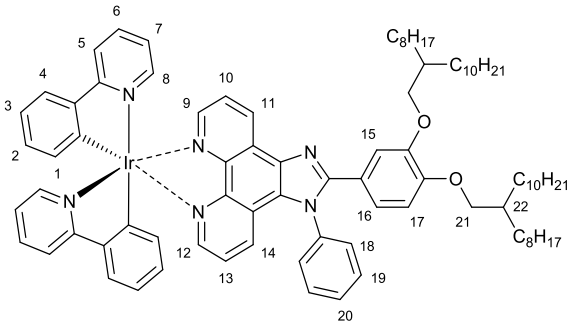

Ir.4.4

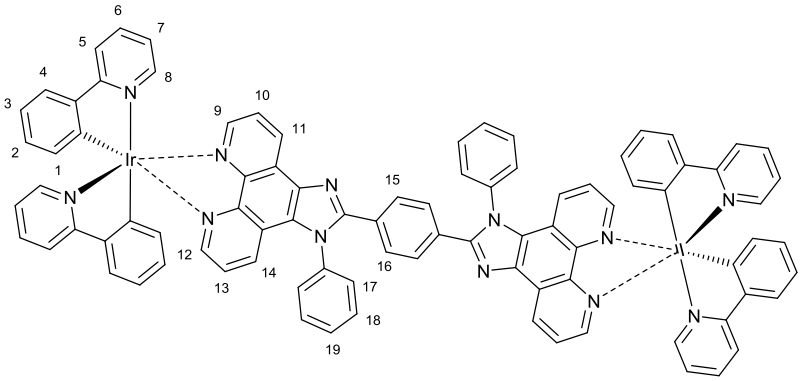

Ir.4.5

^{1}H NMR (400 MHz, $CDCl_3$ + EtOH) and ^{13}C NMR (125 MHz, C_2D_6O) of 2,6-Diactetylpyridine-bis(4-methoxyphenylhydrazone) (2)

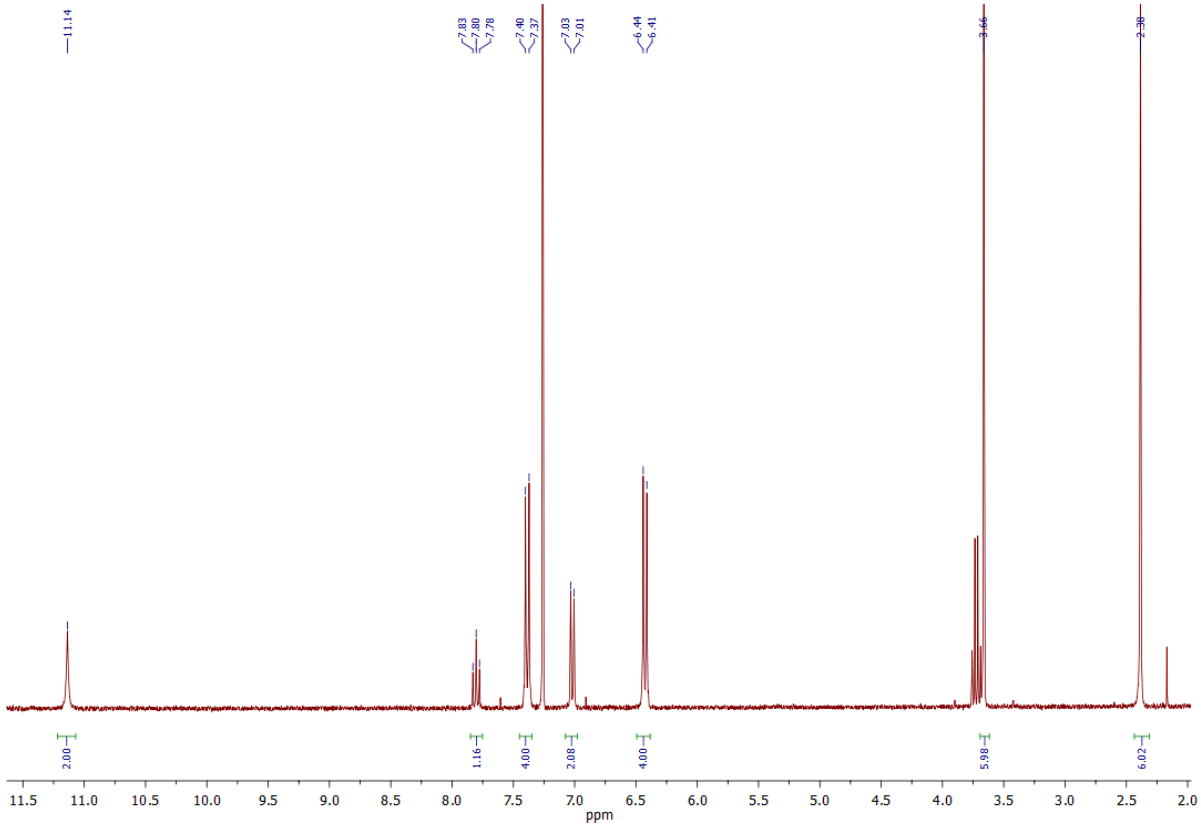

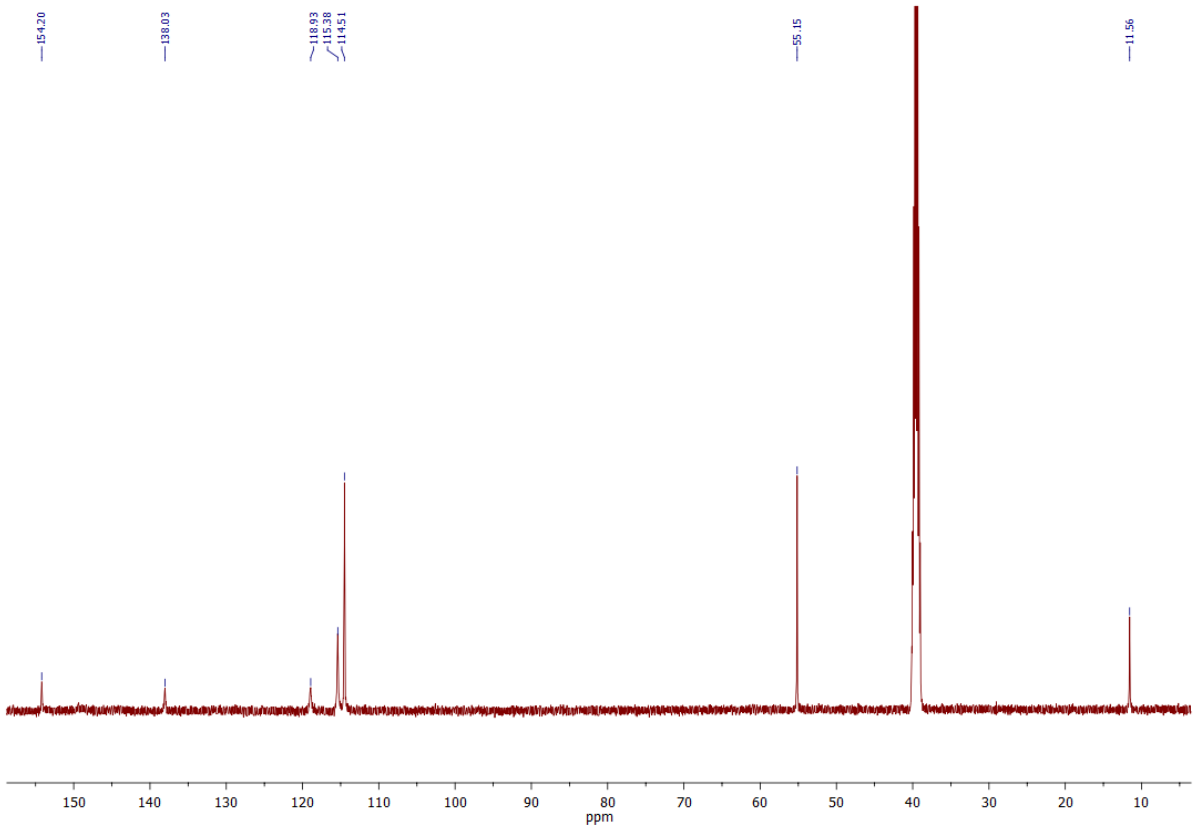

^{1}H NMR (500 MHz, MeOD) and ^{13}C NMR (125 MHz, MeOD) of 2,6-Diactetylpyridine-bis(4-trifluoromethoxyphenylhydrazone) (3)

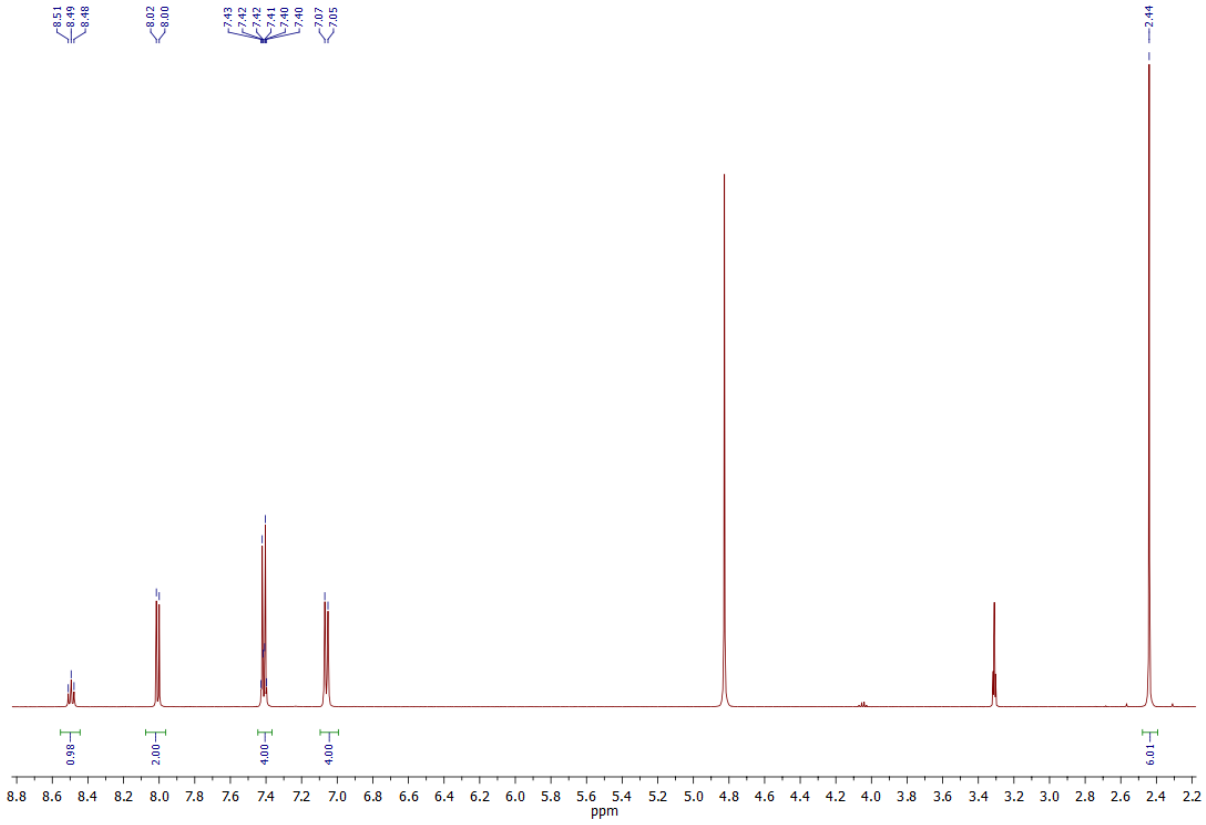

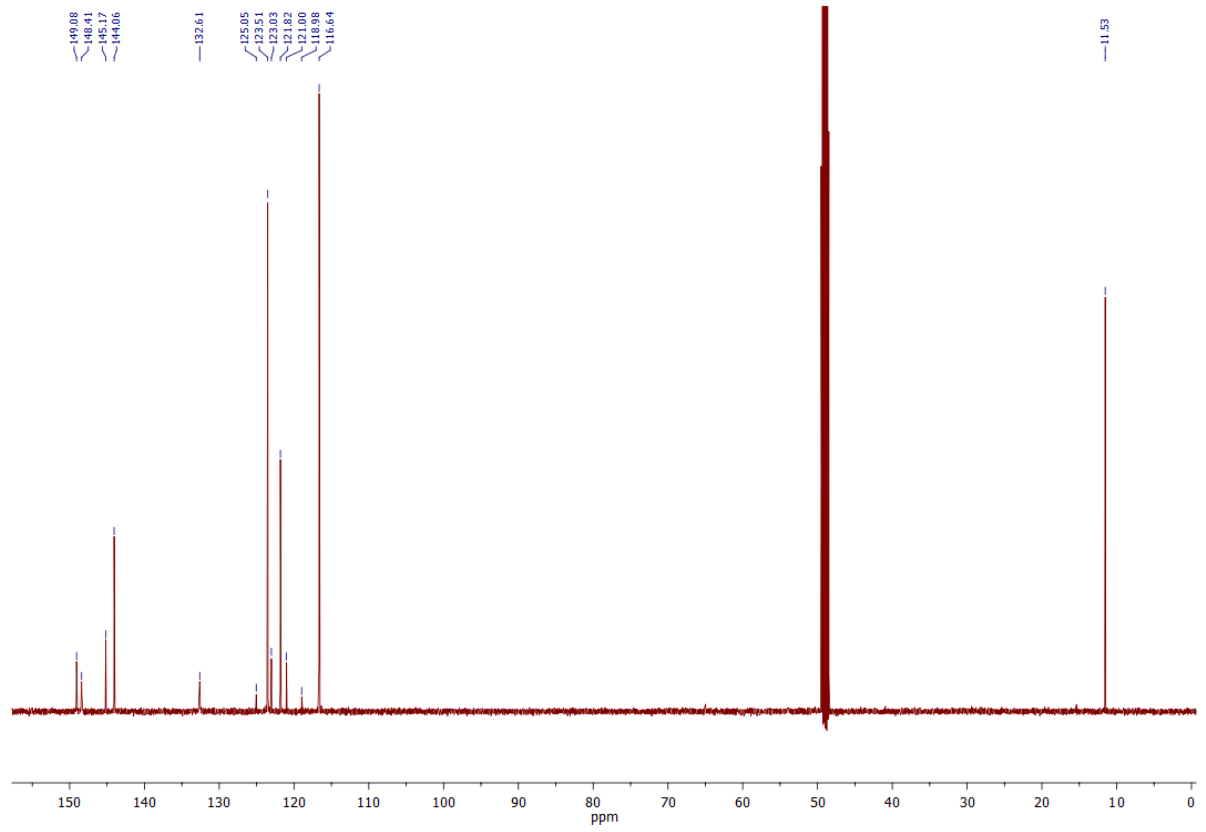

^{1}H NMR (500 MHz, $CDCl_3$) and ^{13}C NMR (125 MHz, $CDCl_3$)of 2,6-Bis[(5-trifluoromethoxy)-1H-indol-2-yl]pyridine (3.2)

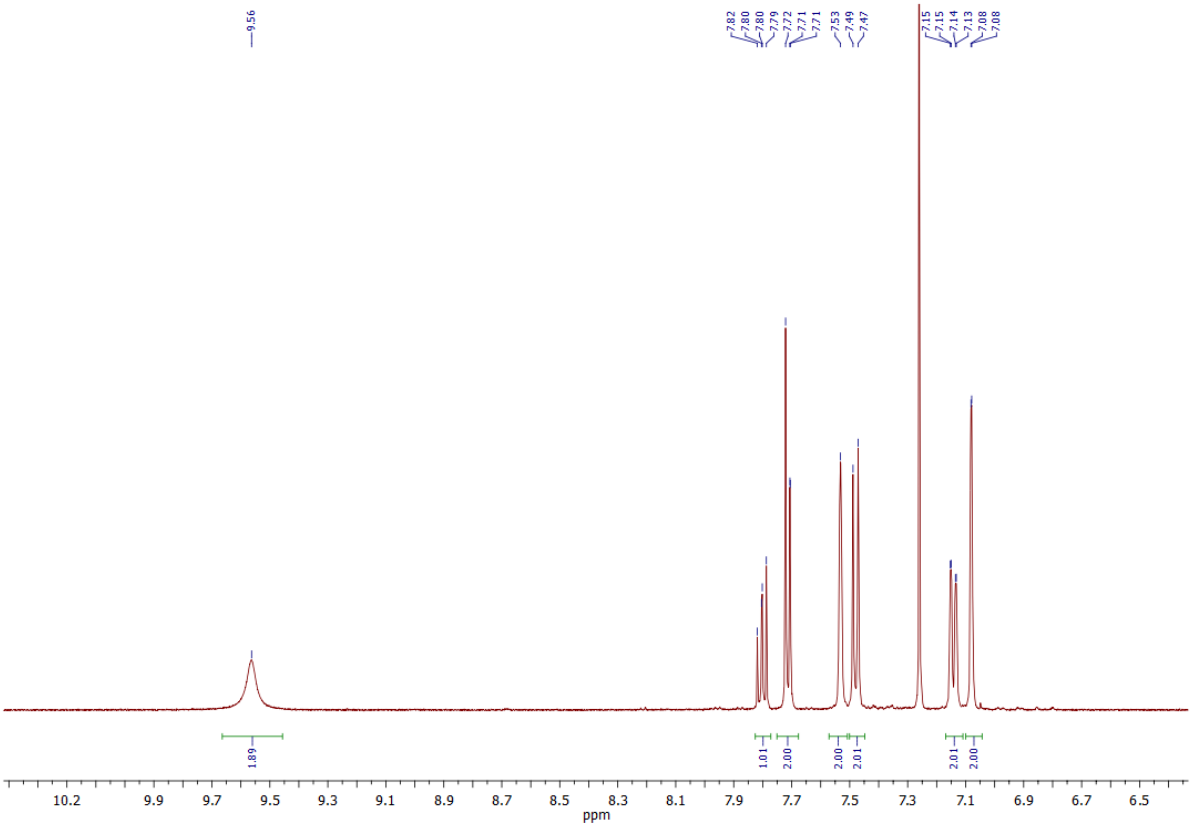

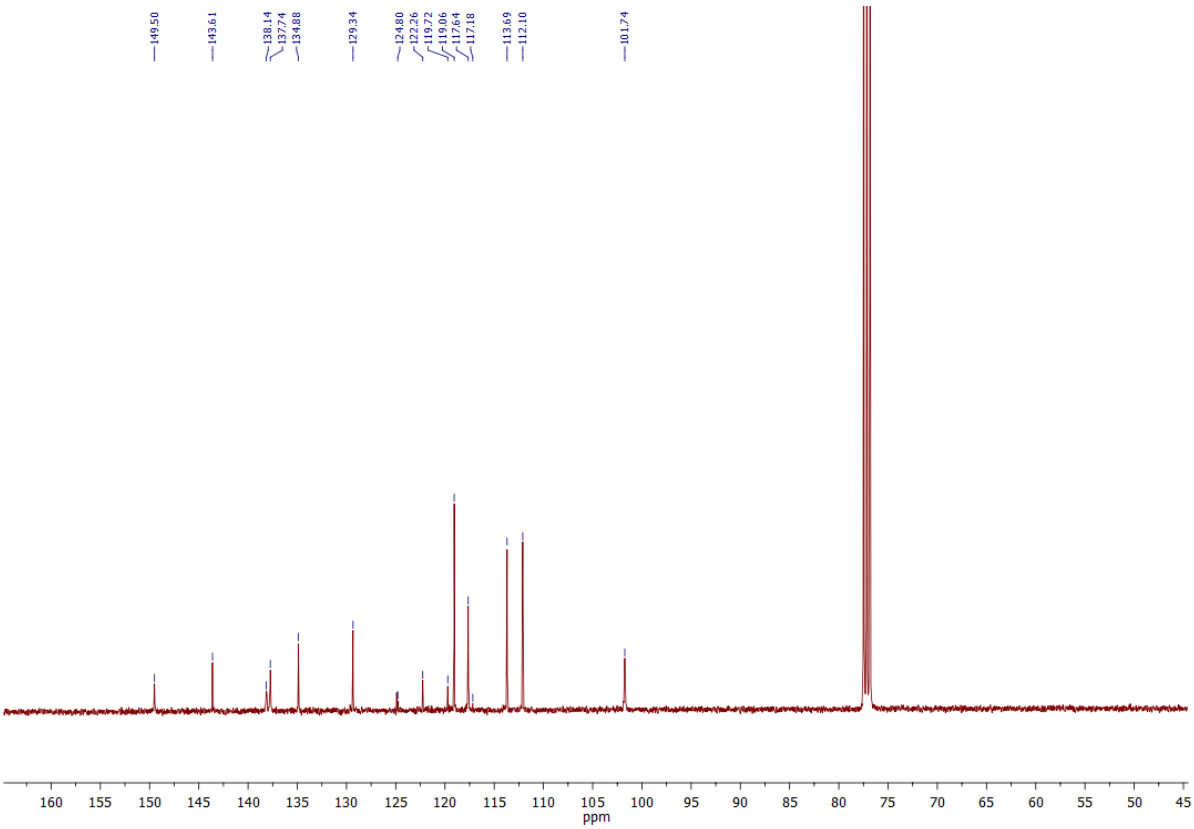

^{1}H NMR (500 MHz, CD_2Cl_2) and ^{13}C NMR (125 MHz, CD_2Cl_2) of 2,6- Bis[(5-methoxy)-1H-indol-2-yl]pyridine (3.3)

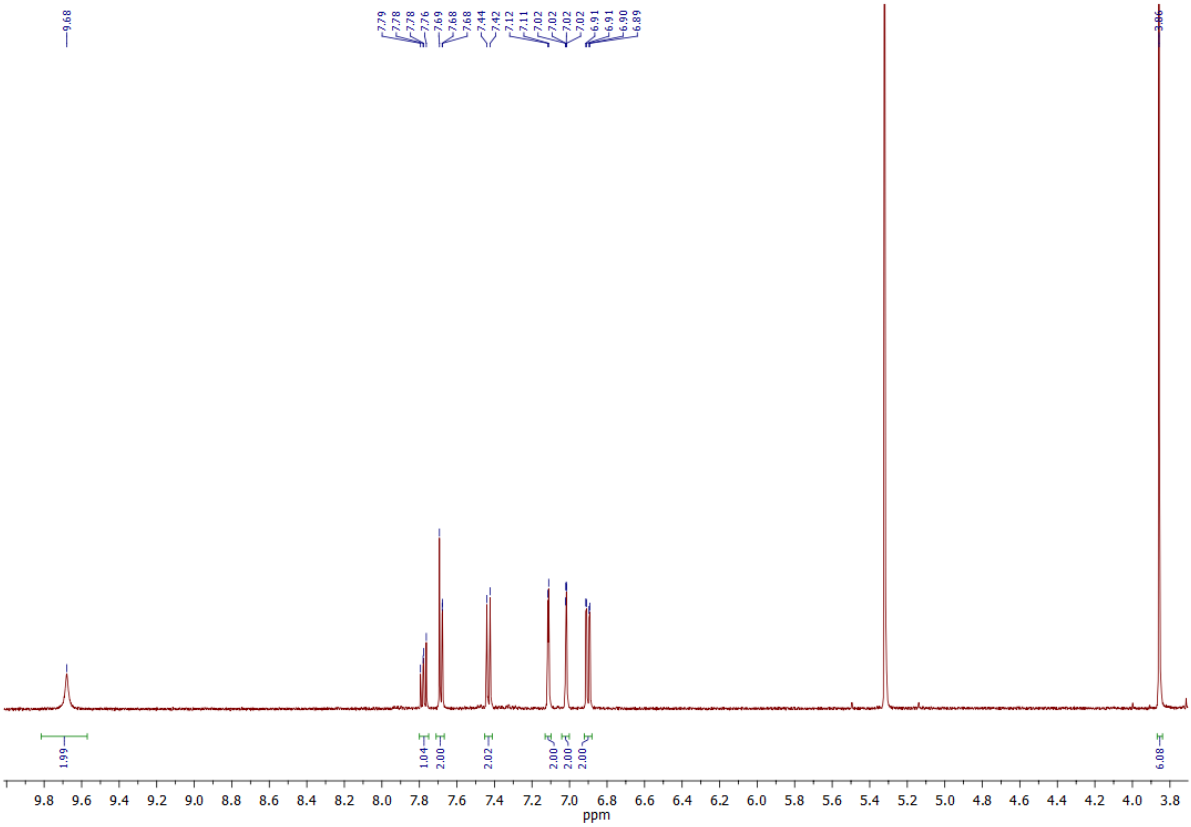

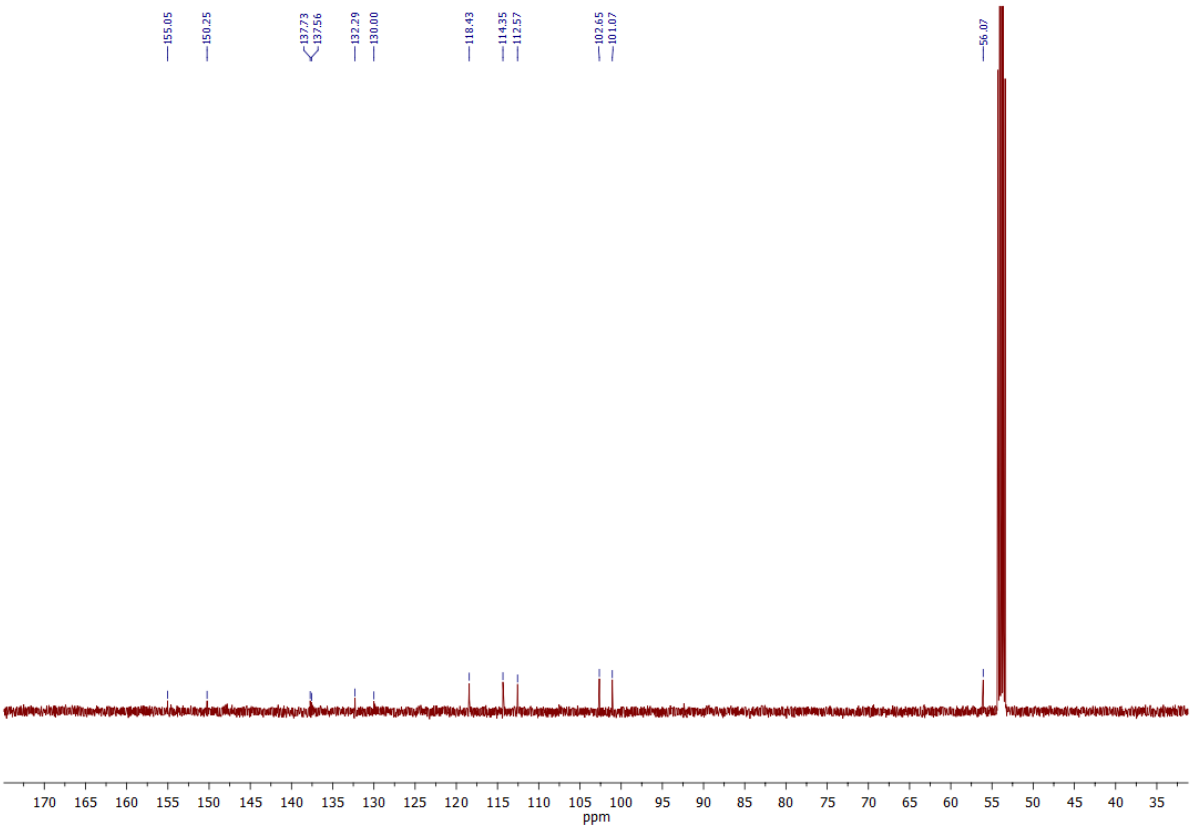

^{1}H NMR (400 MHz, CD_3CN) and ^{13}C NMR (125 MHz, CD_2Cl_2) of 2,5-Bis[(5-methoxy)-1H-indol-2-yl]thiophene (3.4)

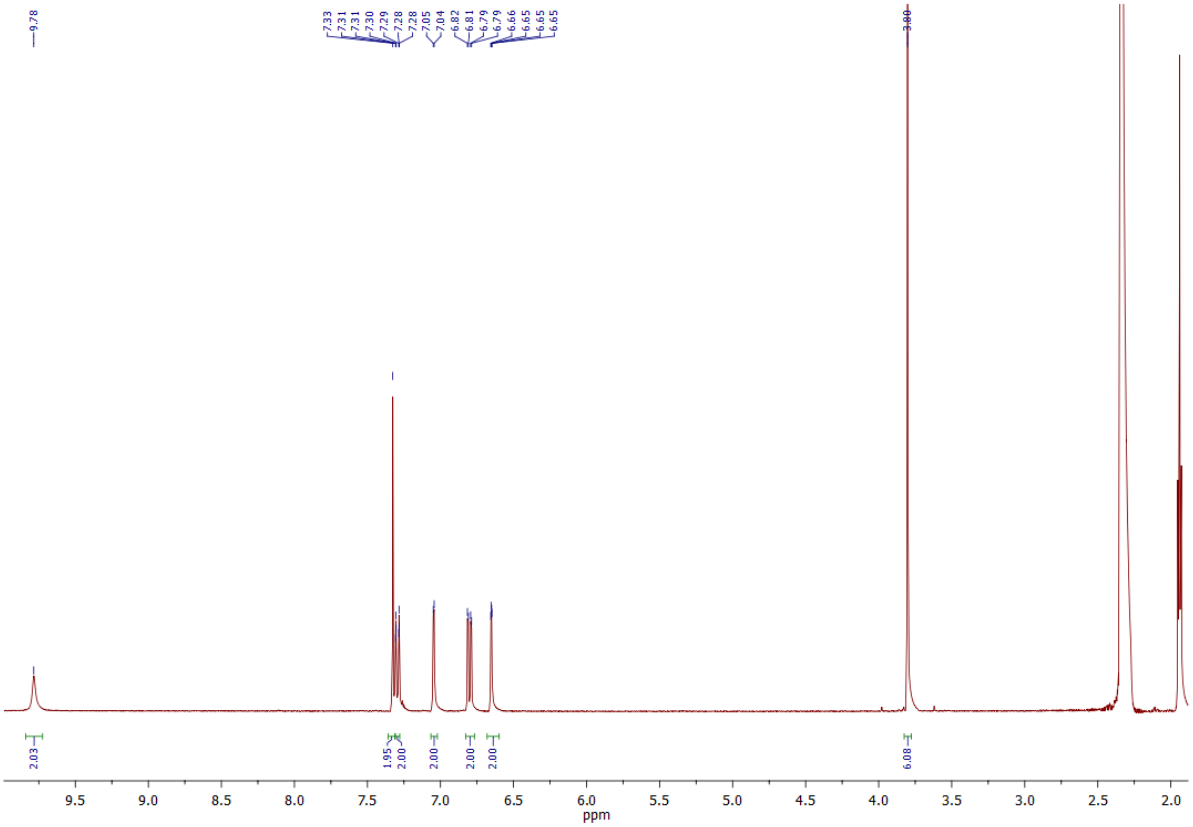

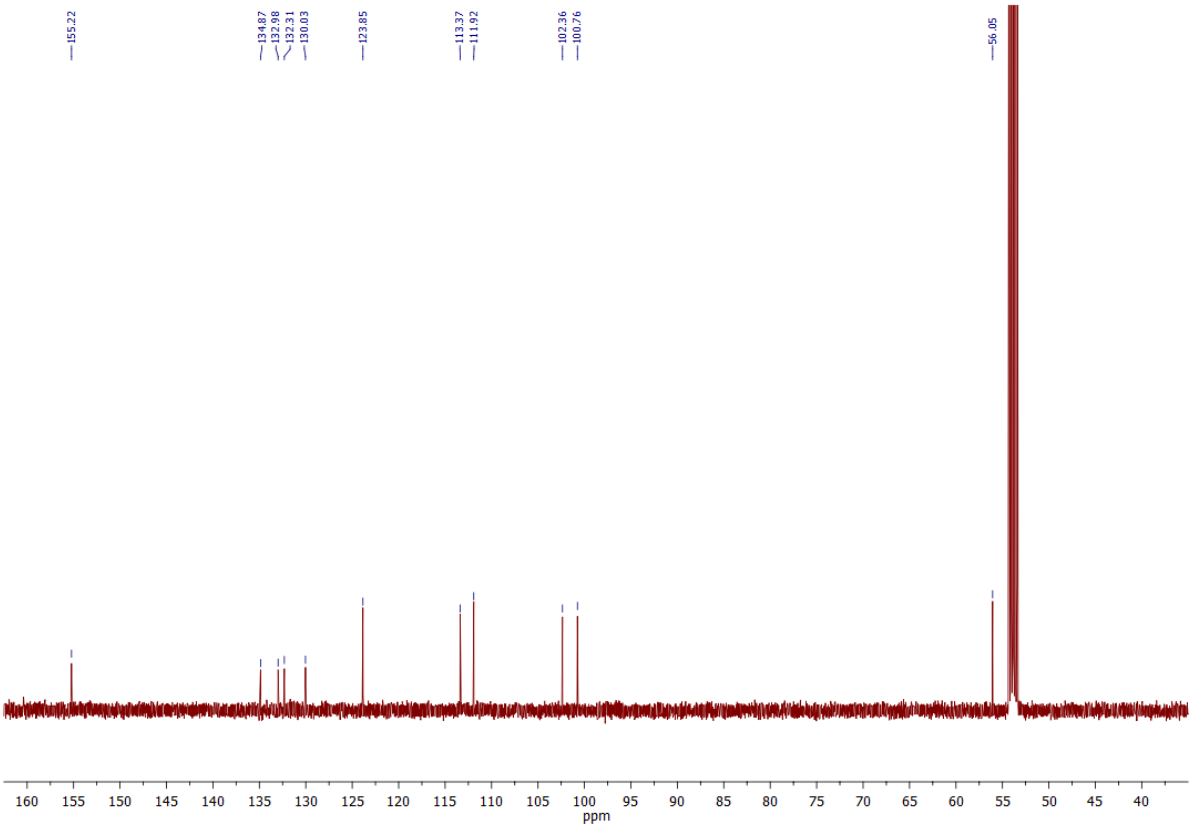

^{1}H NMR (300 MHz, $CDCl_3$) of 2-Bromo-3-*n*-butyl-5-methoxy-1H-indole (10)

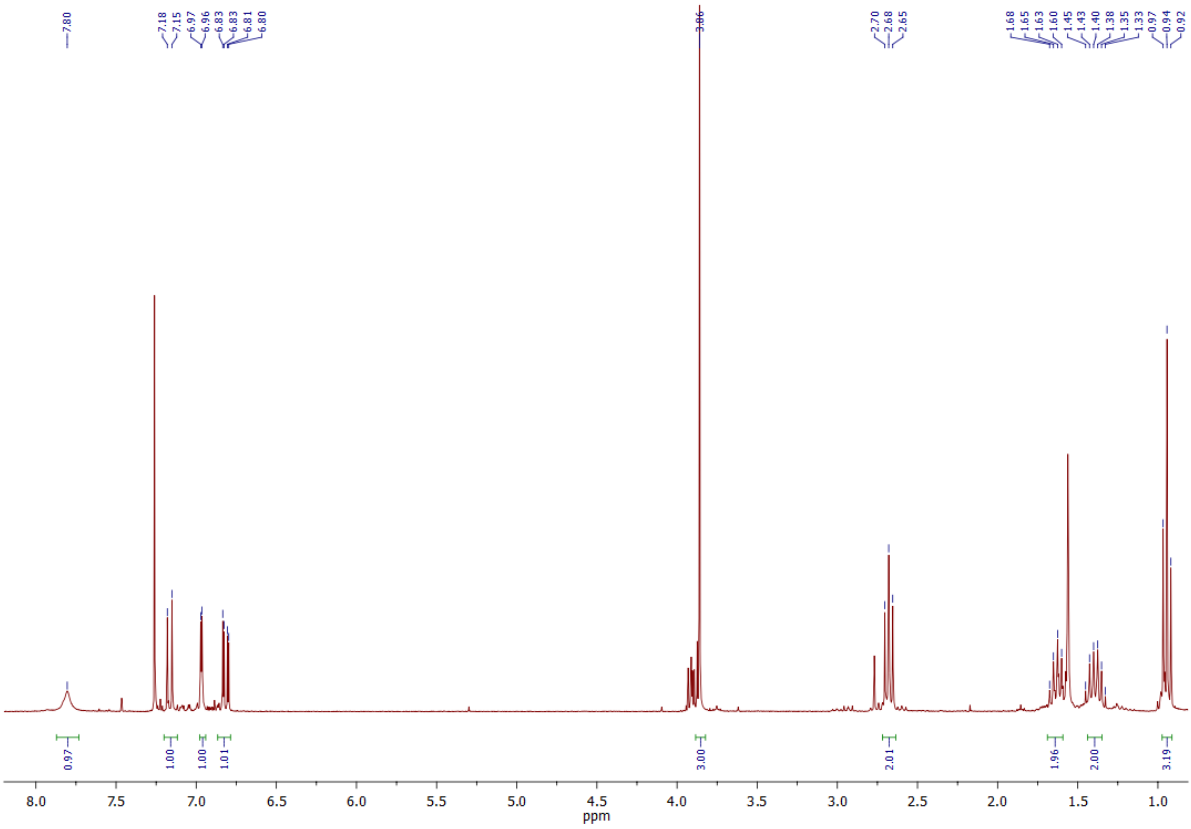

^{1}H NMR (500 MHz, $CDCl_3$) of 2,6-Dibromo-3-*n*-butyl-5-methoxy-1H-indole (11)

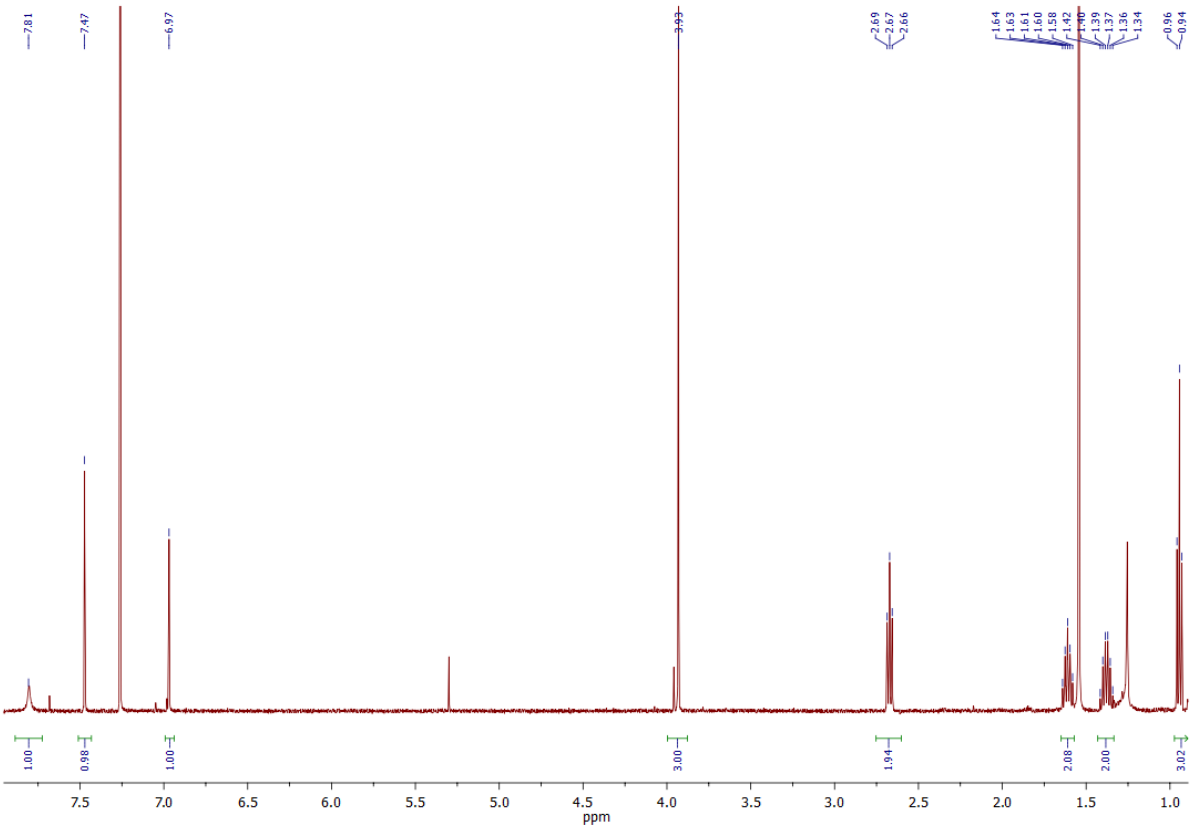

^{1}H NMR (500 MHz, CD_2Cl_2) and ^{13}C NMR (125 MHz, CD_2Cl_2) of 3-*n*-Butyl-5-methoxy-1-phenylsulfonylindole (13)

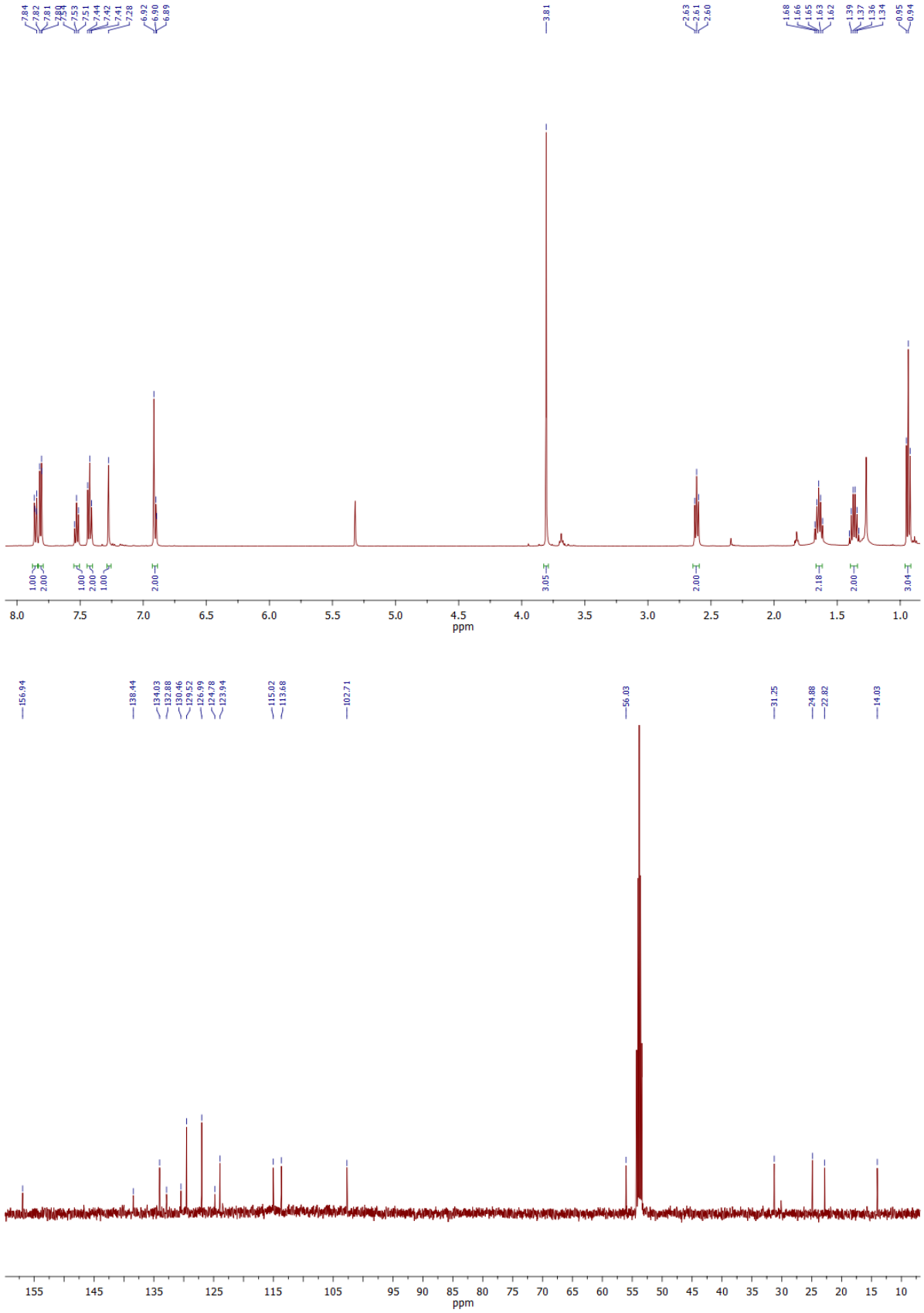

^{1}H NMR (500 MHz, C_2D_6O) and ^{13}C NMR (125 MHz, C_2D_6O) of 5-Methoxy-3-phenyl-1-phenylsulfonyl-2-trimethylstannylindole (16)

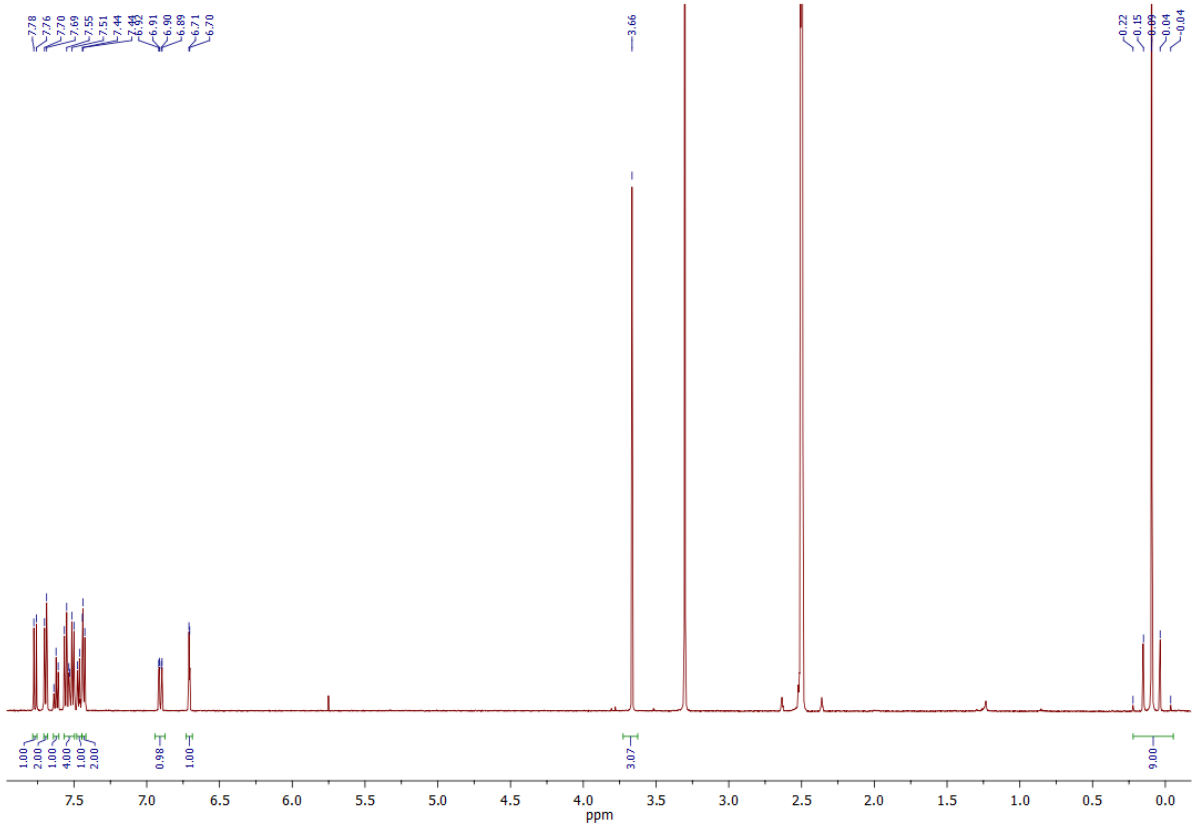

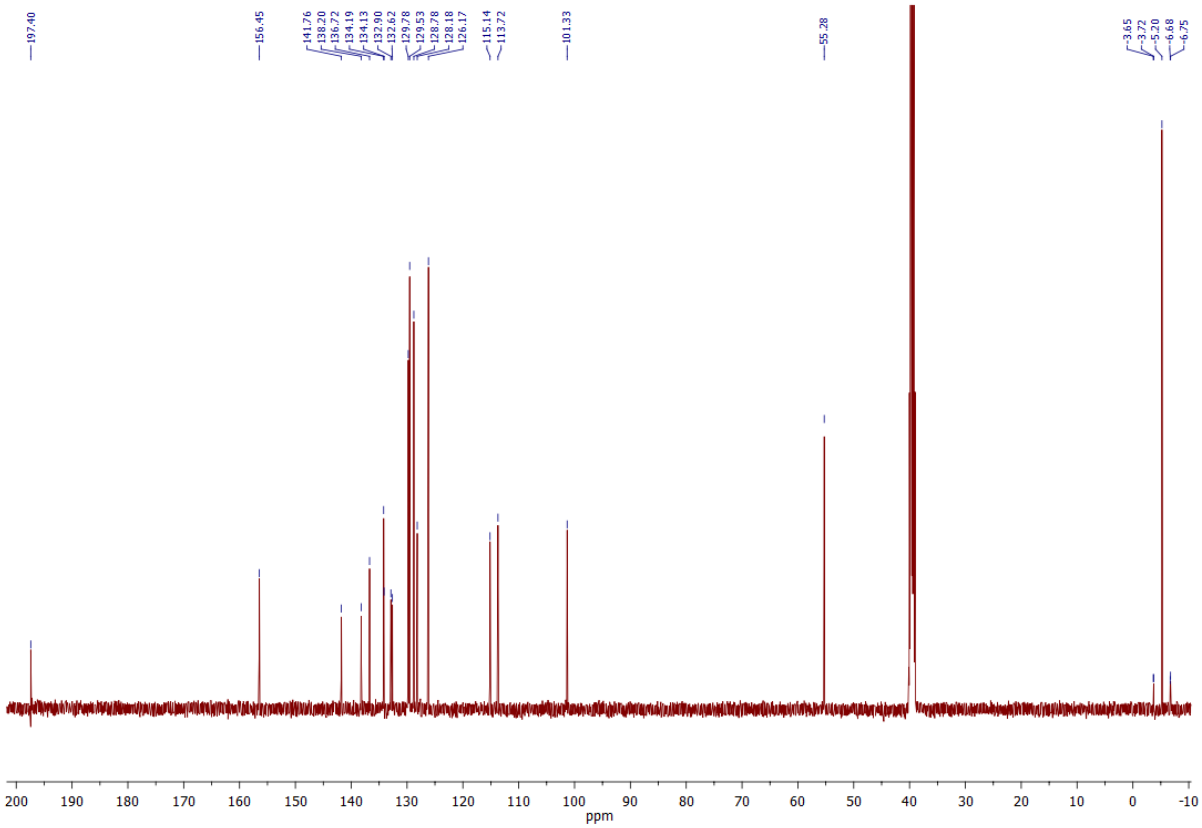

^{1}H NMR (500MHz, C_2D_6O) and ^{13}C NMR (125 MHz, C_2D_6O) of 5-Methoxy-3-phenyl-1-[(2'-trimethylstannyl)phenylsulfonyl]-2-trimethylstannylindole (17)

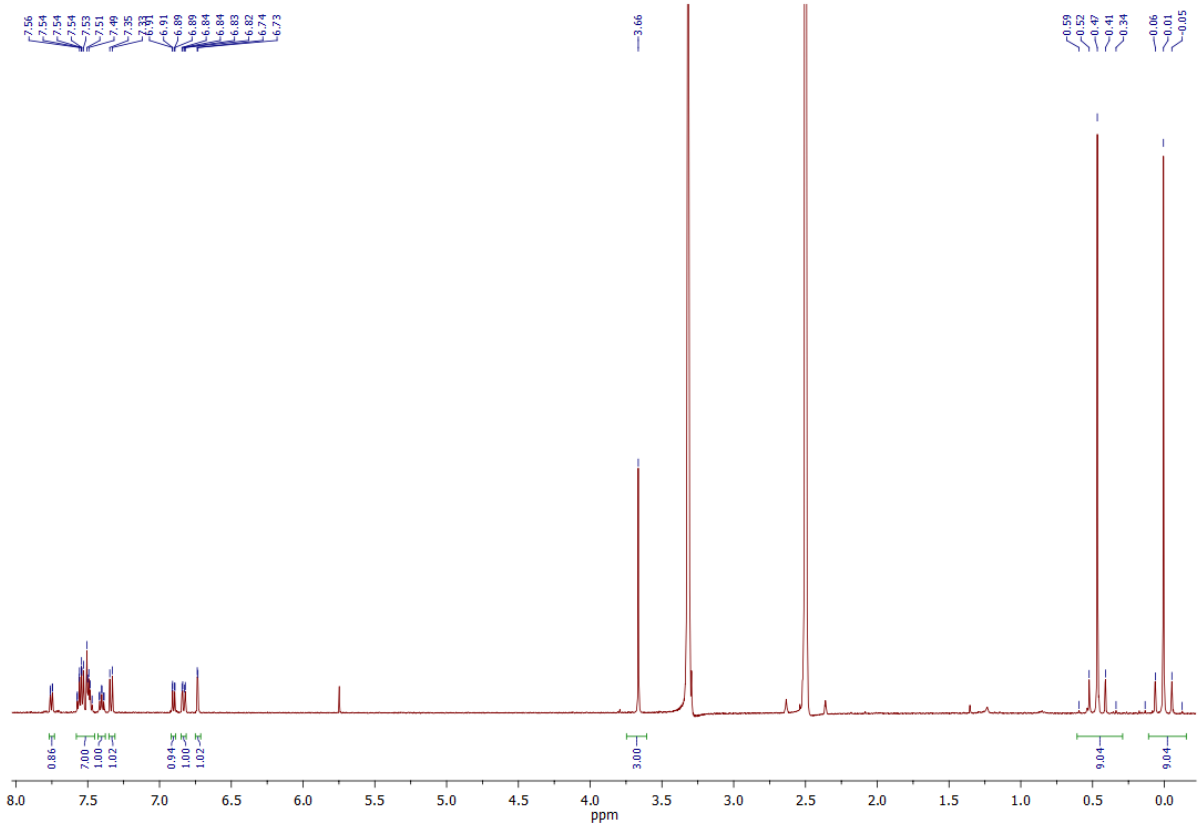

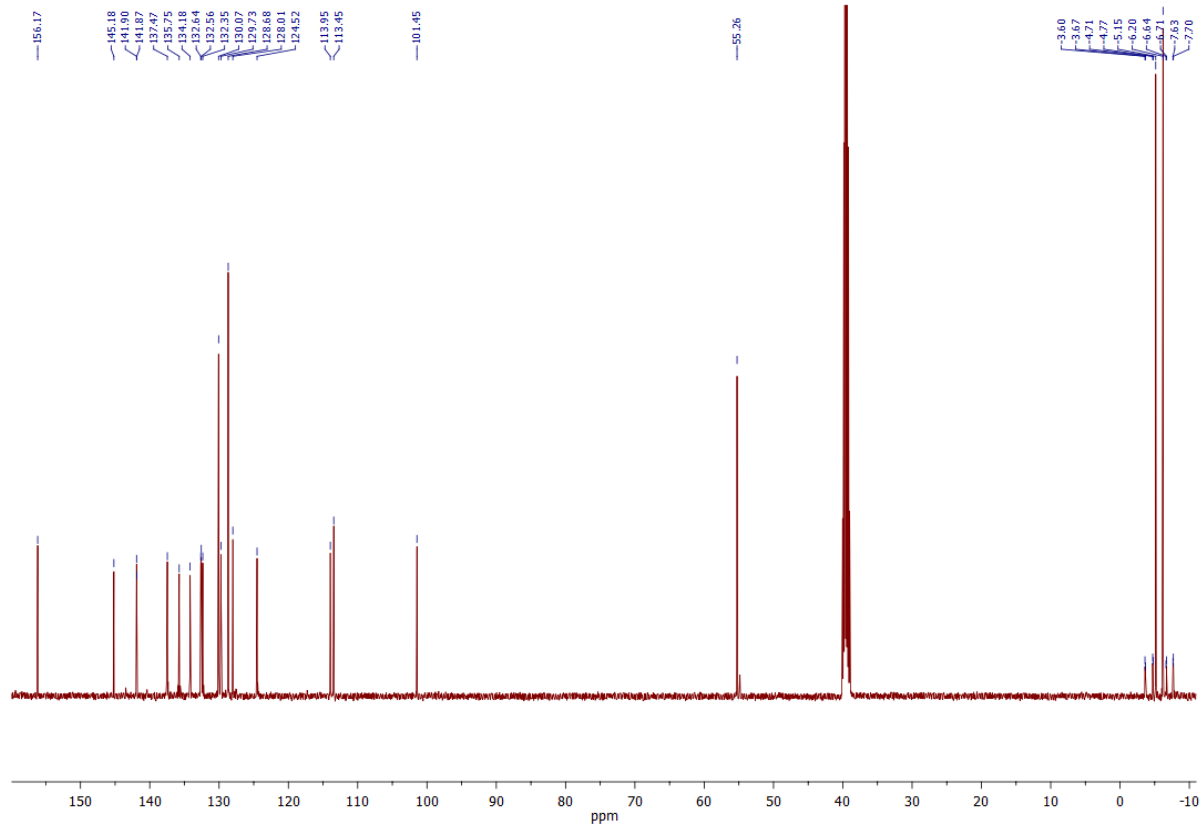

^{1}H NMR (500 MHz, $CDCl_3$) and ^{13}C NMR (100 MHz, $CDCl_3$) of 5-Methoxy-1-phenylsulfonyl-2-trimethylstannylindole (18)

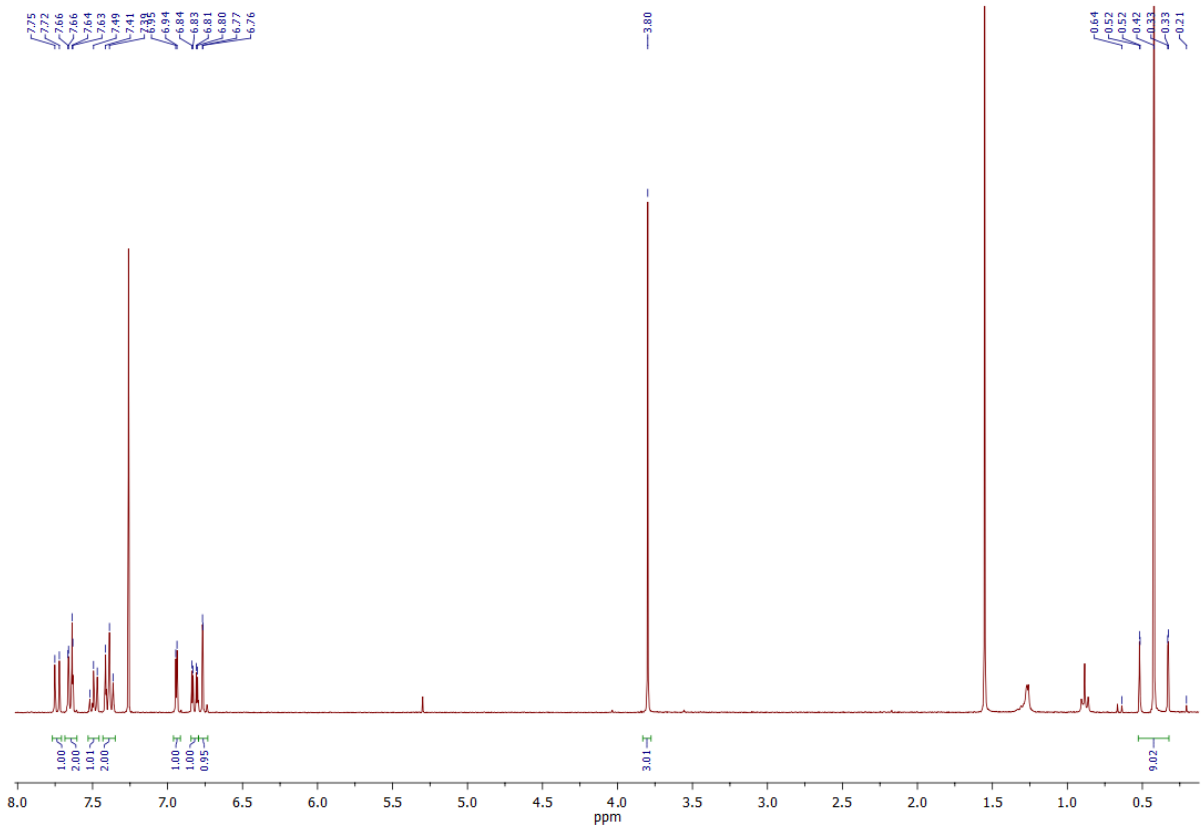

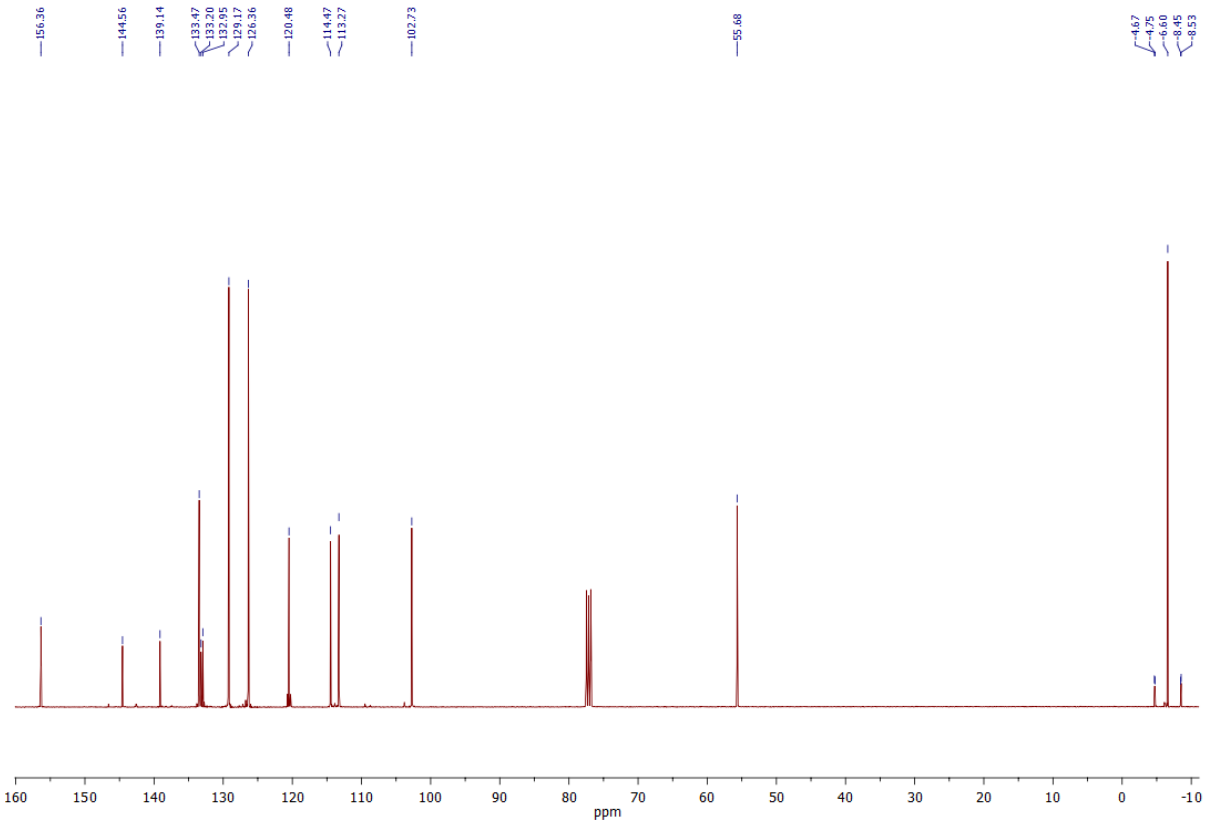

^{1}H NMR (500 MHz, DMSO) and ^{13}C NMR (125 MHz, DMSO) of 6-(5-Methoxy-3-phenyl-1-phenylsulfonylindol-2-yl)-2-bromopyridine (20)

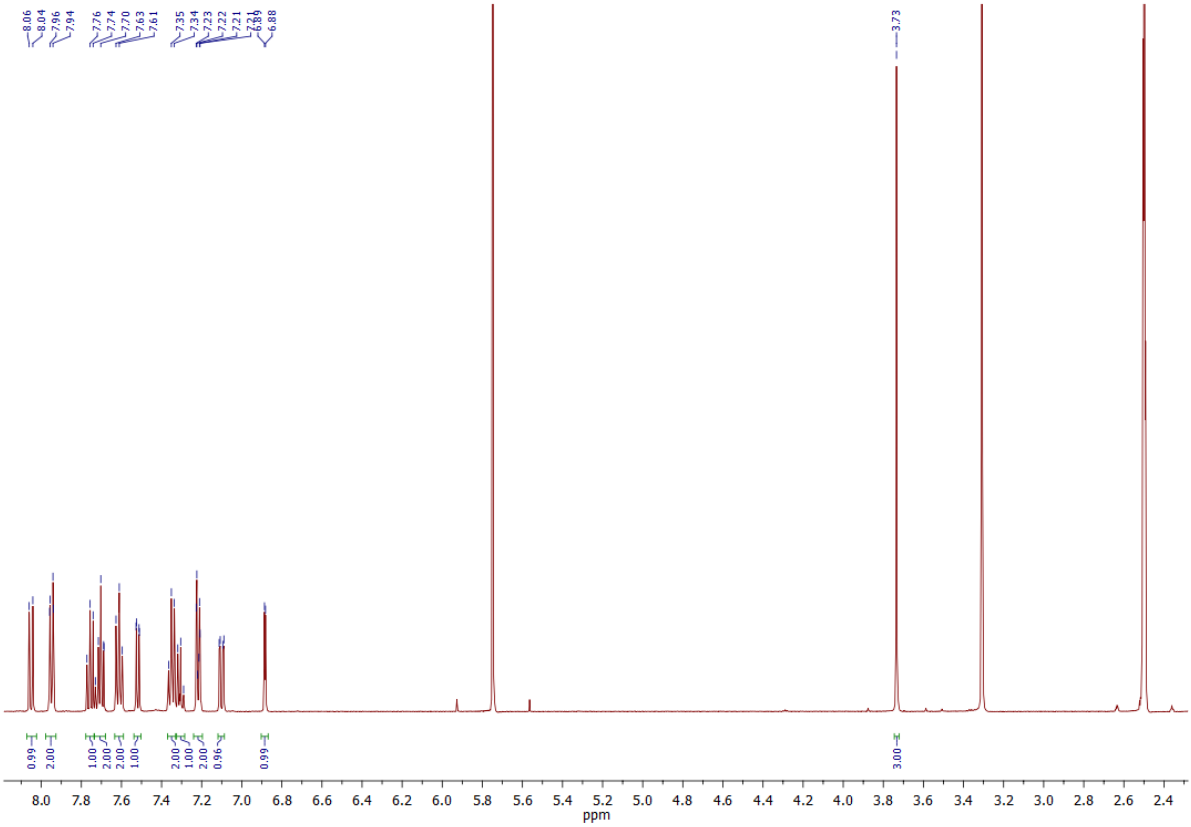

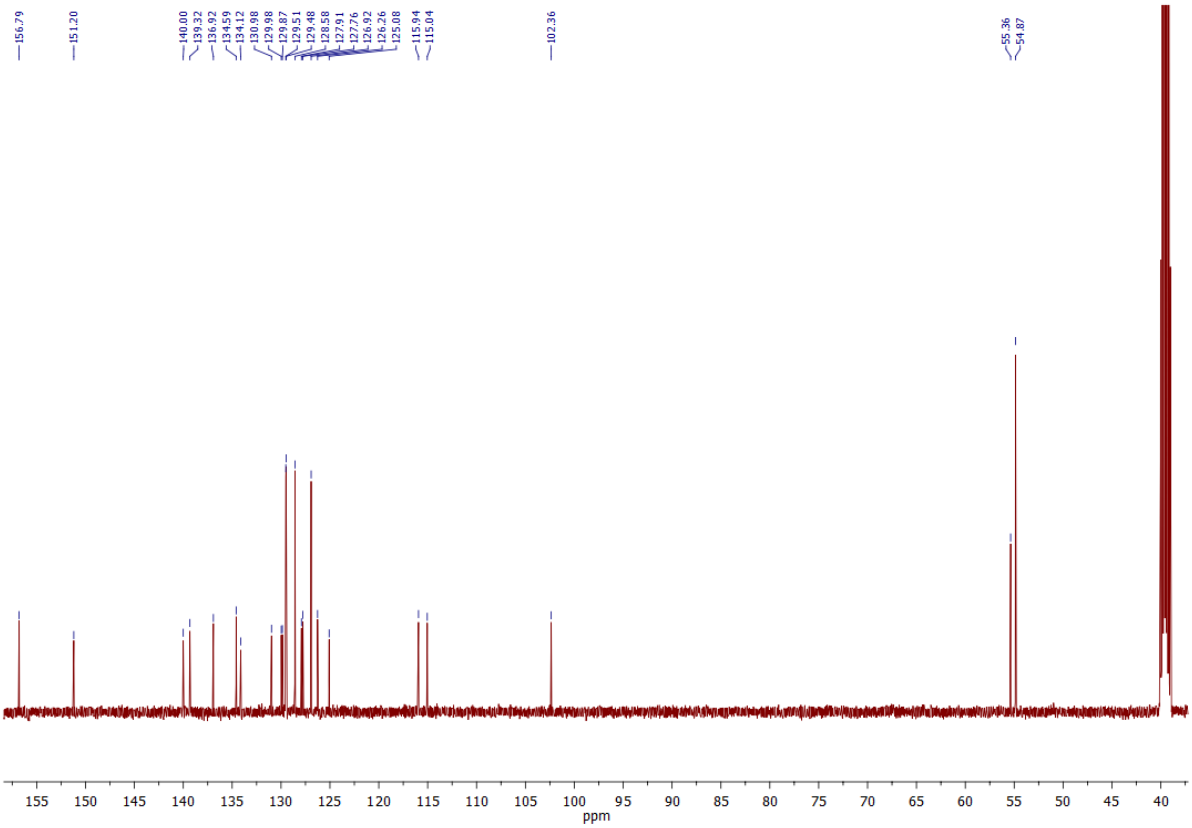

^{1}H NMR (400 MHz, $CDCl_3$) and ^{13}C NMR (100 MHz, $CDCl_3$) of 1,3-Bis(5-Methoxy-1-(phenylsulfonyl)-1H-indol-2-yl)benzene (21)

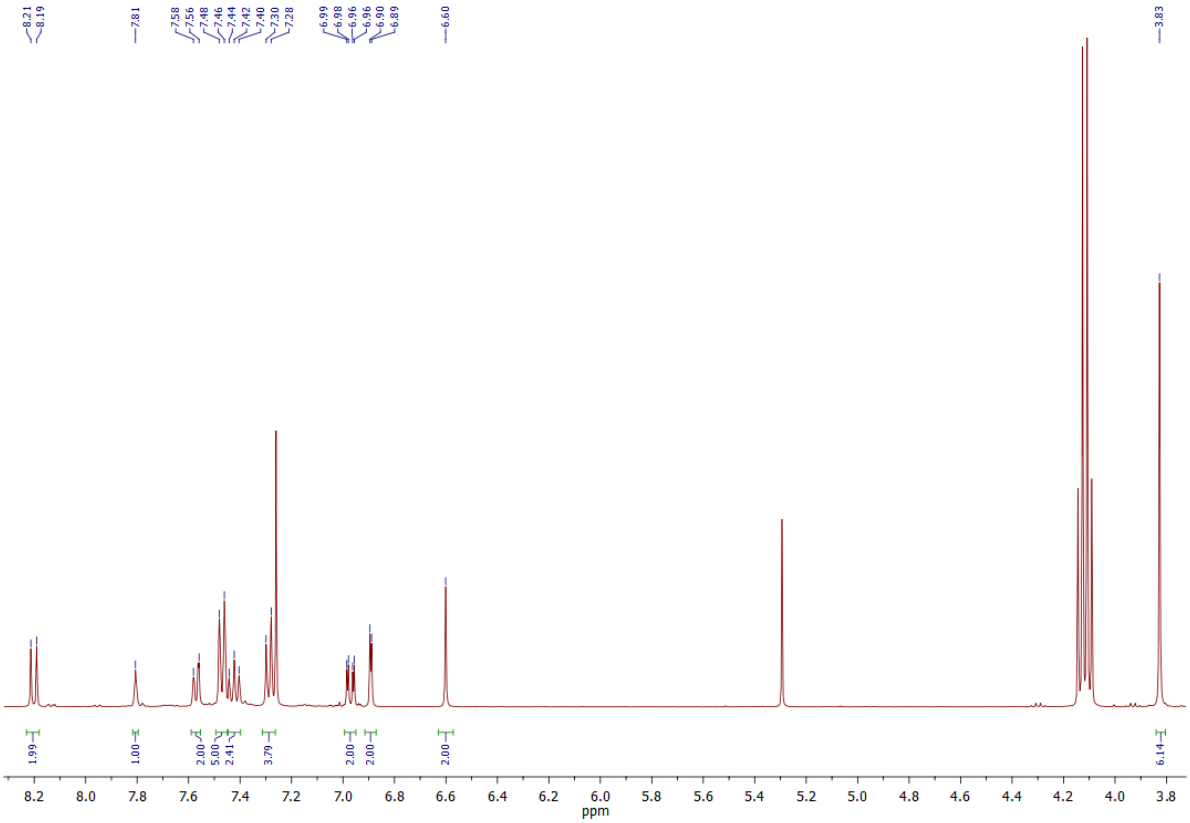

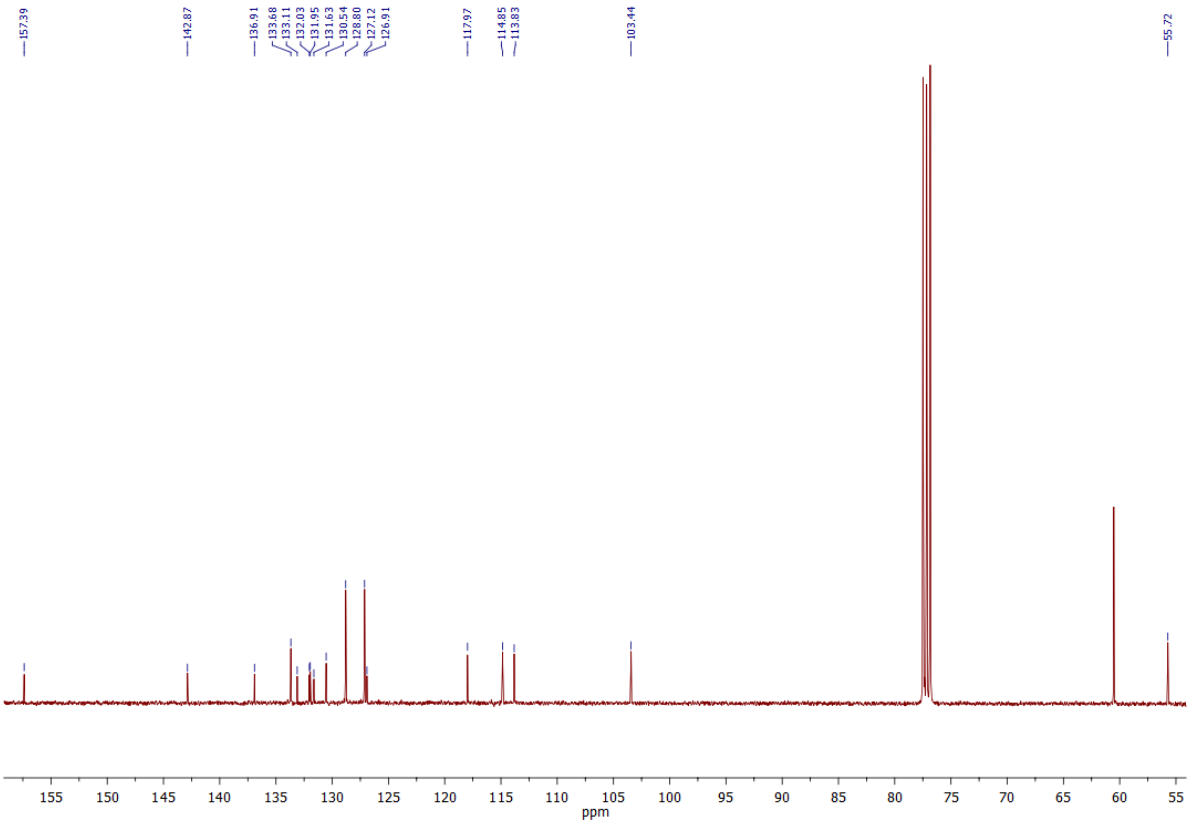

^{1}H NMR (500 MHz, CD_2Cl_2) and^{13}C NMR (125 MHz, CD_2Cl_2) of 2,6-Bis(5-methoxy-1-phenylsulfonylindol-2-yl)pyridine (22)

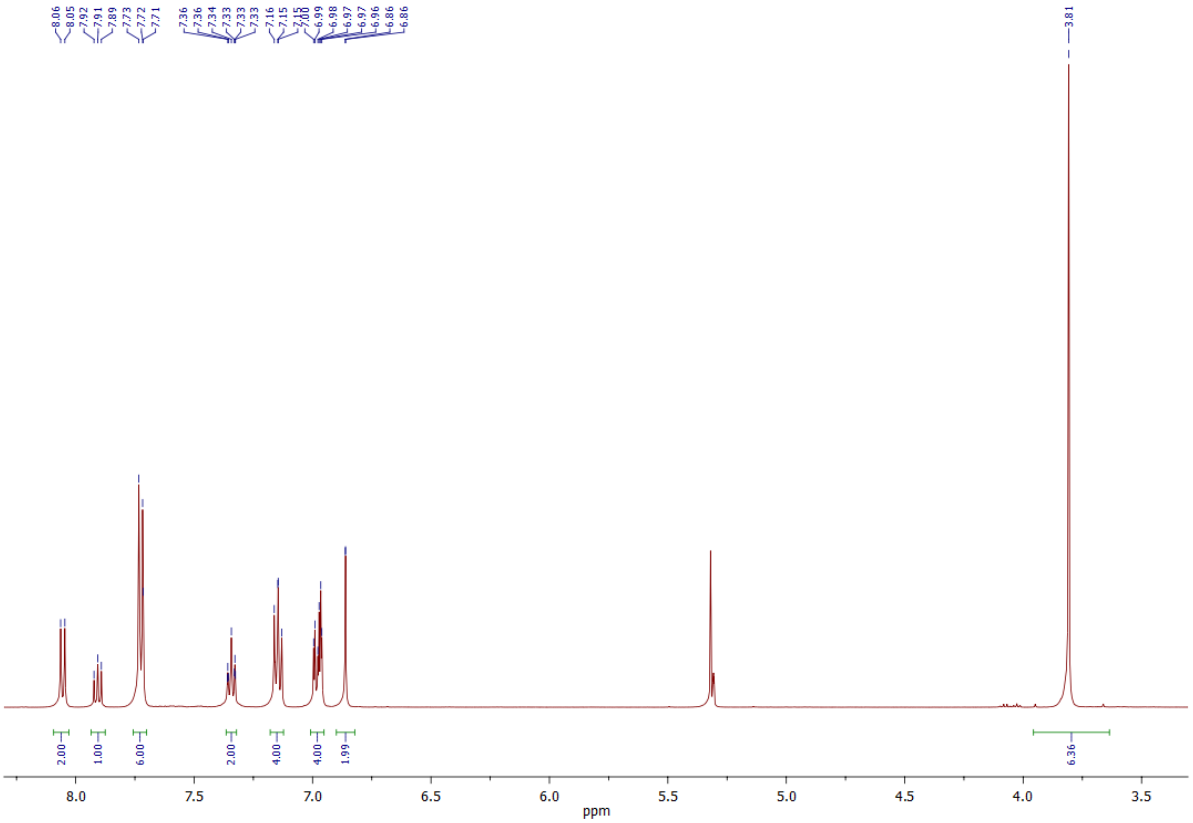

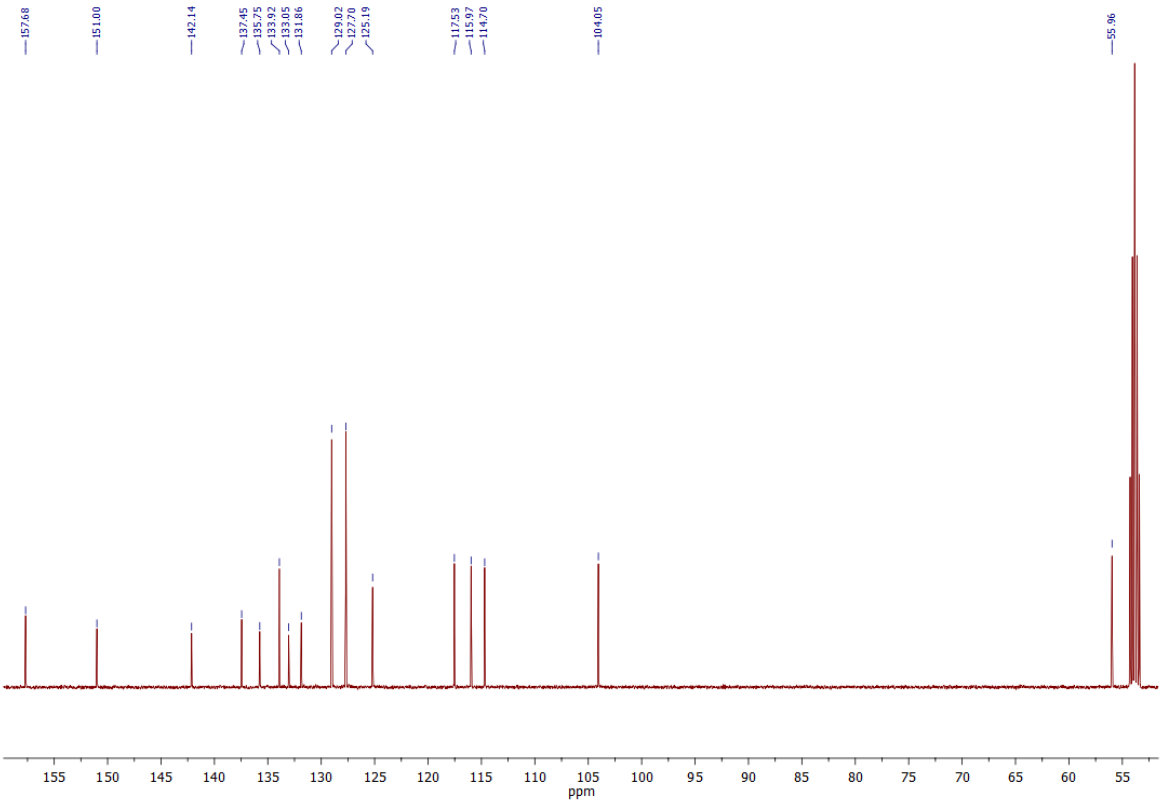

^{1}H NMR (500 MHz, $CDCl_3$) and ^{13}C NMR (125 MHz, $CDCl_3$) 2,5-Bis(5-methoxy-1-phenylsulfonylindol-2-yl)thiophene (24)

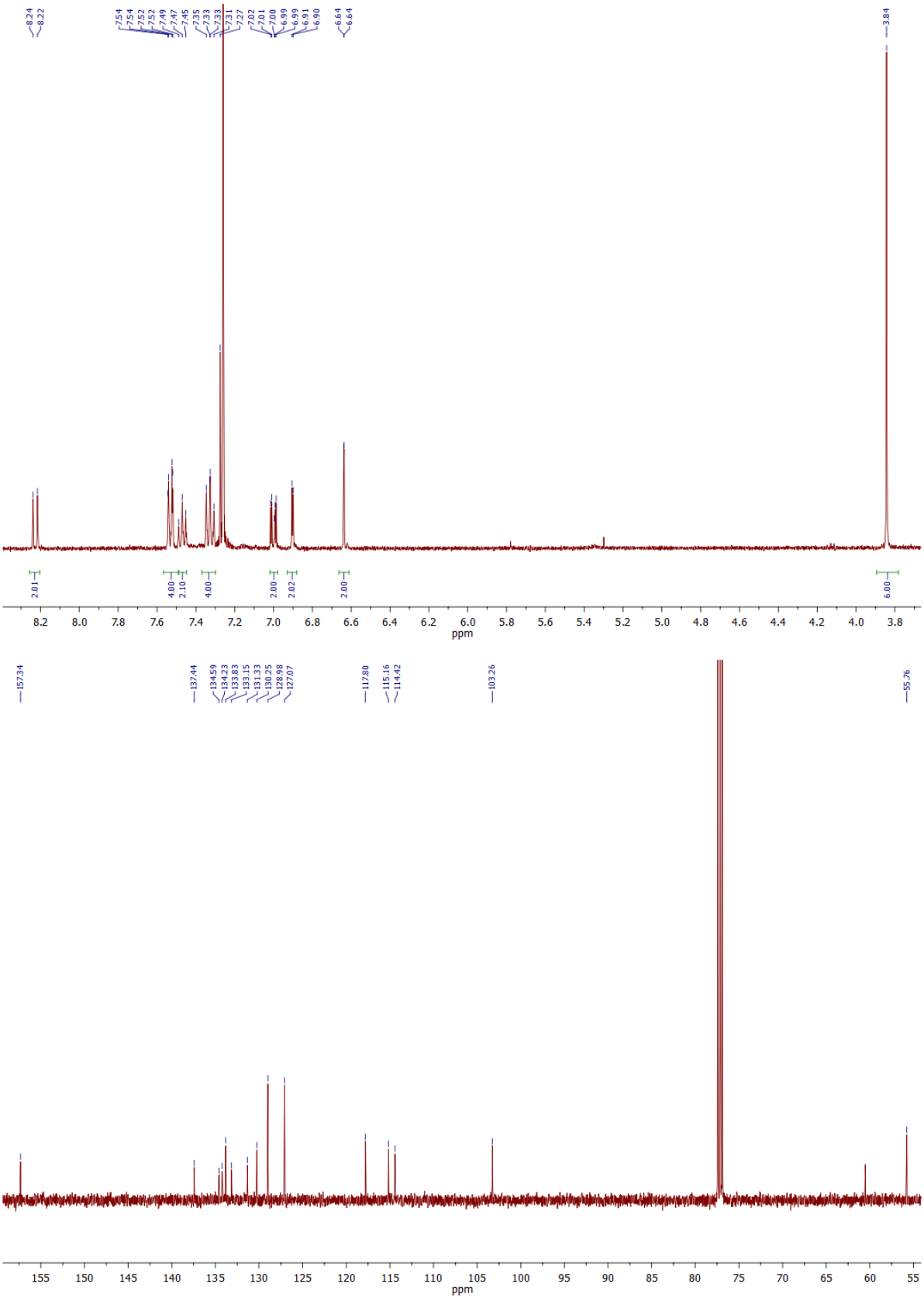

^{1}H NMR (300 MHz, CD_2Cl_2) of 2,5- Bis(5-methoxy-1-phenylsulfonylindol-2-yl) thiazole (25) (Crude NMR spectrum)

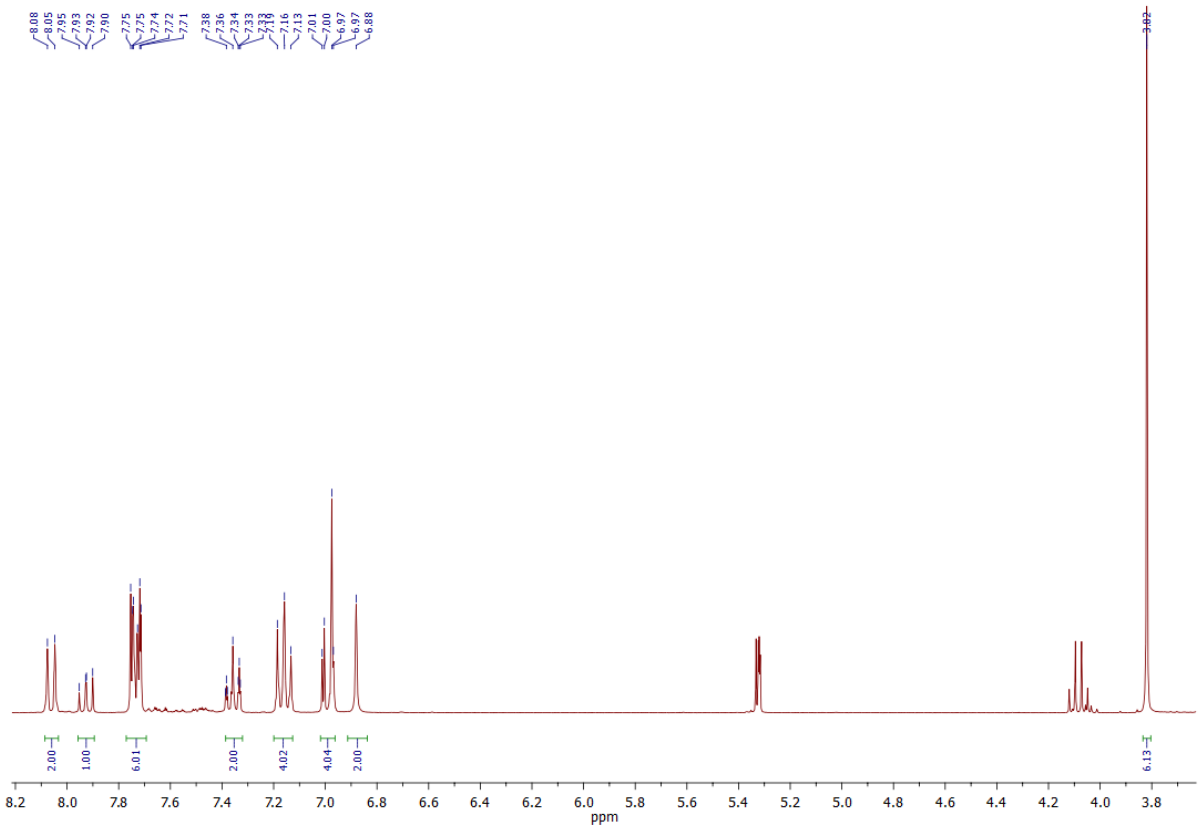

^{1}H NMR (400 MHz, $CDCl_3$) of Bis(5-methoxy-1-phenylsulfonylindol-2-yl) (28)

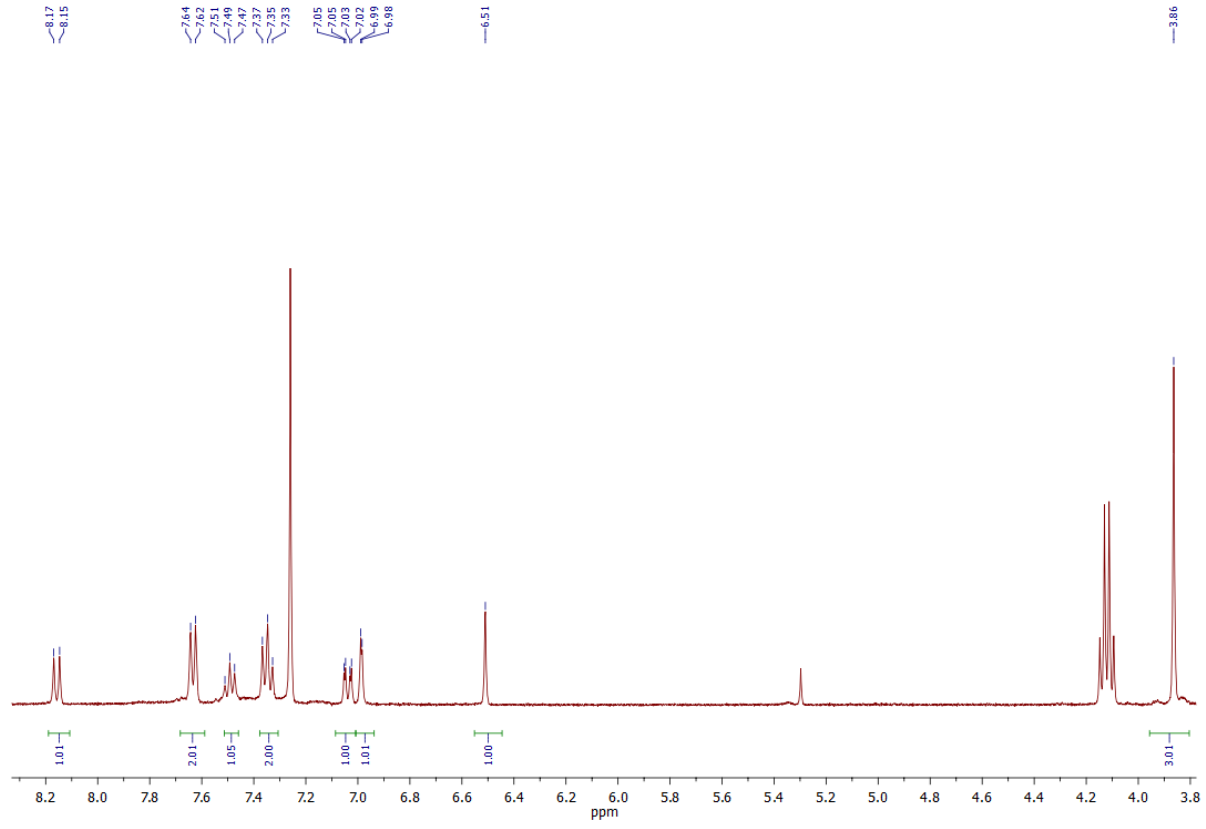

^{1}H NMR (500 MHz, $CDCl_3$) and ^{13}C NMR (125 MHz, $CDCl_3$) of 2-(5-Methoxy-1-phenylsulfonylindol-2yl)-5-(5-methoxy-1H-indol-2-yl)thiophene (29)

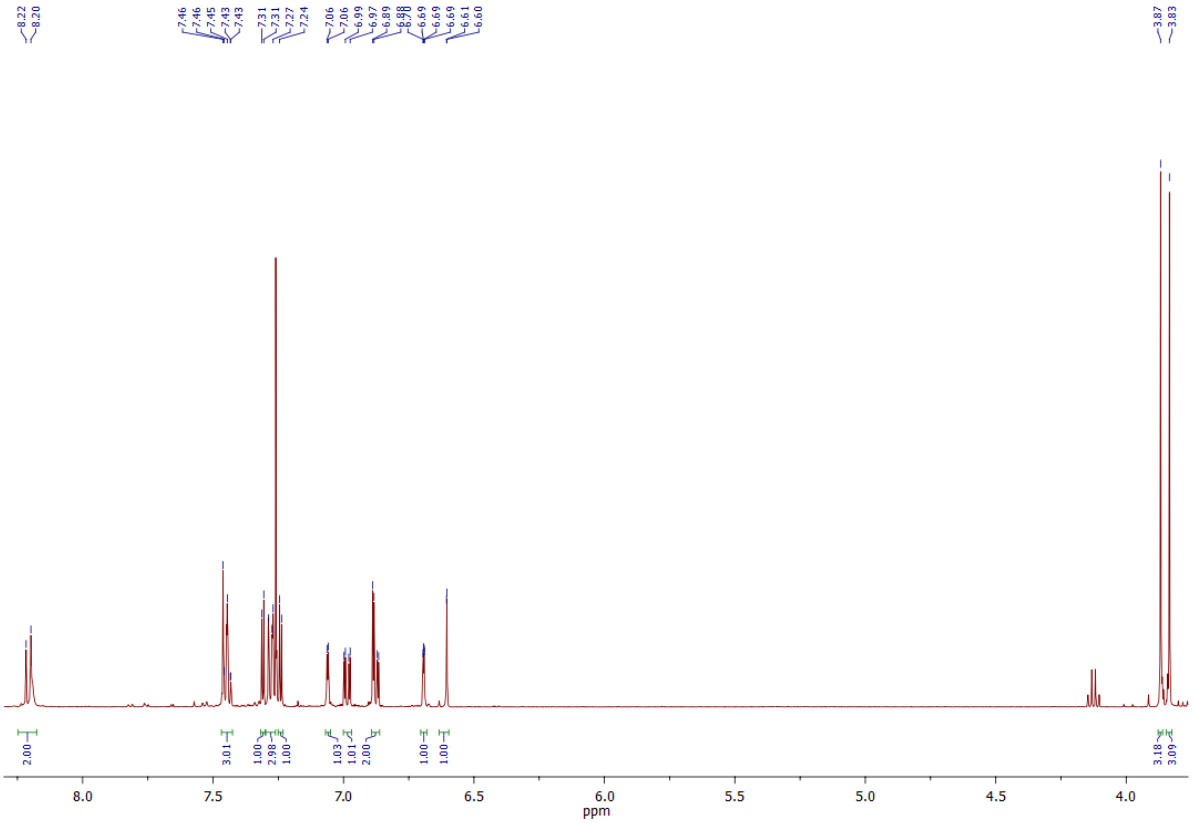

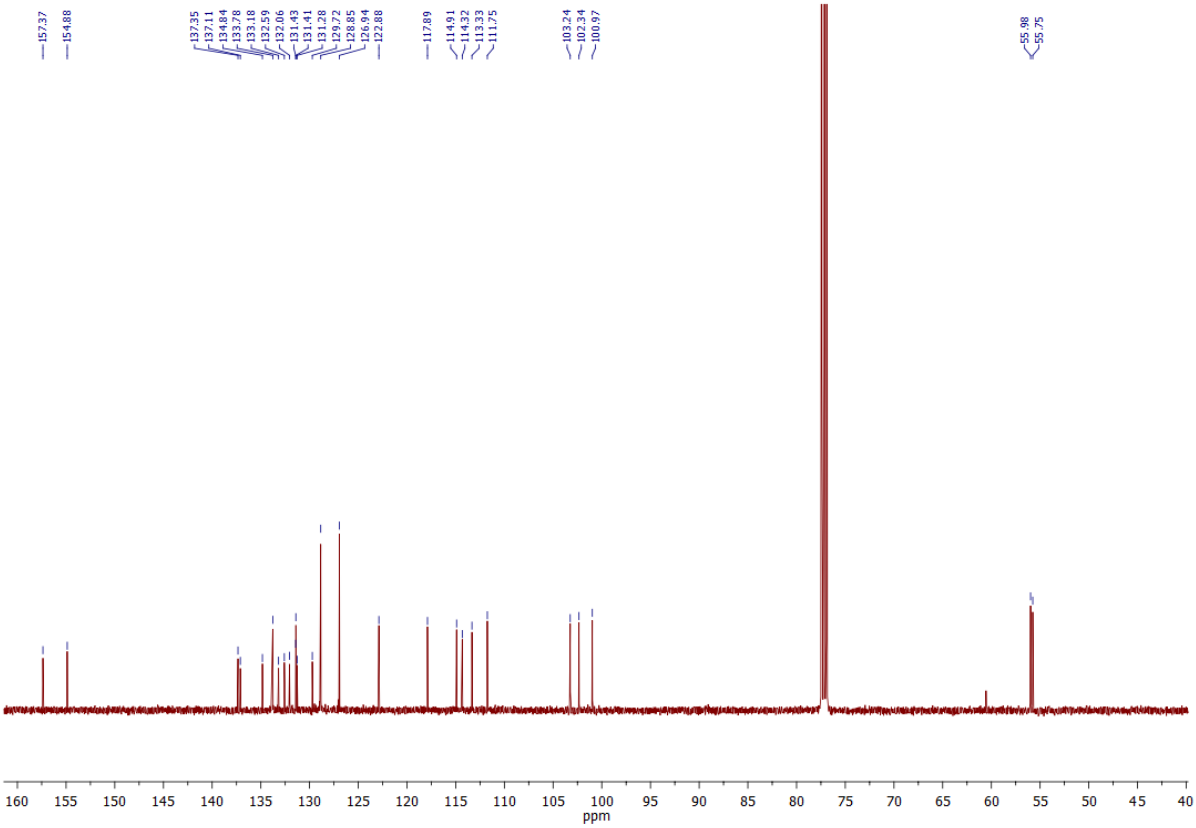

^{1}H NMR (400 MHz, $CDCl_3$) and ^{13}C NMR (100 MHz, $CDCl_3$) of (±)-4-[(2-Octyldodecyl)oxy]benzaldehyde (34)

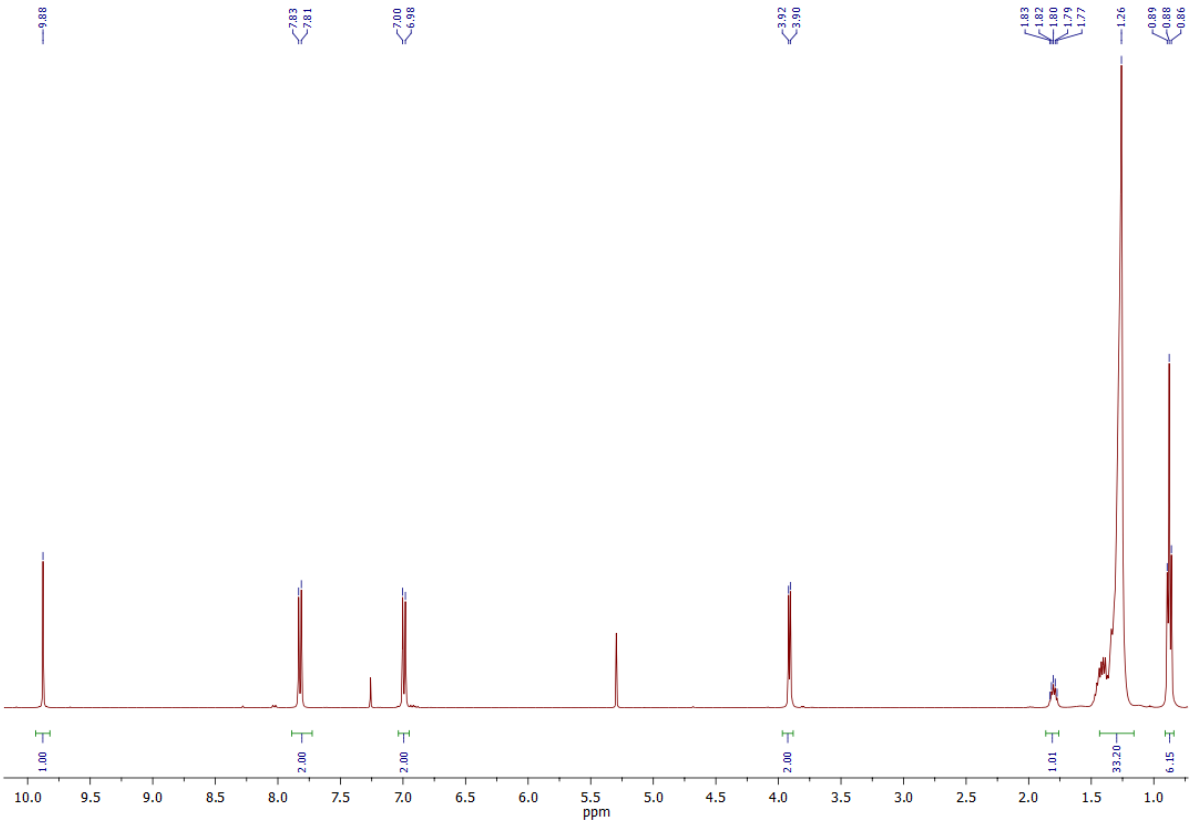

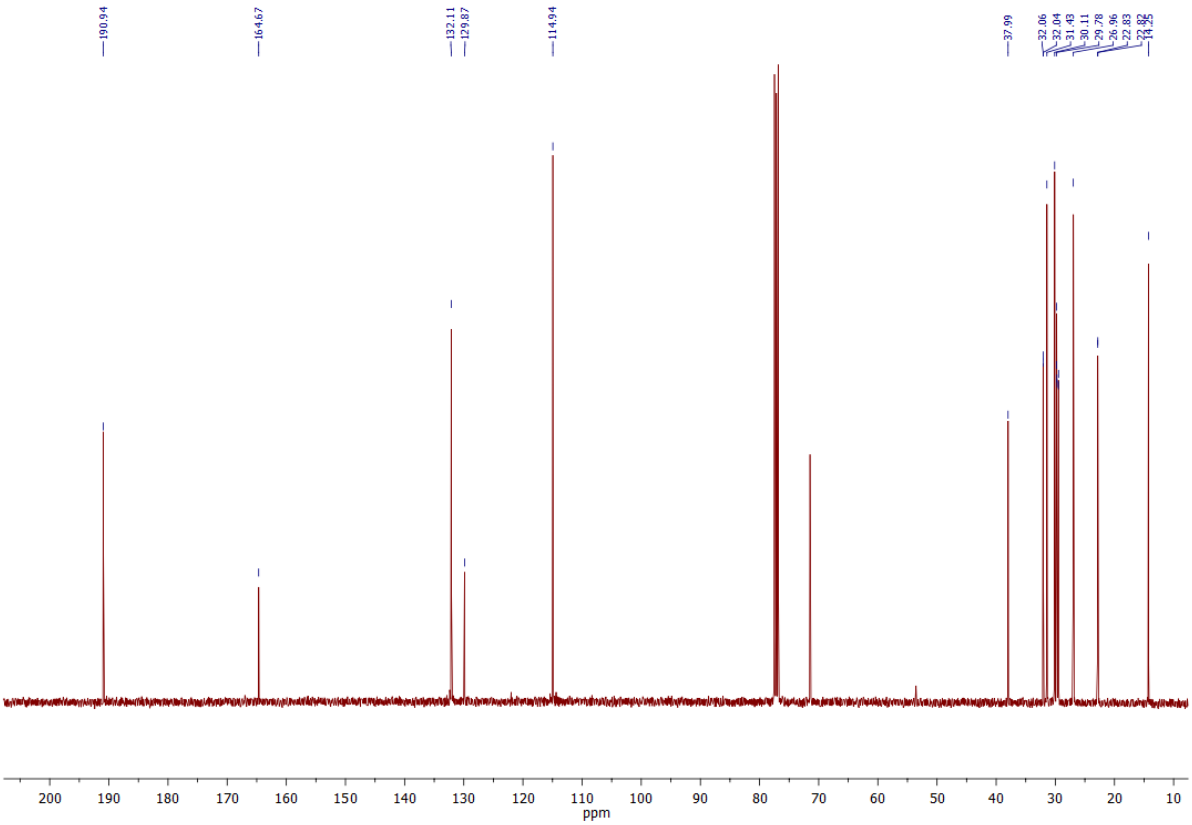

^{1}H NMR (400 MHz, $CDCl_3$) and ^{13}C NMR (100 MHz, $CDCl_3$) of 3,4-Bis[(2-octyldodecyl)oxy]benzaldehyde (35)

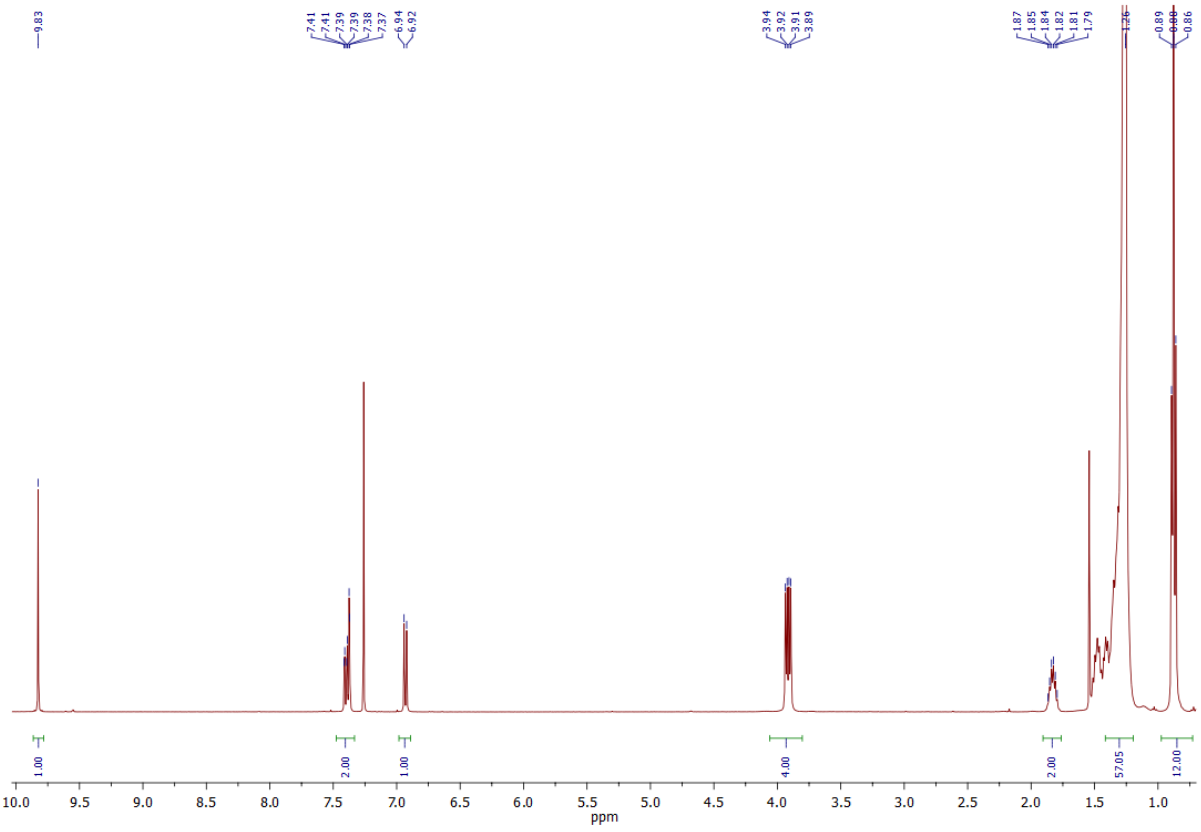

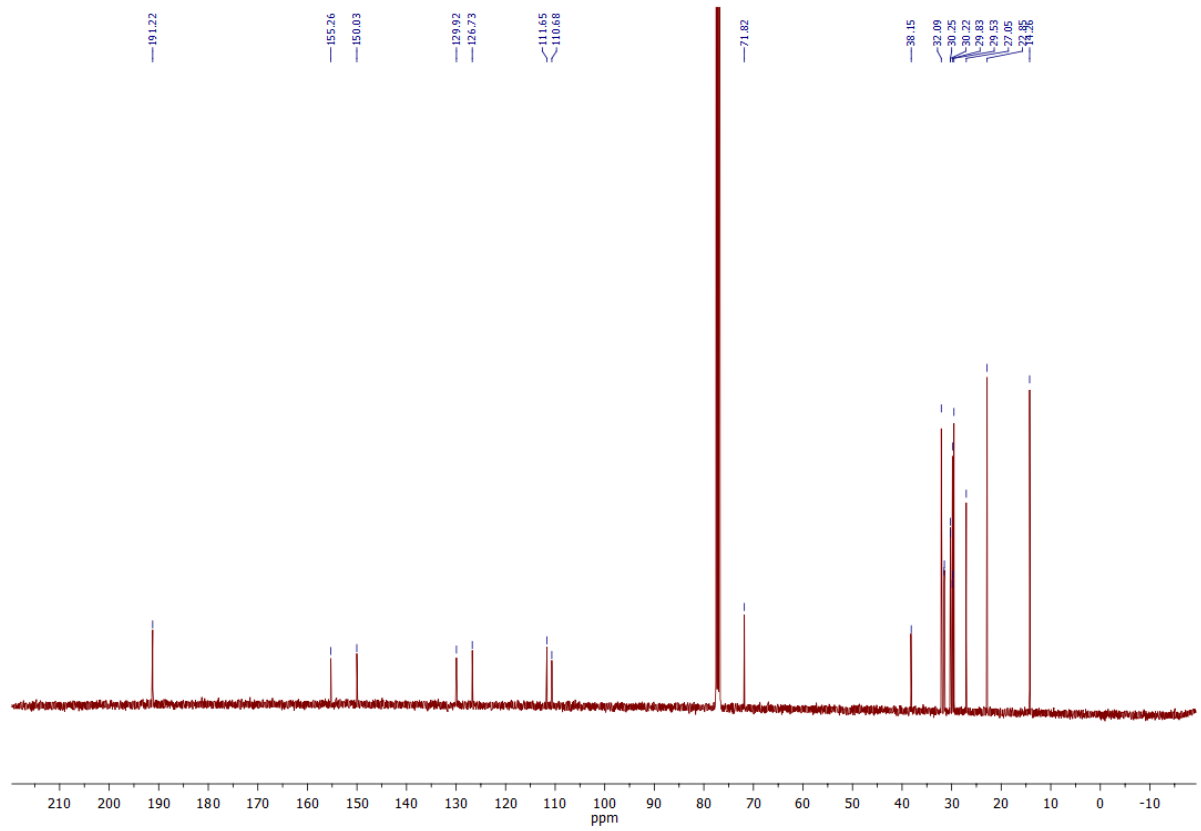

^{1}H NMR (400 MHz, $CDCl_3$) and ^{13}C NMR (100 MHz, $CDCl_3$) of 3-Hydroxy-4-[(2-octyldodecyl)oxy]benzaldehyde (36)

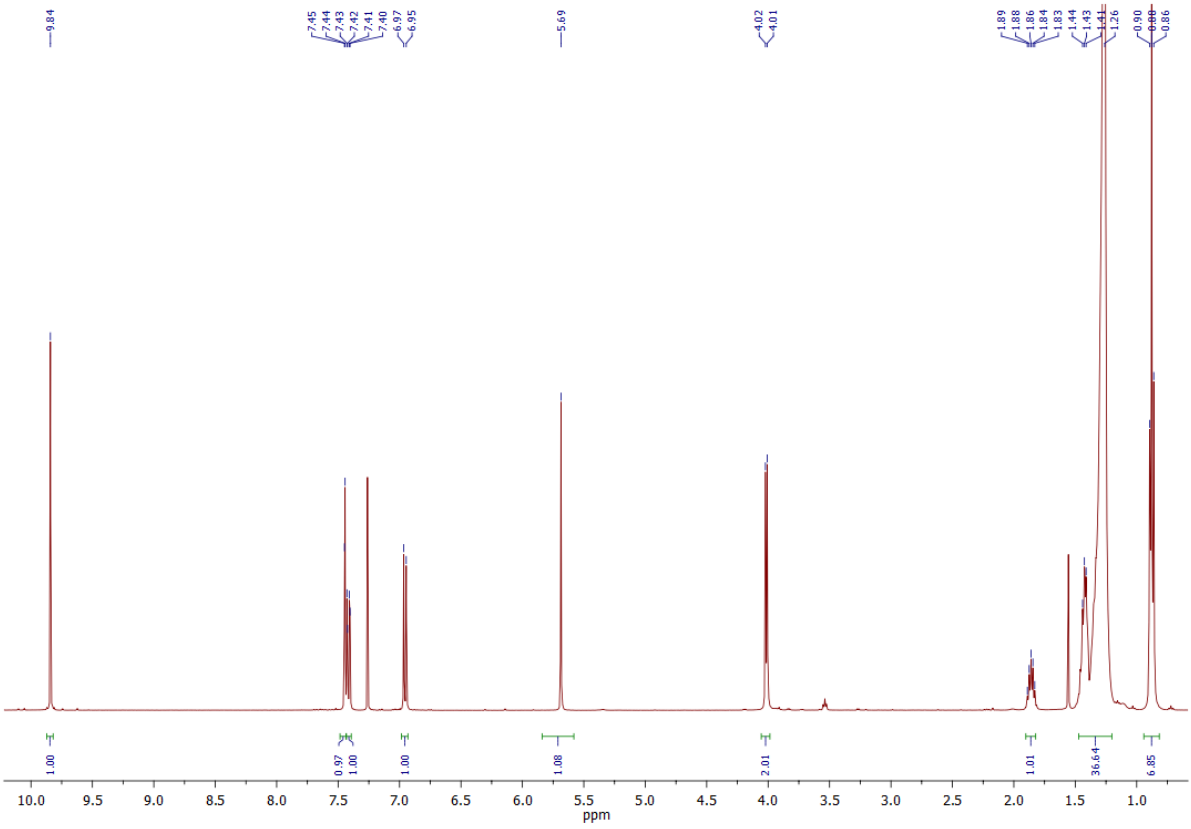

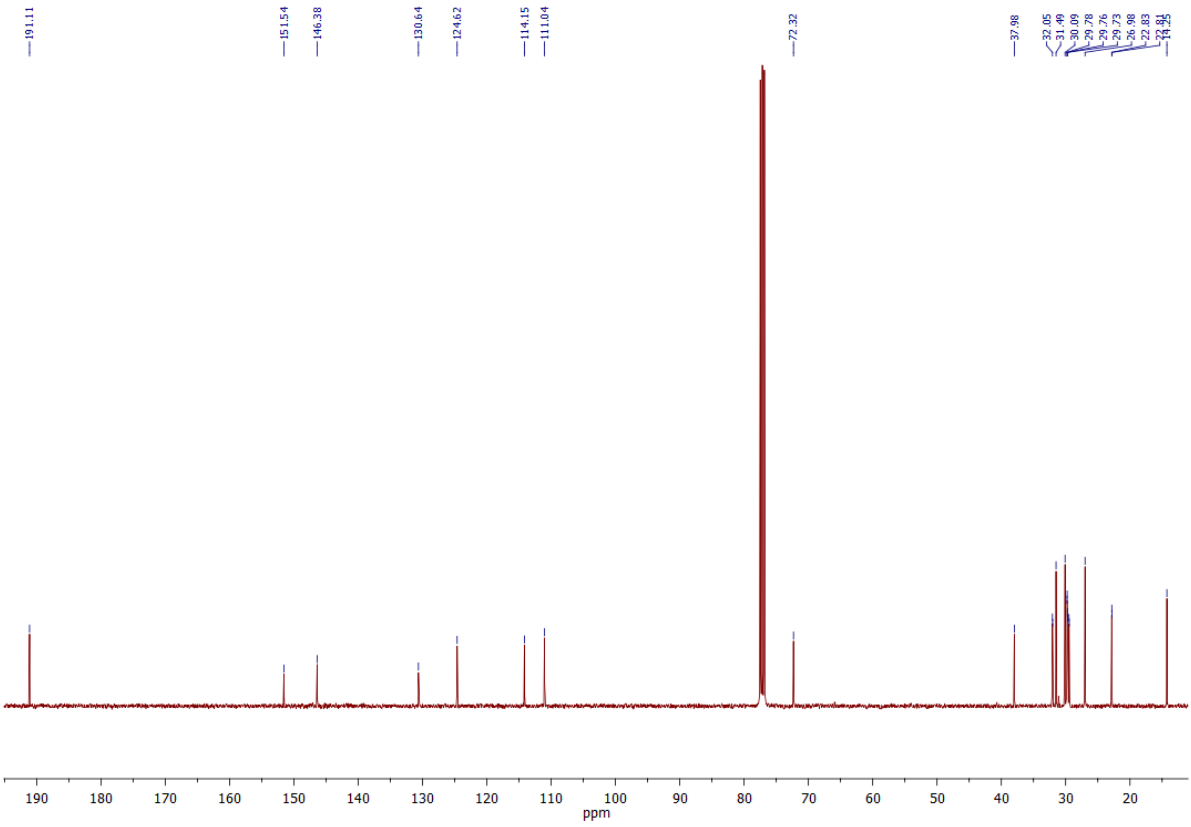

^{1}H NMR (400 MHz, $CDCl_3$) and ^{13}C NMR (100 MHz, $CDCl_3$) of (±)-2-{4-[(2-octyldodecyl)oxy]phenyl}-1H-imidazo[4,5-f][1,10]phenanthroline (4.1)

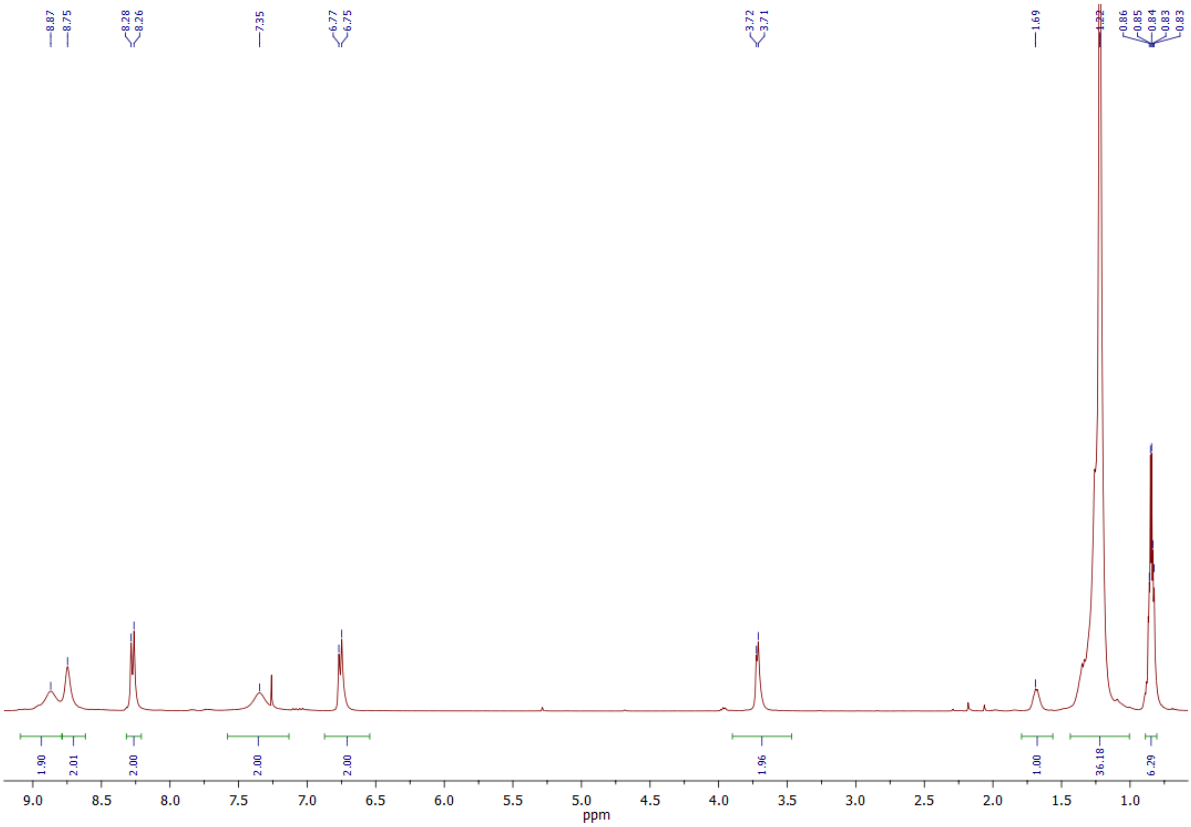

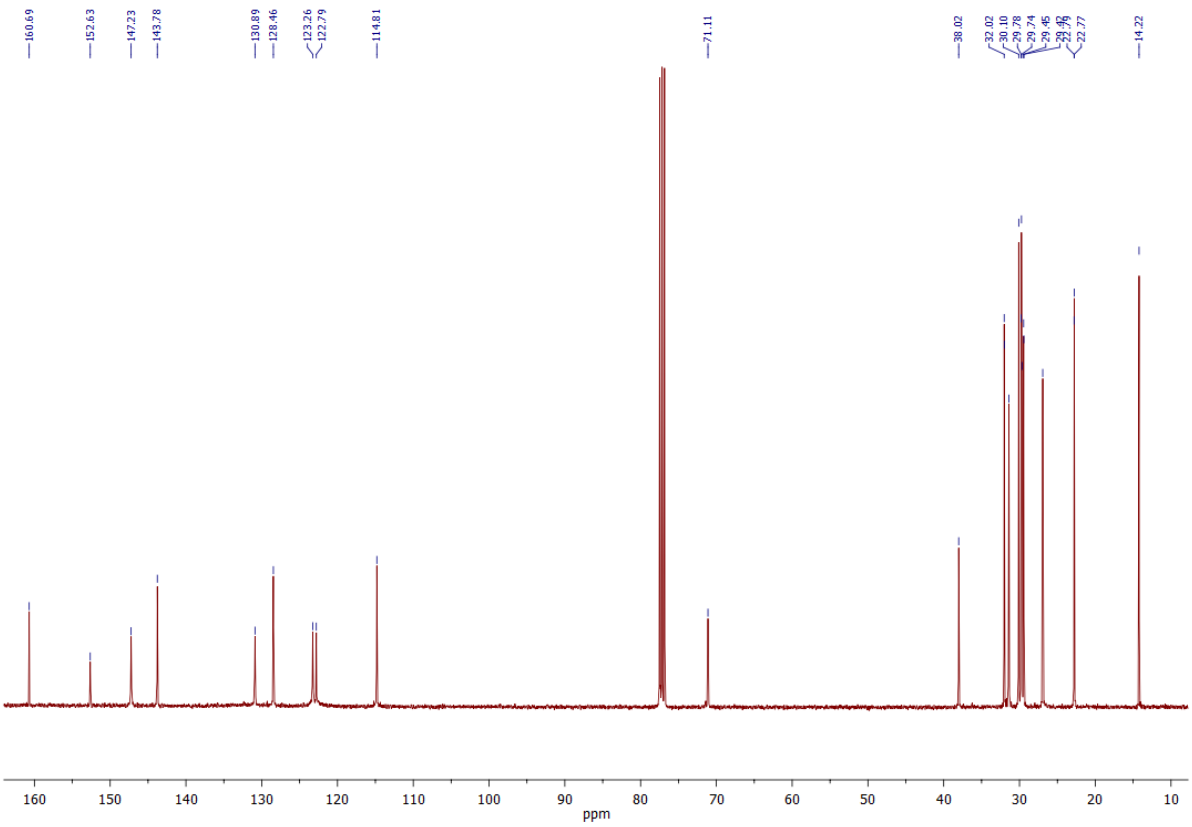

^{1}H NMR (400 MHz, $CDCl_3$) and ^{13}C NMR (100 MHz, $CDCl_3$) of

(±)-2-{4-[(2-octyldodecyl)oxy]phenyl}-1-phenyl-1H-imidazo[4,5-f][1,10]phenanthroline (4.2)

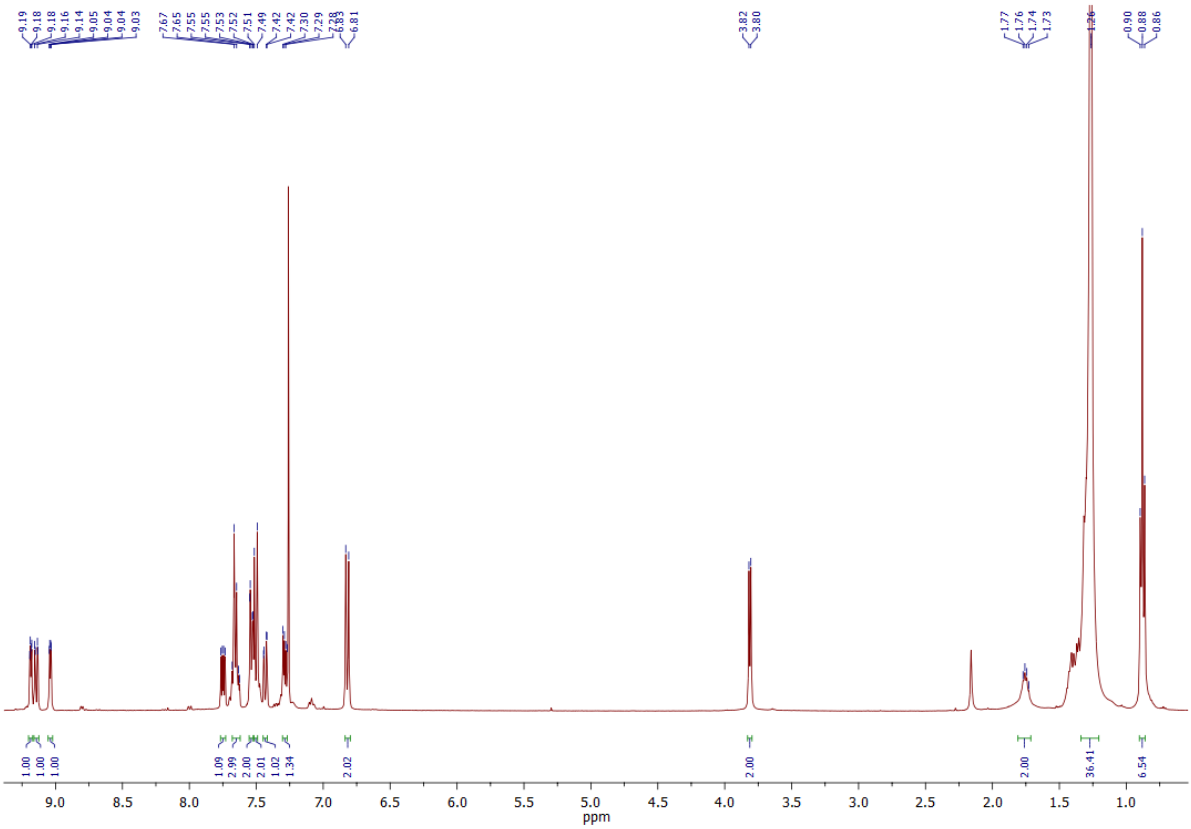

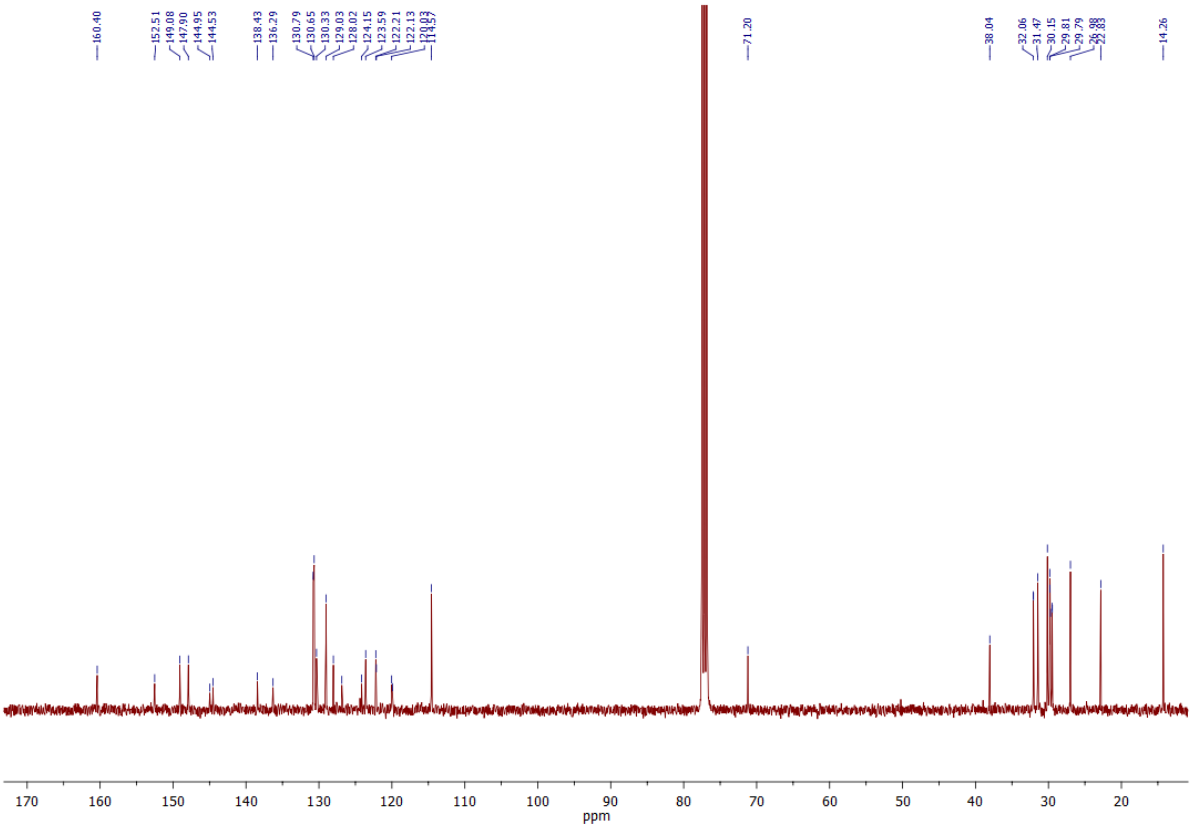

^{1}H NMR (400 MHz, $CDCl_3$) and ^{13}C NMR (100 MHz, $CDCl_3$) of

2-{3,4-bis[(2-octyldodecyl)oxy]phenyl}-1H-imidazo[4,5-f][1,10]phenanthroline (4.3)

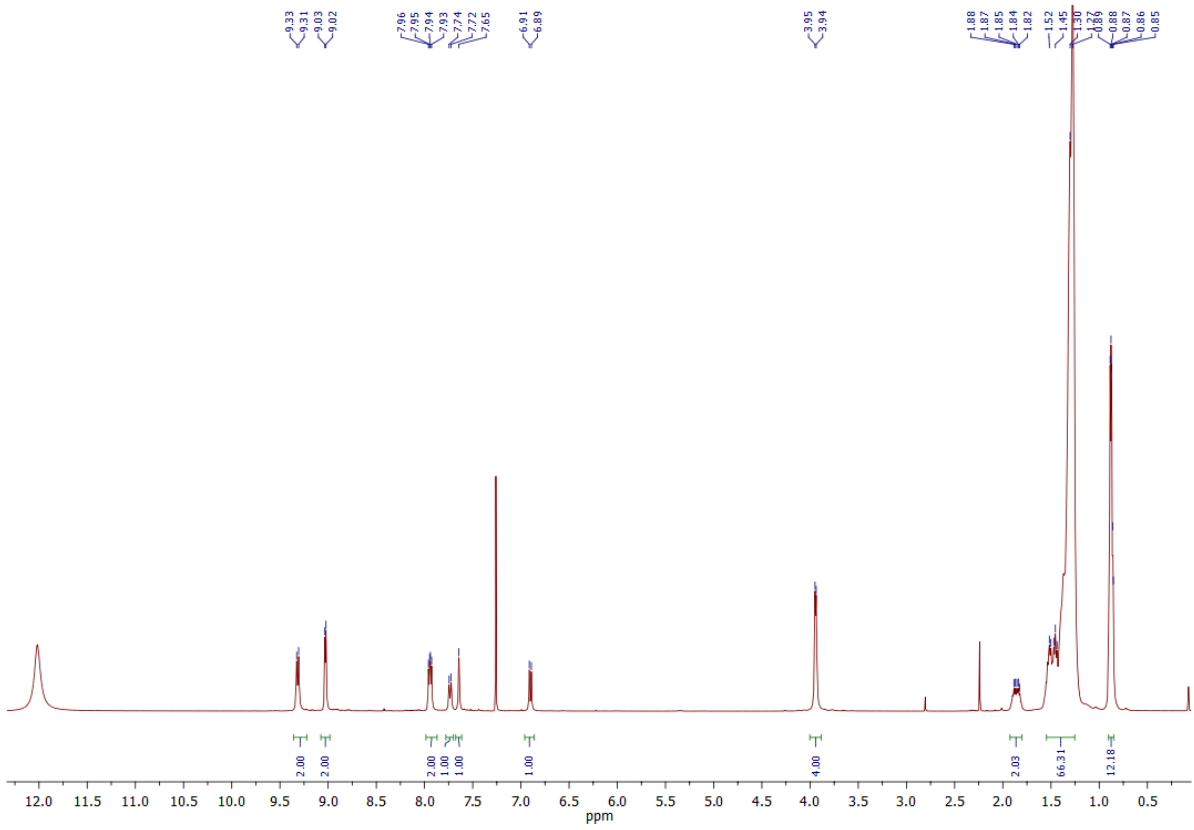

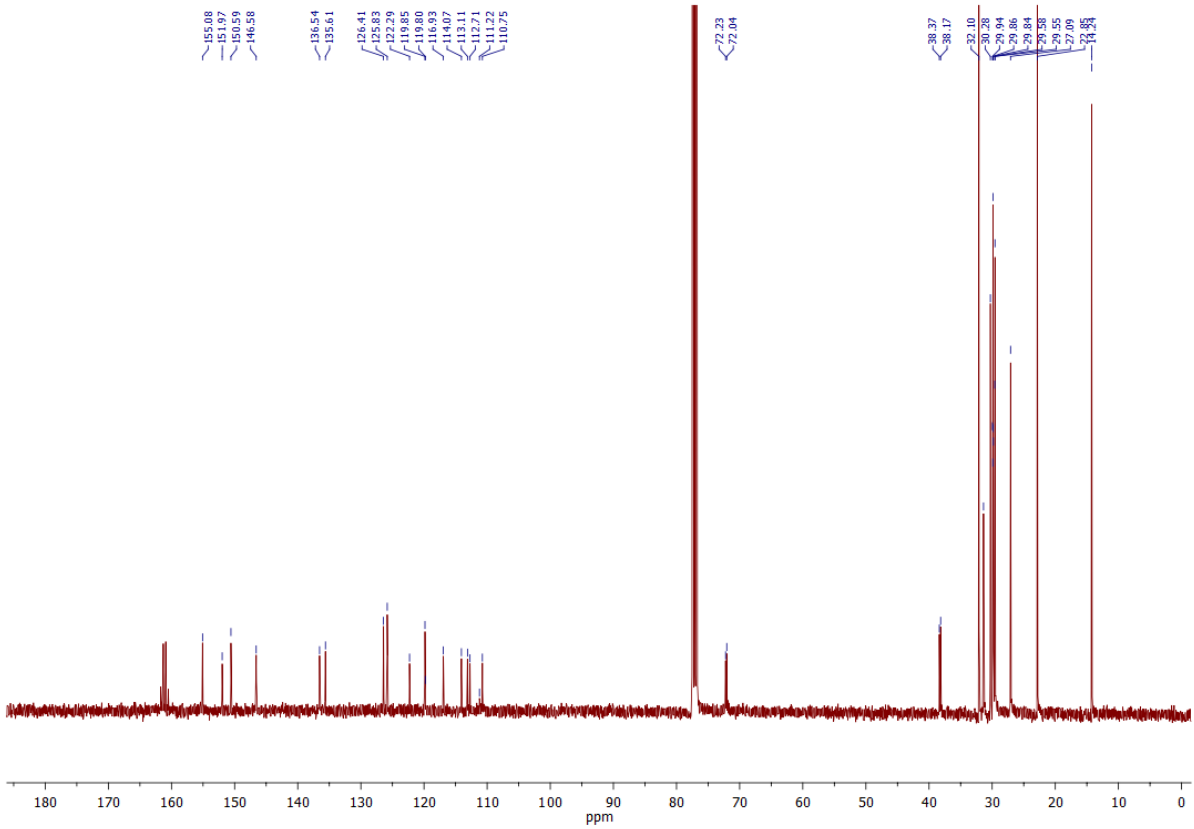

^{1}H NMR (400 MHz, $CDCl_3$) and ^{13}C NMR (100 MHz, $CDCl_3$) of

2-{3,4-bis[(2-octyldodecyl)oxy]phenyl}-1-phenyl-1H-imidazo[4,5-f][1,10]phenanthroline (4.4)

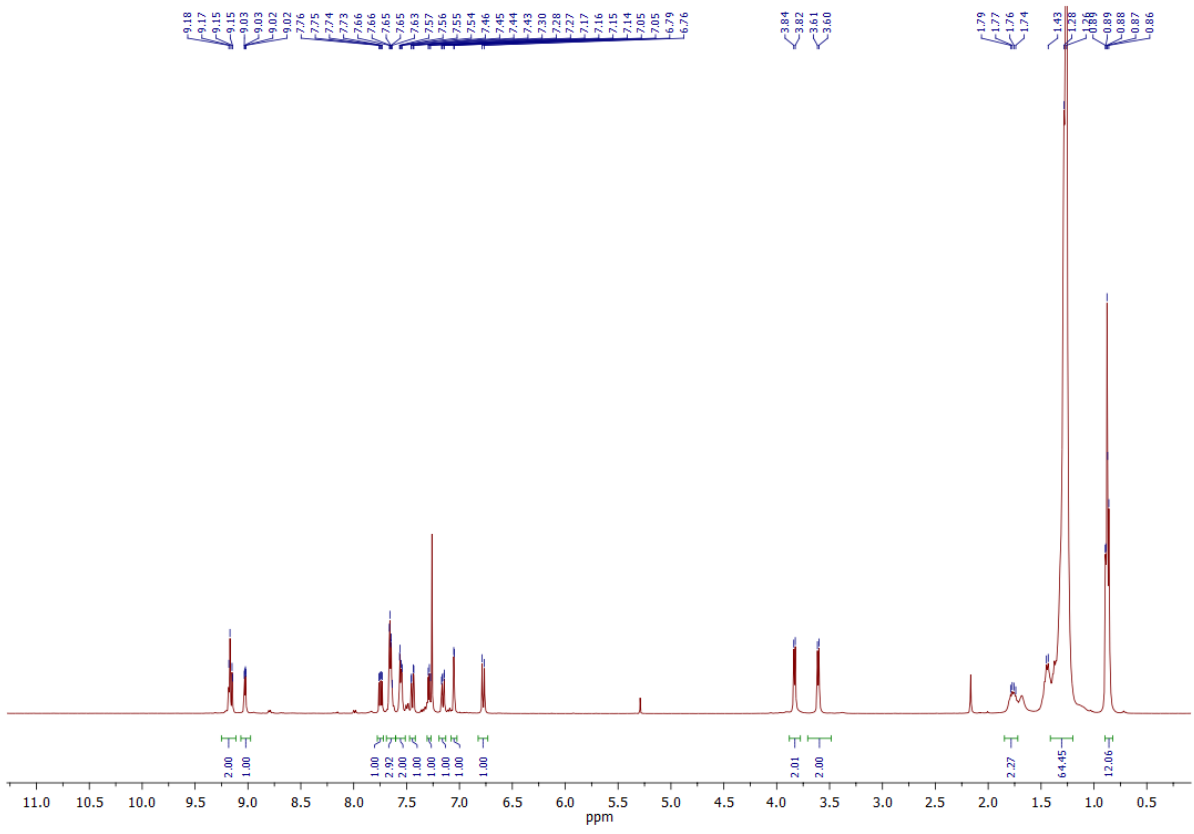

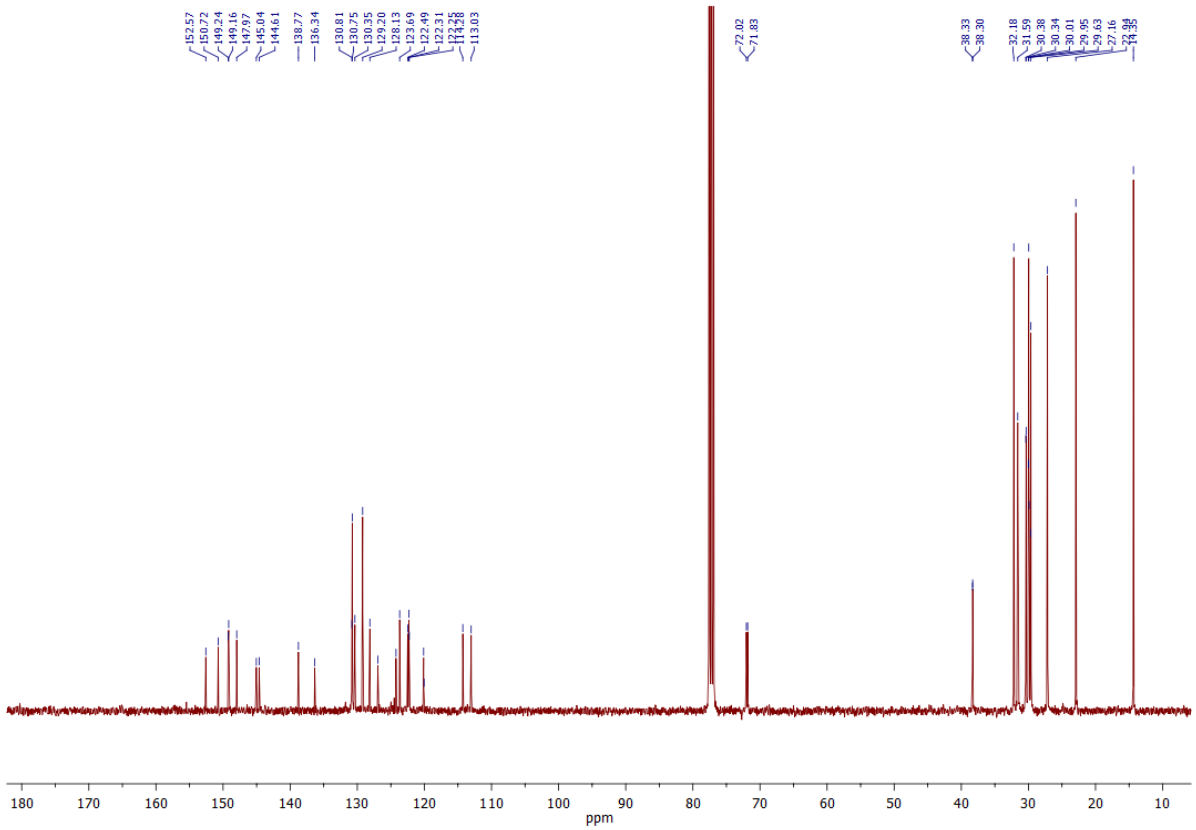

^{1}H NMR (400 MHz, $CDCl_3$) and ^{13}C NMR (100 MHz, $CDCl_3$) of 1,4-bis(1-phenyl-1H-imidazo[4,5-f][1,10]phenanthrolin-2-yl)benzene (4.5)

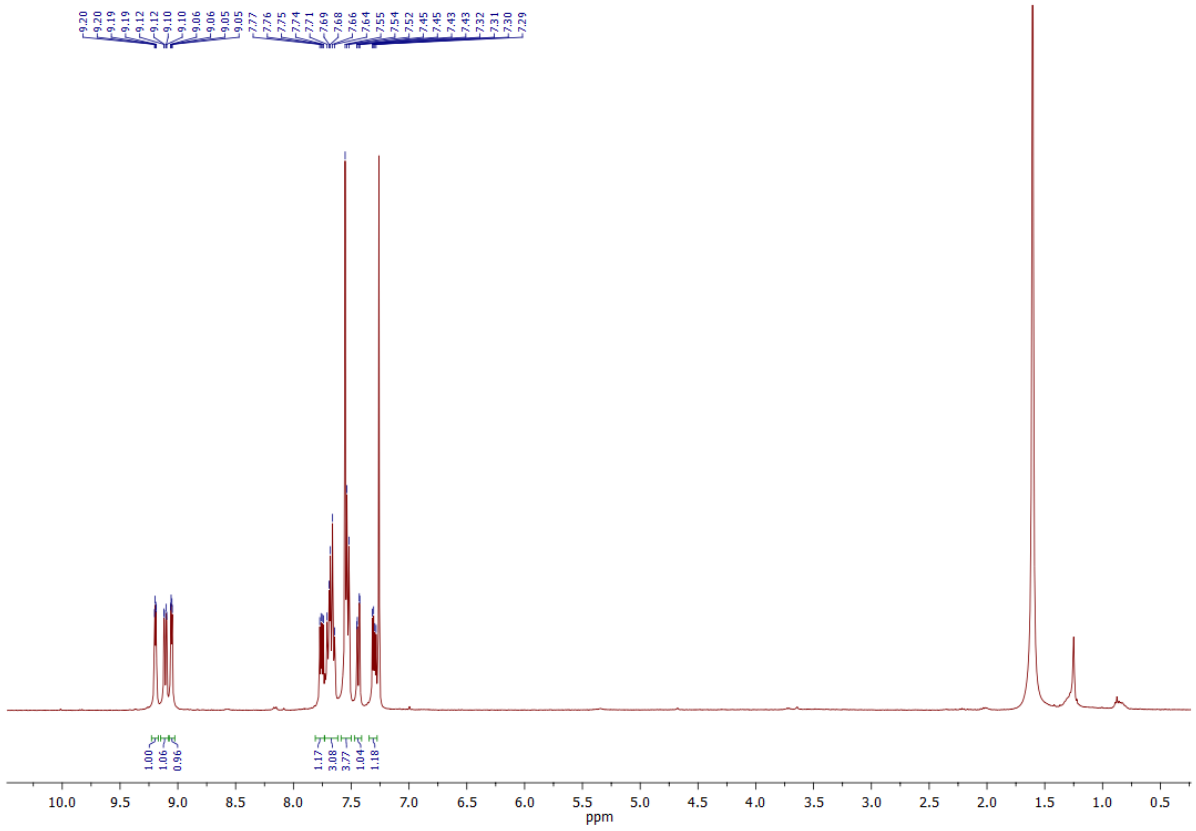

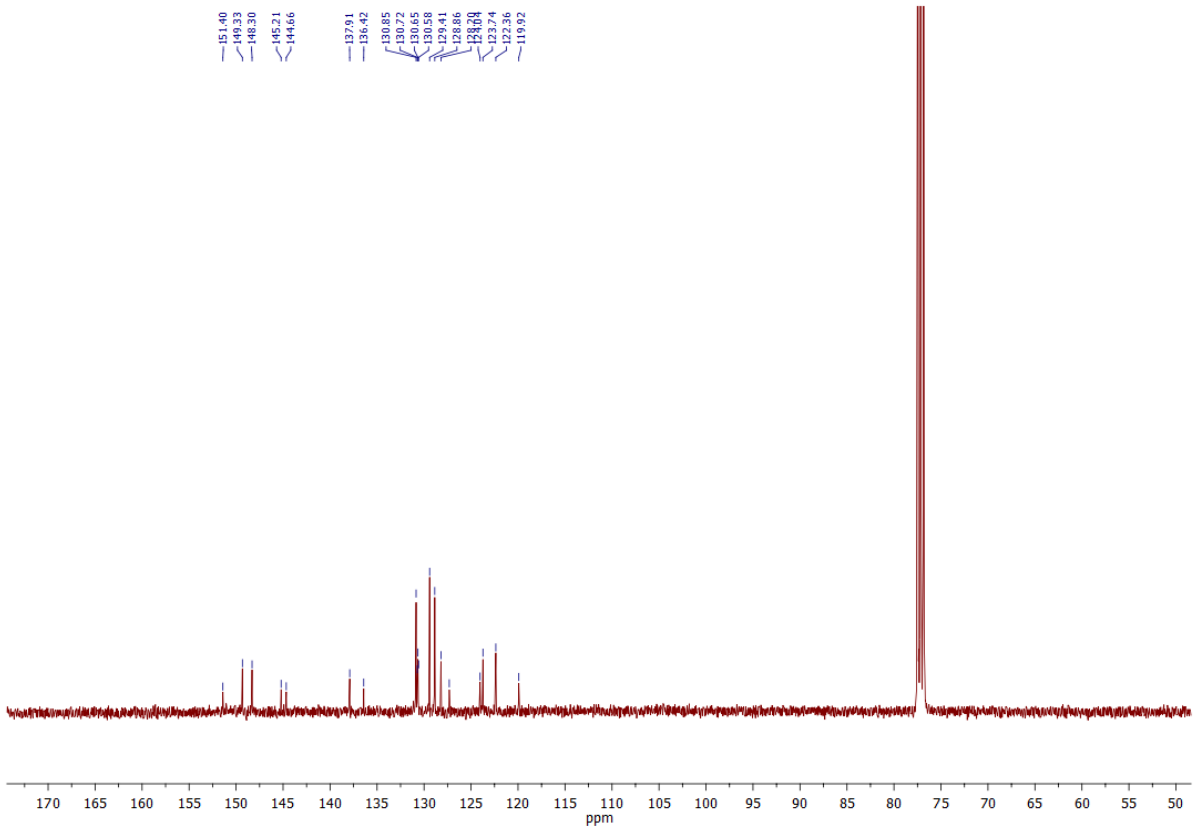

[Ir(ppy)$_2$(4.1)]$^+$(Ir.4.1)

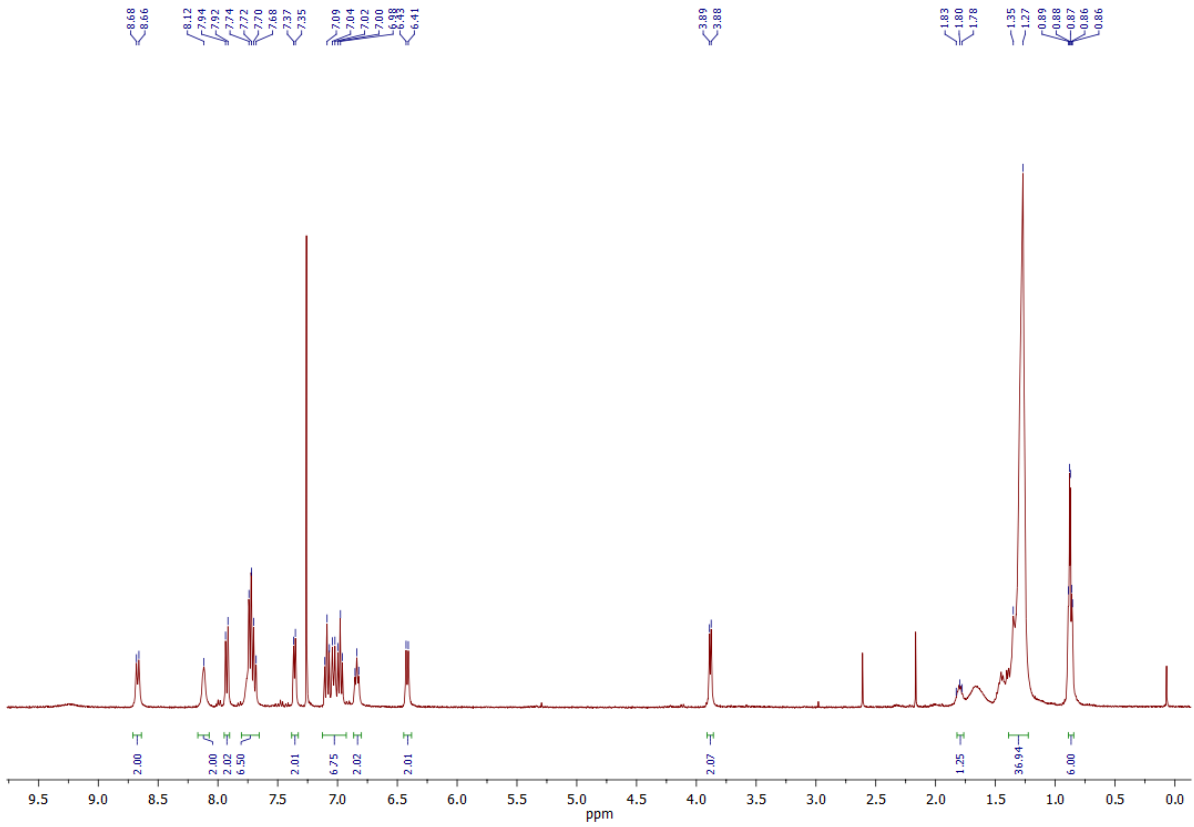

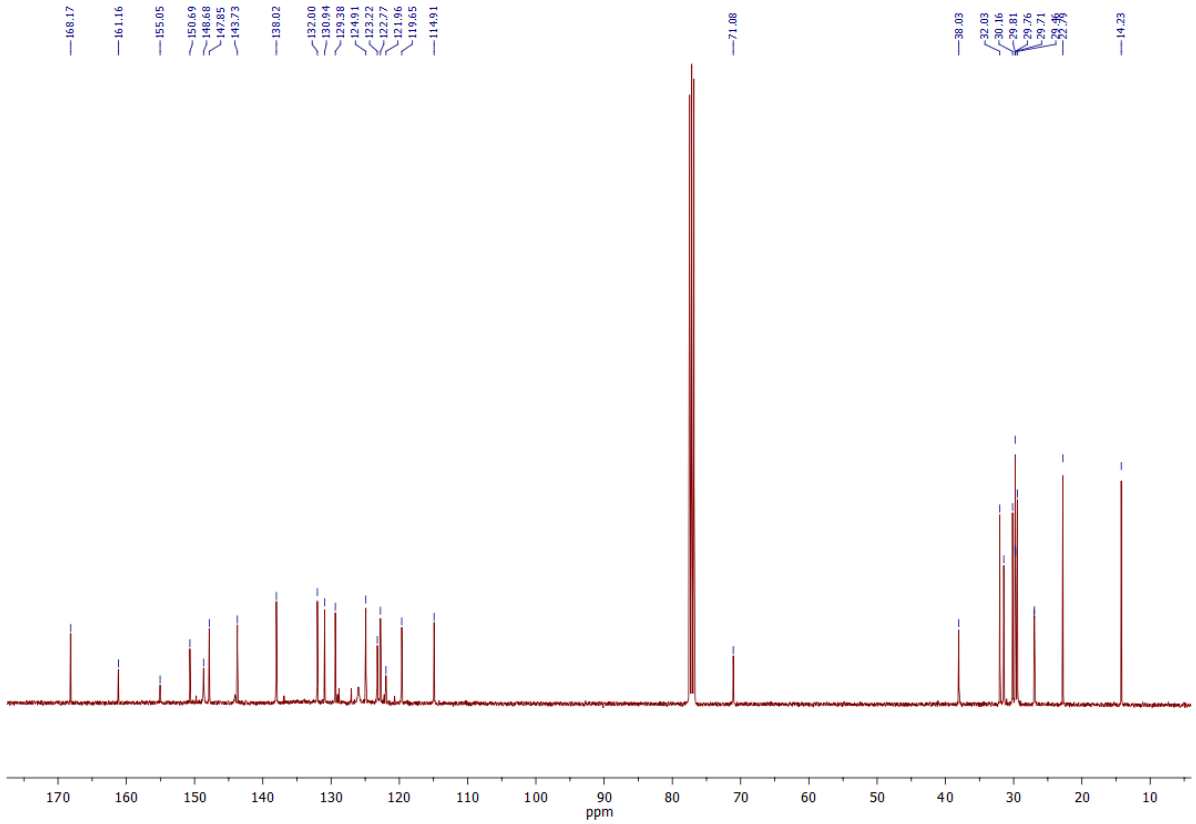

[Ir(ppy)$_2$(4.2)]$^+$(Ir.4.2)

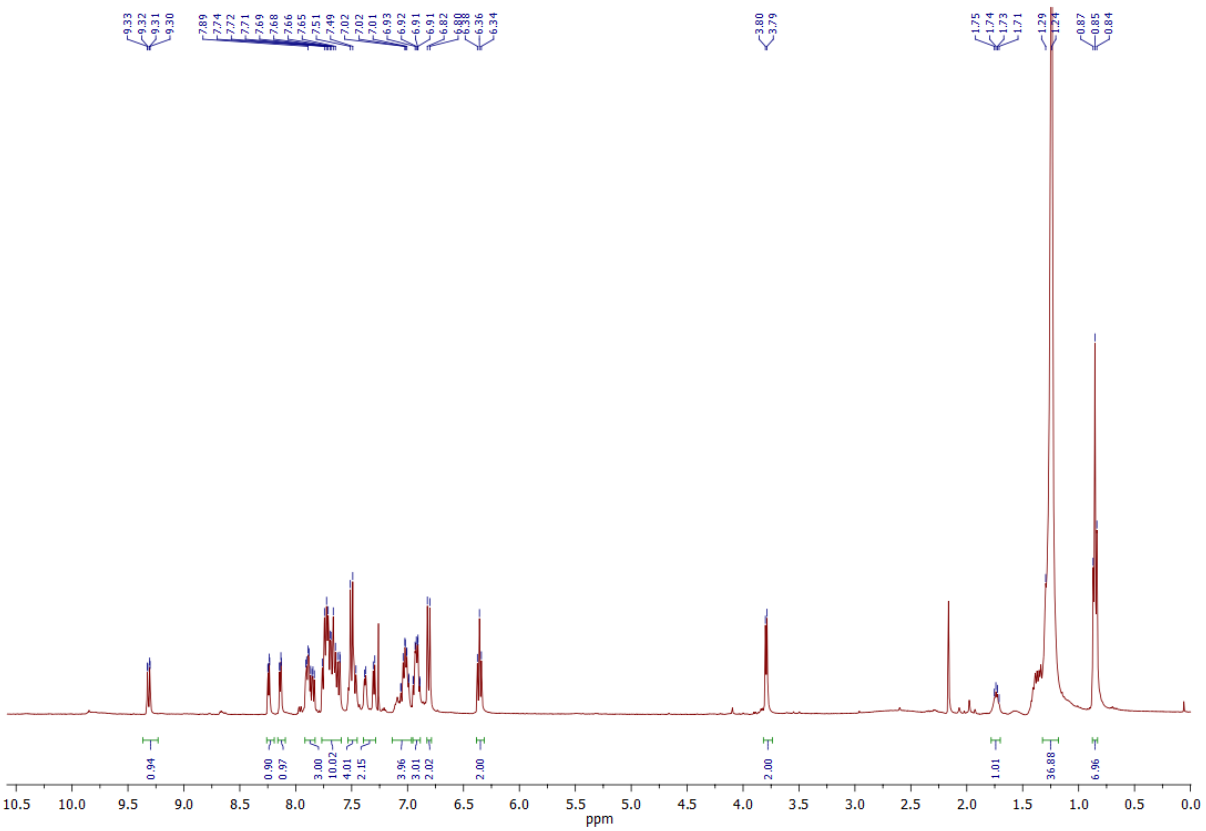

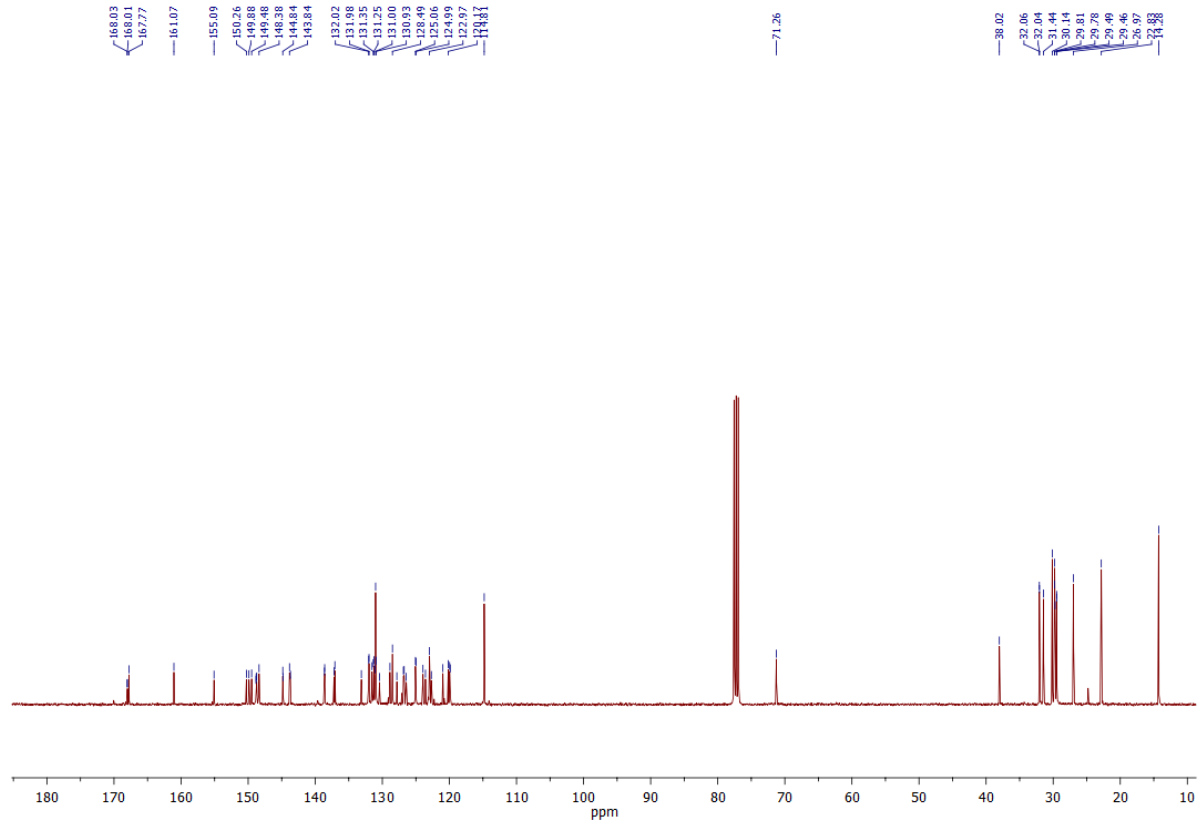

[Ir(ppy)$_2$(4.3)]$^+$(Ir.4.3)

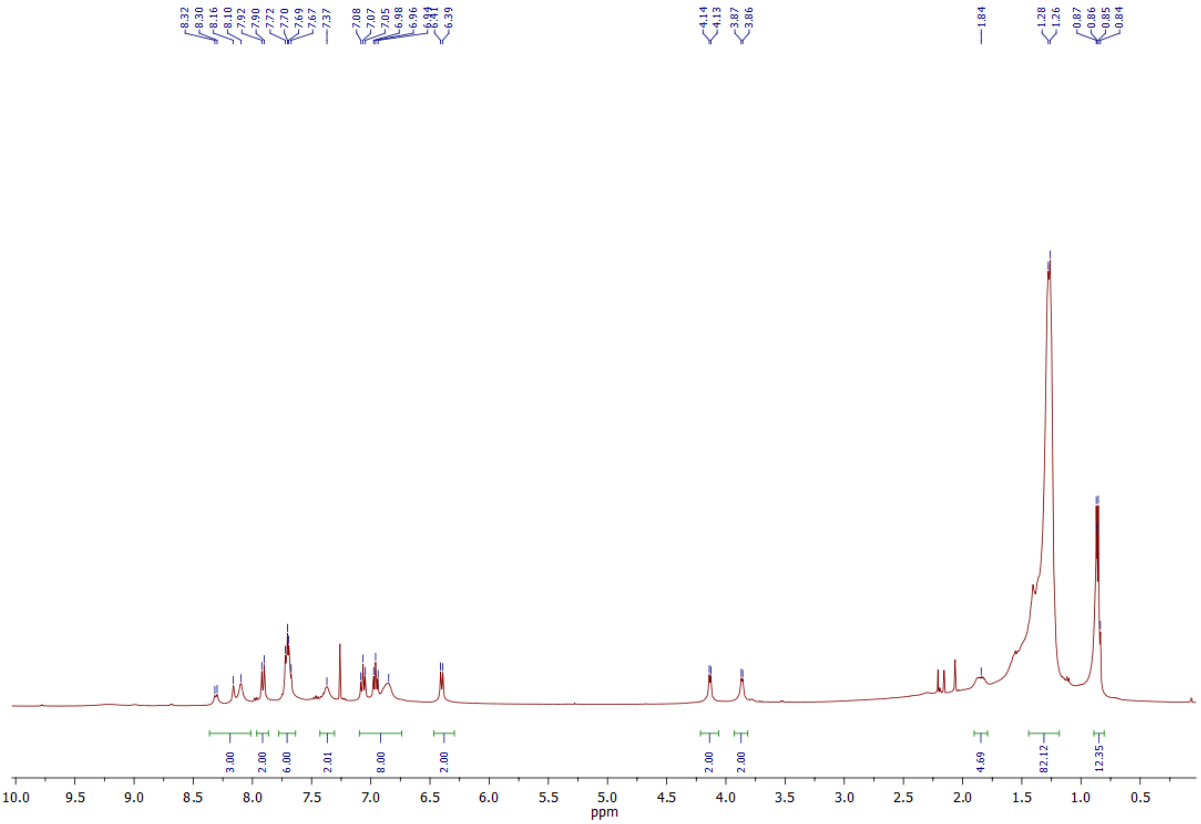

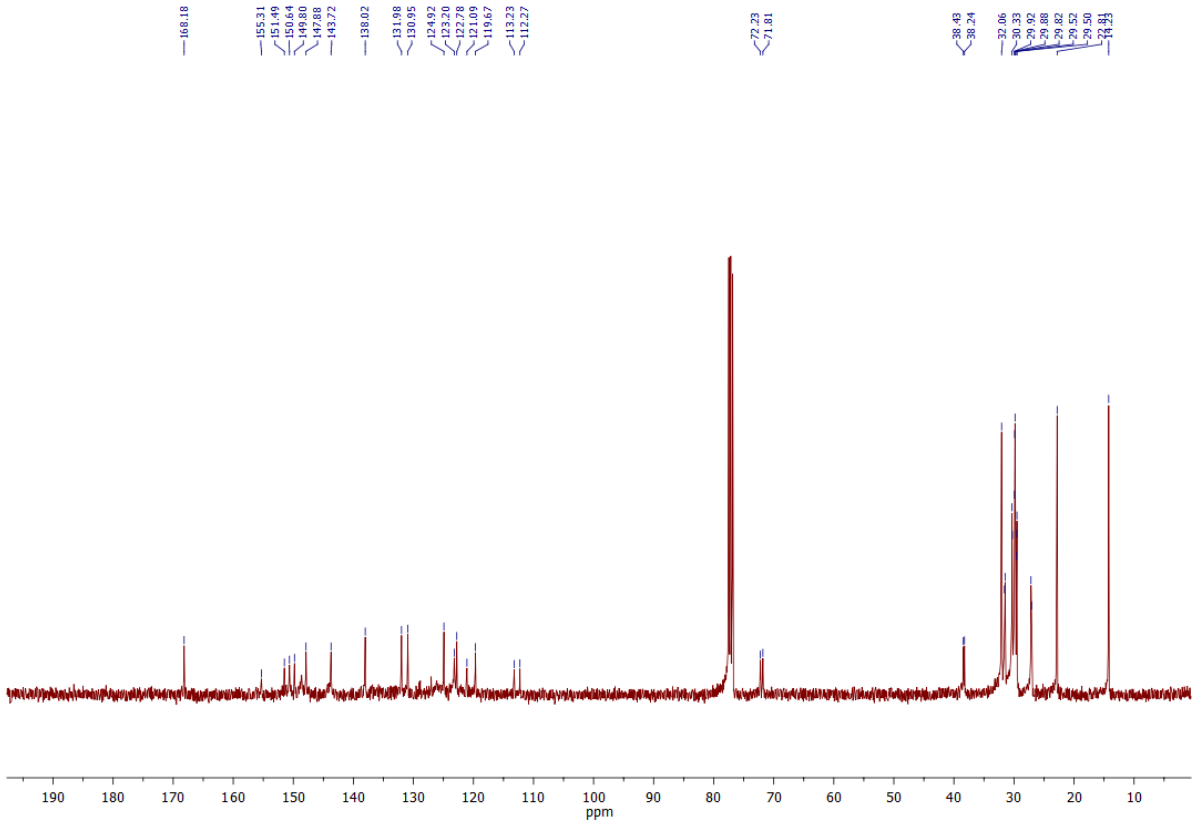

[Ir(ppy)$_2$(4.3)]$^+$(Ir.4.4)

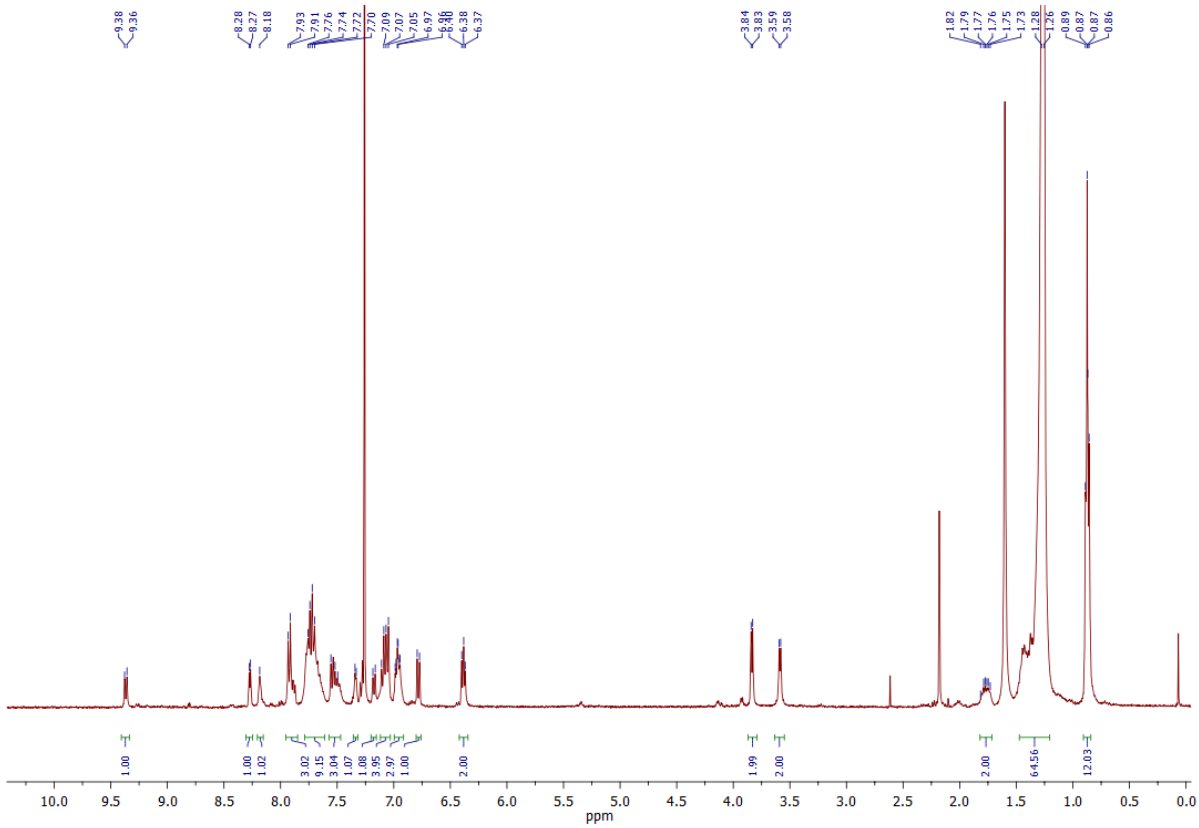

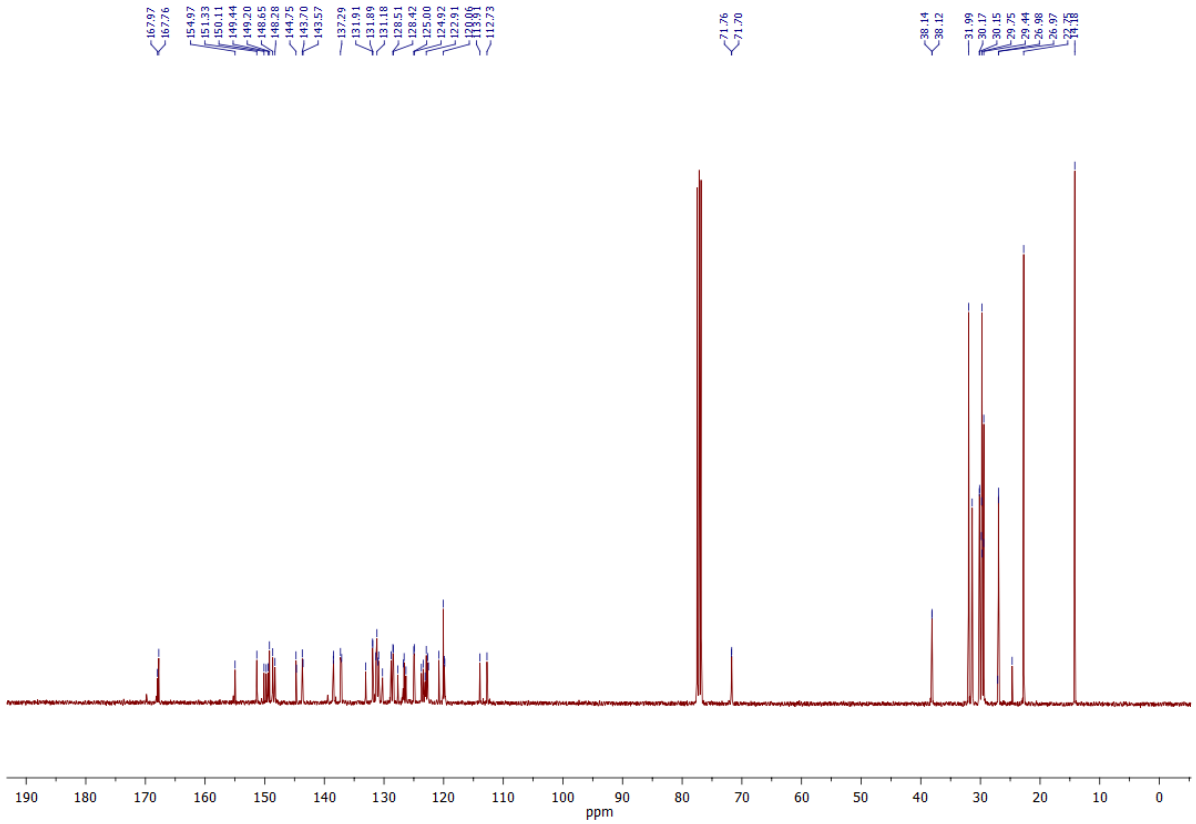

[Ir(ppy)$_2$(4.3)]$^+$(Ir.4.5)